LOCA and Air Ingress Accident Analysis of a Pebble Bed Reactor

by

Tieliang Zhai

Submitted to the Department of Nuclear Engineering
In partial fulfillment of the requirements for the degrees of

Nuclear Engineer
and
Master of Science in Nuclear Engineering

at the

MASSACHUSETTS INSTITUTE OF TECHNOLOGY

AUGUST, 2003

Author……
Department of Nuclear Engineering
August 15, 2003

Certified by……..……..
Prof. Andrew C. Kadak
Thesis Supervisor

Certified by …….……..
Prof. Hee Cheon No
Thesis Reader

Accepted by……...
Prof. Jeffrey A. Coderre
Chairman, Department Committee on Graduate Students

LOCA and Air Ingress Accident Analysis of a Pebble Bed Reactor

by

Tieliang Zhai

Submitted to the Department of Nuclear Engineering
In partial fulfillment of the requirements for the degrees of

Nuclear Engineer
and
Master of Science in Nuclear Engineering

Abstract

The objective of this thesis was to investigate the key safety features of the pebble bed reactor under challenging conditions. The first part of the thesis explored the "no meltdown" claim of the proponents of the technology without the use of any active emergency core cooling systems after a loss of coolant accident. Using a conservative HEATING-7 analysis, it was shown that the peak fuel temperature was approximately 1640 °C after the initial loss of coolant which is about 1500 °C below the UO_2 fuel melting temperature. Sensitivity studies also showed that the peak fuel temperature was insensitive to thermal properties, such as the soil conductivity, emissivities of the concrete wall and the pressure vessel. It was established that although the fuel would not melt, the temperature of the reactor vessel and the reactor cavity concrete exceeded design limits. A separate study by Professor Hee Cheon No using new code developed for this application (PEB-SIM) confirmed the HEATING-7 peak temperature results without convection cooling in the reactor cavity. His analysis was extended to perform a sensitivity study to determine how much air would have to be circulated in the reactor cavity to bring the temperatures of the reactor vessel and reactor cavity within design limits. This study showed that approximately 6 m/s of air-flow would be required. This study also showed that the peak fuel temperature was unaffected by the reactor cavity cooling system. The conclusion was that although the core will not melt even under these very conservative conditions by a large margin, some form of reactor cavity cooling system will be required to keep the reactor vessel and reactor cavity concrete within design limits. Future work in this area will be the design of a passive reactor cavity core cooling system based on the design inferences identified in this study.

The second part of this thesis was to develop a better understanding of the details of air ingress accidents in pebble bed and prismatic reactors. A theoretical study of an open cylinder of pebbles to better understand the key processes involved in air ingress was performed using the previous results from the LOCA analysis as initial conditions. The HEATING-7 model with side calculations to model the buoyancy and resistance to flow in a pebble was used to predict the peak fuel temperatures and air ingress velocity. The results of this simple analysis showed that

heat source contribution from the chemical reaction was relatively low and confined to the lower reflector region. The peak temperature increase from the non-chemical LOCA analysis was about 20 °C (a maximum of 1660 °C at 92 hours). Dr. No's analysis using PEB-SIM with cheimical reactions showed similar results (peak temperature of 1617 °C at 92 hours). The other interesting result was that the air ingress velocity decreased after about 350 °C. This negative feedback could be a significant factor in air ingress accidents in real reactors since the average post LOCA temperature in the reactor is on the order of above1300 °C. Using these fundamental insights, attention focused on developing a benchmarked computational fluid dynamics modeling capability for air ingress events. Two series of tests were used to benchmark the CFD code selected for this analysis – FLUENT 6.0. The first series of tests were performed at the Japan Atomic Energy Research Institute (JAERI). These tests were aimed at understanding the fundamental processes of air ingress accidents in separate effects tests. There were initial diffusion, natural circulation and the chemical reactions with heated graphite in a prismatic reactor configuration. Particularly, A multi-component diffusion model, surface reaction model and volume reaction model were developed. The FLUENT model and methodology developed was able to predict quite accurately each of these tests. The second experimental benchmark was the Julich Research Center test performed at the NACOK facility. This series of tests was to model natural circulation in a pebble bed reactor under varying hot and cold leg temperatures to assess air mass flow rate. The FLUENT methodology developed was able to predict the mass flow rates for the 40 experiments with very good results. This work will be used to benchmark the NACOK chemical corrosion tests in the future. A outline for a work plan for continuation of this work has been prepared for development of a benchmarked CFD capability to analyze the details of air ingress accidents.

Thesis supervisor: Andrew C. Kadak
Title: Professor of Practice of Nuclear Engineering

Acknowledgments

I would like to express my deepest gratitude and affection to my advisor, Prof. Andrew Kadak, for his guidance, patience and constant support. I feel especially privileged to have worked and studied under the guidance of such a fine mentor and a gifted educator. Among other things, I learned a great deal from him about conducting research and pursing a professional career.

Grateful and sincere thanks to my thesis reader, Dr. Hee Cheon No who has always been willing to help and offered many constructive ideas on my work. His independent models have confirmed my calculation, and his advises have broadened my view on various aspects of the research.

I wish to thanks Prof. Ronald Ballinger, Prof. Mujid Kazimi, who talked with me about my work and gave me many wonderful advises. Thank also go to Dr. Walter Kato, for many early discussions on the LOCA analysis.

Many thanks to the other members of my engineer committee: Prof. George Apostolakis, Prof. Michael Driscoll and Dr. Lin-wen Hu. Their comments and insightful suggestions have help to strengthen the work and improve the organization of the final document.

The PBMR group has been a stimulating and enjoyable place to work. Jing Wang, Heather MacLean, Chunyun Wang are all wonderful friends. I can always remember the many happy occasions and what I learned from you all.

Special thanks to my family: my dear daughter Michelle who is now 11-month-old, my wife Ruirong for her love and help, my parents and parents-in-law for their help to take care my daughter. I love you all.

This research was financially supported by Idaho National Engineering and Environment Laboratory and by Nuclear Regulatory Commission.

TABLE OF CONTENTS

LIST OF FIGURES

LIST OF TABLES

LIST OF APPENDIX

1. Introduction

1.1. Introduction

As a promising future energy option, HTGR technology is once again receiving increasing interest in many countries. The main attractiveness of this technology is the modular design concepts and passive safety. These features offer the promise of an economically competitive electricity generation option, suitable for construction and operation in both industrialized and developing countries. The high temperature capability and smaller unit size also provides the prospect of non-electrical applications for high temperature process heat and for hydrogen production, as well as low temperature energy supply for desalinization through cogeneration.

The Modular Pebble Bed Modular Reactor (MPBR) is a new type of high temperature helium gas-cooled, graphite moderated nuclear reactor, which is recognized worldwide as an inherently safe reactor type [1]. The pebble bed reactor is being developed at MIT and in South Africa. It is a reactor where the inherent safety objective can be reasonably attained due to its low power density and high heat capacity of the core. The most remarkable feature of this reactor is that it has natural deterministic attributes that do not require active engineered safety systems to prevent the core from melting in accident situations such as the complete loss of coolant.

While the overall safety of the pebble bed reactor is generally accepted, there are two specific accidents that need to be analyzed and understood to validate these claims. The first is a loss of coolant accident which is the standard type of accident assumed for light water reactors and the second is more unique to high temperature graphite reactors – air ingress. The loss of coolant accident in light water reactors requires active engineered safety systems to provide cooling water quite quickly to prevent the core from melting. In high temperature pebble bed gas reactors, the large amount of graphite which has a tremendous capability to store and transfer heat and the low power density of the core, allows the reactor core to increase temperature very slowly (80 hours) without active engineered systems and does not reach temperatures that will melt the fuel.

The air ingress accident is important because of the potential for chemical reactions of air with the graphite (carbon) in the reactor. Under certain circumstances, the graphite which makes up much of the internals of the reactor, can aggressively react with the air contributing an additional internal heat source and possibly burn. The details of the analysis are complex and only generally understood. The purpose of this thesis is to develop a methodology using advanced computational fluid dynamics methods to understand the complexities of the air ingress accident.

1.2. Description of MPBR [2]

The reactor consists of an annular core (3.5 meters in diameter) surrounded by graphite blocks. There are about 300,000 graphite fuel pebbles in the core region, and each pebble consists of ~15,000 fuel micro-spheres. In the central region of the core, there are 110,000 graphite pebbles consisting of no fuel. Each fuel micro-sphere is composed of a uranium dioxide pellet (enriched to 8% U-235), enclosed in a three-layer ("TRISO") coating consisting of a layer of silicon carbide sandwiched by two layers of pyrolytic carbon. The "TRISO" fuel has exhibited good fission product retention in German tests up to temperatures of about 1600 °C [3]. Both the core and the graphite reflectors are installed in the pressure vessel. The normal operation pressure is 80 bars, and the safety limit temperature is 480 °C for the pressure vessel. An under-ground reactor cavity is designed to reduce the possibility of radioactivity release and to transfer the decay heat to the soil surrounding the cavity in the accident scenarios.

The temperature resistance of the fuel and the use of a single-phase-helium gas coolant enable the reactor to operate at a coolant temperature of about 900 °C, considerably higher than the operating temperature of LWRs. The higher temperature alone allows the reactor to achieve a thermal efficiency of 45% (Table 1-1 shows the key PBMR plant parameters). The pebble bed reactor can use either a direct or indirect gas turbine cycle (known as the Brayton cycle).

In the normal operation, fuel pebbles are continuously loaded at the top of the core, flow downward, and are discharged at the bottom (shown in Figure 1-1). Shutdowns would be required only for maintenance purposes because the PBMR is fueled while operating. Because the MPBR is continuously refueled, the excess reactivity can be kept low. Also, the design has a

more negative fuel temperature coefficient than LWRs, as the Doppler feedback is greater for the less-thermal neutron spectrum associated with a graphite moderator. These features reduce the risk of reactivity accidents for most scenarios.

A major component of the PBMR safety basis is a low power density (an order of magnitude below that of an LWR) and large thermal capacity (as a result of the large mass of graphite in the core), together with the high-temperature resistance of the fuel. The maximum power rating of each module (265 MWth) and the high surface-to-volume ratio of the core were chosen so that in the event of a loss of coolant from the primary system, adequate cooling would be provided without the need for forced convection. In the event of a total loss of primary coolant and no operator intervention, the core heat-up rate would be slow and the maximum fuel temperature would not exceed the target value (not safety limit) 1600 °C. Thus, the design does not include conventional emergency core cooling systems, which are required for LWRs to provide emergency water sources in the event of a loss-of-coolant accident.

Due to the high safety of MPBR, there are significant opportunities to reduce some of the costly and, for the MPBR, unnecessary requirements that apply to the current generation of U.S. nuclear plants. These proposals include (1) use of a confinement building instead of a robust containment capable of preventing a large release of radioactive materials in the event of severe core damage; (2) a reduction of the size of the emergency planning zone (EPZ) from 16 kilometers to 400 meters; (3) a reduction in the number of staff; and (4) a reduction in the number of systems that are required for the safety of light water reactors.

Thermal power	265MW
Core height	10.0 m
Core diameter	3.5 m
Pressure vessel height	16 m
Pressure vessel radius	5.6 m
Number of fuel pebbles	360,000
Micro-spheres/fuel pebble	11,000
Fuel	UCO or UO_2
Fuel pebble diameter	60 mm
Fuel pebble enrichment	8%
Uranium mass/fuel pebble	7 g
Coolant	Helium
Helium mass flow rate	120 kg/s (100% power)
Helium entry/exit temperatures	522 °C/900 °C
Helium pressure	80 bar
Mean power density	3.54 MW/m^3
Number of control rods	6

Table 1-1: MPBR Plant Parameters [1]

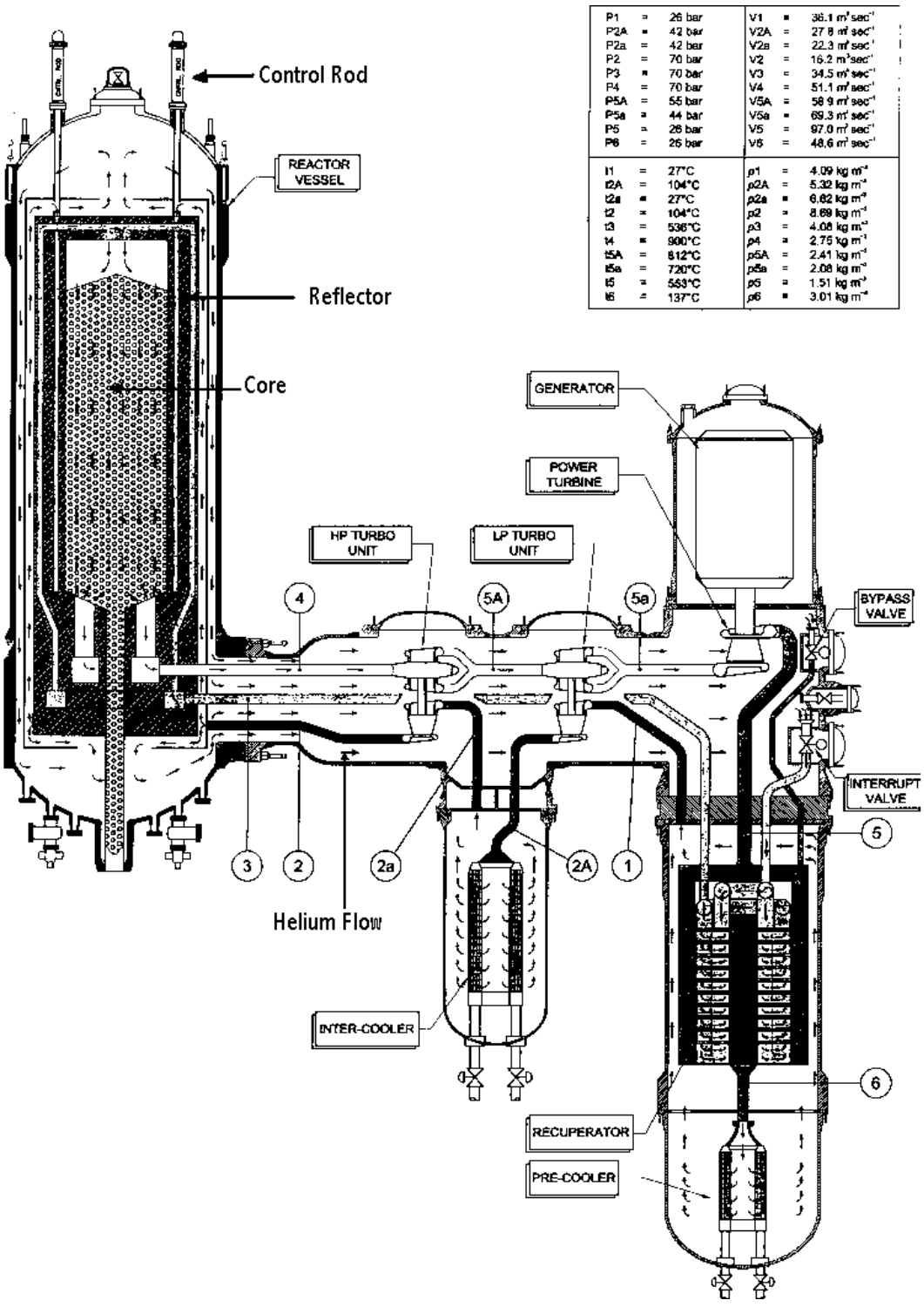

Figure 1-1: The Profile of the PBMR [1]

1.3. Contributions of This Thesis

Unlike LWRs, the PBMR does not have the benefit of thousands of reactor-years' worth of operating experience. In addition, the reported graphite burning during the Chernobyl accident has raised public concerns about the behavior of other graphite moderated reactor types under severe accident conditions, especially when air enters the primary circuit after a failure of the primary system boundary. The consequences of an extensive graphite fire could be severe, undermining the argument that a conventional containment is not needed. Radiological releases from the Chernobyl accident were prolonged as a result of the fires which some allege was due to the burning of graphite, which continued long after other fires were extinguished. Even though the temperature of a graphite fire might not be high enough to severely damage the fuel micro-spheres, the burning graphite itself would be radioactive as a result of neutron activation of impurities and contamination with "tramp" uranium released from defective micro-spheres [3]. Although there is a difference of opinion as to whether the graphite actually burned at Chernobyl, the air ingress accident needs to be understood which is the main purpose of this thesis.

This thesis is divided into two parts, Part 1 deals with the Loss Of Coolant Accident (LOCA). A detailed model is developed using HEATING-7 [4] to study the consequences of the accident, especially the characteristics of the peak temperatures for the regions we most concerned. All the key components that may significantly influence the heat transfer are modeled, and for the unknown factors, conservative assumptions are made. This study will confirm the previous findings of no core melting and identify significant needs to address the temperature limits of the reactor vessel and reactor cavity. This analysis will also provide the initiating event conditions for the air ingress accident.

In Part 2, the air ingress accident is studied in a step-by-step method. The goal of this work is to understand the phenomenon of air ingress in a graphite core and develop a methodology using computational fluid dynamics tools to more accurately model the air ingress for both pebble and prismatic cores. There are many complicated processes involved in the air ingress accident:

diffusion, natural convection, dynamic and multiple chemical reactions in a complex geometry. To address the complexities of the analysis a simplified theoretical study was performed to gain an appreciation of the processes at work. This was followed by a CFD benchmarking program based on experimental work performed by JAERI (Japanese Atomic Energy Research Institute) in which the basic phenomenon of diffusion, natural circulation and chemical reactions are separately tested to understand main mechanisms involved in the air ingress accident. This work is applicable to prismatic reactors. To benchmark the pebble bed reactors, natural circulation experiments performed by Forschungszentrum Julich GmbH were simulated using the CFD code, FLUENT6.1 to develop a CFD method for the analysis of the air ingress accidents in the pebble bed plants.

2. LOCA Analysis

2.1. Introduction

The inherent properties of the Modular Pebble Bed Reactor (MPBR) facilitate the design with high degree of passive safe performance compared with other type of reactors. This analysis examines the performance of the pebble bed reactor in response to a complete Loss of Coolant Accident (LOCA) without the any active engineered features.

The loss-of-coolant accident is one of the most severe accidents for an MPBR. The challenge in a LOCA is to remove the heat released by radioactive decay of fission products without core damage by passive means only. This objective of this reactor concept is such that it should be designed in such a way that the temperature limits will not be exceeded in such an accident, even if no active heat removal measures are taken. While this might not be completely possible, this analysis will identify the critical components that need to be addressed to assure that temperature limits are not exceeded.

The purpose of the analysis presented below is to determine the peak temperatures for the core, pressure vessel and concrete wall after a LOCA with depressurization which proceeds with no means of core and reactor cavity cooling except for conductive and radiation heat transfer to the soil surrounding the reactor cavity and natural convection from the enclosed top of the reactor cavity to the air.

Once these peak temperatures are calculated, mitigating measures would need to be identified to avoid exceeding temperature limits. This study assumes a reactor shutdown with a complete depressurization as if caused by a double-ended guillotine break of the connecting vessel and pipes. This is judged to be a more severe accident than a pressurized loss of coolant accident (loss of flow).

The Modular Pebble Bed Reactor will be modeled for the detailed study. Once the baseline calculation is concluded, a detailed sensitivity study will be conducted to identify critical parameters or conditions that can enhance the passive heat removal processes for future designs.

2.2. Physical Phenomena

This analysis will model an equivalent double-ended guillotine break with an instantaneous depressurization after operation for full power for an equilibrium core. The reactor is assumed to be shutdown with the insertion of the shutdown rods. Within a very short period (about several seconds), the pressure will be balanced between the reactor pressure vessel and the reactor cavity as a result of the rapid blow-down. No active cooling system is assumed to remove decay heat from the reactor. The decay heat generated in the reactor is transferred from the core through the reactor vessel by conduction; from the reactor to the concrete reactor cavity by radiative heat transfer; from the reactor cavity to the surrounding soil, which is the ultimate heat sink, by conduction. Natural convection to the air from the top of the reactor cavity is also assumed.

The HEATING7 [4] code will be used as the code to calculate the heat transfer from the fuel region through the reflector, the reactor vessel and through the reactor cavity to the earth as a final heat sink. The initial power distribution for the modular pebble bed reactor will be obtained from the VSOP code, which is the basic core neutronics code, used in pebble bed analysis[5].

2.3. Model Description

A three-dimensional model of the MPBR was developed for input to the HEATING-7 code. The model divides the components involved into 21 regions, as shown in Figure 2-1, which are composed of seven different materials: pebbles, graphite, helium, 2-1/4 Cr-Mo steel, air, concrete, and soil. The core void is filled with stagnant helium. In some cases when the properties for these materials could not be fully determined, conservative values were chosen as a basis, and sensitivity analyses were performed on these undetermined parameters.

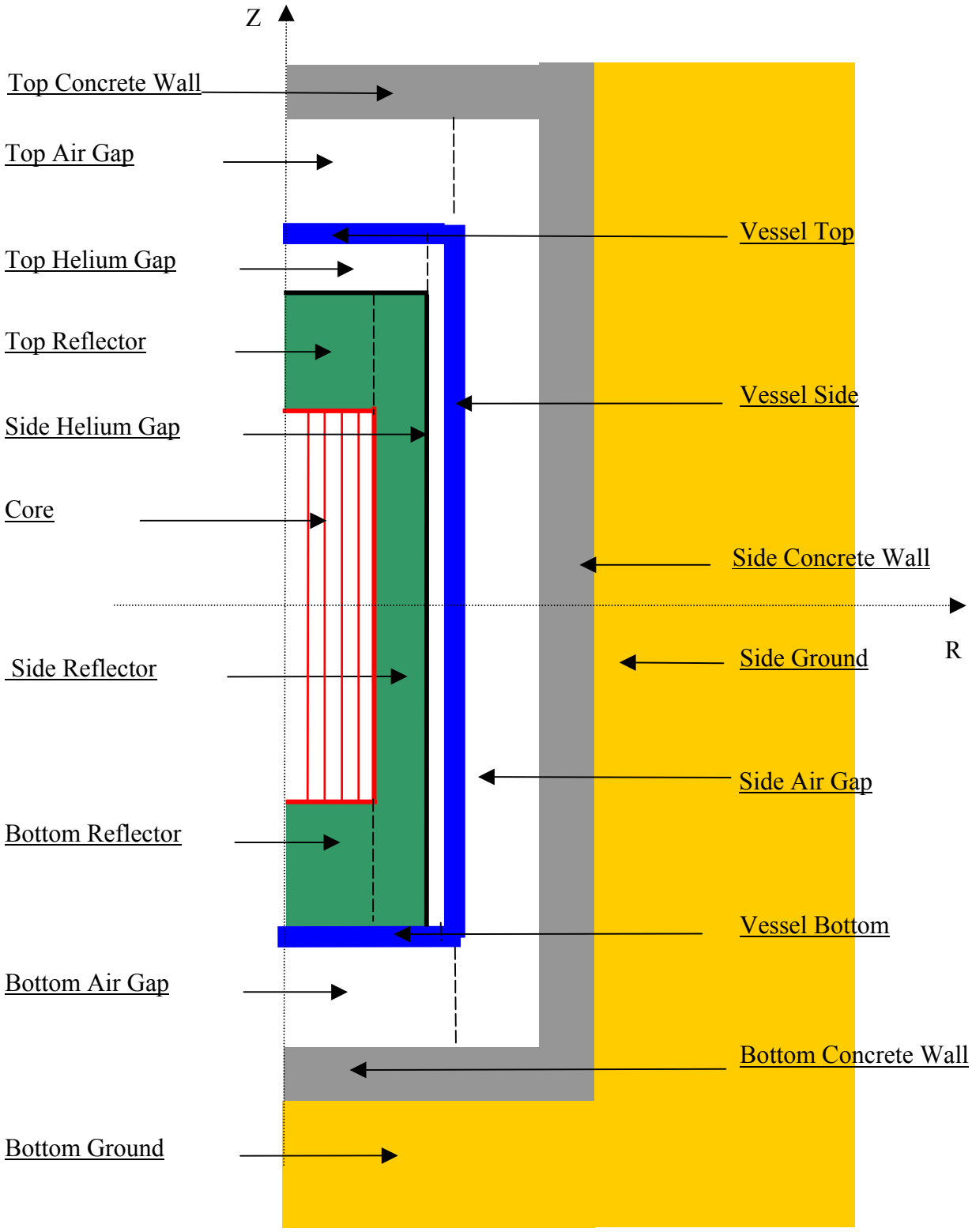

Figure 2-1: HEATING-7 Model for LOCA Analysis

2.3.1. HEATING-7 Description [4]

HEATING-7 is a general-purpose conduction heat transfer program written in Fortran 77. The name HEATING is an acronym for Heat Engineering and Transfer In Nine Geometries (although with modifications there are now 12 geometries). HEATING-7 can solve steady state and/or transient heat conduction problems in one-, two-, or three-dimensional Cartesian, cylindrical, or spherical coordinates. A model may include multiple materials, and the thermal conductivity, density, and specific heat of each material may be both time- and temperature-dependent. The thermal conductivity may also be anistotropic. Materials may undergo change of phase. Thermal properties of materials may be input or may be extracted from a material properties library. Heat-generation rates may be dependent on time, temperature, and position, and boundary temperatures may be time- and position-dependent. The boundary conditions, which may be surface-to-surface or surface-to-environment, may be specified temperatures or any combination of prescribed heat flux, forced convection, natural convection, and radiation. General gray-body radiation problems may be modeled with user-defined factors for radiant exchange. The mesh spacing may be a variable along each axis. The code uses free-form-reading subroutines to interpret the input data file, which is subdivided into data blocks identified by keywords.

2.3.2. Regions and Mesh

In the 3-Dimensional model, a cylindrical coordinate is adopted and the complicated system is divided into many regions mainly based on their thermal properties. For each edge in the inner regions, all the edge lengths are 0.1 meter, and the total number of nodes in the model is 58,106 according this mesh schedule (For mesh details, see Appendix 1). Table 2-1 indicates the regions involved in this model and their other properties. In this table, the reference numbers are used to represent the regions. The center point of the core is selected as the origin of the cylindrical coordinate system.

The core region is divided into 5 channels, and each channel consists of several layers based on the fuel properties. There are 57 layers in the 5 channels: 9 layers in channel 1, 10 layers in

Channel 2, 11 layers in Channel 3, 12 layers in Channel 4 and 15 layers in Channel 5 (Shown in Figure 2-2) [5]. (For the detailed description on the layers, see Appendix 2.) Each layer consists of 11 patch, the reference number, power density and volume are shown in Appendix 3.

Region Name	Reference Number	Materials	R_{min} (m)	R_{max} (m)	Z_{min} (m)	Z_{max} (m)
Channel 1	1	Pebble	0	0.69	-3.77	3.77
Channel 2	2	Pebble	0.69	1.01	-3.77	3.77
Channel 3	3	Pebble	1.01	1.27	-3.77	3.77
Channel 4	4	Pebble	1.27	1.50	-3.77	3.77
Channel 5	5	Pebble	1.50	1.75	-3.77	3.77
Top Reflector	101	Graphite	0	1.75	3.77	5.33
Side Reflector	102	Graphite	1.75	3.31	-5.33	5.33
Bottom Reflector	103	Graphite	0	1.75	-5.33	-3.77
Top Helium Gap	104	Helium	0	3.31	5.33	5.83
Side Helium Gap	105	Helium	3.31	3.41	-5.33	5.83
Top Region of the Vessel	107	2-1/4 Cr-Mo Steel	0	3.41	5.83	5.93
Side Region of the Vessel	108	2-1/4 Cr-Mo Steel	3.41	3.51	-5.43	5.93
Bottom Region of the Vessel	109	2-1/4 Cr-Mo Steel	0	3.41	-5.43	-5.33
Top Region of the Air Gap	110	Air	0	3.51	5.93	6.93
Side Region of the Air Gap	111	Air	3.51	4.82	-6.43	6.93
Bottom Region of the Air Gap	112	Air	0	3.51	-6.43	-5.43
Top Concrete Wall	113	Concrete	0	4.82	6.93	7.13
Side Concrete Wall	114	Concrete	4.82	5.02	-6.63	7.13
Bottom Concrete Wall	115	Concrete	0	4.82	-6.63	-6.43
Side Soil	116	Soil	5.02	25.02	-6.63	7.13
Bottom Soil	117	Soil	0	25.02	-26.63	-6.63

Table 2-1: The Regions

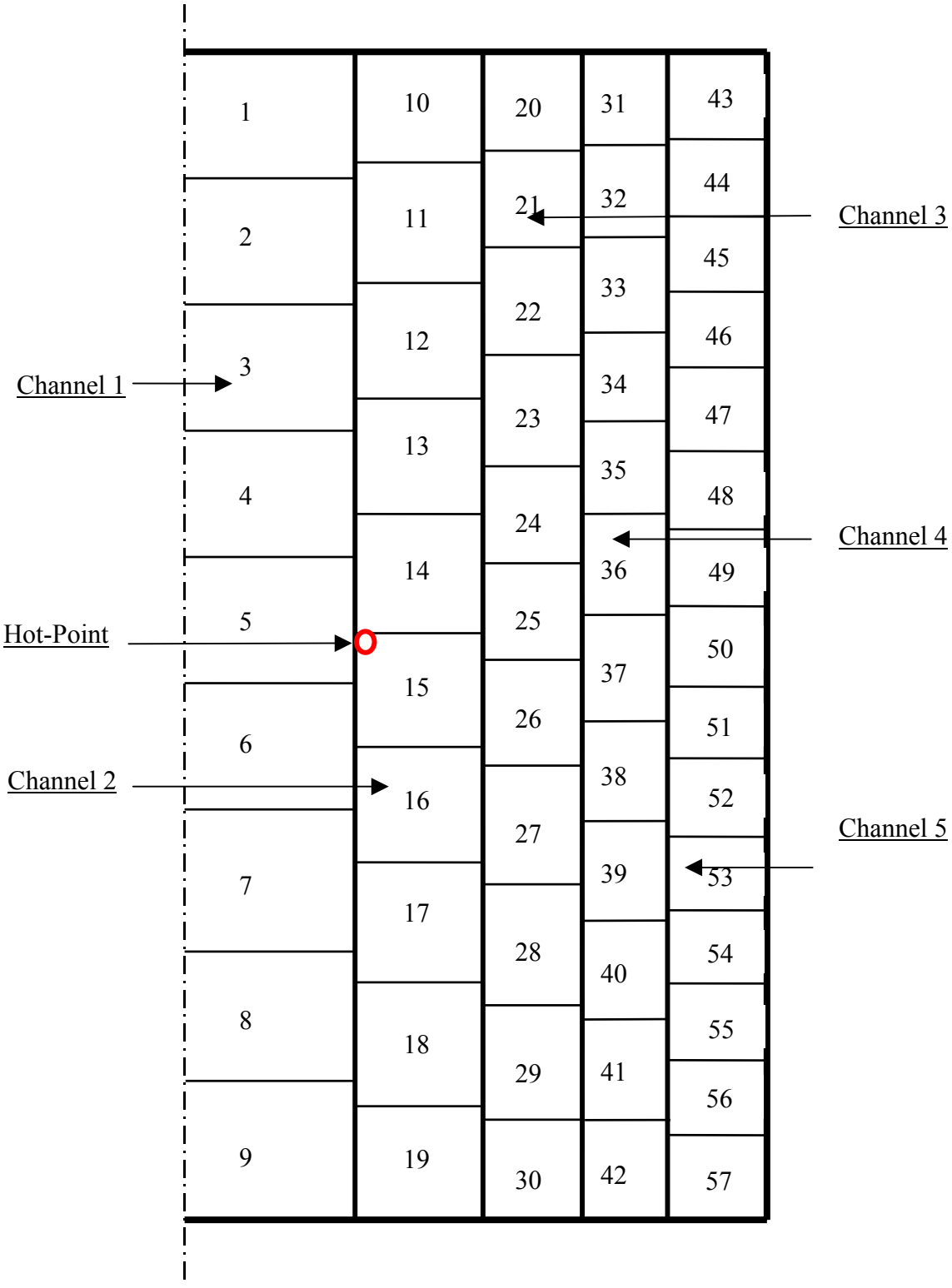

Figure 2-2: Regions in the Core Region

2.3.3. Assumptions

Although all the soil surrounding the cavity is the ultimate heat sink, the soil outer dimension of the models is limited to 26 m. This assumption is made since heat transfer in soil is so slow that only the soil surrounding the cavity is involved in the heat transfer over a long period of time. The temperature distribution calculation confirmed this estimation and justified limiting the outer radius. Heat removal by natural circulation is not considered since HEATING 7 cannot handle convection processes. This makes the analysis more conservative. For this phase of the work, chemical reactions are ignored leaving decay heat as the only source of heat addition to the system. Components are assumed to maintain their geometric configuration. The core barrel region, which is made of steel with high thermal conductivity relative to the other materials, is neglected because of its low thermal resistance. In addition, the complicated geometry in the bottom of the core is simplified: with the volumes unchanged, the original geometry of each layer in the core bottom is modified to a regular one similar to the layers in the central region of the core.

2.3.4. Initial Conditions and Boundary conditions

Initial equilibrium cycle core conditions at the time of reactor depressurization and shutdown were obtained from calculations performed using the VSOP code by Lebenhaft [5]. The core modeled was the ESKOM pebble-bed reactor being proposed in South Africa, which is being used by MIT as the reference core design. Table 2-2 shows the initial conditions, where the temperature is spatially dependent, the figures that display them are identified in the table. In Figure 2-3, the five curves show the temperature distribution from the bottom (-3.77 meter) to the top (+3.77 meters). The temperature distribution in the reflectors only depends the height of the reflectors. In Figure 2-4 and Figure 2-5, lower Z refer to lower part of the reflectors. For the side reflector, its peak temperature locates in the lower part since the helium flow from the top to the bottom in the normal operation. The air in the reactor cavity region is assumed to be stagnant and heat transfer occurs only by conduction and radioactive heat transfer as previously described. The initial temperature of the pressure vessel is assumed to be the temperature of the helium gap

since the conductivity of the pressure vessel is high. Very conservatively, the initial temperature of the air in the cavity is equal to the pressure vessel temperature. The initial temperature of the concrete wall and the soil were assumed to be 50 °C and 35 °C respectively. The boundary temperatures are assumed to be the temperatures of the soil – 35 °C.

In the helium and air gaps, the heat is transferred by conductivity and by radiation between facing surfaces. There is no forced convection in the two gaps. In the model, the heat transfer is governed by the following formula:

$$h_{eff} = h_c + h_r[T_s^2 + T_b^2][T_s + T_b] + h_n[T_s - T_b]^{he} \qquad \text{Eq. 2-1}$$

where

T_s = surface temperature, °C

T_b = boundary temperature, °C

h_c = forced-convection heat transfer coefficient, W/m^2-°C

h_r = radiation coefficient, W/m^2-°C^3

h_n = natural convection multiplier, and

h_e = natural convection exponent.

Although HEATING-7 cannot model heat transfer by convection directly, it can consider the convection as an extra heat transfer term on the boundaries if the user provide heat transfer coefficients on the boundaries. But the heat transfer coefficients must have the following strict format as shown in Eq. 2-1.

Region	Initial Temperature
The Core	Figure 2-3
Top Reflector	Figure 2-4
Side Reflector	Figure 2-5
Helium Gap	279 °C [5]
Pressure Vessel	279 °C
Air Gap	279 °C
Concrete Wall	50 °C
Earth	35 °C

Table 2-2: The Initial Temperatures [5]

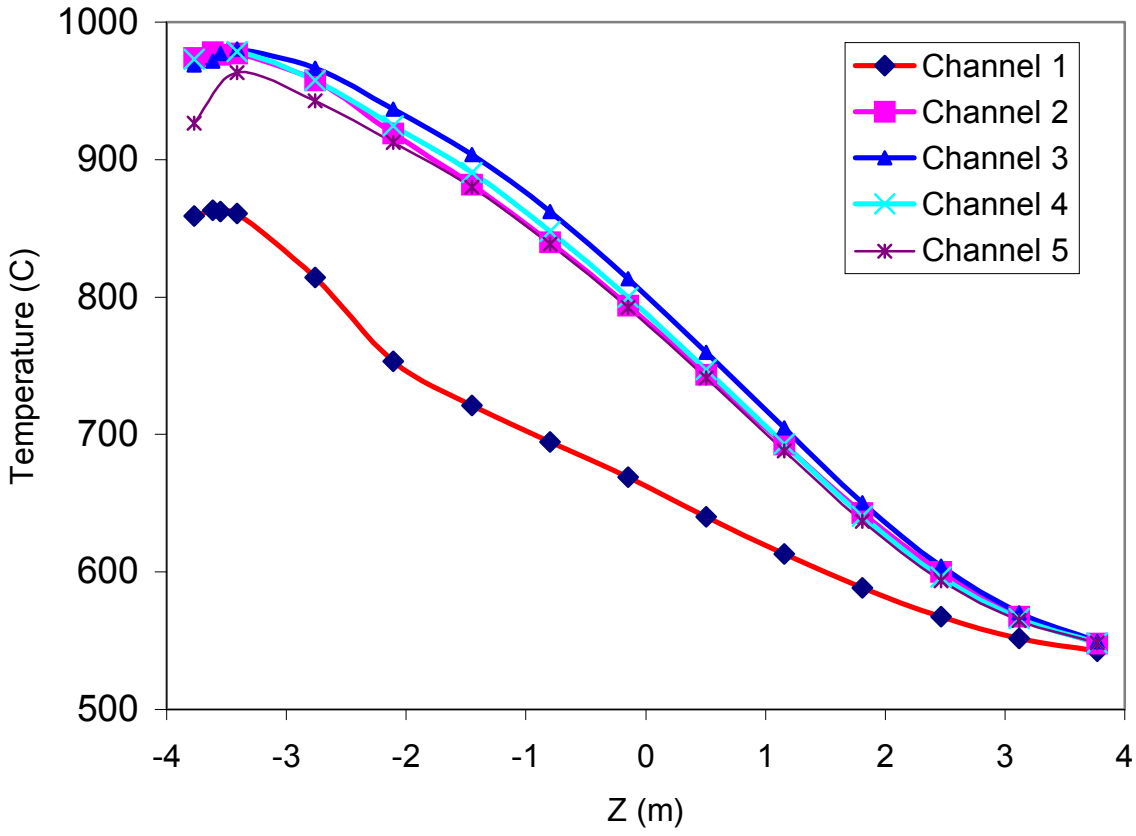

Figure 2-3 Initial Temperature of the Channels [5]

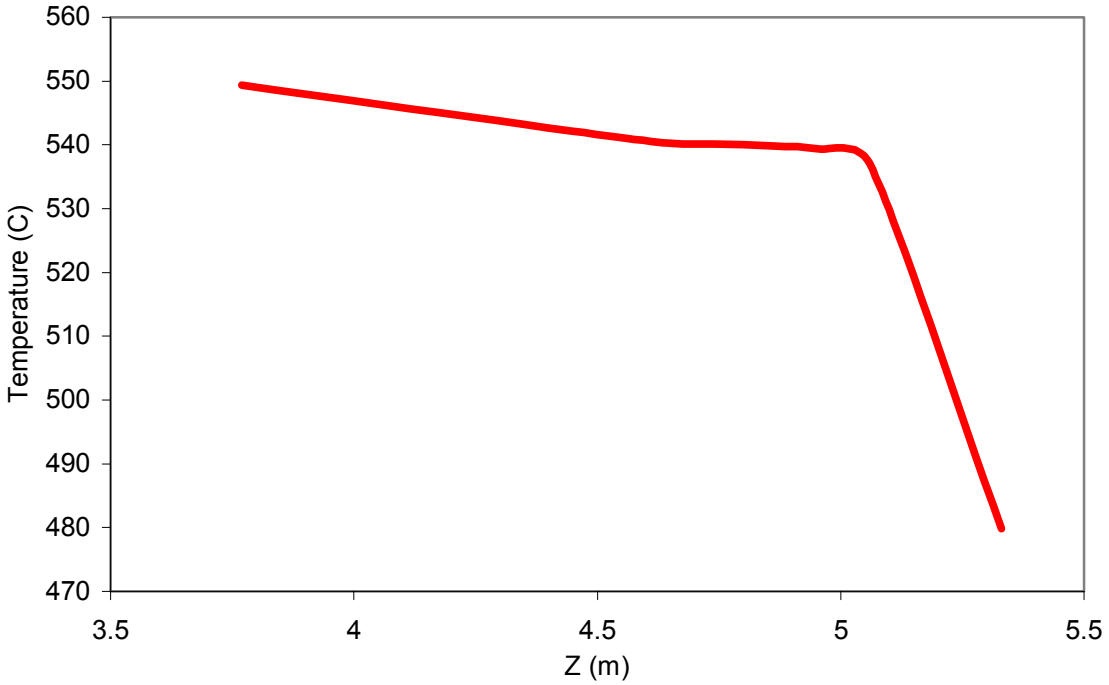

Figure 2-4 Initial Temperature of the Top Reflector [5]

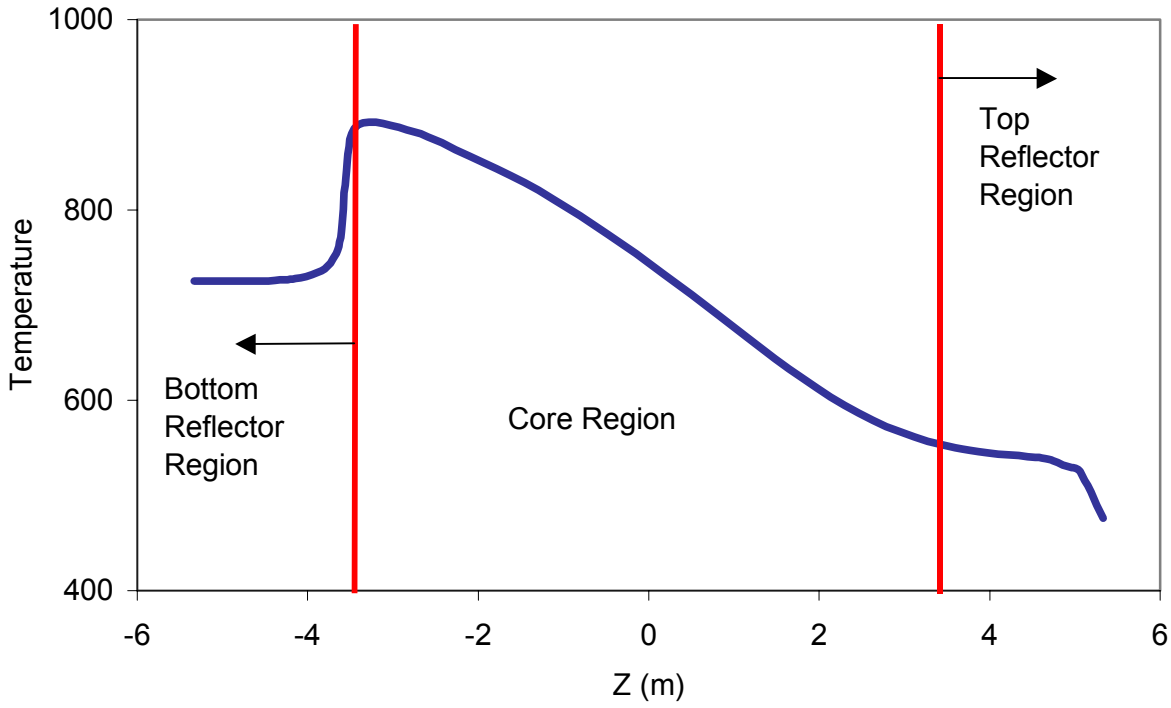

Figure 2-5 Initial Temperature of the Side Reflector [5]

2.3.5. Decay Heat Generation

After reactor shutdown, fission power induced by delayed neutrons subsides rapidly, and thereafter the heat released by radioactive decay of fission products dominates the reactor power. The decay heat depends primarily on the operating history of the reactor, including the reactor power level prior to shutdown, and on the duration of the shutdown period. The following empirical formula from KFA [6] is used to approximate the power released by radioactive decay:

$$Q_{DH}(t_0,t_s)=Q_T A(t_s^{-a}-(t_0+t_s)^{-a}) \qquad \text{Eq. 2-2}$$

where

Q_T = reactor power prior to shutdown,

t_s = reactor shutdown time,

t_0 = reactor operating time, and

A and a are constants given for different time intervals in Table 2-3.

Time Intervals (seconds)	A	a
$10^{-1}< t_s<10^{1}$	0.0603	0.0639
$10^{1}<t_s<1.5*10^{2}$	0.0766	0.181
$1.5*10^{2}<t_s<4.0*10^{6}$	0.130	0.283
$4.0*10^{6}<t_s<2.0*10^{8}$	0.266	0.335

Table 2-3: Constants A and a in Eq. 2-2

The decay heat curve using this formula is shown in Figure 2-6.

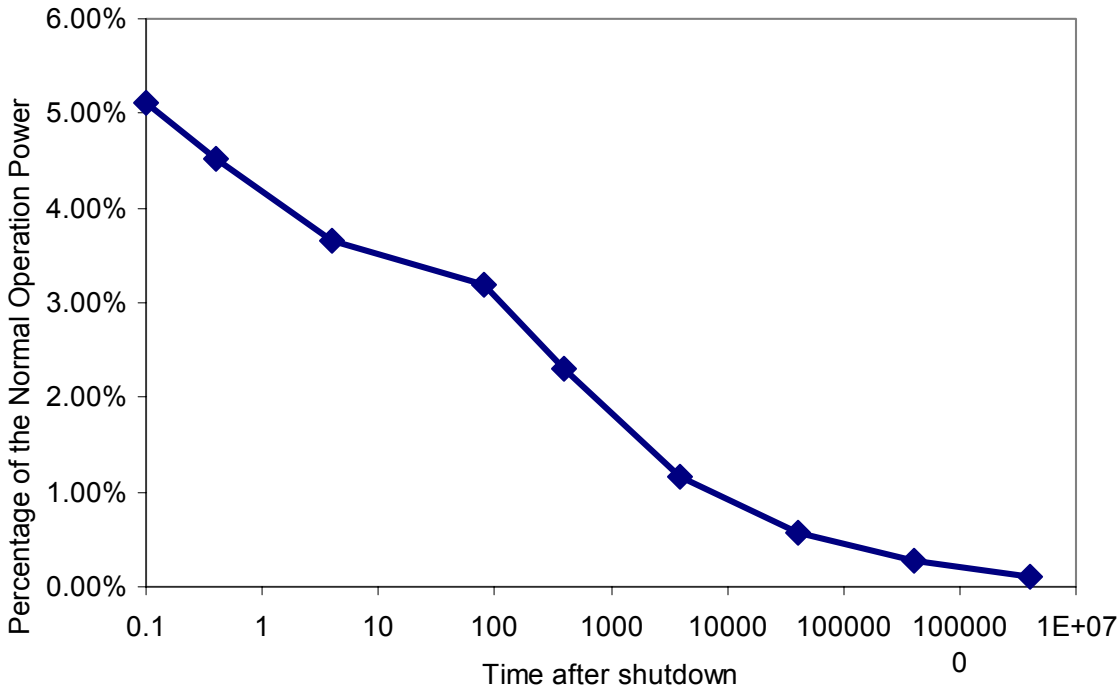

Figure 2-6: Decay Heat

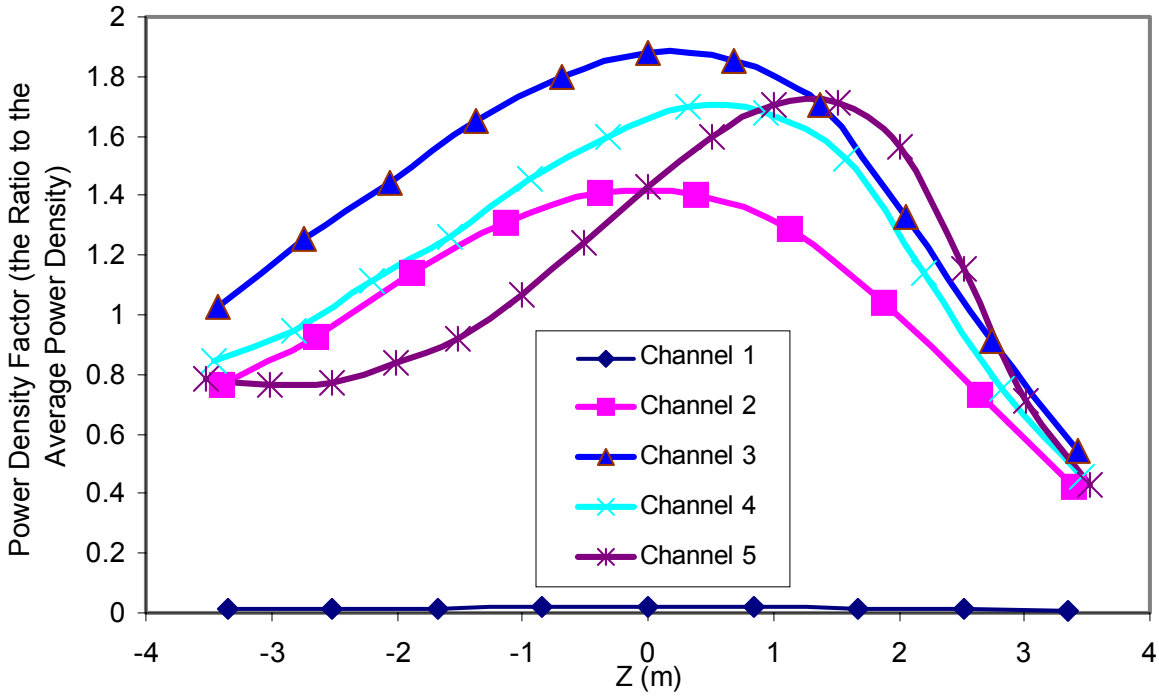

Figure 2-7: Power Density for the 5 Channels [5]

2.3.6. Material Properties

The Pebbles

Heat transfer in the core involves both thermal conduction through fuel elements and radiation through the voids between pebbles. The inner reflector is made of graphite pebbles that have the same geometry as the pure fuel pebbles. Here, we ignore the heat convection between helium and fuel pebbles. The density of the pebble bed region is 729.5 kg/m^3 [6]. General Electric developed a correlation for the calculation of the pebble bed thermal conductivity which depends only on core temperature and is given by [6] and shown in Figure 2-8:

$$K(T) = 1.1536*10^{-4}(T-173.16)^{1.6622} \quad \text{Eq. 2-3}$$

The specific capacity ($\rho_{ij}C_{pij}$) can be determined by the correlation given by [6]:

$$\rho_{ij}C_{pij}(T_{ij})=1.75(1-\varepsilon)[0.645+3.14((T_{ij}-T_0)/1000)-2.809((T_{ij}-T_0)/1000)^2+0.959((T_{ij}-T_0)/1000)^3] \quad \text{Eq. 2-4}$$

Where

ε = Void fraction of the pebble bed,

T_{ij} = Nodal temperature, K,

T_0 = 273.16K,

$\rho_{ij}C_{pij}$ = nodal heat capacity density, J/K-CM^3.

The void fraction of the pebble bed could be calculated using the following formula[23]:

$$\varepsilon = 0.78/[(D/d)^2]+0.375 \quad \text{Eq. 2-5}$$

Where,

D: The diameter of the vessel,

d: The diameters of the pebbles.

For the PBMR, the diameter of the reactor vessel is 3.5 meters, and the diameter of the pebble is 0.06 meter. Thus, the average void fraction (porosity) is ~0.375.

The Graphite Reflectors [6]

The density of the side reflector is 1394.8 kg/m^3. The conductivity of graphite depends on temperature, and it is shown in the Figure 2-8. The Specific Heat of graphite is shown in Figure 2-10.

The Helium Gap

The density and conductivity of Helium depends on temperature, and it is given in theFigure 2-7 and Figure 2-8, respectively. Its' Specific Heat is a constant-5193.0 J/kg.°C[6].

The Pressure Vessel - 2-1/4 Cr-Mo Steel

The density of the 2-1/4 Cr-Mo Steel used as the reactor material is assumed to be constant at 7833.35 kg/m^3[6]. The thermal conductivity of the vessel as a function of temperature is computed by the following formula[6]:

$$K_{2\text{-}1/4Cr\text{-}Mo}(T)=49.341695-0.017228.T \qquad \text{Eq. 2-6}$$

Where

T, Vessel temperature in (K)

$K_{2\text{-}1/4Cr\text{-}Mo}$, the thermal conductivity in (W/m-K)

The Specific Heat of the vessel as a function of temperature is computed by the following formula [6] (shown in Figure 2-10):

$$Cp_{2\text{-}1/4Cr\text{-}Mo}(T)=380.962+0.535104*T-6.10413*10^{-4}*T^2+3.02469*10^{-7}*T^3$$

Eq. 2-7

The emissivity of the pressure vessel is a constant, 0.73[8].

The Air [7]

The density, thermal conductivity and specific heat of the air as a function of temperature are shown in Figure 2-8, Figure 2-9 and Figure 2-10.

The Concrete Wall

Assume the thermal conductivity, density and specific heat of the concrete wall as a function of temperatures are constant at 0.79 w/m.°C, 1930.0 kg/m^3, 880.0 J/kg.°C, respectively[6]. The emissivity of the concrete wall is a constant, 0.7[8].

The Soil

Assume the thermal conductivity, density and specific heat of the concrete wall as a function of temperatures are constant at 0.83 w/m.°C, 1900.0 kg/m^3, 1500 J/kg.°C, respectively[6].

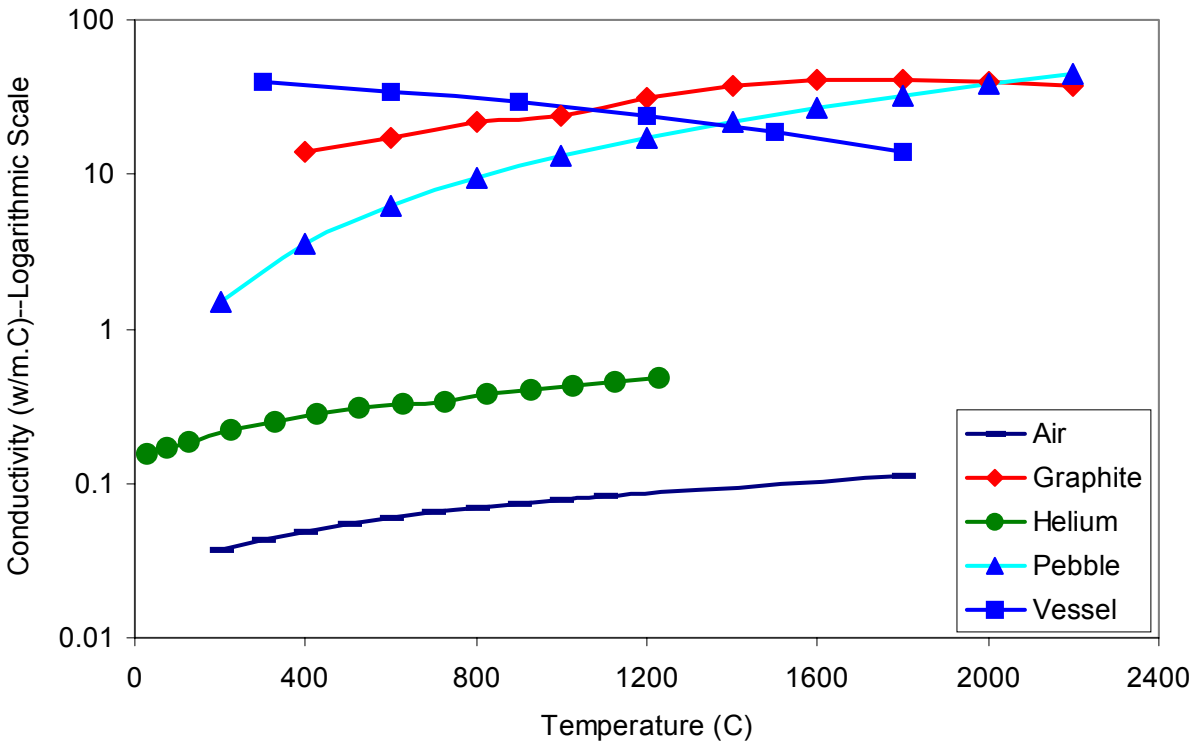

Figure 2-8: Conductivities of Air, Graphite Reflector, Helium, Pebble and Vessel

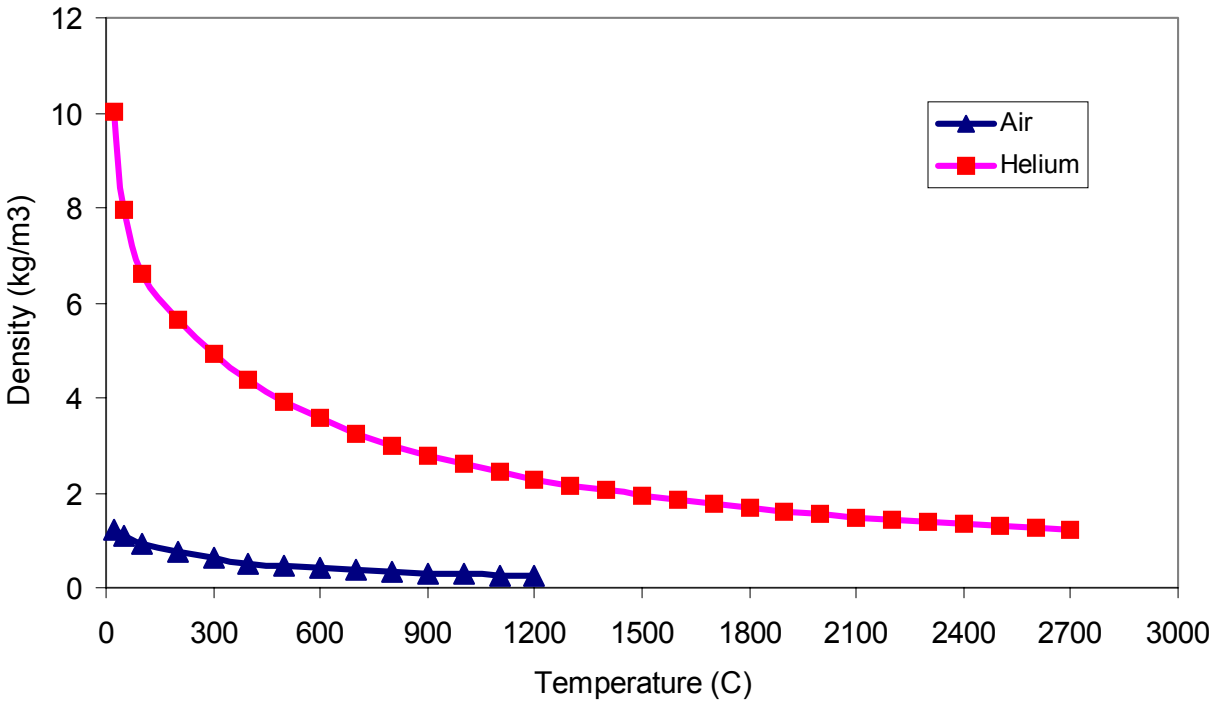

Figure 2-9: Density of Air and Helium

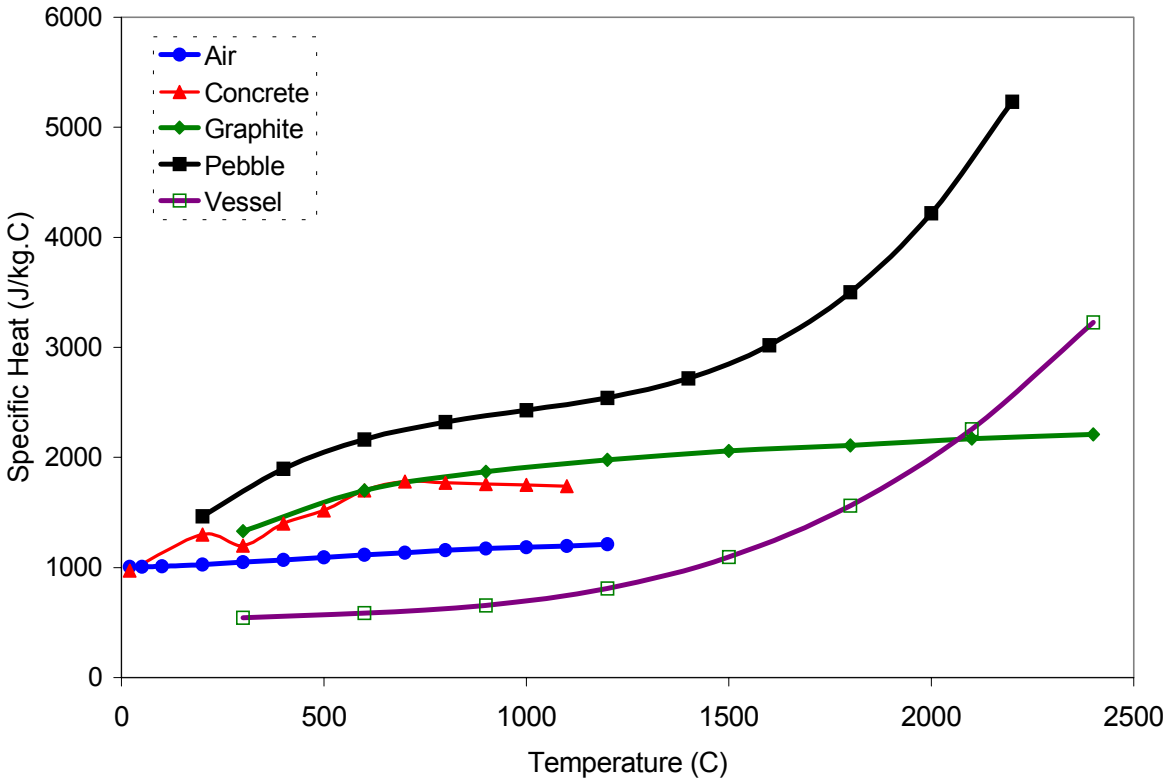

Figure 2-10: Specific Heat of Air, Concrete,
Graphite Reflector, Pebbles and Pressure Vessel

2.4. Analysis and Results

According to the format requirements of HEATING-7, The data blocks were written for the LOCA analysis. The input files are in Appendix 1 and the CD attached. The geometry, material thermal properties (density, thermal conductivity, specific heat and emissivity), and the decay heat were defined as functions of position and time using tables in the data block. The initial time step is 1 second, and the following time steps were increased or decreased by a factor of 1.1 based on the current convergence speed. In every time step, the temperature distribution, the decay heat and thermal properties as functions of time and local temperature was updated for the following heat transfer calculation, The temperature distributions for specific time were saved in the output file. Before the running of HEATING-7, initial time, maximum running time for the problem, time step and convergence criteria were also defined in the first data block. It takes about half hour to run the benchmark calculation, and an output file (shown in CD) is generated, which shows the node maps and the temperature distribution for concerned.

In this analysis, three hot points were identified – the hot points for the core, the pressure vessel and the concrete wall respectively. Figure 2-12 shows the results of the benchmark calculation. The maximum core hot-point temperature is calculated to be 1642 °C in the 92nd hours after the initial loss of coolant, and after that, the hot-point temperature goes down slowly. The slow cooling-down phenomenon is because that the heat transfer resistance between the heat source (core) and the ultimate heat sink (soil) grows with the progress of the heat transfer although the decay heat goes down rapidly.

The hot-point lies in the Channel 2 (shown in Figure 2-2), not in the central channel - Channel 1 since there are no fuel pebble in the central channel. In the normal operation, due to the helium flows from the top to the bottom, the bottom part of the core has a higher temperature. This temperature distribution is also the initial temperature condition. In this model, a constant temperature boundary is set up for the heat transfer above the ground, which is a more effective mechanism heat transfer than the heat transfer to the bottom soil only by conductivity. Therefore, the hot point is not stationary. It moves slowly from the bottom to the center height of the core.

Figure 2-13 Shows the temperature profile on the 73rd day from the reactor to the soil. The lower soil and concrete conductivity dominates the heat transfer in which most of the temperature drop occurs in the soil and the concrete wall. Consequently, there is not much of a temperature difference between the core, pressure vessel and the inner side of the concrete wall.

This analysis indicates that no fuel melting will occur under the conservative assumption of no convective core cooling – the melting temperature of UO_2 fuel is 2700 °C, which is 1000 °C above the calculated peak core temperature. Although the decay heat goes down with time, the core hot-point temperature stays above 1400 °C for the first 3 months. This result demonstrates the exceptional safety characteristics of the PBMR.

The calculation also indicates that the hot points in the pressure vessel and the concrete wall will reach their peak values at 1311 °C and 1306 °C, respectively, in 1680 hours (about 73 days) after the shutdown of the reactor. The peak temperature of the pressure vessel and the concrete wall are only about 5-20 °C apart because of very low thermal resistance resulting from large radiation transport between the reactor vessel and the concrete wall at such as high temperatures while the thermal resistance of the soil is very high. This is due to the lower thermal resistance of the reactor cavity compared with the thermal resistance of the soil and the concrete wall. The effective heat transfer distance in the soil is only about 3 meters even 73 days later. Therefore, most of the decay heat will accumulate in this small volume, which leads to the higher temperature inside the cavity.

2.5. Sensitivity Study

The MPBR program is still in the conceptual design stage: Many key parameters have not been established. Based on engineering experience and theoretical estimation, the crucial parameters that affect the temperature field were identified and a sensitivity analysis was performed. The sensitivity analyses were performed on: the emissivity of the vessel and the concrete wall, the decay heat, the conductance of the concrete wall and the soil. Since the concrete wall and the

reactor vessel have the about same hot-point temperature, the figures in the sensitivity study only show the temperature curves for concrete wall.

2.5.1. Peak Temperature Sensitivities to the Emissivities of the Vessel and the Concrete Wall

Reference [8] indicates that the emissivity of the reactor vessel is 0.73 and the average emissivity of the concrete wall is 0.7. Therefore, in the emissivity sensitivity analysis, Two extreme scenarios are studied: the concrete wall and reactor vessel with the lowest emissivity 0.01 and both with the highest emissivity 1. The best estimate emissivity value used in the analysis is 0.73.

For the case with lowest emissivity, the hot-point temperature of the core is higher than the benchmark, and always above 1600°C after the peak value in the first 3 months (Shown in Figure 2-14). Moreover, due to the isolation function by the lower emissivities, most of the heat will be deposited inside of the vessel at the beginning, so the concrete wall has a lower temperature in the first 900 hrs. 900 hours later, the soil becomes the main heat sink instead of the core region, and most of the temperature drop will be in the soil. Consequently, the concrete will have a higher hot point peak temperature (about 1400°C) than the benchmark (1307°C) due to the higher thermal resistance from the emissivities. But there is no obvious shift of the temperature curve between the case with emissivity of 1.0 and the case with emissivity of 0.73(benchmark calculation). Thus, emissivity does not appear to be a critical factor in peak core temperature.

2.5.2. Peak Temperature Sensitivities to the Conductivity of the Soil and the Concrete Wall

In the sensitivity analysis on the conductivity of soil and concrete wall, the conductivity of the soil and concrete wall were adjusted at the same time. In Figure 2-15, we can see a surprising result: even if the soil has the conductivity of the Mercury (the conductivity of mercury is 10.3w/m.°C at 200°C, and will increase for the higher temperature), there is almost no change of

the core peak temperature. Although the peak temperatures of concrete wall and pressure vessel decrease dramatically, they are still at 535 °C, which is higher than their safety limitations. The safety limitations for the vessel and concrete wall are 482 °C and 177 °C, respectively. Thus, while the unproved conductivities of the soil and concrete wall will help reduce the peak temperature of the concrete wall and pressure vessel, the peak core temperature is unaffected.

2.6. Independent Verification Using PBR_SIM

As an independent confirmatory check, calculations were performed by Hee Cheon No to benchmark the HEATING-7 results [10]. Dr. Hee Cheon No independently developed the PBR_SIM (Pebble Bed Reactor_SIMulation). Following is a brief description of his model [10]:

a. Nodal scheme in primary system:

- 12 axial divisions: 10 core nodes, 1 lower reflector, 1 upper reflector, top reactor vessel and containment, bottom reactor vessel, containment, and soil.
- 20 radial divisions: 5 pebble and divisions, 1 outer reflector, 1 core barrel node, 1 reactor vessel, 1 air gap, 3 concrete and 8 soil divisions.

b. Heat transport scheme in primary system (Shown in Figure 2-11):

- Core nodes: radial and axial conduction + radiation, axial convection from the top to the bottom
- Air gap region: axial convection from the bottom to the top, the wall convective heat transfer by combination of both air natural convection and forced convection
- He gap regions between the core barrel and the inner surface of the reactor vessel, and between the outer surface of the reflectors to the inner surface of the reactor vessel: radial radiation transport between solid walls.
- Other solids: radial conduction heat transfer
- Easy adoption of realistic boundary condition with constant temperature on 25 m from the center of the core or of constant temperature boundary conditions of the

concrete, the soil, and the reactor vessel provided by the active/passive concrete cooling system and the He cooling system.

c. Main assumptions involved in models in primary system

- Constant temperatures of structures and air above the top containment
- Averaged temperatures in the top and bottom reactor vessel and containment
- No radial convective mixing in the gas region

d. Capability of the Code

- Core thermal-hydraulic dynamic analysis for system control
- Core thermal-hydraulic analysis in operational transients and depressurization accident
- Analysis for passive or active concrete cooling system or decay heat residual cooling system.

Dr. No's summary conclusions are shown on Figure 2-16. The benchmark case (0 m/s coolant velocity) agrees well with HEATING-7 prediction assuming no convective cooling. His calculation indicates that the fuel temperature reaches a maximum one of 1679 °C at 108 hours (the fuel peak temperature is 1642 °C at 92 hours). In addition, PBR-SIM has the capability to model convective cooling in the reactor cavity to determine the flow velocity necessary to keep the hot-point temperatures below their safety limit PBR_SIM calculations indicate that with a convective coolant flow in the reactor cavity of approximately 6 meters per second, the concrete peak temperatures can be maintained within allowable limits, but the reactor vessel temperatures are still above the allowable range. Moreover, there is no significant temperature drop of the core hot-point temperature with the coolant velocities of 2m/s, 4m/s and 6m/s. This suggests that some form of convection cooling is required to maintain the reactor vessel and reactor cavity concrete within design limits.

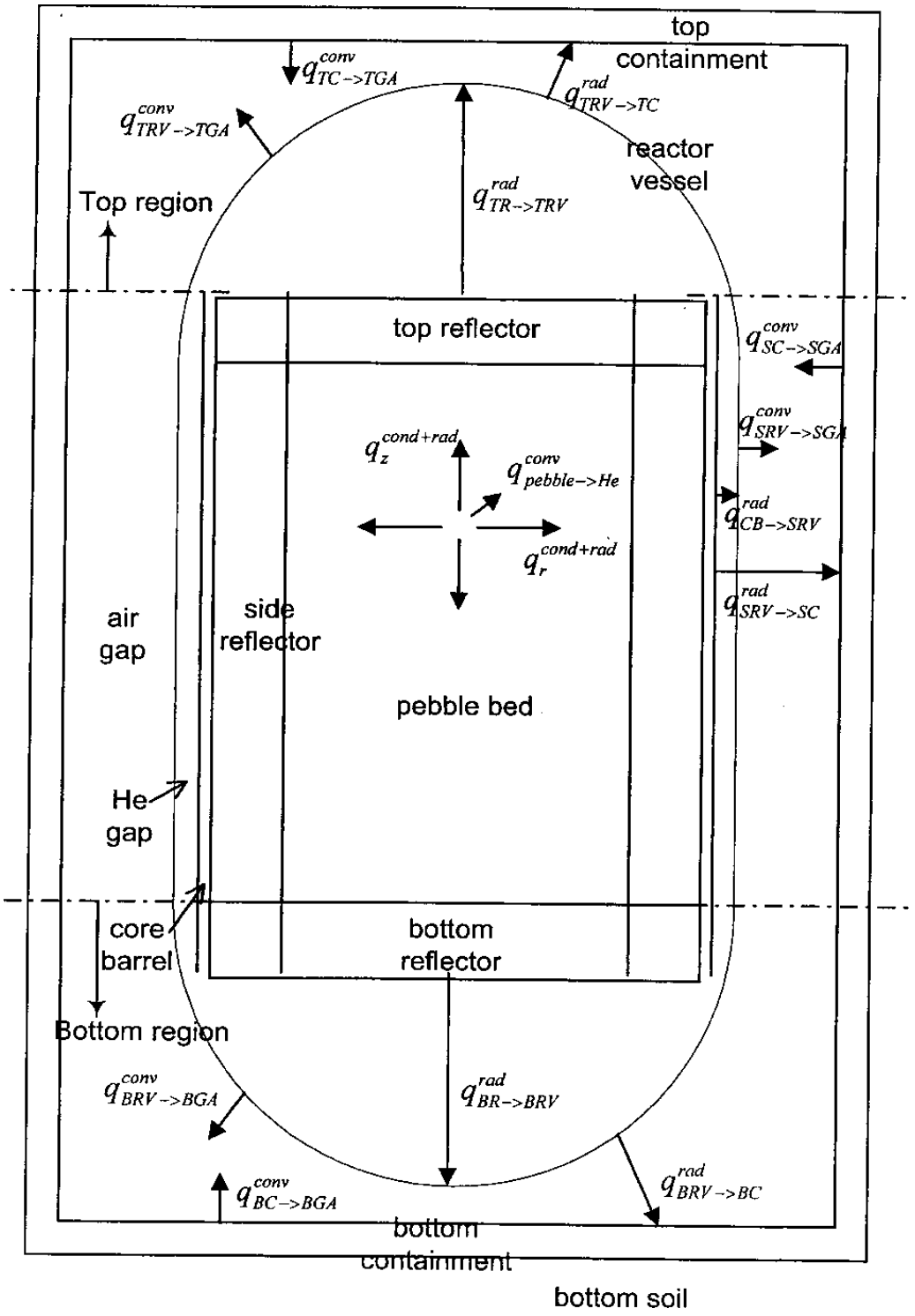

Figure 2-11: Calculation Domain and Hat Transport Mechanisms Involved in Each Region [10]

2.7. Conclusions

From the benchmark, sensitivity study and Dr. No's independent verification, the following critical conclusions are reached:

- No meltdown occurs

The power density of the PBMR is low, 3.54MW/m^3, and there is huge volume of graphite with high specific heat, including the graphite pebble and graphite reflectors in the pressure vessel. In first several days with higher decay heat generation, the graphite absorbs most of the heat. Therefore, even under the extreme conservative assumptions, the hot-point temperature of the core is only 1642 °C much lower than the fuel melting point.

- Changes in reactor vessel emissivity do not change peak fuel temperature.
- Increases in conductivity in the concrete and soil do not change peak fuel temperature, but do decrease peak reactor vessel and concrete wall temperature.
- The temperatures of the concrete wall and the steel pressure vessel are above their safety limit.
- The heat transfer resistance in soil and concrete wall becomes the dominant factor in the LOCA.
- Means need to be found to increase the heat transfer to the ultimate heat sink (soil or air).

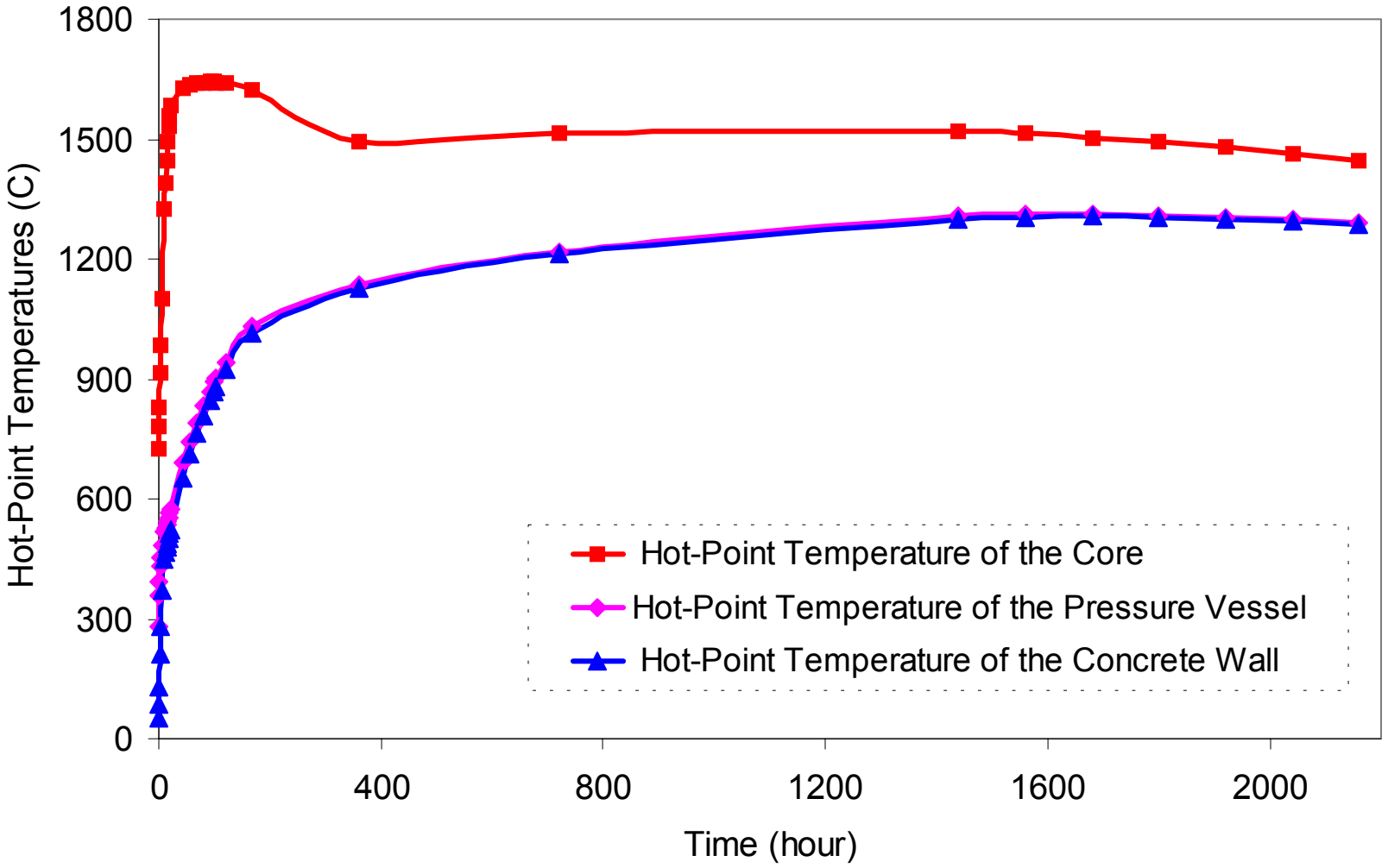

Figure 2-12: Hot-point Temperatures for LOCA

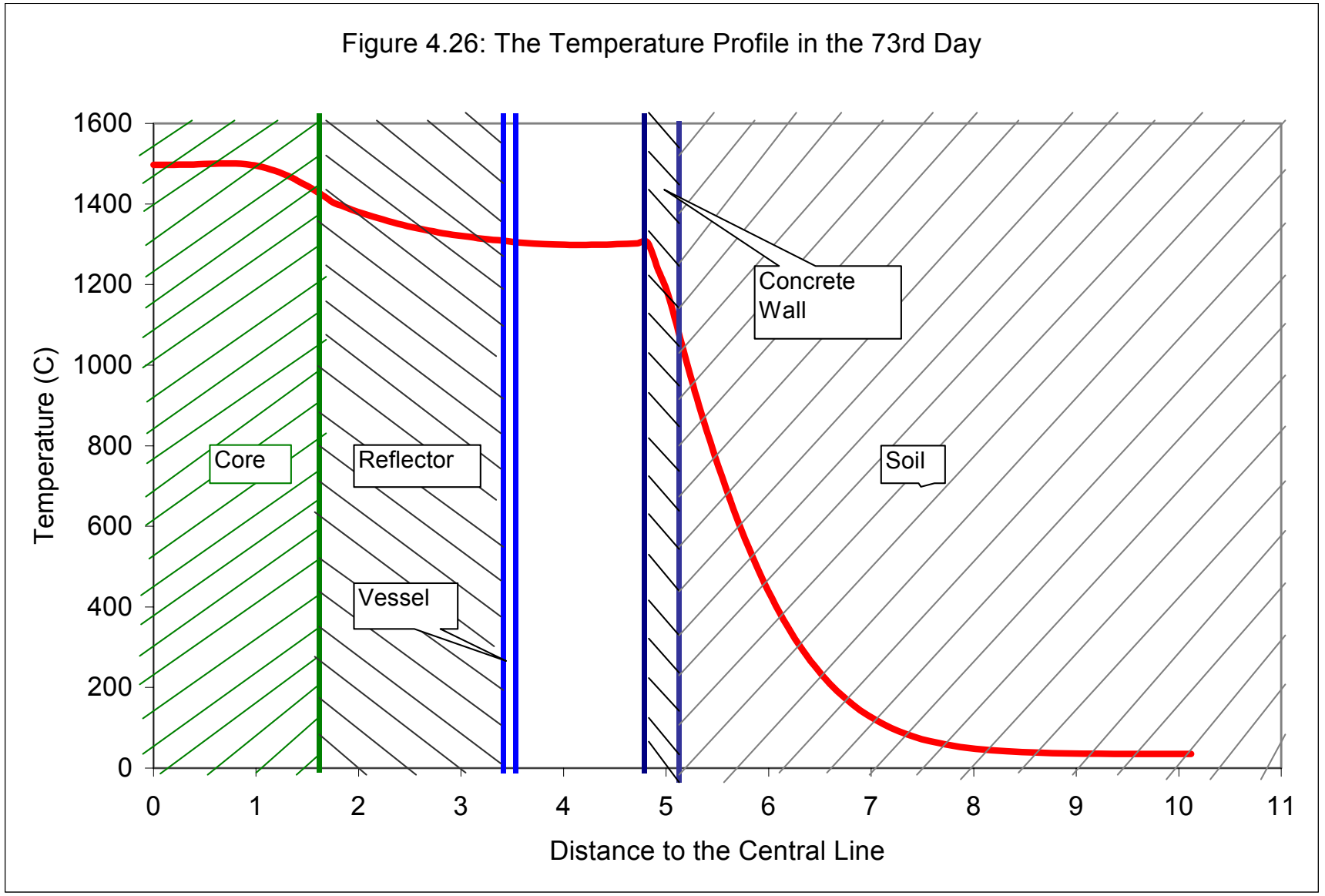

Figure 2-13: The Temperature Profile on the 73rd Day in LOCA Analysis

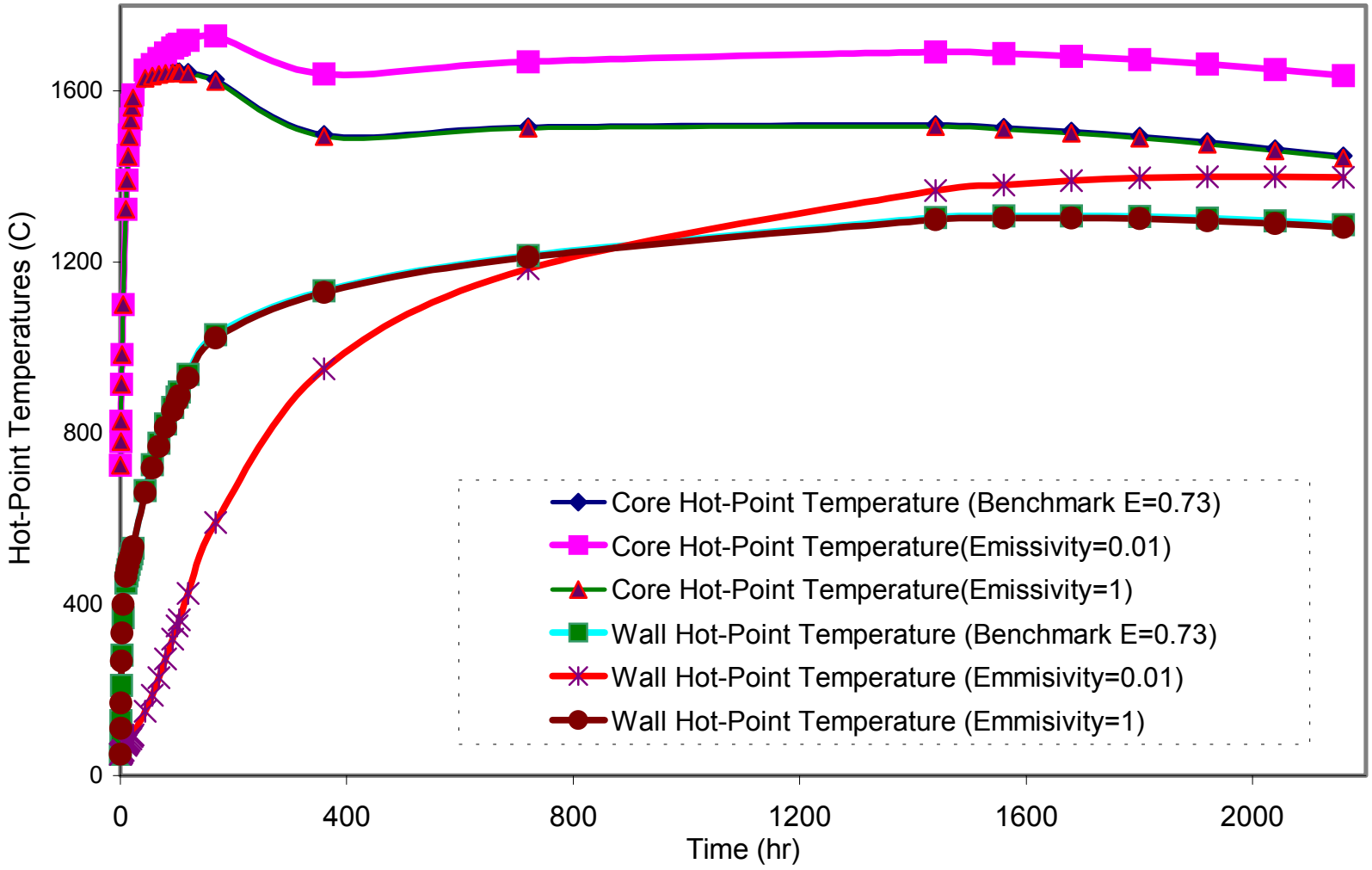

Figure 2-14: Hot-point Temperature Sensitivity to Emissivities of Vessel and Concrete Wall in the LOCA Analysis

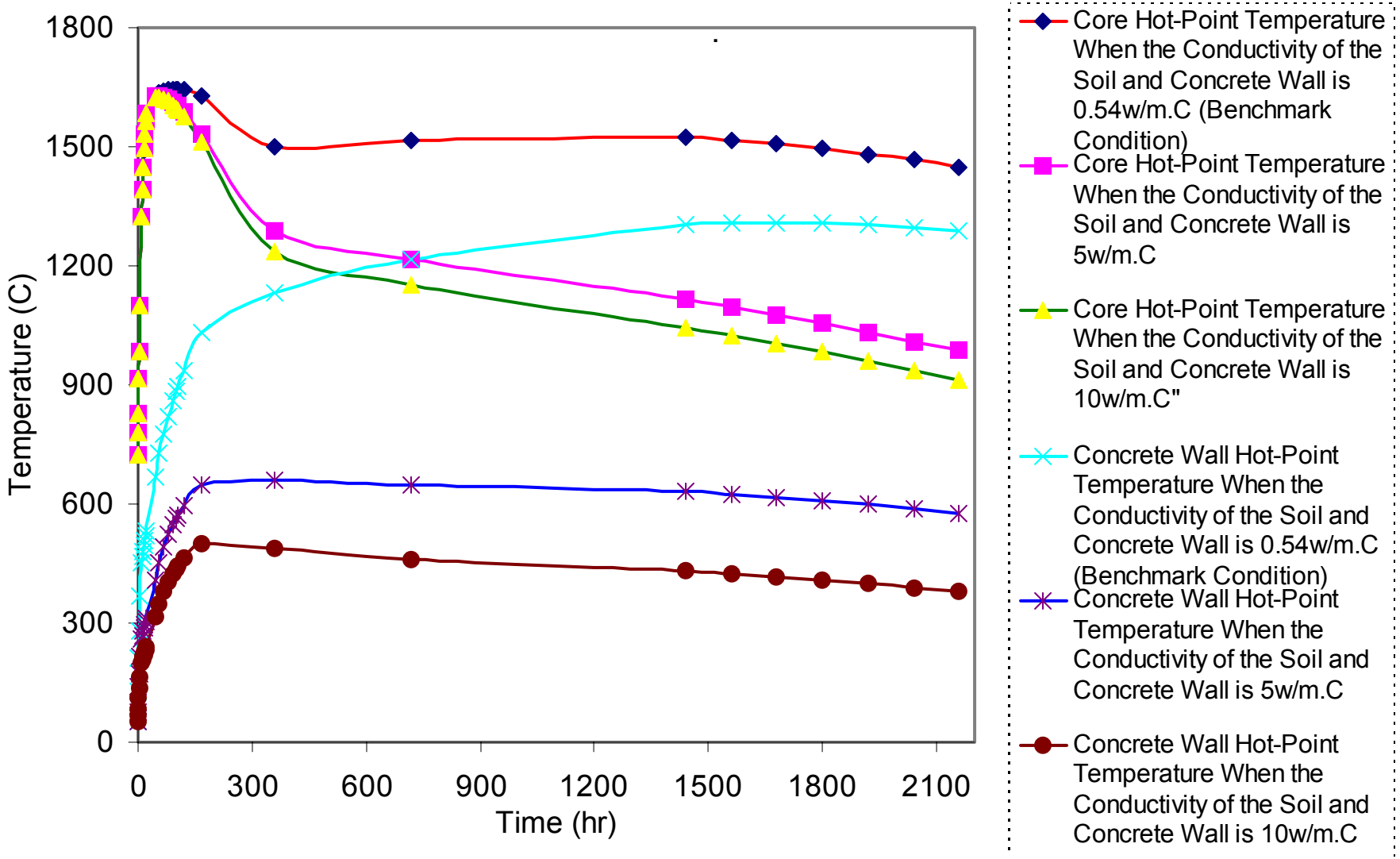

Figure 2-15: Hot-point Temperature Sensitivity to the Conductivity of Soil and Concrete Wall in the LOCA Analysis

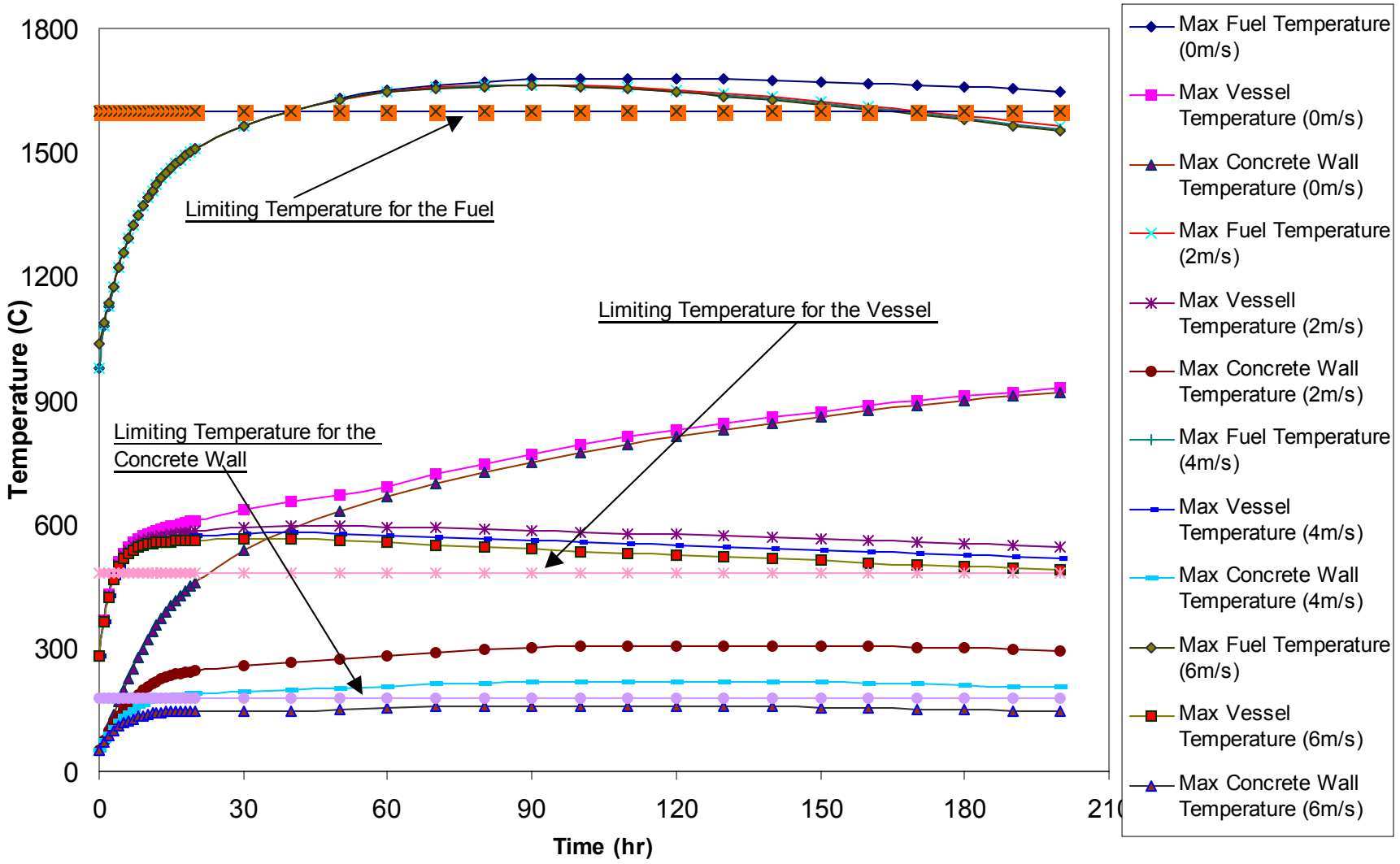

Figure 2-16: Trends of Maximum Temperature for 0, 2,4,6 m/s of Air Velocity in the Air Gap Region

3. The Air Ingress Accident

3.1. Introduction

In the LOCA study discussed above, no chemical reactions were assumed to occur. If the air enters the reactor, as it will after the depressurization, air will react chemically with graphite in the reflector and the pebbles. The air ingress accident is another accident sequence that must be analyzed for pebble-bed and prismatic high temperature gas reactors.

Massive ingress of air into the core of a PBMR is among the accidents with a low occurrence frequency but possibly severe consequences. The likelihood of a large air ingress accident is very low largely because of the nature of the vessels in the primary system and the relatively small piping penetrations, 0.06-0.57 meter in diameters [16]. For direct cycle reactors such as the South African pebble bed reactor and the General Atomics prismatic high temperature gas reactor designs, the plant consists of several large vessels connected by another large vessel containing the hot and cold leg piping. For the indirect cycle plant design such as the MIT pebble bed reactor, the inlet and outlet piping is contained in an outer pipe, which carries high temperature helium gas to an intermediate heat exchanger.

There are gaps in the detailed understanding of air ingress accident progression. While experiments have been done in the past, none have been conclusive regarding the potential for burning of graphite in actual reactor conditions. For the hypothetical accident study of a complete rupture of the coaxial hot gas duct, an experimental apparatus named NACOK (**Na**turzug im **Co**re mit **K**orrosion) in KFA (Jülich Research Center, Germany), and another in JAERI (Japan Atomic Energy Research Institute) had been set up to study the ingress of air into the core as a result of natural circulation. Some initial experimental and theoretical studies have been done to investigate the air ingress phenomena and develop the passive safety technology for dealing with air ingress and graphite corrosion. Although the HTGR in JAERI has a prismatic core structure, which is

different from that of MPBR, the research on this reactor has provided an additional source of information for understanding the fundamental phenomenon for all such high temperature graphite reactors.

Except for some theoretical studies on the physical processes, a sufficiently detailed and realistic study could not be found for this challenging problem in which many complicated phenomena are involved, such as mass transfer, chemical reactions, and heat transfer by conduction, natural convection and radiation. Most of the analysis on real reactors, Fort. St. Vrain, HTR-10 in China and the proposed pebble bed plant in South Africa, the analysis assumes gross corrosion properties for graphite and a limited supply of air available to assess how much graphite is consumed. Once all the air contained in the reactor cavity is consumed, the accident is assumed to be terminated. This analysis typically shows a limited quantity of graphite consumed which is confined to the graphite lower reflector, limited temperature rise in the fuel which is still below the peak temperatures allowable and no fuel interaction with the oxygen since essentially all the oxygen is consumed in the lower reflector. This work is intended to contribute towards improving the understanding of processes taking place during air ingress accidents. The objective of this aspect of the thesis will be to develop a fundamental understanding of key air ingress variables leading to the development of a model to analyze the consequences of the event.

Therefore, the key questions for the air ingress analysis are:

- What are the dominant factors for this accident?
- How long is the diffusion period? (time before massive air ingress)
- What is the oxidation rate of the graphite in the different regions?

In order to develop such detailed understanding, a Computational Fluid Dynamics (CFD) computer code is employed to model the complex fluid dynamics and chemical processes in such an event. The code chosen for this analysis is, it is important to benchmark the FLUENT 6 code[17][18] which has recently been upgraded to handle such chemical

reactions. The challenge of this aspect of the thesis is to develop a benchmarked capability to model the fundamental processes underway using FLUENT 6.0.

There are two series of experiments that have been conducted on air ingress which have been published:

The first is done in Japan by JAERI in which a series of three experiments were conducted in sequential order to develop a fundamental understanding of the three key phenomenon [11] [12] [13]:

a. Pure diffusion in an isothermal environment,
b. Diffusion and the natural convection in a thermal environment,
c. Diffusion, natural convection and chemical reactions in a thermal. These experiments were intended to simulate the environment in prismatic reactors.

The second series of air ingress tests were conducted in Germany at the Juelich Research Center. These tests were performed at the NACOK facility [14]. There were two tests conducted and a third planned. These tests were conducted in a much larger facility simulating the performance of pebble bed reactors. The first test, which is a natural circulation test, will be benchmarked in this thesis [15].

3.2. Air Ingress Accident Progression

Figure 3-1 shows the air flow in an air ingress accident. Generally, the air ingress accident can be divided into three major stages[19]:

Stage 1 is defined as the depressurization state during LOCA shown in Figure 3-2. In stage 2, helium gas remains in the reactor vessel under essentially atmospheric conditions as shown in Figure 3-3. The air/helium gas mixture in the reactor cavity has a volume concentration ratio of about 1 to 1. This means that the gas layers become stable, because helium is lighter than an air/helium gas mixture. In addition, the buoyancy force between

a high-temperature coolant passage (hot leg) and a medium-temperature passage (cold leg) in the reactor is not large enough to cause natural circulation of the gas mixture (composed of N_2, O_2, CO_2 and CO) throughout the reactor. Hence, air enters the reactor vessel mainly by molecular diffusion which is very slow process. Whatever oxygen enters the reactor, it will react with graphite components and produce CO and CO_2. In addition, the resulting gas mixture is transported by natural convection in many local spaces inside the reactor vessel. This period may last for several hours to several hundred hours depending on different break and geometry scenarios. Although the second stage may last for a long time, the total amount of air entering the reactor in this stage is very small.

As a time passes, the density of the gas mixture in the reactor increases and the buoyancy force caused by density differences between the high-temperature and medium-temperature passages also increases. Finally, because of these buoyancy forces, natural circulation of air takes place throughout the reactor which defines stage 3. That is, air enters the reactor from the breach of the inner tube of the primary pipe and passes through the high-temperature passage and medium-temperature passage. It goes out from the reactor through the breach of the outer tube of the primary pipe. Figure 3-4 shows the flow path of the air ingress event upon onset of natural circulation.

Analyses performed by the Germans, Japanese and Chinese on their reactors have shown that this accident is manageable and does not create unacceptable consequences in terms of off-site releases, due largely to the smaller size of the break assumed and the ability to stop the air ingress within several days [20].

While these assumptions are quite reasonable, this research project will focus on the development of analytical tools to address the physical phenomenon in a more realistic way to understand the behavior of the complicated interactions involved using a computational fluid dynamics code (FLUENT 6) to better predict the performance of the core during the event. It is expected that the methodology developed can be used to address the phenomenological questions that will result as part of the licensing of these

reactors in the future without the need to make conservative assumptions in analysis or to apply potentially non-conservative assumptions that lead to accident termination.

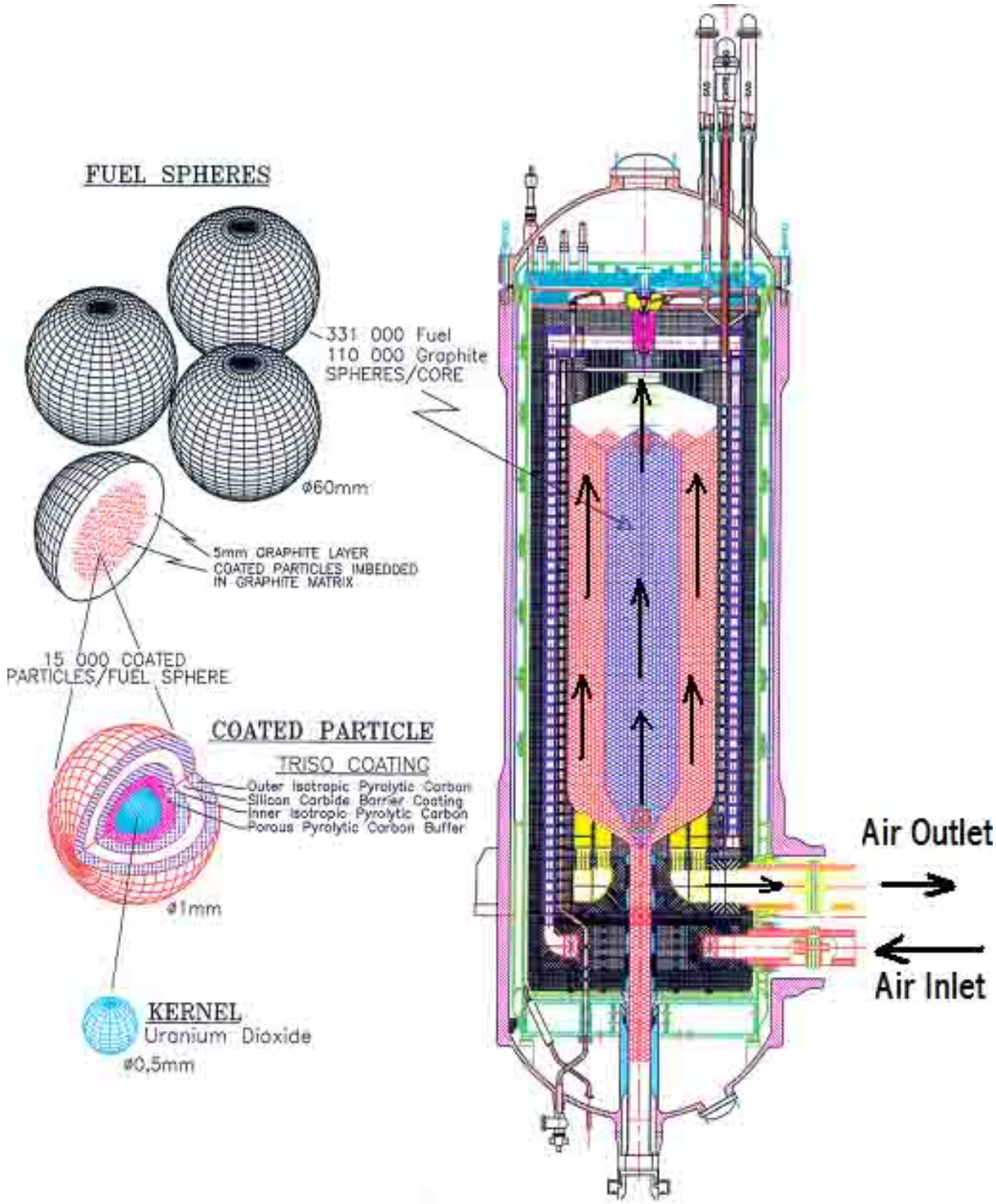

Figure 3-1: Air Flow in Air Ingress Accident [1]

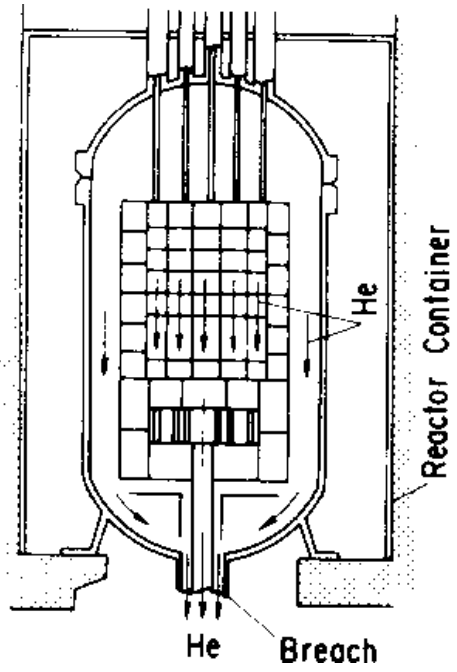

Figure 3-2: Stage 1: Depressurization [12]

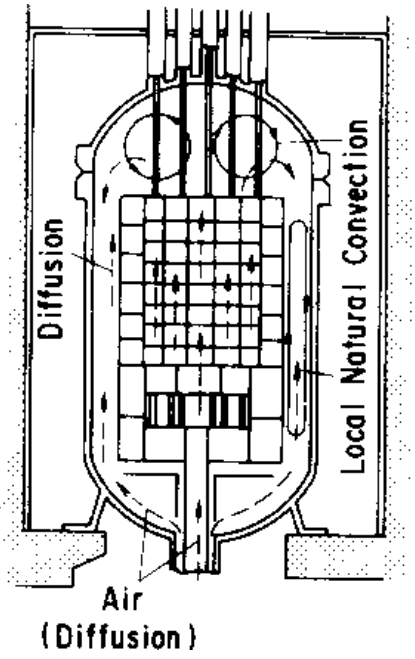

Figure 3-3: Stage 2: Molecular Diffusion [12]

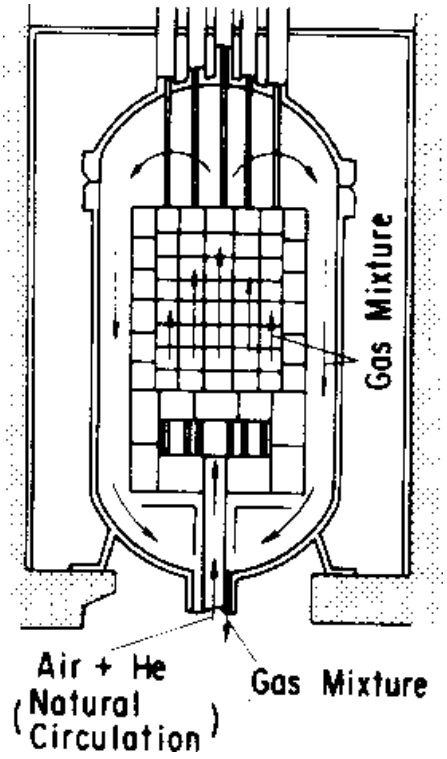

Figure 3-4: Stage 3: Natural Circulation [12]

3.3. Initial Theoretical Study

The initial theoretical study was aimed at understanding the fundamental phenomenon at work during an air ingress event. This study analyzed a simple cylinder open on the top and bottom containing a reflector on the sides and the bottom with the central region filled with pebbles to model the "chimney" effect. The HEATING 7 code was used to model the heat transfer from the reactor with simplifying assumptions that conservatively treated the expected processes. This analysis provided useful information for more detailed analysis that followed.

In this study, a scenario referred to as the "chimney effect" is assumed. Figure 3-5 illustrates the flow paths in the "chimney." Based on the former LOCA sensitivity study and the limitation of the code HEATING-7, which cannot model the chemical reactions directly, we made the following assumptions:

- The vessel is assumed to be an open-ended cylinder at both ends for initial studies.
- There is enough fresh air supply, no moisture in the air, and the inlet air temperature is 300 °C (average temperature in reactor cavity).
- The gas temperature is at all times assumed to follow the temperature of the solid structures. This is generally a good assumption because of the very slow transients and the low heat capacity of the gases.
- Did not consider the diffusion process on the pebble and reflector surface
- The initial conditions, boundary conditions, thermal properties and decay heat are same as the LOCA model.
- The only product is CO_2, which is produced immediately at the graphite surface.
- No conductive cooling due to the limitation of HEATING-7.

The air consists of only 20% (in volume) O_2 and 80% (in volume) N_2, which are considered as ideal gases. After the air enters into the vessel, all of the air will be

consumed proportional to the contact area between the oxygen and the graphite. The experiment found that the diffusion process would dominate the chemical reaction in this air ingress accident. Due to the challenge from the diffusion, very conservatively, the resistance from the diffusion was not considered in this study.

The key parameters are shown in Table 3-1.

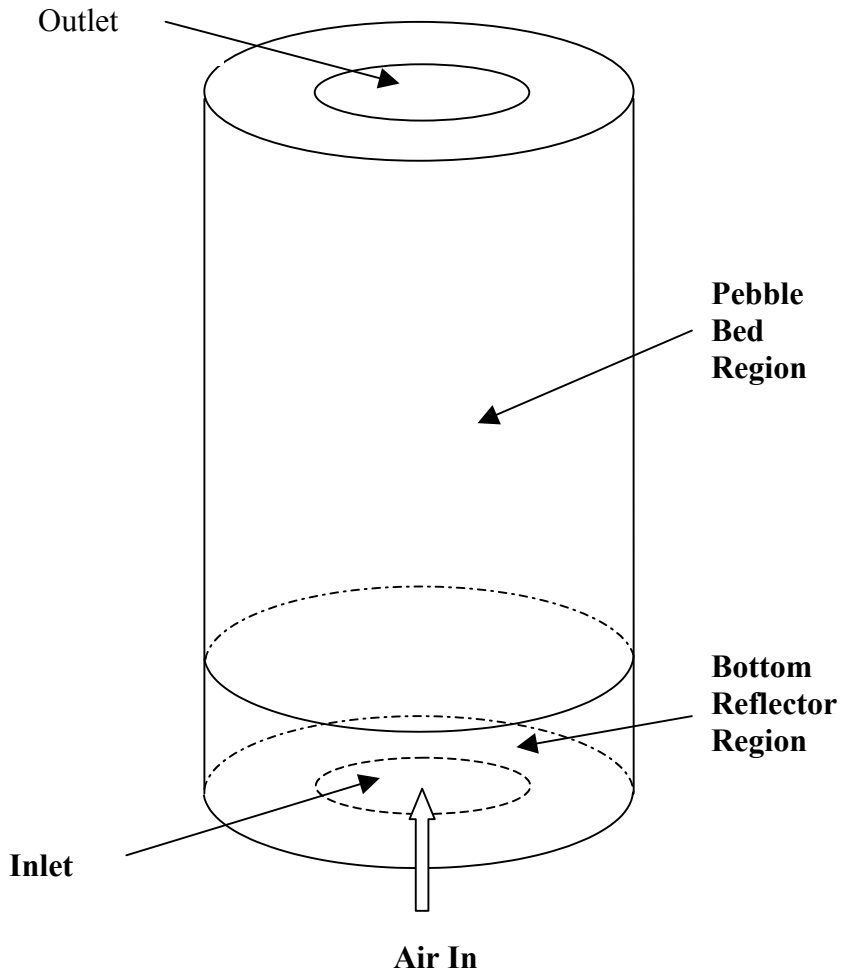

Figure 3-5: Schematic Diagram of Air Ingress Model

In the MathCad calculation, the constants used are shown in the following table:

Height of the core, H	7.54 m
Diameter of the core: D	3.5 m
Diameter of the pebbles, d	0.06 m
Gravitational acceleration, g	9.8 m/s^2
Porosity of the pebble bed, ε	0.39
Temperature of the fresh air, T_air_in	20 °C
Pressure of the atmosphere, P_atm	$1.01*10^5$ Pa

Table 3-1: The Parameter in the Theoretical Study

The thermal properties of the air, such as density, specific heat, conductivity and viscosity are obtained from [7].

3.3.1. Chemical Reactions

In contrast to its excellent thermal, mechanical and neutron physical properties, graphite possesses only a comparably low resistance to oxidizing gases. The possible chemical reactions are:

$2C + O_2 \rightarrow 2CO$ $(\Delta H = -110.52$ KJ/mole) [1] Eq. 3-1

$C + O_2 \rightarrow CO_2$ $(\Delta H = -393.51$ KJ/mole) Eq. 3-2

$C + CO_2 \leftrightarrow 2CO$ $(\Delta H = +172.47$ KJ/mole)

[1] ΔH represents the difference between the enthalpy of the system at the beginning of the reaction compared to what it is at the end of the reaction: $\Delta H = H_{final} - H_{initial}$ Thus: if the system has higher enthalpy at the end of the reaction, then it absorbed heat from the surroundings (endothermic reaction); if the system has a lower enthalpy at the end of the reaction, then it gave off heat during the reaction (exothermic reaction).Therefore: For endothermic reactions $H_{final} > H_{initial}$ and ΔH is positive ($+\Delta H$); For exothermic reactions $H_{final} < H_{initial}$ and DH is negative ($-\Delta H$) .

Eq. 3-3

$2CO + O_2 <---> 2CO_2 \quad (\Delta H = -565.98 KJ/mole)$

Eq. 3-4

The reactions may be described as occurring in four major steps. First, oxygen gas must be transported to the graphite surface. Second, the gas must diffuse into the graphite pores to the oxidation location. Third, the actual chemical reaction must occur. Last, the reaction products must diffuse out of the media to allow more oxygen to reach the graphite [9].

Reactions of oxygen with graphite will commence at temperatures higher than 400 °C. Countermeasures to stop the oxidation process are either to cool down the core below 400 °C by the main heat sink or to stop the air ingress. In the low-temperature regions (less than 600 °C), chemical reactions are slow and the time required for oxygen transport may be neglected. Oxidation is assumed to proceed uniformly throughout the graphite in this temperature region by in-pore diffusion; then the diffusion rate determines the graphite conversion rate. Boundary layer diffusion occurs at high temperatures. In general, the higher the temperature, the greater the proportion of CO formed. Above 900 °C, the products consist almost entirely of CO [21].

This is a very complicated process. Besides CO, CO_2, N_xO_x, Carbon-oxygen surface complex (Complex: a chemical association of two or more species (as ions or molecules) joined usually by weak electrostatic bonds rather than covalent bonds) is formed. For the reaction above 1000K, CO is the dominant reaction product. It proceeded through the formation of a surface oxide, C_3O_4, which formed very rapidly and then decomposed in the presence of Carbon and oxygen. At temperatures above 1100 °C the reaction favored the formation of CO. Increasing the velocity of the gases flowing over the carbon suppressed the formation of CO_2. CO_2 is the product of the secondary reaction between CO and O_2[22].

For the graphite pebbles and graphite reflector, one of the crucial issues is the graphite burning. Burning is defined as self-sustained combustion of graphite. Combustion is defined as rapid oxidation of graphite at high temperatures. Self-sustained combustion produces enough heat to maintain the reacting species at a fixed temperature or is sufficient to increase the temperature. From experiments, CO burns in air at concentrations above 12.5 and below 74 volume percent [9]. The factors needed to determine whether or not graphite can burn in air are: graphite temperature, air temperature, air flow rate (in a limited range), ratio of heat lost to the heat produced [9].

3.3.2. Calculation Procedures

Since there are no diffusion, natural convection and chemical reaction models in the code HEATING-7 code, many hand calculations were performed to include these effects aided by the code MathCad code. The key assumption made in the theoretical study is that no significant changes occur in the temperature field in several minutes due to the higher heat capacity of the graphite and the low rate of change in the heat generation from the chemical reactions and the decay heat. The calculation procedure is shown on Figure 3-6, HEATING-7 was run for every 5-minute time step.

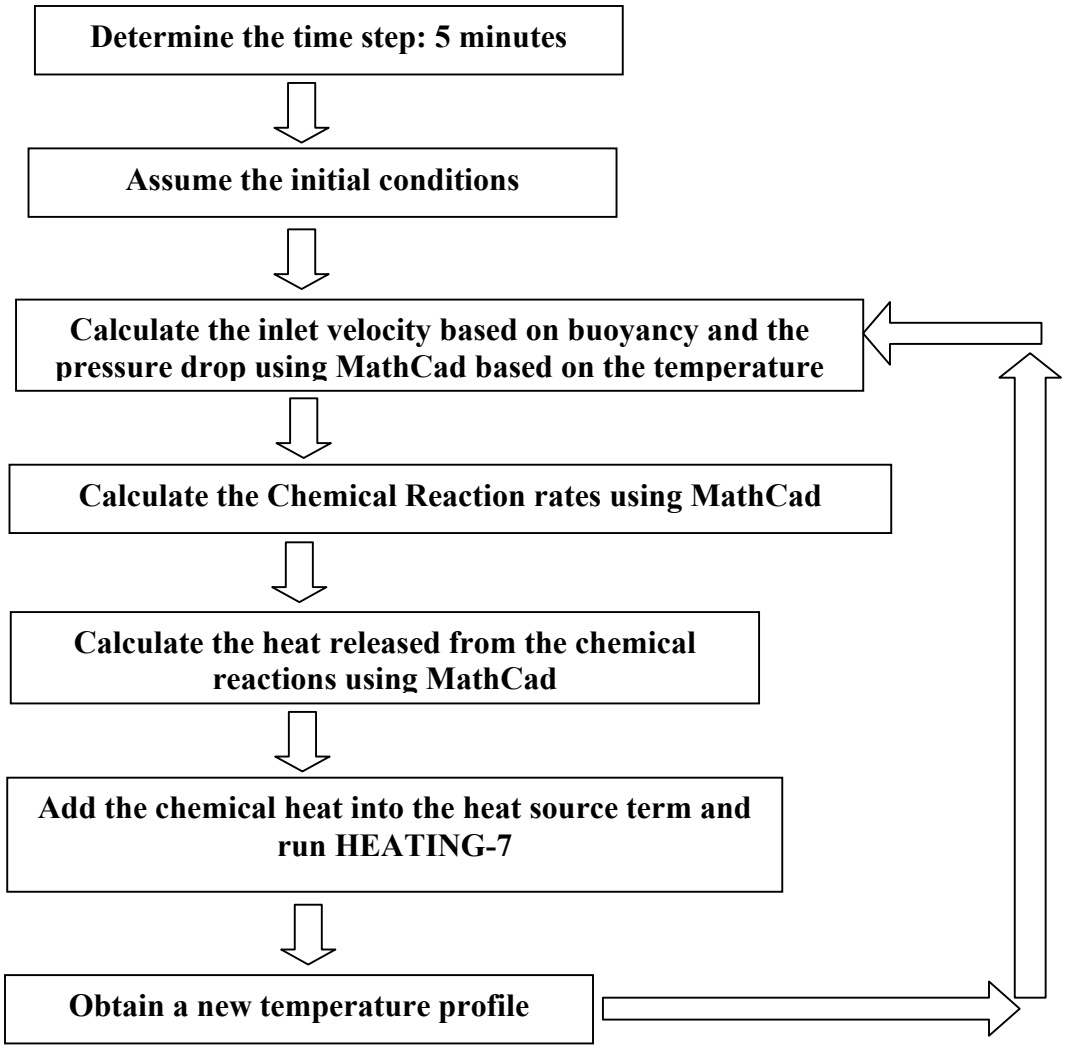

Figure 3-6: Procedures for Theoretical Study

In brief, the calculation procedures are:

Step 1: Based on the initial temperature profile of the current time step, the air inlet velocity was calculated from the balance between buoyancy (shown in Eq. 3-6) and pressure drop (shown in Eq. 3-7) aided by MathCad (shown in (The MathCad file is shown in Appendix 4). The steady state balance equation solved is $P_b = \Delta P$ as shown in Eq. 3-6 and Eq. 3-7.

It is assumed that the final product is CO_2, and the heat released from the chemical reactions is added into the heat source term of the HEATING-7. Then HEATING-7 is rerun to provide the temperature profile for the calculation of next time step.

Step 2: Calculate the chemical reaction rate. The chemical reaction rate by kinetics is described as[21]:

$$R=K_1*\exp(-E_1/T)(PO_2/20900) \quad \text{Eq. 3-5}$$

When T<1273K: K_1=0.2475, E_1=5710;
When 1273K<T<2073K, K_1=0.0156, E_1=2260;

Step 3: Add the heat by chemical reaction to the energy term of Code Heating-7

Step 4: Run heating-7

Step 5: Calculate the air velocity, graphite combustion rate and mole fraction of oxygen. The buoyancy is calculated using the following formula:

$$P_b = (\rho_c - \rho_h) * g * \frac{H}{2} \quad \text{Eq. 3-6}$$

where,
ρ_c: the average density of cold leg,
ρ_h: the average density of hot leg,
g: gravitation,
H: the height of the reactor vessel.

For the pressure drop in the pebble bed, the following formula are adopted [23]:

$$\Delta p = \psi \frac{H}{d} \frac{1-\varepsilon}{\varepsilon^3} \frac{\rho}{2} u^2 \quad \text{Eq. 3-7}$$

$$\psi = \frac{320}{\frac{\mathrm{Re}}{1-\varepsilon}} + \frac{6}{(\frac{\mathrm{Re}}{1-\varepsilon})^{0.1}}$$

Eq. 3-8

Where ψ is the pressure drop coefficient, which is dependent on the Reynolds number, which is defined as

$$\mathrm{Re} = \frac{du\rho}{\eta}$$

Eq. 3-9

H: the height of the pebble bed

d: the diameter of the pebbles

ρ: the fluid density

η: fluid dynamic viscosity

u: the gas velocity

ε: the porosity of the pebble bed

Equation Eq. 3-7 is confirmed by experiments up to $\mathrm{Re}/(1-\varepsilon)=5*10^4$. The first term of equation represents the asymptotic solution for laminar flow, the second for turbulent flow.

The average porosity of the pebble bed ε_t is dependent on D/d as in the following formula (D is the diameter of the pressure vessel, and d refers to the diameter of the pebbles):

$$\varepsilon_t = \frac{0.78}{(D/d)^2} + 0.375$$

Eq. 3-10

The calculation of air inlet velocity is an iterative process. For a given temperature distribution, the thermal properties of the air are calculated using the ideal gas formula. Then, the air inlet velocity is adjusted in order to balance the pressure drop and the buoyancy, and the final air inlet velocity calculated is the value at which the two forces equal each other (as discussed in step 1).

3.3.3. Results and Conclusions of the Theoretical Open Cylinder Study

In this model, the air inlet velocity in the pebble bed reactor as a function of the graphite average temperature is studied. The calculations of the pebble bed show that the air inlet velocity does not always increase when the core is heated (Shown in Figure 3-7). The air inlet velocity reaches its peak value at about 350 °C. As pebble temperature increases beyond this point, the inlet air velocity goes down. This negative feedback is a very positive result for the air ingress accident study, because the core temperature is almost always well above 350 °C, which limits air ingress.

The reasons for this phenomenon are: first, with the increase of the temperature, the viscosity of the gas increases. Second, if the temperature of the air becomes higher, air density becomes lower, which would create a higher air velocity in the core (shown in Eq. 3-6). However, the pressure loss is proportional to the velocity squared (shown in Eq. 3-7). In other words, the resistance increases much faster than the buoyancy with the increase of the average graphite temperature (assumed to be the gas temperature). The net effect is a reduction in air ingress velocity with higher temperature. When the air ingress is modeled for the open cylinder in the HEATING-7 analysis, the air ingress as a function of time is shown on Figure 3-8.

The heat generation rate of the carbon-oxygen chemical reaction was included in the HEATING-7 calculations which had previously included the decay heat term. Because this is a very slow transient and because of the very low heat capacity of the gases, the gases were assumed to have a temperature distribution similar to that of the solid structure.

Figure 3-9 shows the peak temperature of the core of 1663 °C, 21 degree higher than the former LOCA study. Similarly, most of the time, the peak temperature moves in the channel 2 of the VSOP/HEATING. The small peak temperature difference is due mainly to the low heat contribution of the chemical reactions which occur in the lower reflector.

In addition, the hot-point temperatures are kept low due to the excellent conductivity of the graphite. Figure 3-8 shows the air inlet velocity as a function time. Figure 3-10 plots the mole fraction of oxygen from the bottom of the reflector to the bottom of the reactor core pebble region. The figure shows that almost all of chemical reactions occur in the bottom reflector or in the several pebble layers of the pebble bed, which is far from the hot-point of the LOCA results presented earlier not considering the effects of air ingress.

In summary, the qualitative theoretical study indicates that:

- Negative feedback mechanism: This negative feedback mechanism on air ingress velocity would reduce significantly the consequences of the air ingress accident, because the core temperature is almost always well above 350 °C in the accident process.
- No meltdown: The conservative theoretical study excludes the possibility of core meltdown. Therefore, peak temperature of core is not the primary concern for his accident as long as the peak temperature is below the silicon carbide degradation temperature.
- The contribution of heat from the chemical reaction to the peak fuel temperature is very small ~ 20 C. Thus, chemical reactions are not expected to impact peak fuel temperatures.
- Even with an open cylinder assumption – a complete chimney – the air ingress velocity is limited to 0.025 meters/sec (0.13 kg/sec). This small amount of air ingress may limit the potential for "burning".
- The bulk of the oxygen is consumed in the lower reflector with little interaction with the fuel pebbles.
- Need for detailed study: The slow diffusion process, which may last several days, was not considered in the theoretical study, and it is assumed that the natural convection begins just after the depressurization stage, and a scenario with two-end open vessel is formed. Actually, the accident sequences and the consequences would be significantly different from that of the initial studies, and they strongly depend on the geometry of the reactor, the diffusion properties of the gases, the surface and volume

reaction rates. To study these phenomena numerically, the transfer functions of momentum, energy and species must be solved in a complicated space. These requirements lead us to the adoption of the powerful CFD code which has been developed with the potential to perform a detailed study of the air ingress accident.

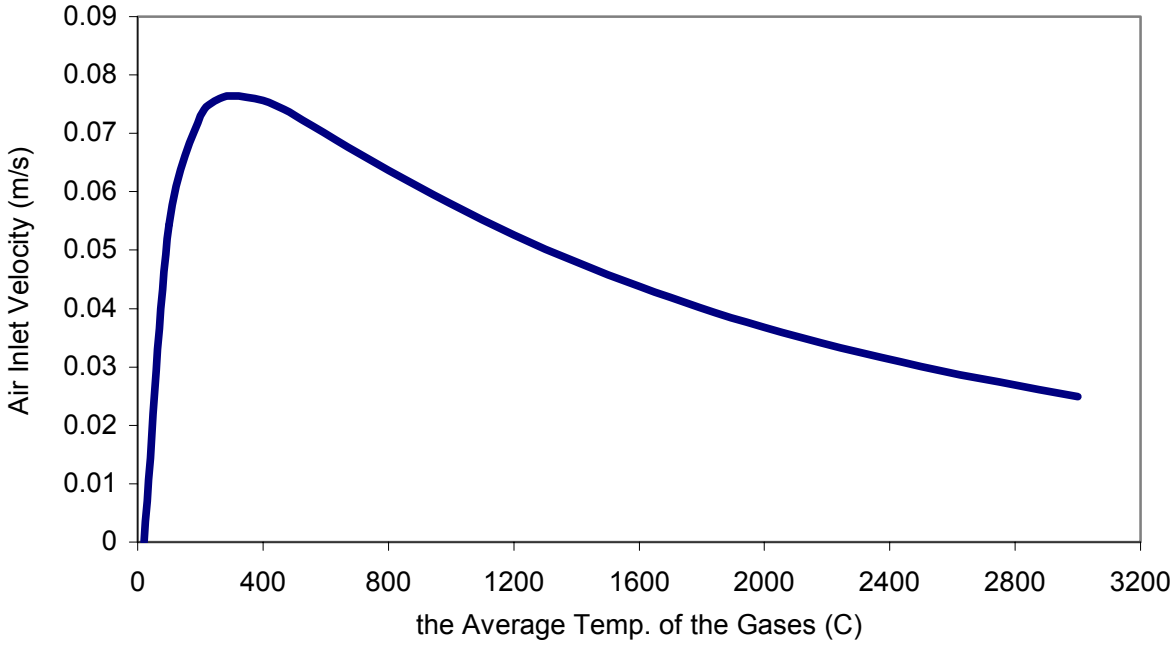

Figure 3-7: The Air Inlet Velocity vs. Pebble Bed's Average Temperature

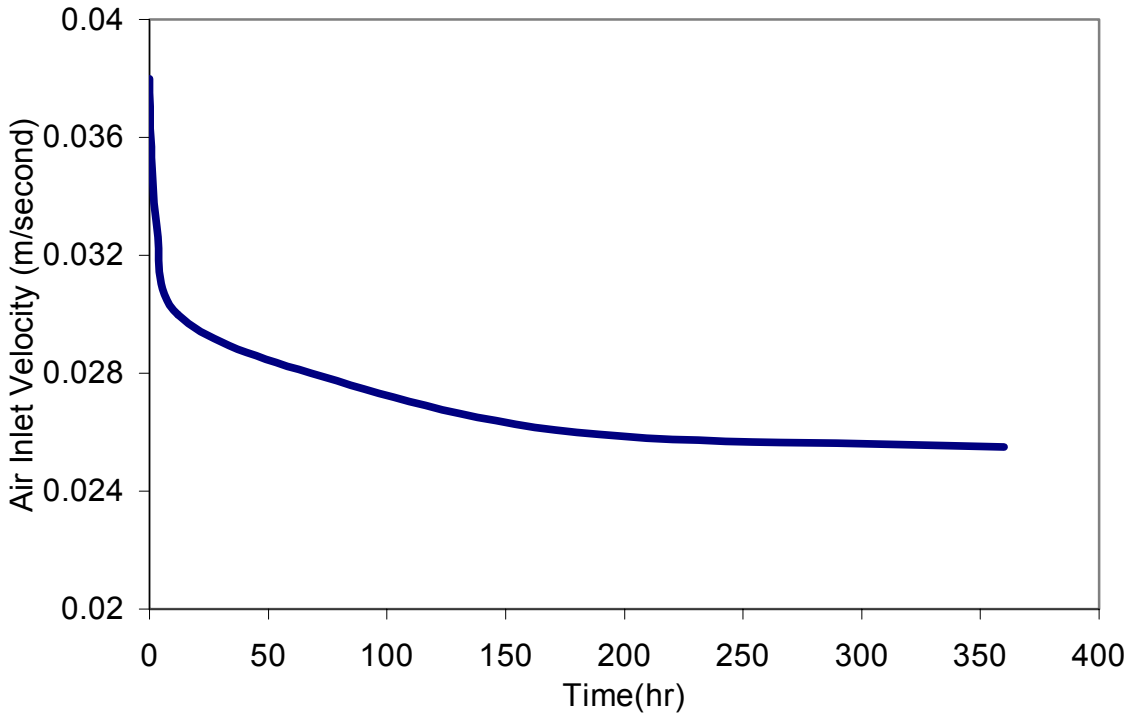

Figure 3-8: Air Inlet Velocity

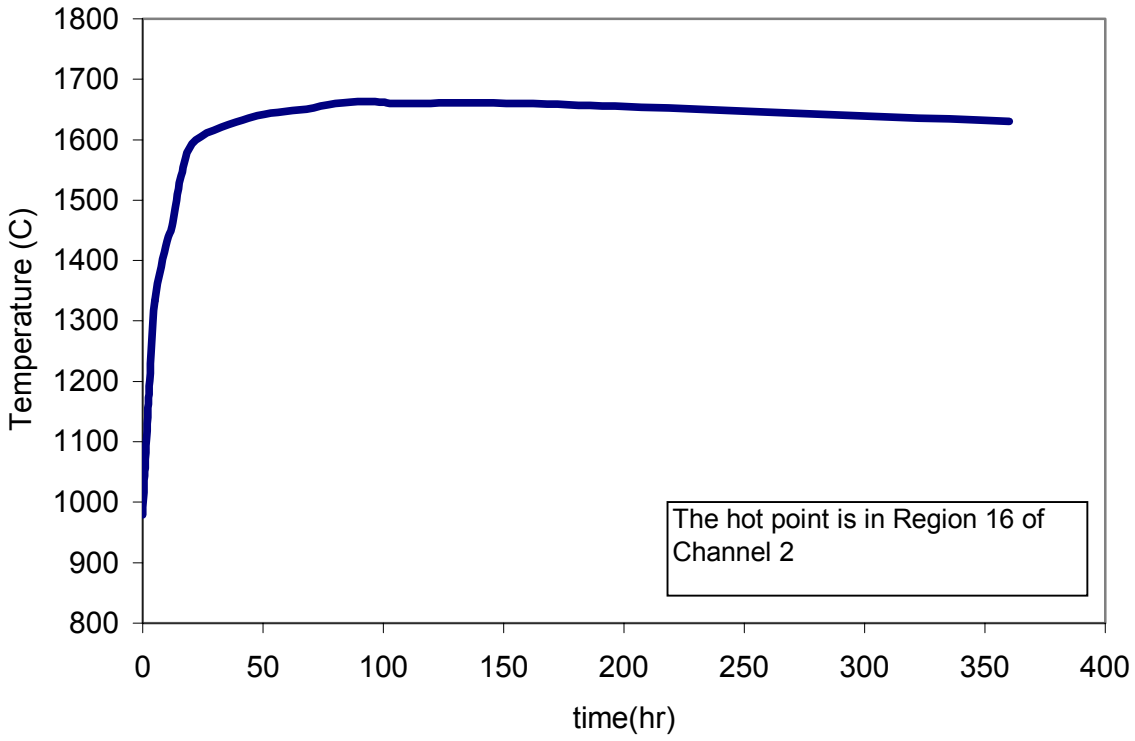

Figure 3-9: The Peak Temperature in the Core for Air Ingress Accident

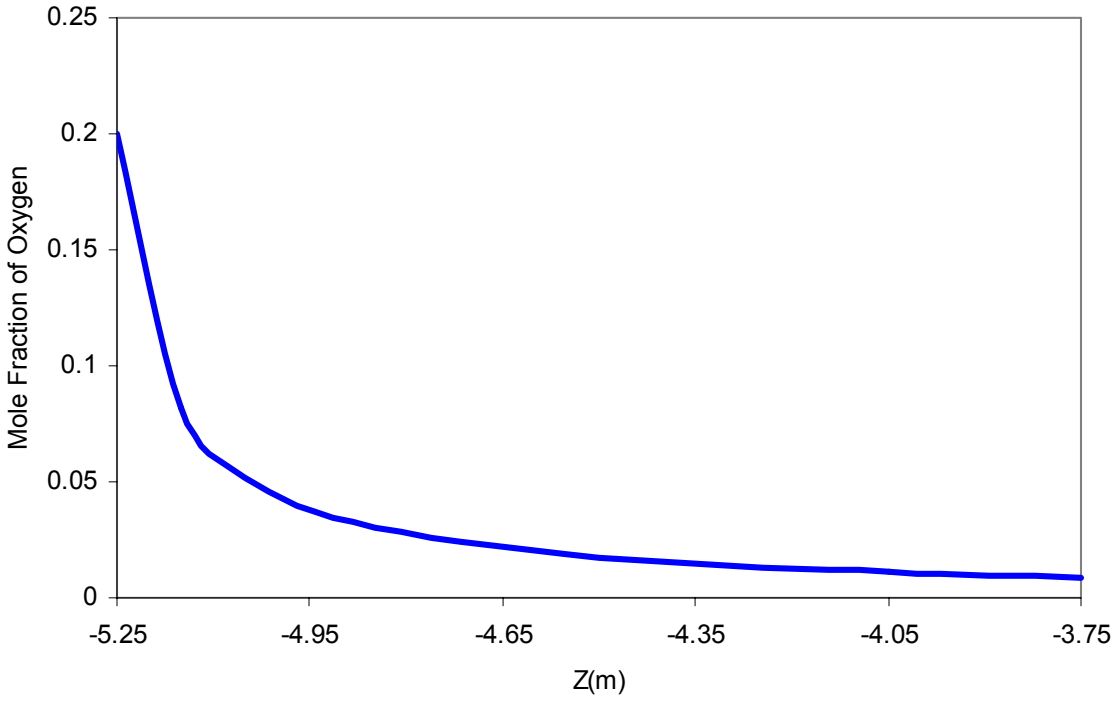

Figure 3-10 Oxygen Mole Fraction in the Bottom Reflector

3.4. Computational Fluid Dynamics Studies

As pointed out in the previous section, phenomenological understanding of the complex processes involved in air ingress requires sophisticated modeling tools. One such code is FLUENT that has recently be upgraded to handle multicomponent chemical reactions. This code will be used to develop a modeling capability for air ingress events for both pebble and prismatic type high temperature gas reactors. In order to accomplish this objective, the code methodology will be benchmarked against air ingress experiments performed in Japan and Germany. The Japanese tests were focused on prismatic reactors while the German tests examined pebble bed reactor configurations.

Based on engineering experience and previous experiments, key factors in air ingress events are:

- Onset time of air ingress post LOCA
- Temperature of the graphite (reflector and pebbles)
- Oxidation and diffusion rates for chemical reactions
- Partial pressure of oxygen and oxidation byproducts (CO, CO_2,)
- Velocity of air ingress
- Concentrations of O_2, CO, CO_2
- Heat removal capability from the core

FLUENT 6.0 was chosen as the tool for this analysis since it has the capability to deal with these factors.

FLUENT is the worlds' largest commercial CFD software, which has a wide range of industrial applications and world wide consulting services. Besides its capacities to model the heat transfer and mass diffusion, surface reaction model was added in its latest version – FLUENT 6.0. FLUENT is a standard CFD tool used in many complex heat transfer calculations. The FLUENT 6 version has been upgraded to allow for the

introduction of chemical reactions through the use of user defined functions that can simulate graphite and oxygen reactions in addition to including all forms of heat transfer including convection. This more rigorous tool will allow more confidence in the results of air ingress analysis.

In order to understand all of the key processes (diffusion, natural convection, and chemical reactions) involved in the air ingress accident, three experiments by JAERI (Japan Atomic Energy Research Institute) and one experiment by Julich Institute of Germany will be studied with increasing complexities using the CFD code FLUENT 6.0.

3.4.1. JAERI Air Ingress Experiments[11][12][13]

In order to understand all of the key processes (diffusion, natural convection, and chemical reactions) involved in the air ingress accident, three experiments by JAERI (Japan Atomic Energy Research Institute) were studied with FLUENT 6.0.

3.4.1.1. Isothermal JAERI Experiment – Diffusion

3.4.1.1.1. Experiment Description

A rough sketch of the experimental apparatus is shown in Figure 3-11 and Figure 3-12. The apparatus consists of a reverse U-Shape tube and a gas tank. A bent pipe connecting the two pipes is also heated. The inner diameter of the tube is 52.7mm.

This experiment was designed to test the first stage of air ingress – diffusion . The entire experiment was conducted at isothermal conditions at 18 C. [6] The two gases used were helium in the tube and nitrogen in the lower tank.

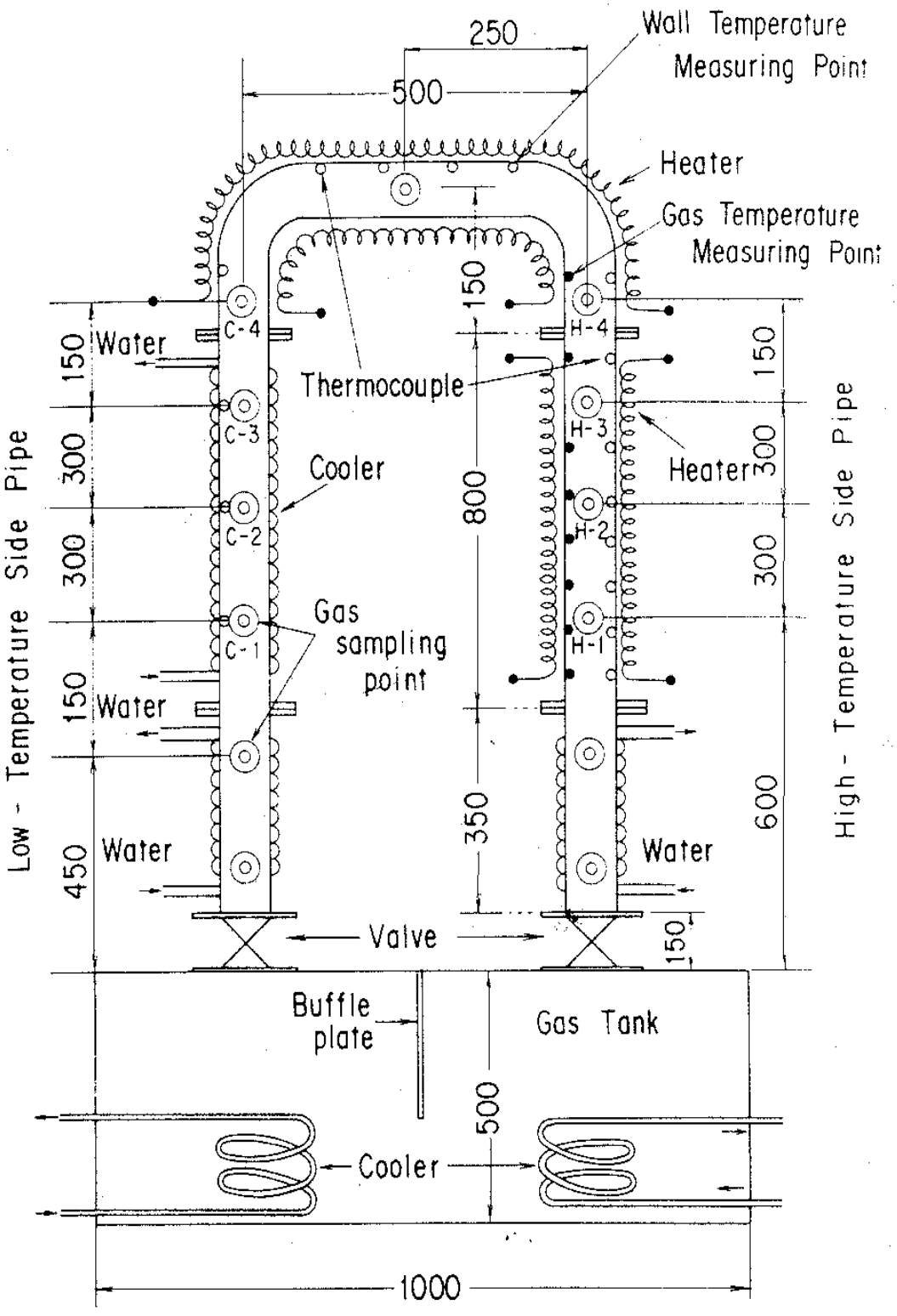

Figure 3-11: Experimental Apparatus for Isothermal and Non-Isothermal Experiments [13]

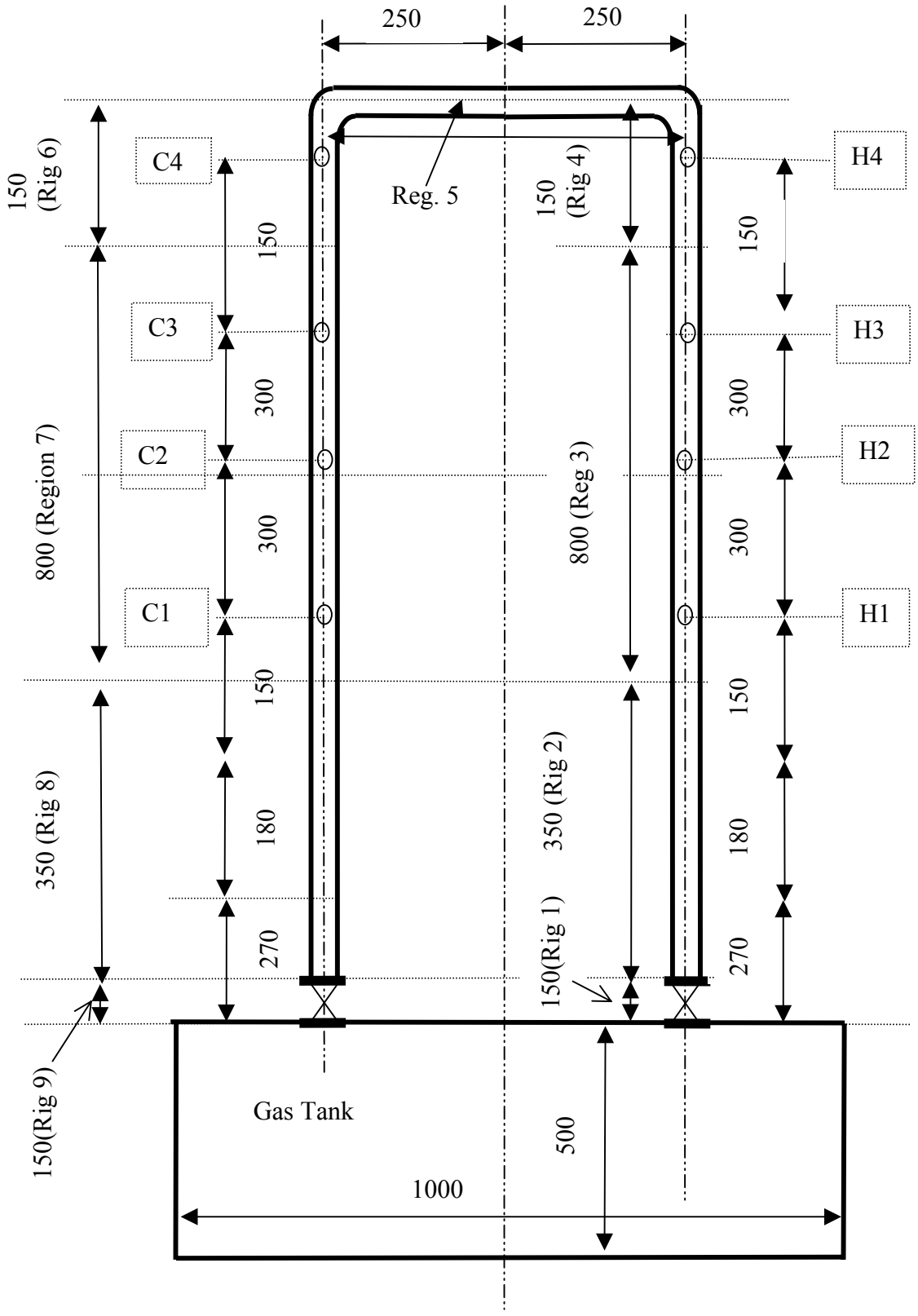

Figure 3-12: FLUENT Model for Isothermal and Non-Isohermal Experiments

The experimental procedures are:

1) Close all-valves between the reverse U-Shape tube and the gas tank;
2) The tube and the gas tank is evacuated by a vacuum pump;
3) Then the tube is filled with lighter gas of He, and heavier gas of N_2 is filled in the gas tank;
4) When a steady state test condition with atmosphere pressure is reached, the ball-valves are open to simulate the pipe rupture accident.

The Figure 3-13 shows the geometry and mesh generation using the preprocessor GAMBIT 2.0. There are 490 hexahedral cells and 1856 mixed cells in this 3-Dimensional model. The properties of He and N_2, such as the specific heat, conductance, density and viscosity, are all from the ideal gas database of FLUENT. The boundary condition is that all the wall temperatures are equal to the environment temperature, 18 °C. Before the valve opening, there is 100% He in the pipe region and 100 % N_2 in the gas tank region. In addition, no disturbance is involved in this pure diffusion process.

In this model, the ideal gas properties, including the density, conductivity, specific heat and viscocities, are adopted as the material properties. For the mass diffusivity, at single value for 18 °C is calculated using the following multi-component formula [26].

$$D_{A-B} = \frac{10^{-7} T^{1.75} [(M_A + M_B)/M_A M_B]}{P(\Sigma_A^{1/3} + \Sigma_B^{1/3})^2}$$

Eq. 3-11

Where,

M_A, the molecular weight of gas A;

M_B, the molecular weight of gas B;

P, the total pressure of the two gases;

Σ_A, the diffusion volume for gas A;

Σ_B, the diffusion volume for gas B;

The molecular weights and the diffusion volumes, Σ, for the gases involved in the accident are shown in the following Table 3-2.

Gas	Molecular Weight	Diffusion volumes
He	4	2.88
N_2	28	17.9

Table 3-2: The Molecular Weight and Diffusion Volume

3.4.1.1.2. Results

Figure 3-14 shows the experimental and calculated mole fraction changes of N_2 at various gas sampling positions for the isothermal experiment. H1, H2, H3, H4 refer to 4 points monitored in the hot leg, and C1, C2, C3, C4 refer to 4 points monitored in the cold leg. The horizontal axis expresses the elapsed time after the simulated pipe rupture. The calculation is in good agreement with the experiment. As the mole fraction distribution of N_2 is the same on both legs, natural convection of the gas mixture does not occur with pure diffusion being the only phenomenon of interest. This benchmarking shows that FLUENT can be used to model the stage 2 of air ingress (Diffusion). (As shown in Figure 3-15, Figure 3-16 and Figure 3-17).

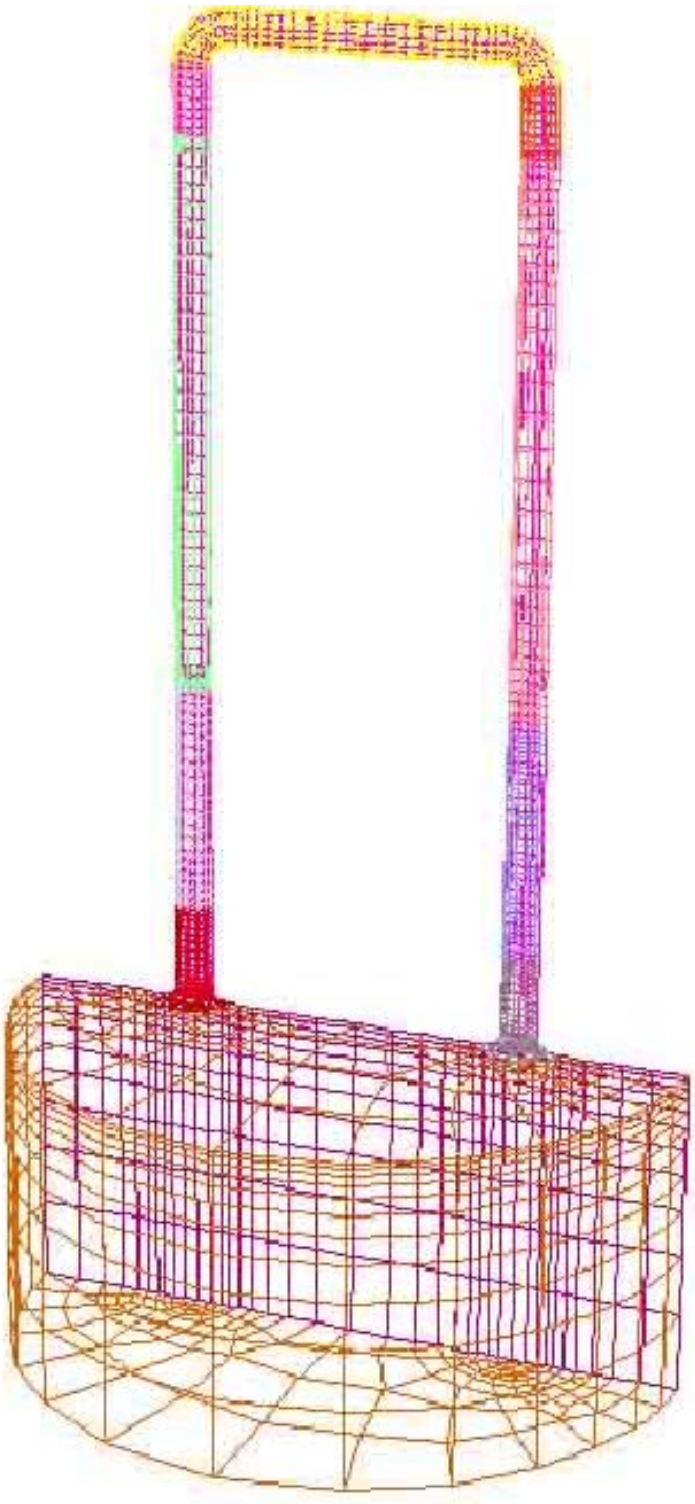

Figure 3-13: The Structured Meshes for Isothermal and Non-Isothermal Experiments

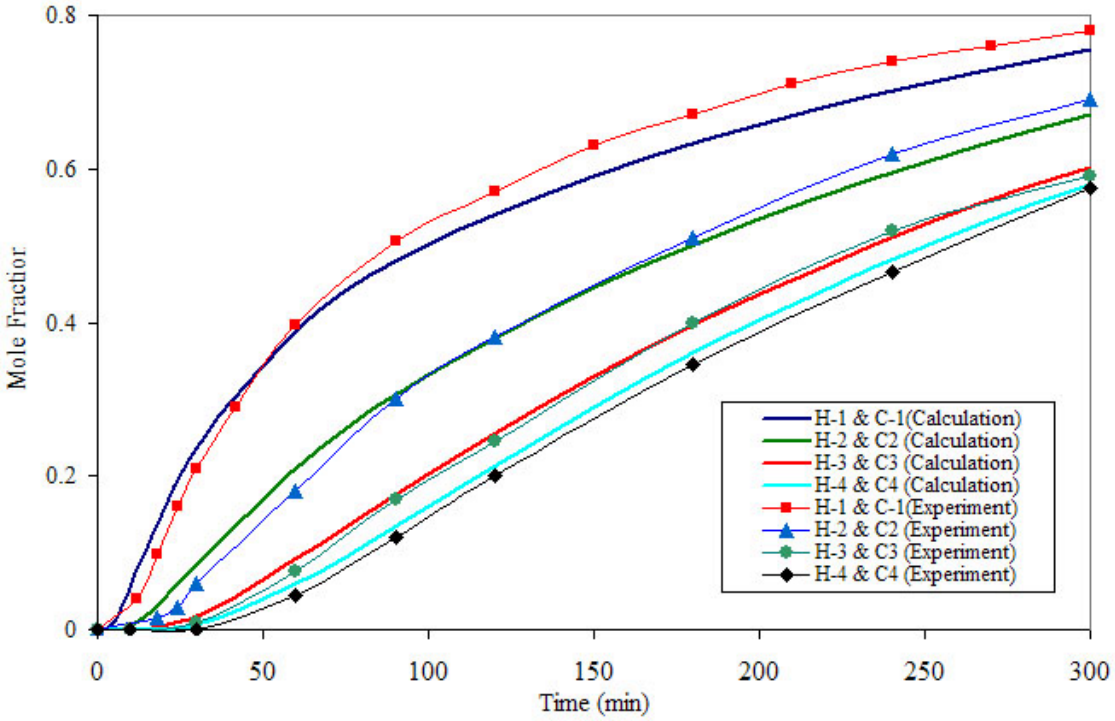

Figure 3-14: Mole Fraction of N_2 Benchmarking of the Isothermal JAERI Experiment

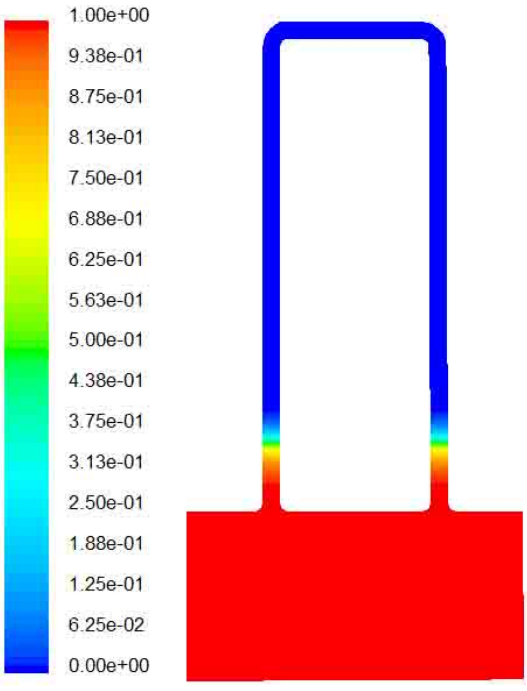

Figure 3-15: N_2 Mole Fraction Contour (t=0.25min)

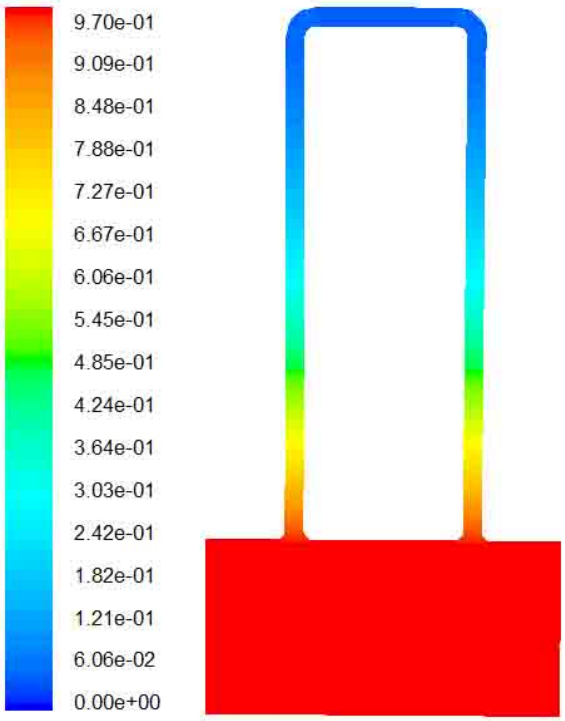

Figure 3-16: N_2 Mole Fraction Contour (t= 60 min)

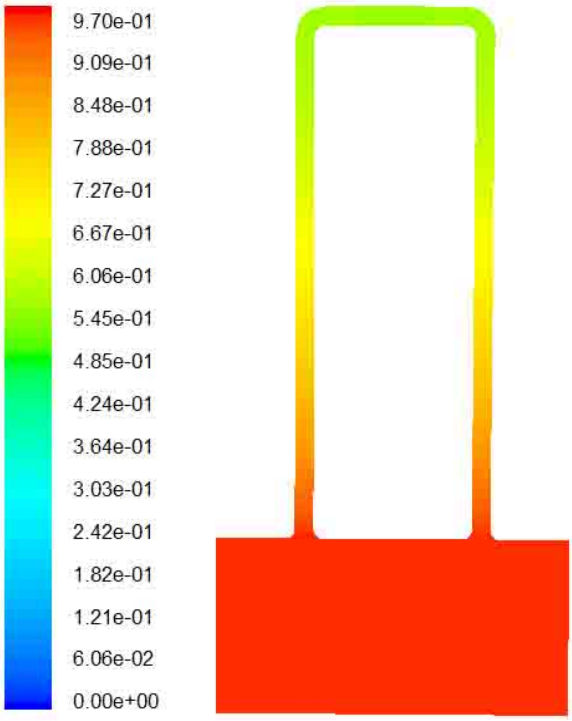

Figure 3-17: N_2 Mole Fraction Contour (t= 180 min)

3.4.1.2. JAERI Non-Isothermal Experiment

3.4.1.2.1. Experiment Description [11]

The non-isothermal experiment is similar to the isothermal experiment except that the objective of this experiment is to provide a temperature gradient between the hot and cold legs to assess the onset of natural circulation. Thus, in addition to modeling the early stage diffusion of nitrogen into the helium, a temperature difference enhances the diffusion process allowing for density differences in each of the legs which ultimately creates a mechanism for natural circulation.

In the Non-Isothermal experiment, the same facility as the Isothermal experiment is used, but the pipes are heated and maintained constant temperature for every segment. The longitudinal average temperature T over each region is, respectively, T_1=19.3 °C, T_2=19.3 °C, T_3=256 °C, T_4=154 °C, T_5=124 °C, T_6=59 °C, T_7=26.3 °C, T_8=17.7 °C, T_9=17.7 °C (the User Defined Function is shown in Appendix 9). The profile is shown in Figure 3-18, and see Appendix 7 and Appendix 8 for detailed information about this model.

3.4.1.2.2. Results

The mole fraction change of N_2 and the initiation time of the natural circulation of pure N_2 agree well with the experimental results (Shown in Figure 3-19, Figure 3-20 and Figure 3-21). The contours of N_2 mole fractions (From Figure 3-23 to Figure 3-32) clearly show the dynamics of the natural circulation process. This process could be well explained by the density difference between the hot leg and the cold leg:

After the initial instability – shown on Figure 3-22 caused by the opening of the valves, the nitrogen diffuses into the hot leg with a higher rate than the cold since the gas with higher temperature has a higher diffusion coefficient. At some point, the density

difference between the two legs is sufficiently large to develop a buoyancy force large enough to overcome the resistance to flow starting the natural circulation process. Figure 3-23 through Figure 3-32 show that the helium is moving from the hot leg to the cold leg as the density difference between the legs is increased. The buoyancy of the hot leg is driving the helium into the cold leg and ultimately back into the nitrogen tank. At 220 minutes, natural circulation is on the verge of beginning with a very rapid flow of nitrogen from the hot leg to the cold leg in less than 1 minute.

The agreement of the FLUENT calculation with the Non-Isothermal experiment is very good, demonstrating the second phase of the air ingress phenomenon using the CFD tool.

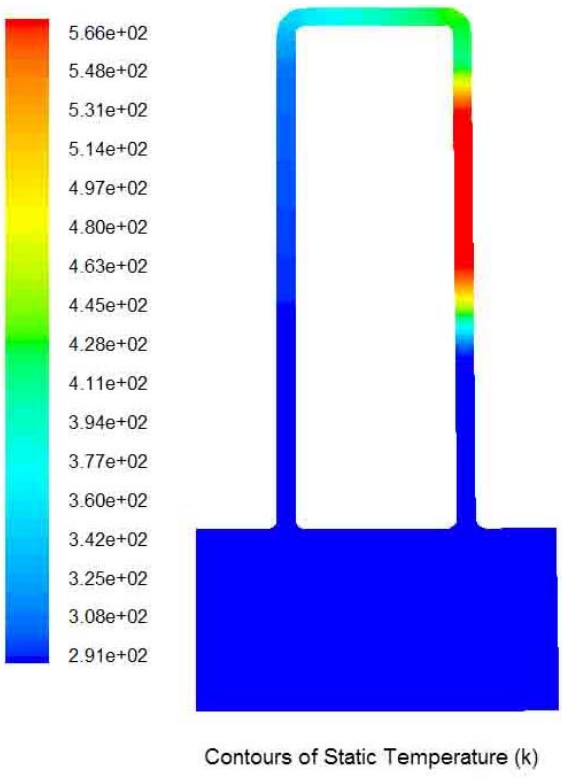

Figure 3-18: The Constant Temperature Boundary Condition

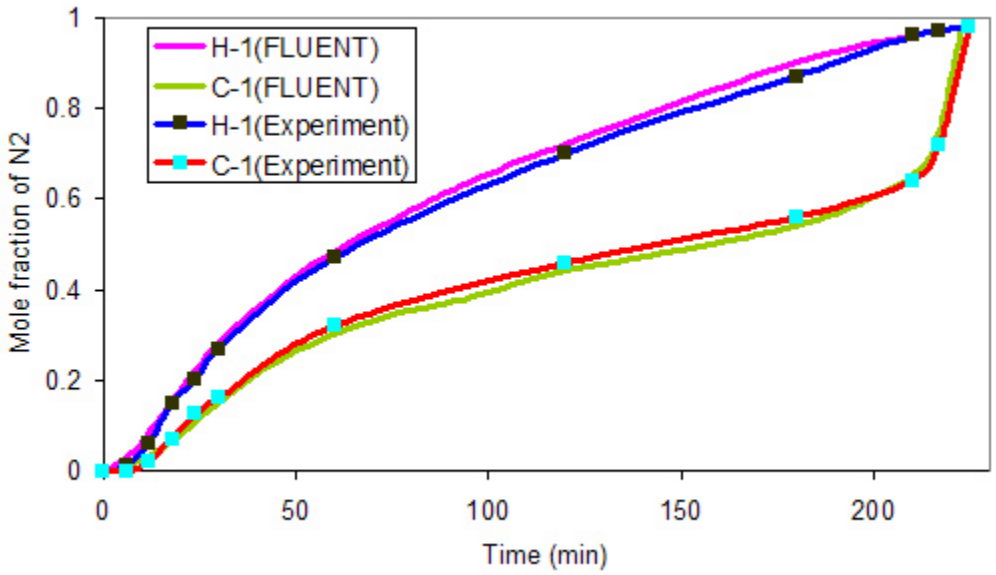

Figure 3-19: Comparison of mole fraction change of nitrogen between the gas sampling positions H-1 and C-1 in the Non-Isothermal experiment

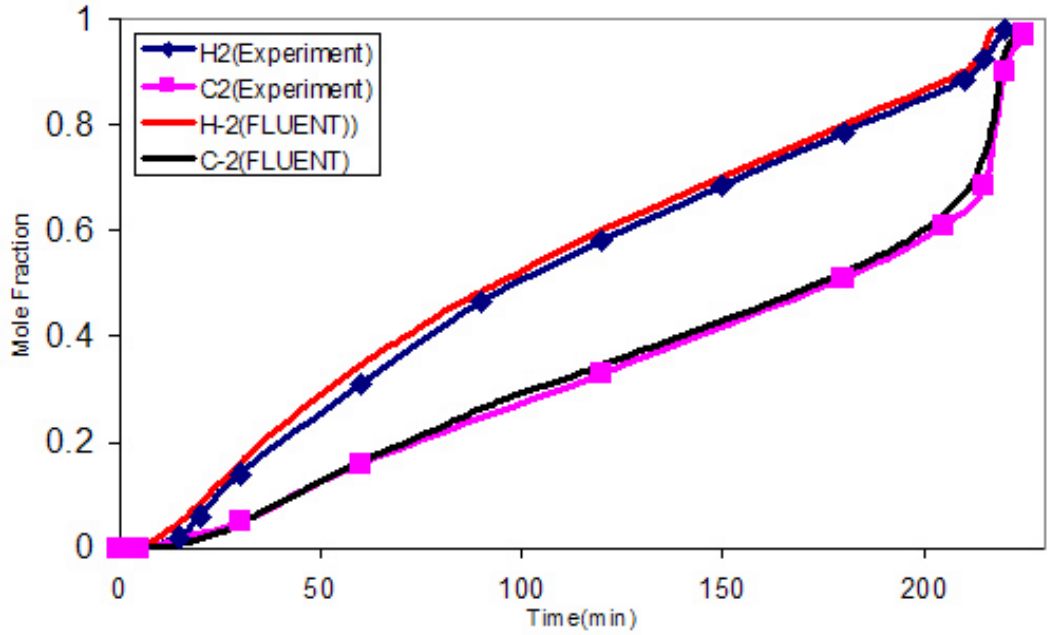

Figure 3-20: Comparison of mole fraction change of nitrogen between the gas sampling positions H-2 and C-2 in the Non-Isothermal experiment

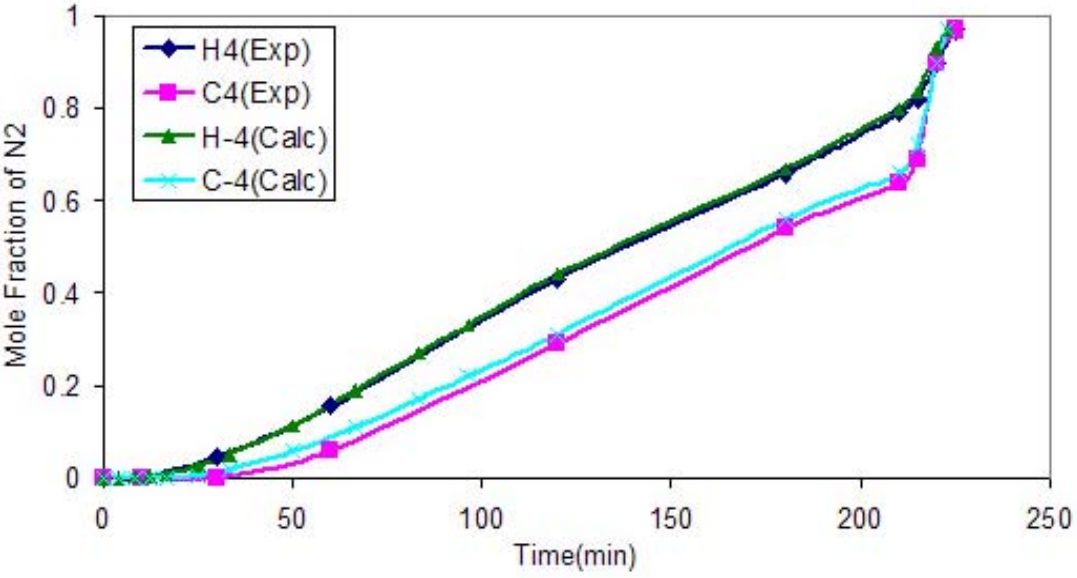

Figure 3-21: Comparison of mole fraction change of nitrogen between the gas sampling positions H-4 and C-4 in the Non-Isothermal experiment

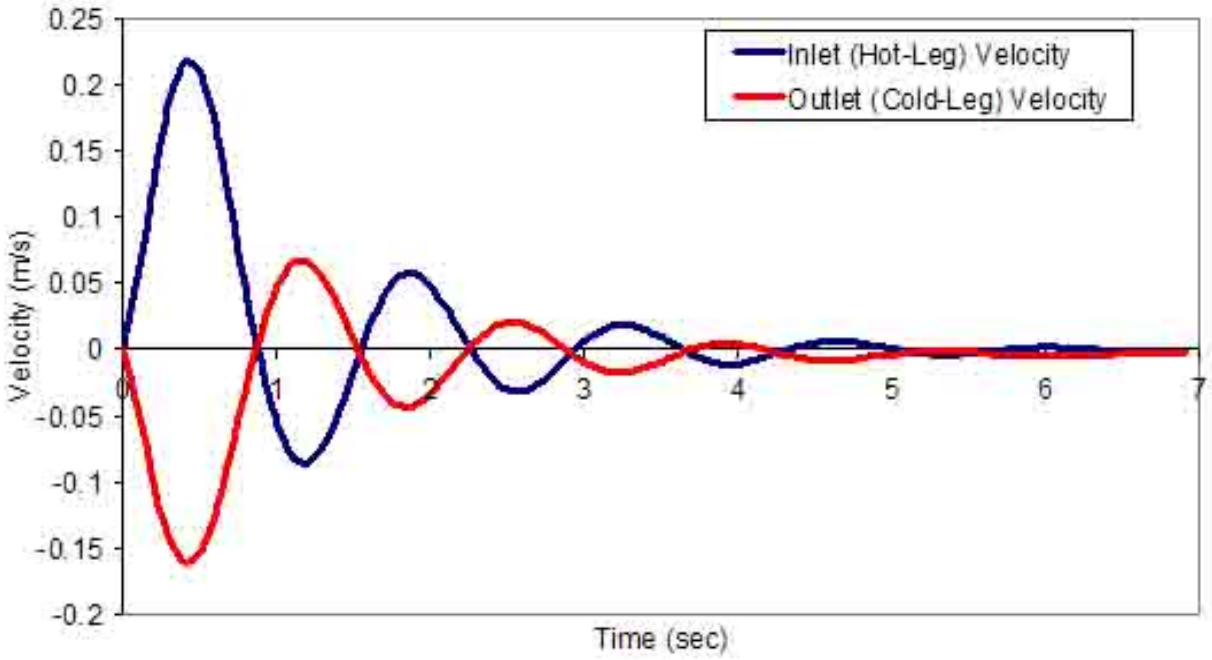

Figure 3-22: The Inlet and Outlet Velocity

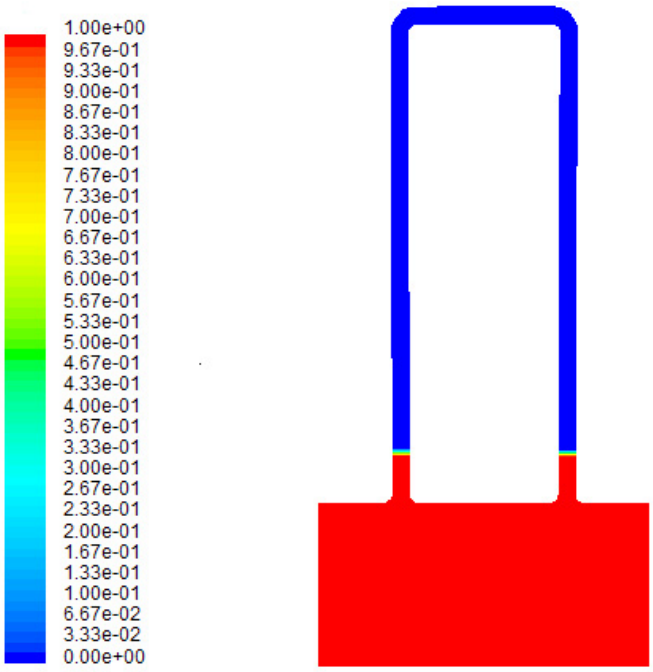

Figure 3-23: Nitrogen Contour (t = 0 min)

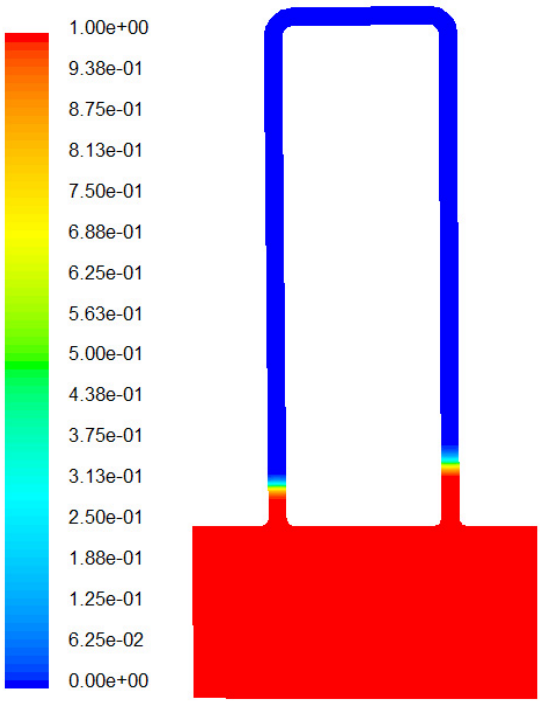

Figure 3-24: Nitrogen Contour (t=1.6 min)

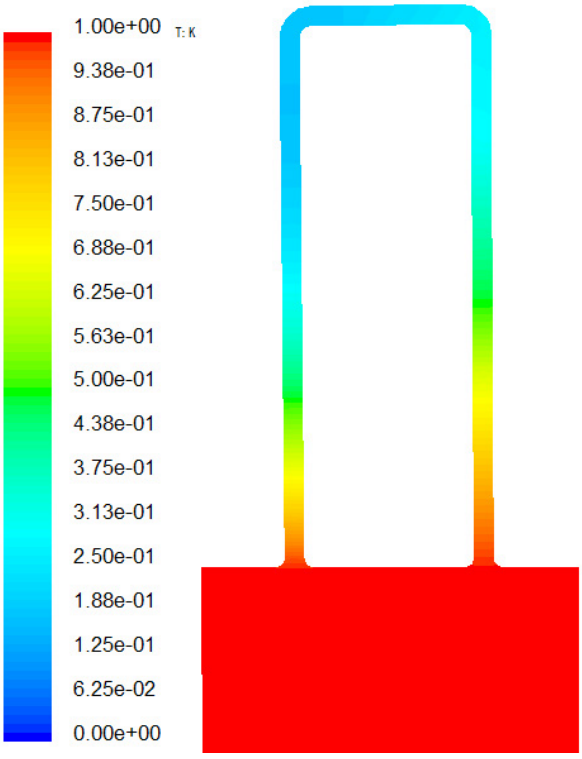

Figure 3-25: Nitrogen Contour (t=75.5 min)

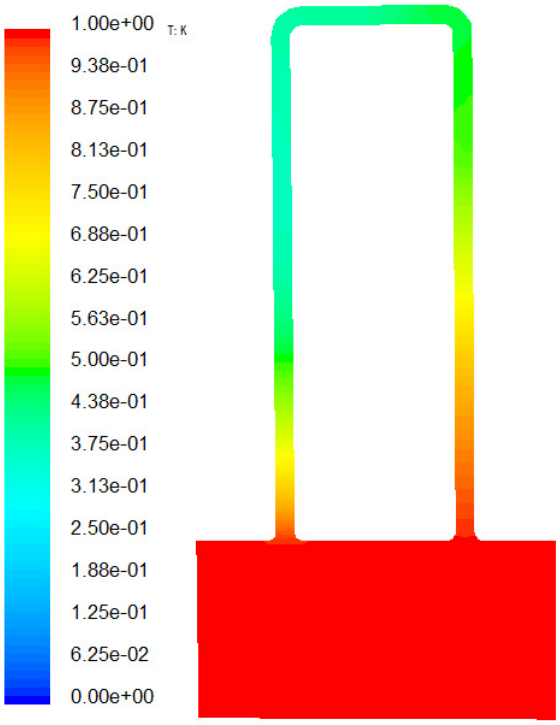

Figure 3-26: Nitrogen Contour (t=123.3 min)

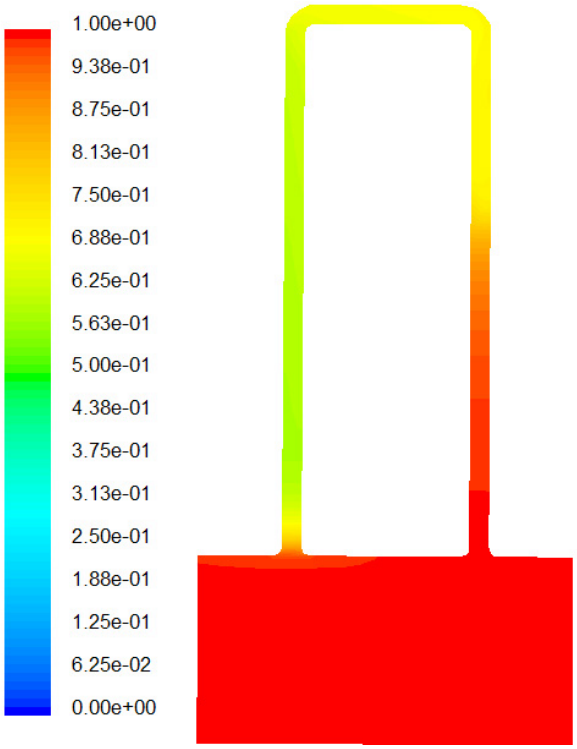

Figure 3-27 Nitrogen Contour (t=220.43 min)

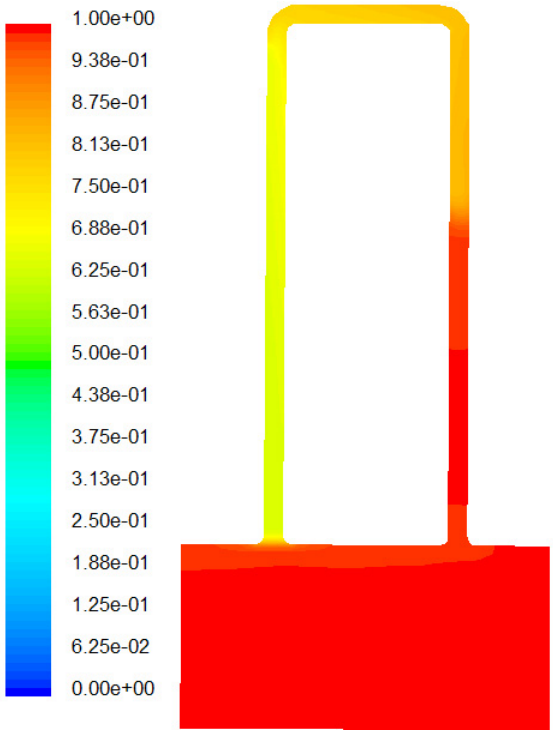

Figure 3-28: Nitrogen Contour (t=222.55)

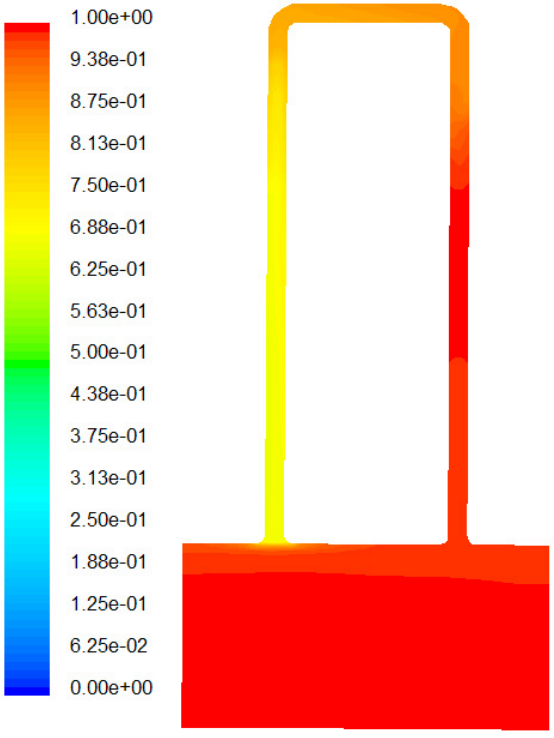

Figure 3-29: Nitrogen Contour (t=223.03 min)

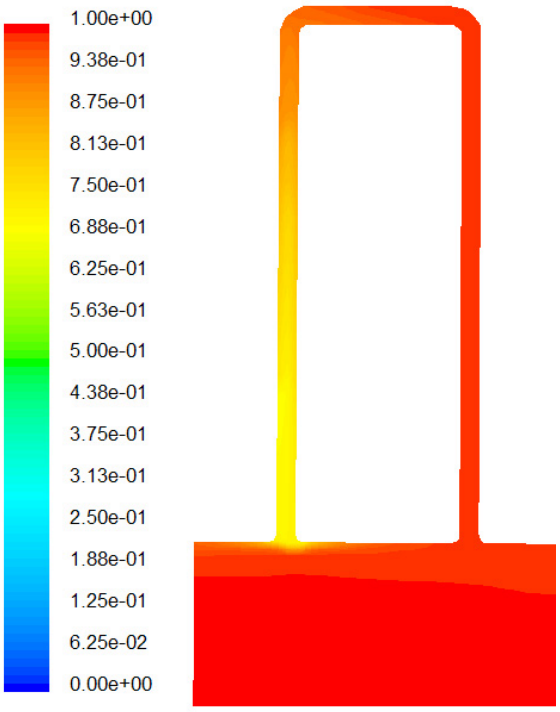

Figure 3-30: Nitrogen Contour (t=223.20 min)

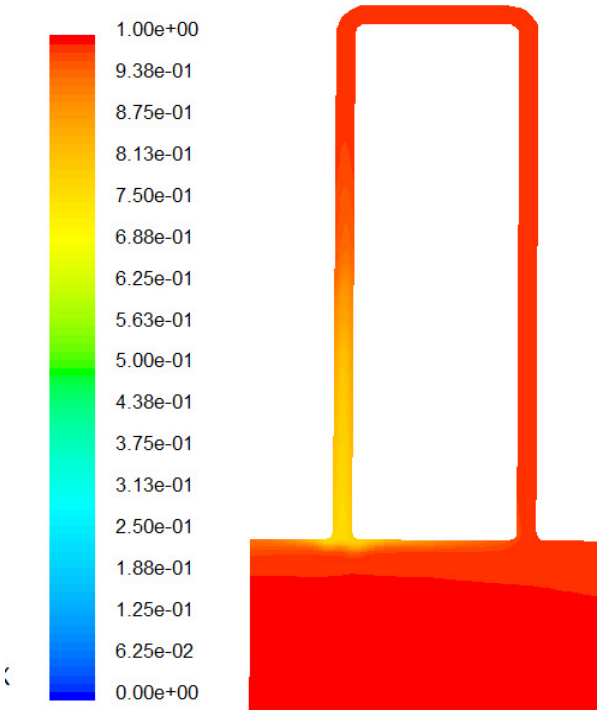

Figure 3-31: Nitrogen Contour (t=223.28 min)

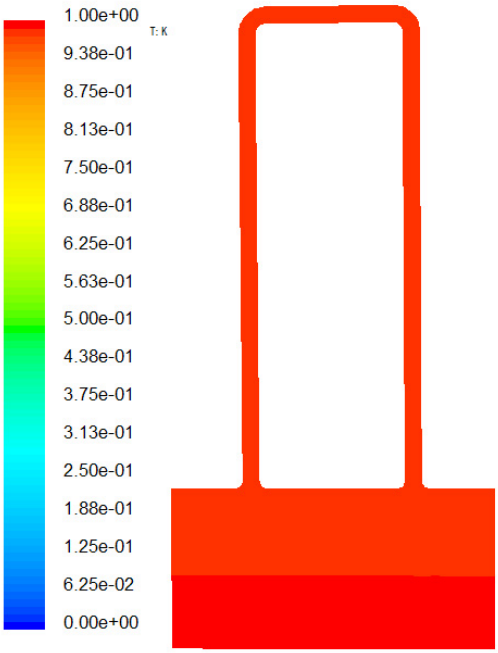

Figure 3-32: Nitrogen Contour (t=224.00 min)

3.4.1.3.Benchmarking of the Multi-Component Model with Chemical Reactions

The last series of experiment conducted by JAERI is the multi-component experiment by which the combined phenomena of molecular diffusion and natural convection with a graphite oxidation reaction in a multi-component gas system were studied to investigate the process of air ingress into a reverse U-shaped tube consisting of a hot and cold leg pipe. The objectives of the multi-component experiment is to investigate the basic features of the flow behavior of the multi-component gas mixture, consisting of He, N_2, O_2, CO, CO_2, etc. This experiment tests all major phenomenon in an air ingress event for prismatic reactors.

3.4.1.3.1. Experimental Apparatus [13]

A rough sketch of the experimental apparatus can be seen in Figure 3-33 and Figure 3-34. The vertical heated pipe, made of inconel, has an inner diameter of 52.5 mm, and outer diameter of 60.3 mm and length of 1300 mm. A graphite pipe is inserted into the inconel heated pipe and it measures 40.5 mm i.d, 52.5 mm o.d. and 450 mm in length. The graphite, IG-110, is from Toyo Tanso Co. The upper and lower inner pipes, which are also inserted in the heated pipe, are made of inconel and have the same diameter as the graphite pipe. The horizontal and bent pipes have an inner diameter of 40.5 mm. The vertical cooled pipe measures 41.2 mm i.d. and 1420 mm in length. A gas tank, cylindrical in shape, has an i.d. of 991 mm and a height of 400 mm [13].

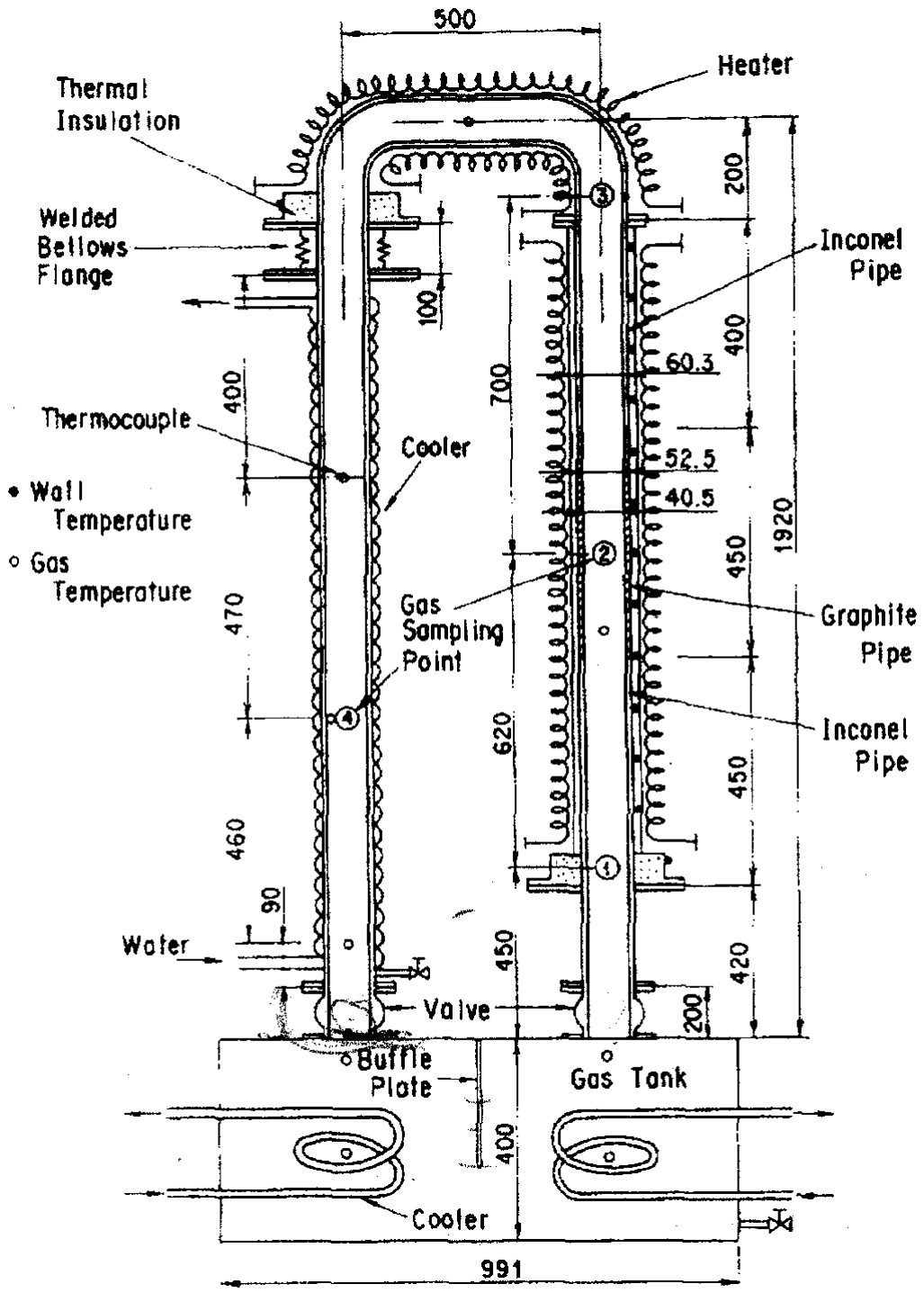

Figure 3-33: Experimental Apparatus for Multi-component Experiment [13]

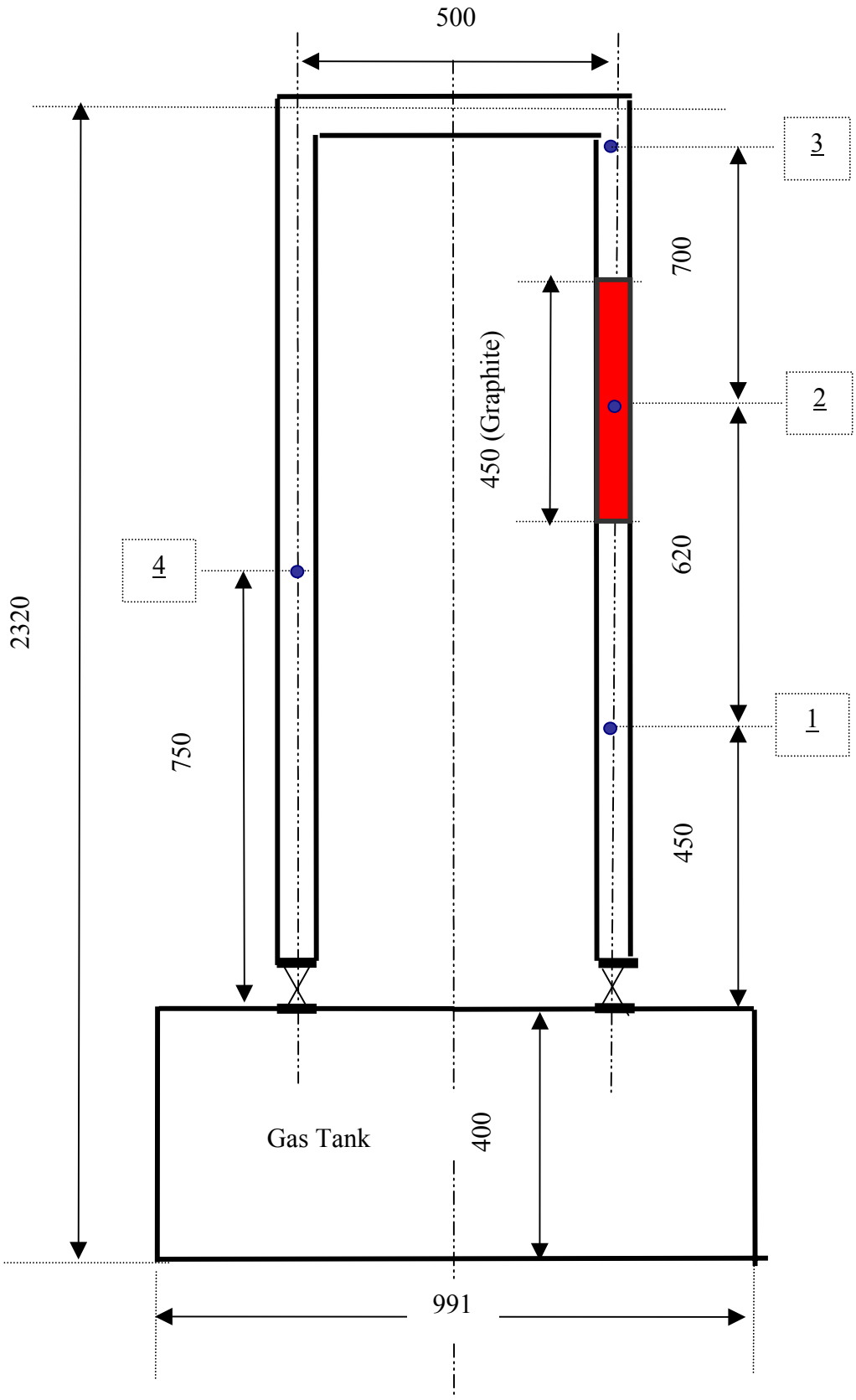

Figure 3-34: FLUENT Model For Multi-component Experiment

The mole fraction of each gas species and the density of the gas mixture were measured at four sampling points shown in Figure 3-34. The density of the gas mixture, the mole fraction of O_2, CO and CO_2 were measured using a gas analyzer (Yokogawa: density-Vibro gas analyzer DG8, O_2-Electrochemical analyzer 6234, CO and CO_2-infrared rays analyzer IR21).

The temperature distribution of the pipe wall was measured by 18 K-type thermocouples and the temperatures of the gas mixture were also measured at nine points using K-type thermocouples. The signals of the voltage from the thermocouples and the gas analyzer were digitallyt sampled and read using a data acquisition control unit (Scanner and DVM: Advantest TR2730 & TR2731). These units were controlled by a Hewlett-Packard Series 9000 Model 216 computer. It is assumed that the onset time of the natural circulation of air is the time when the gas temperature at the cooled pipe exceeds 100 °C. As the natural circulation of N_2 occurs, the gas temperature at the upper part of the cooled pipe increases rapidly. The time required for the gas temperature to be increased from 20 to 100°C is about 10 seconds.

In consideration of the errors induced by the thermocouples, scanner junction and DVM accuracy, the entire accuracy of the temperature measurement was within ±0.3°C. The measurement accuracy of the density analyzer and the concentration analyzer(O_2, CO, CO_2) were ±1% F.S. and ±1.7% F.S., respectively. The relative uncertainty in the density of the gas mixture was found to be ±4%. The uncertainties in the mole fraction of O_2, CO, and CO_2 were found to be ±2.3%, ±4.4% and ±4.4%, respectively. The uncertainty in the onset time of the natural circulation of air was estimated to be 12% [13].

3.4.1.3.2. Experimental Procedure [13]

The experimental procedures are as follows: The ball valves between the reverse U-shaped tube and the gas tank were closed and the tube was evacuated using a vacuum pump. Helium and air was injected into the tube and the gas tank, respectively. Then, the high-temperature side pipe and the connecting pipe were heated from about 400 °C to

800 °C (the longitudinal average temperature of the high-temperature side pipe). When the temperature of the gas and the pipe wall reached a steady-state condition, the gas pressure in the reverse U-shaped tube was equalized to the atmospheric pressure by the opening a small release valve. Then, the two ball valves were open at the same time to simulate a pipe rupture accident. During the experiment, the temperature change of the pipe wall was held within ±2 °C.

The initial conditions for the multi-component experiment are: the total pressure is equal to the atmosphere pressure, no gas flow before the opening of the valves, there is 100% helium in the pipe region above the valves, and 100% air in the tank and the pipe region below the valves. A steady state is reached for the helium in the pipes and the air in the tank. No disturbance is introduced by the opening of the valves. The temperature profile of the wall is kept constant for each segment (see Figure 3-35 and Figure 3-38). The temperature profile was defined using User Defined Functions (UDF) (see Figure 3-36), which were subroutine written in C language (Appendix 11, Appendix 12, Appendix **13**).

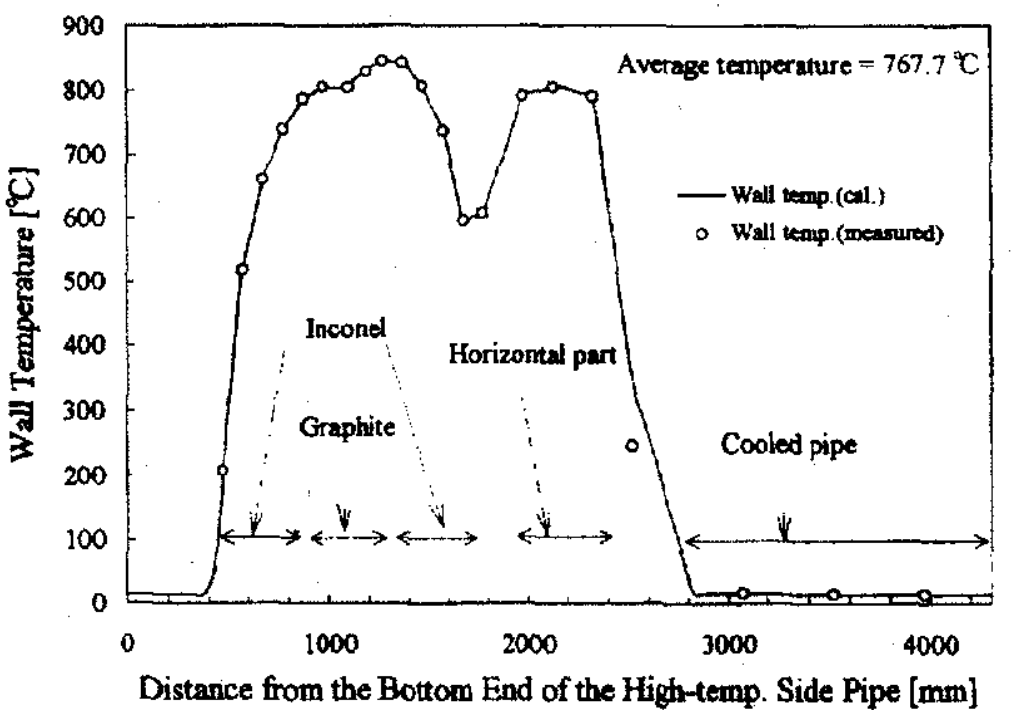

Figure 3-35: Distribution of the Measured Wall Temperature in the Whole Tube [13]

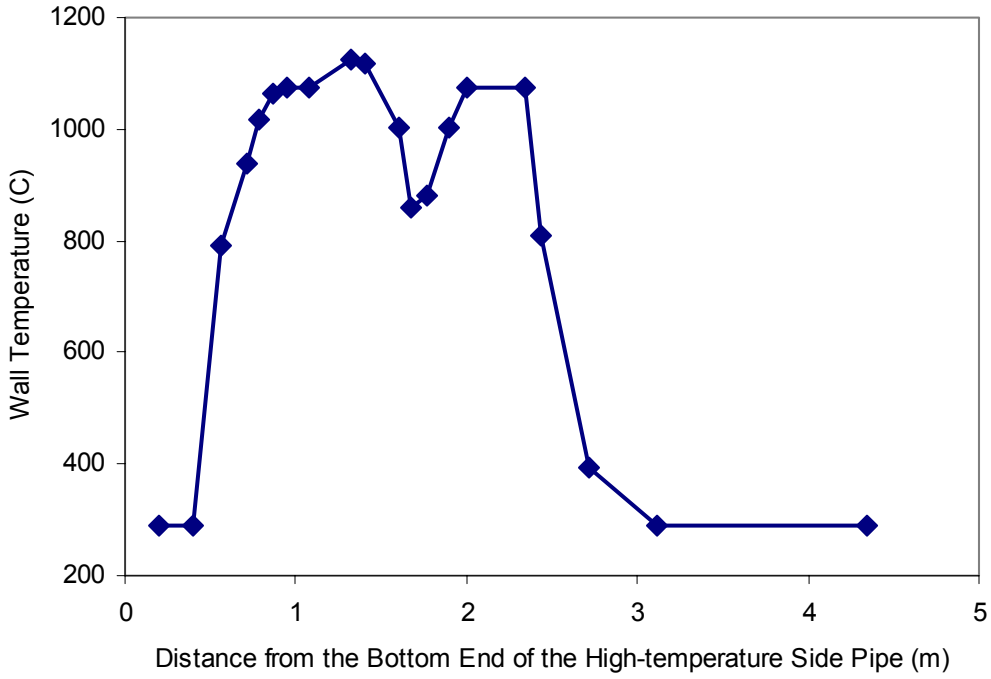

Figure 3-36: Distribution of the Wall Temperature in the Whole Tube Defined by UDF

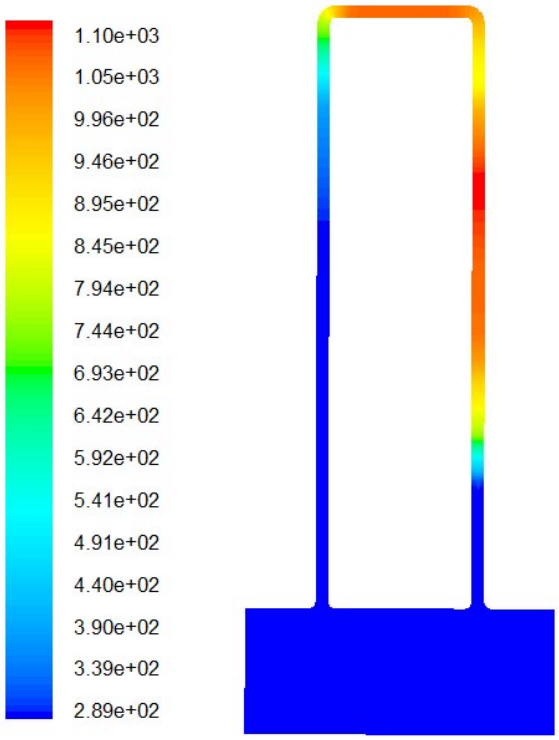

Figure 3-37: The Temperature Profile for the Multi-component Experiment

3.4.1.3.3. Diffusion Coefficients

The multi-component diffusion model is adopted for the diffusion process. For FLUENT 6.1, the definition of the multi-component diffusion coefficient could not be input directly using the formula in Eq. 3-11, and this formula was converted into the following form using Taylor Expansion:

$$D=A_1+A_2T^1+ A_3T^2+ A_4T^3+ A_4T^4$$

Eq. 3-12

There are 6 species of gases involved in the diffusion: He, N_2, O_2, H_2O, CO, CO_2, therefore, 15 diffusion coefficients need to be defined. The constants of A_1, A_2, A_3, A_4, and A_5 are shown in Table 3-4.

The molecular weights and the diffusion volumes, Σ, for the gases involved in the accident are shown in the Table 3-3.

Gas	Molecular Weight	Diffusion volumes
He	4	2.88
O_2	32	16.6
N_2	28	17.9
CO	28	18.9
CO_2	44	26.9

Table 3-3: The Molecular Weight and Diffusion Volume

	O_2-CO	O_2-CO_2	O_2-He	O_2-H_2O	O_2-N_2
A1	-4.300E-06	-3.400E-06	-1.520E-05	-5.600E-06	-4.400E-06
A2	3.966E-08	3.146E-08	1.400E-07	5.147E-08	4.039E-08
A3	1.492E-10	1.184E-10	5.266E-10	1.937E-10	1.520E-10
A4	-1.658E-14	-1.316E-14	-5.852E-14	-2.152E-14	-1.689E-14
A5	1.919E-18	1.523E-18	6.774E-18	2.491E-18	1.955E-18
		CO-CO_2	CO-He	CO-H_2O	CO-N_2
A1		-3.400E-06	-1.450E-05	-5.500E-06	-4.300E-06
A2		3.145E-08	1.334E-07	5.042E-08	3.996E-08
A3		1.183E-10	5.019E-10	1.897E-10	1.503E-10
A4		-1.315E-14	-5.578E-14	-2.108E-14	-1.671E-14
A5		1.522E-18	6.456E-18	2.440E-18	1.934E-18
			CO_2-He	CO_2-H_2O	CO_2-N_2
A1			-1.210E-05	-4.500E-06	-3.500E-06
A2			1.114E-07	4.105E-08	3.199E-08
A3			4.193E-10	1.545E-10	1.204E-10
A4			-4.660E-14	-1.717E-14	-1.337E-14
A5			5.394E-18	1.987E-18	1.548E-18
				He-H_2O	He-N_2
A1				-1.770E-05	-1.480E-05
A2				1.633E-07	1.366E-07
A3				6.144E-10	5.139E-10
A4				-6.828E-14	-5.710E-14
A5				7.903E-18	6.609E-18
					H_2O-N_2
A1					-5.600E-06
A2					5.140E-08
A3					1.934E-10
A4					-2.149E-14
A5					2.488E-18

Table 3-4 The Constants to Define the Diffusion Coefficients

3.4.1.3.4. Chemical Reaction Rates [13]

The graphite oxidation reaction(C-O_2)reaction) and the carbon monoxide combustion (CO-O_2 reaction) are taken into account. The chemical equation of the graphite reaction is expressed as [13]:

$$C + z \cdot O_2 \rightarrow x \cdot CO + y \cdot CO_2$$

Eq. 3-13

The reaction rate is described as

$$r_{c-o} = K_0 \exp(-\frac{E_0}{RT}) p_{o_2}^n$$

Eq. 3-14

where,

K_0=360, reaction constant,

E_0=209 [kJmole^{-1}], activation energy,

P_{O2}, the oxygen partial pressure.

The units of R, T, r_{c-o} and P_{O2} are [Jmole^{-1}K^{-1}], [K], [kg.kg^{-1}s^{-1}] and [pa], respectively. The value of the exponential index, n, in terms of the oxygen partial pressure ranges from 0.75 to 1 for PGX[2]. For this type of graphite, the value used in this analysis is 1 following JAERI's recommendation[13].

The production ratio of CO to CO_2 (x/y=A) is correlated as follows:

$$A = K_1 \exp(-\frac{E_1}{RT})$$

Eq. 3-15

K_1=7943,

E_1=78.3 [kJmole^{-1}], activation energy,

[2] The name of the graphite used in the multi-component experiment.

Where K_1 is the constant and E_1 the activation energy. The reported ratios differ over a wide range because the production ratio depends on experimental conditions, such as the catalytic effects of the impurities contained in the graphite and the grade of graphite. There is no data on these effects, thus, it is assumed that the production ratio of CO to CO_2 is constant since the wall temperature is assumed constant.

The mole number for the reaction term of O_2 and for the generation term of CO and CO_2 of Eq. 3-13 can be obtained from the following relation, respectively [13].

$$z = N_{o2} = \frac{A+2}{2(A+1)}$$

Eq. 3-16

$$x = N_{co} = \frac{A}{A+1}$$

Eq. 3-17

$$x = N_{co2} = \frac{1}{A+1}$$

Eq. 3-18

The chemical equation of the CO combustion is expressed as [13]

$$CO + \tfrac{1}{2} O_2 \rightarrow CO_2$$

Eq. 3-19

$$\frac{dC_{co}}{dt} = -r_{co-o2}.C_{co}.C_{o2}^{0.5}.C_{H2O}^{0.5}[mol.m^{-3}s^{-1}]$$

Eq. 3-20

where,

$$r_{co-o2} = K_2 \exp(-\frac{E_2}{RT})$$

Eq. 3-21

$$C_{co} = \frac{\rho_{co}}{M_{co}} = \frac{\rho.\omega_{co}}{M_{co}}$$

Eq. 3-22

$$C_{O2} = \frac{\rho_{o2}}{M_{o2}} = \frac{\rho.\omega_{o2}}{M_{o2}}$$

Eq. 3-23

$$C_{co} = \frac{\rho_{co}}{M_{co}} = \frac{\rho.\omega_{co}}{M_{co}}$$

Eq. 3-24

$$C_{H_2O} = C.X_{H_2O} = \frac{\rho}{M}.X_{H_2O}$$

Eq. 3-25

Here, K_2=1.3x10^8 [m^3.mol^{-1}.s^{-1}], E_2=126[kJ.mol^{-1}].

3.4.1.3.5. Mesh

A grid adaptation of FLUENT was used in this multi-component model. In the pipe and tank region near the ball valve, denser meshes are generated since the species gradients would be higher in these regions. In addition, through grid adaptation technology, the mesh regions with higher mesh densities move with the species gradient frontiers which determines the convergence speed of every time step. For the grid adaptation technology, see the Chapter 23 of Reference [17].

3.4.1.3.6. Results

In the transient calculation of the multi-component experiment, lower time steps, 0.001-0.01 second, are used for the initial simulation due to the higher species concentration gradients near the ball valve regions. With the decrease of the gradients, time steps are increased to 1.5 seconds. Compared with the former two cases, Isothermal and Non-Isothermal experiments, this is much more time consuming calculation since besides the heat transfer and the natural convection, complicated mass transport and chemical reactions are modeled in the multi-component. For detailed model summary, see the

Appendix 10. Figure 3-38, Figure 3-39 and Figure 3-40 show the comparisons between the calculation and the experiment for the mole fraction changes of O_2, CO and CO_2 at various locations in the experiment. The results show quite good agreement with experiment at the measured points for O_2, CO and CO_2 mole fractions. The FLUENT code also predicts well the onset of natural circulation.

Shown on Figure 3-38 are the point 1 mole fractions calculated compared to the experimental results for O_2, CO and CO_2. While the oxygen is slightly over-predicted below the heated graphite region, there is good agreement with the CO and CO_2 mole fractions as a function of time. The onset of natural circulation is predicted to within less 10% of the actual experimental result.

Shown on Figure 3-39 are the point 3 mole fractions just above the heated graphite zone. This figure shows that all of the oxygen is consumed in the graphite zone until natural circulation begins rapidly. This figure also shows that the predominant species at Point 3 is CO_2 and that the concentration of CO is relatively low (less than 3%). This potentially an important finding relative to "burning" since CO is subject to oxidation forming CO_2 which can be considered "burning.

At Point 4, on the cold leg, Figure 3-40 shows that the oxygen level initially increases due to cold leg diffusion but it is then reduced by the CO and CO_2 gas mixture which diffuses to Point 4. In addition, some of the oxygen reacts with the CO to form CO_2 increasing its mole fraction while reducing the oxygen.

Once natural circulation starts, the dominate species is oxygen as shown on all figures with the concentrations of CO and CO_2 dropping quickly and dramatically. During the natural circulation phase, the air ingress velocity is calculated to be 0.04m/s. In addition, the graphite consumption rate shown on Figure 3-41 dramatically increases as expected to 2.3E-07 kg/s from 1.3E-8 kg/s during the diffusion process. This higher reaction rate is due to the surface chemical reaction rather than the volumetric diffusion reaction experienced during the diffusion stage. This is because the gas mixture moves at a higher

velocity through the graphite pipe before it can diffuse into the graphite for the volumetric reaction.

More important, through the CFD calculation, many critical points are identified for further numerical study on the air ingress accident:

- The ratios between the CO and CO_2 on the graphite surface should be measured for the further CFD simulation.
- Besides the influence of the temperature, the roles played by graphite impurity should be studied carefully in the surface and the volume reactions.
- The reverse chemical reactions must be modeled in the dynamic processes (they are modeled in FLUENT model).
- The diffusion coefficients in the multi-component system are key parameters because they depend on the local concentration of all the gases involved, and the onset of the natural convection is mainly determined by the diffusion of the heavier gases.

In conclusion, natural circulation occurs in the multi-component experiment when the buoyancy produced by density difference between the hot and cold leg is high enough to overcome the friction in the flow path. Almost all the oxygen will be consumed in the diffusion stage, but in natural circulation stage, most of the oxygen will escape from the graphite pipe. Moreover, the dominant reaction production is CO_2, not CO due to the rapid CO oxidation rate and high oxygen concentration, while most of the immediate product at the graphite surface is CO.

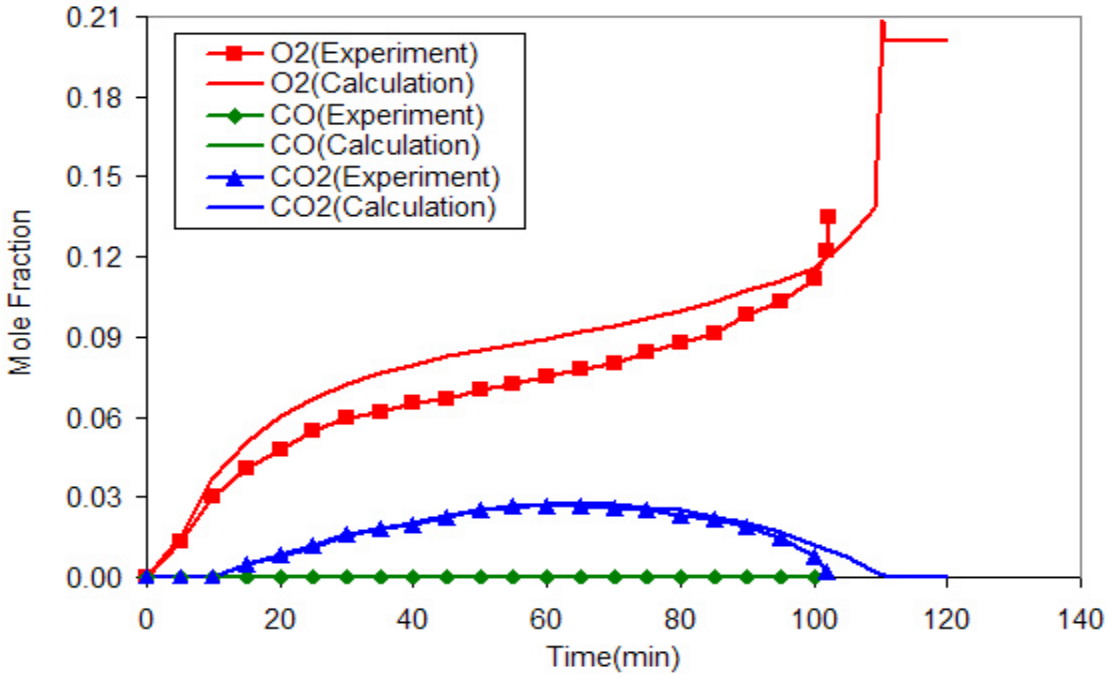

Figure 3-38: Mole Fraction at point-1

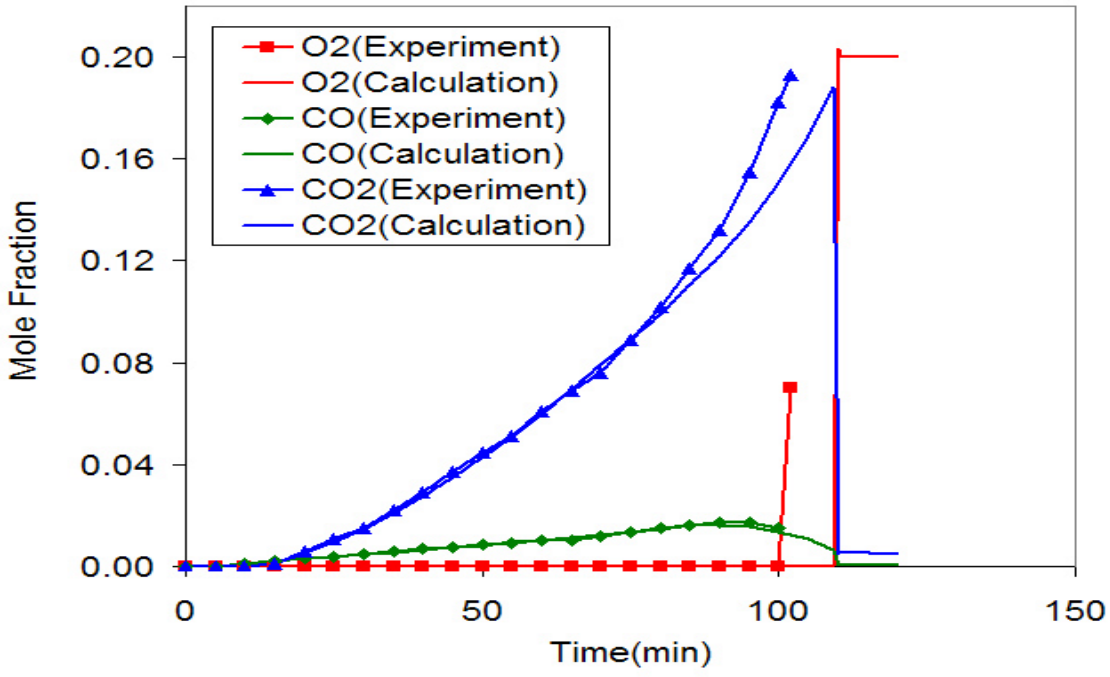

Figure 3-39: Mole fraction at point-3

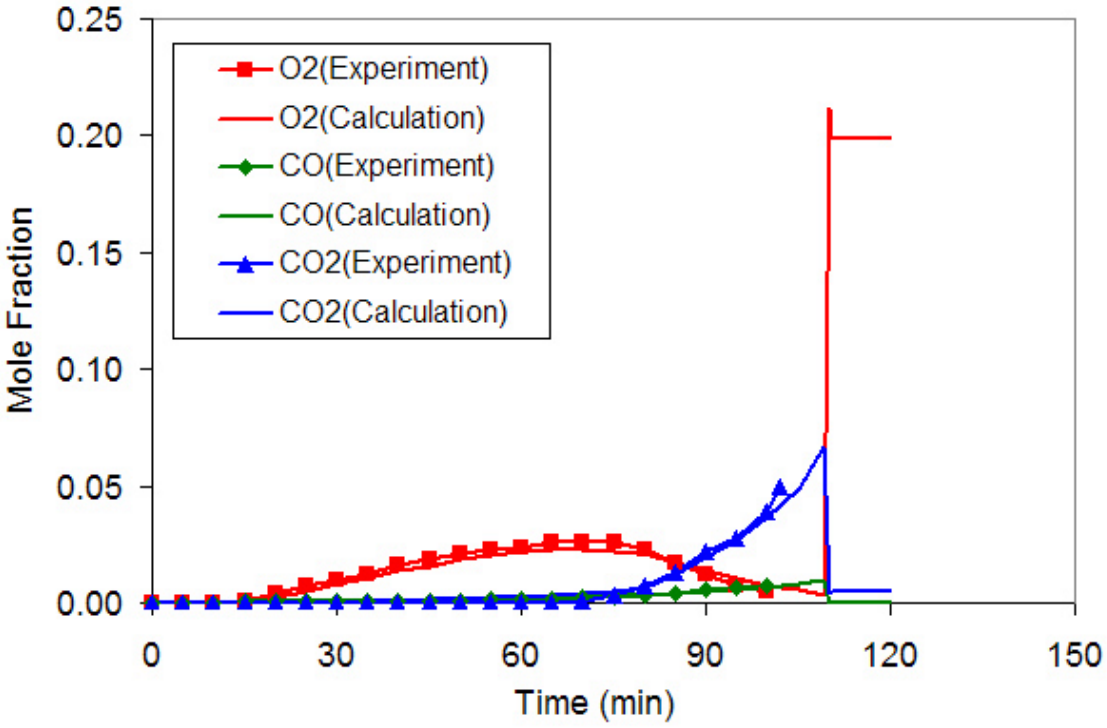

Figure 3-40: Mole Fraction at point-4

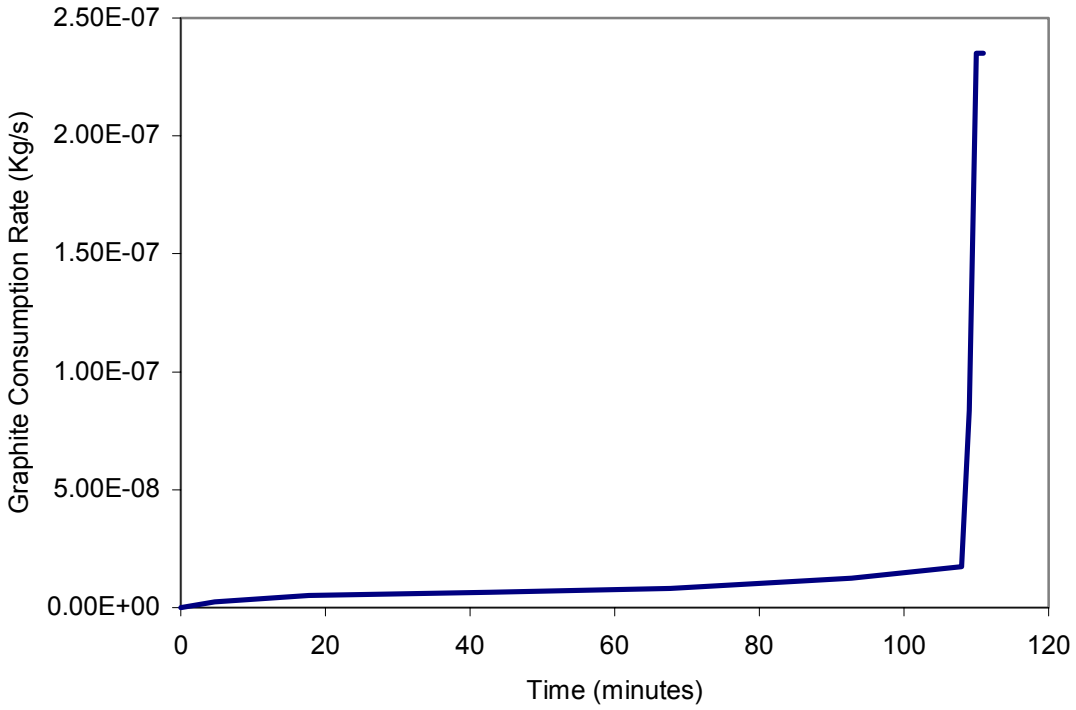

Figure 3-41: Graphite Consumption Rate (FLUENT6.0 calculation)

3.4.2. The NACOK Natural Convection Corrosion Experiment

NACOK Natural Convection Corrosion experimental facility [**Na**turzug im **Co**re mit **K**orrosion] at the Julich Research Center in Germany was built to study air ingress accidents in pebble bed reactors. There have been two significant air ingress tests performed at the facility. The first is a natural circulation flow test measuring mass flow rates at various hot and cold leg temperature through actual size ceramic pebbles. The second test was to an open chimney corrosion test simulating the lower reflector and smaller graphite pebbles[14]. Both tests are important research contributions to improved understanding of the unique characteristics of air flow in pebble bed reactors. In this thesis, the FLUENT code will be used to model the first series of mass flow tests.

3.4.2.1. Experimental Apparatus

The NACOK experimental facility is shown on Figure 3-42. It is schematically represented in Figure 3-43, and the Figure 3-44 shows the profile defined by GAMBIT Code. The left square channel is called experiment channel, and the right pipe return pipe. The left channel, with 0.3m x 0.3m square cross section, has a height of 7.3 meters, and the pebble bed with a height of 5 meters is installed in the experiment channel. The horizontal and the returning pipe have a diameter of 0.125 meter.

In the mass flow experiment, forty individual runs in four series were made to study the features of the mass flow rates corresponding to the different temperature distributions in the experiments. For the first series of experiments, the temperature in the returning pipe is kept at 200 °C while the temperatures in the experiment channel are 250°C, 300°C, 350°C, 400°C, 450°C, 500°C, 550°C, 600°C, 650°C, 700°C, 750°C, 800°C, 850°C, 900°C, 950 °C and 1000°C respectively. Similarly, for the second series of experiments, the temperature in the returning pipe is kept at 400 °C while the temperatures in the experiment channel are 450°C, 500°C, 550°C, 600°C, 650°C, 700°C, 750°C, 800°C,

850°C, 900°C, 950°C and 1000°C respectively. Table 3-5 shows the temperatures for the experiment channel and the returning pipe.

Series	Average wall temperature of the Returning Pipe	Average wall temperature of the Experiment Channel
1	200	250°C, 300°C, 350°C, 400°C, 450°C, 500°C, 550°C, 600°C, 650°C, 700°C, 750°C, 800°C, 850°C, 900°C, 950 °C and 1000°C
2	400	450°C, 500°C, 550°C, 600°C, 650°C, 700°C, 750°C, 800°C, 850°C, 900°C, 950°C and 1000°C
3	600	650°C, 700°C, 750°C, 800°C, 850°C, 900°C, 950°C and 1000°C
4	800	850°C, 900°C, 950 °C and 1000°C

Table 3-5: The Temperatures for the Experiment Channel and the Returning Pipe

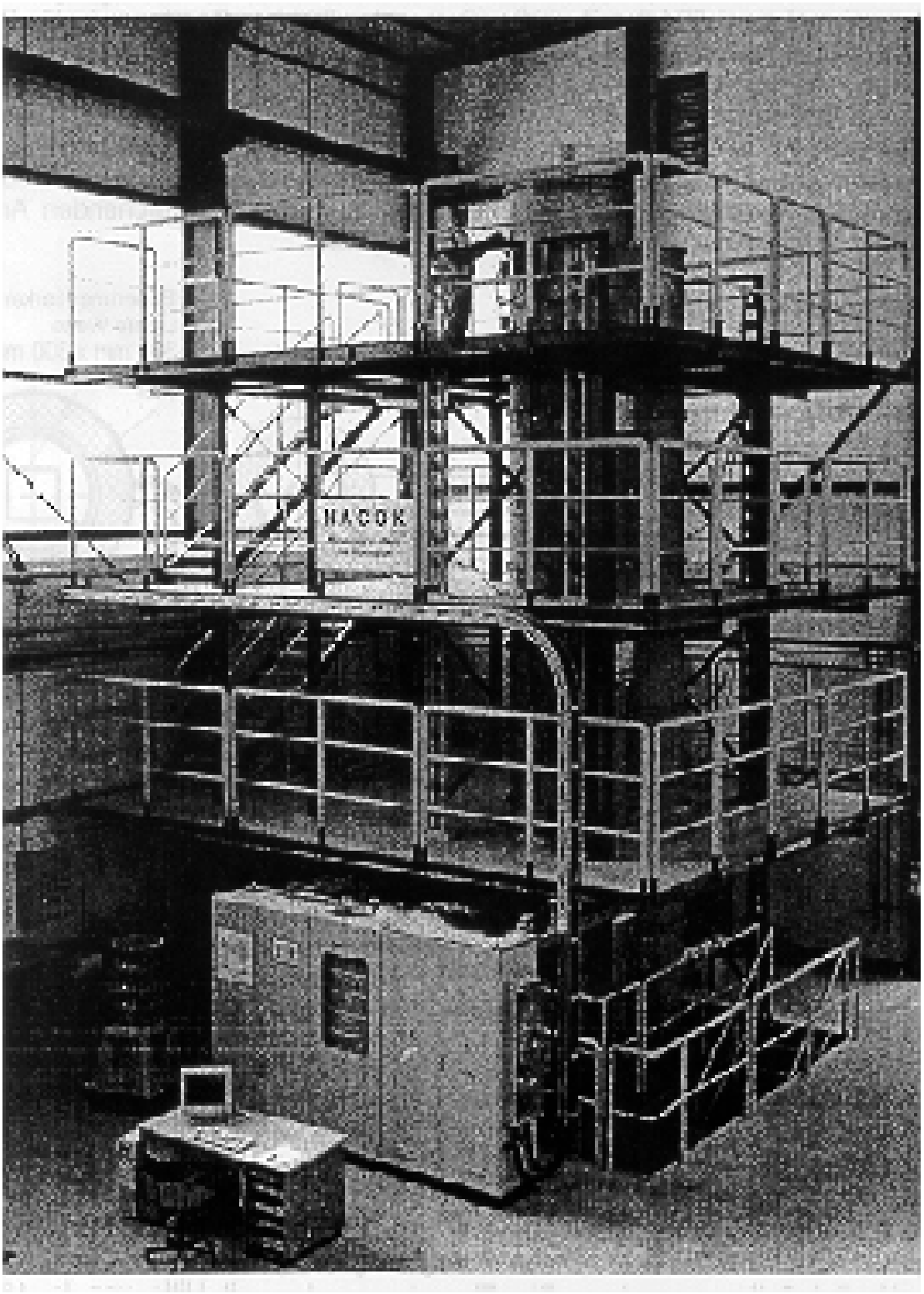

Figure 3-42: NACOK Experimental Apparatus [14]

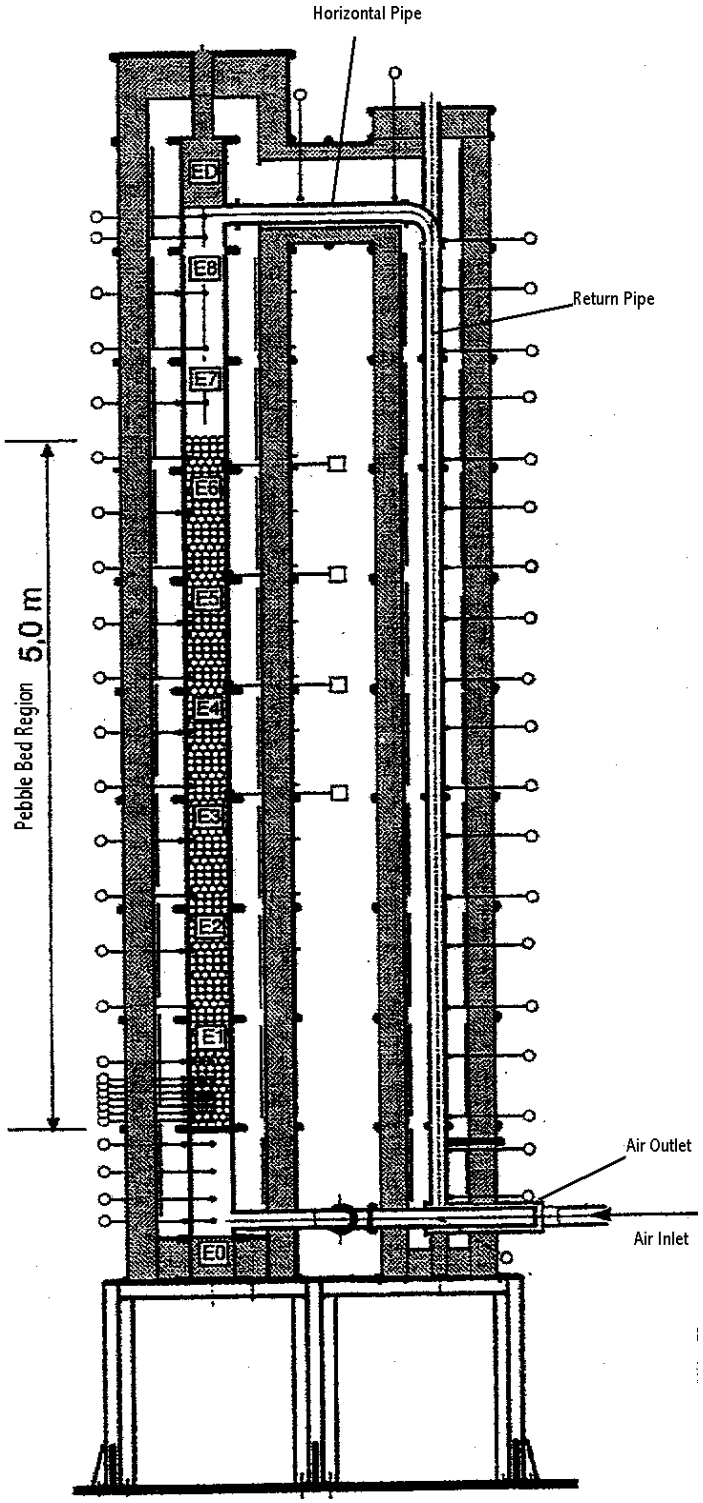

Figure 3-43: The Profile of the NACOK Experimental Apparatus [14]

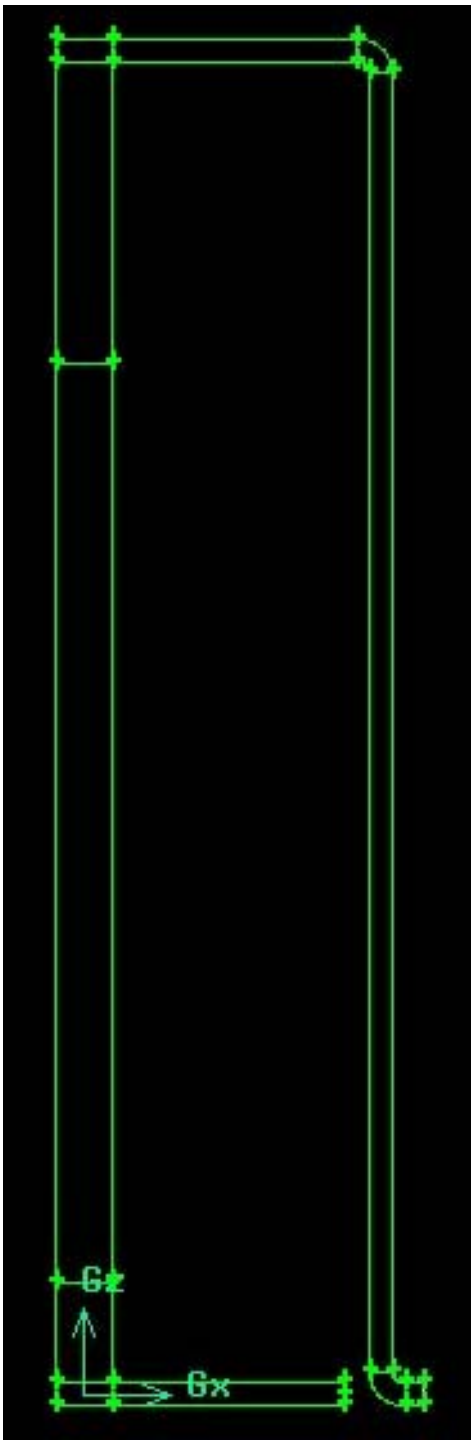

Figure 3-44: The Profile of the NACOK Natural Ccirculation Experiment Defined by GAMBIT

3.4.2.2.FLUENT Model

One of the key challenges in modeling experiments is knowing the exact test configuration. Actual size 6 cm ceramic pebbles were arranged in the experimental channel in a 5 x 5 configuration (see Figure 3-45). In order to calculate the average porosity, the total number of the pebbles needs to be obtained. Figure 3-46 shows the regular distribution of the pebbles. It is clear that Pebble A, D and E are in one plane, and the half distance between Pebble A and D is $(\sqrt{2})*r$. From Figure 3-47, the height of a layer should be equal to $(\sqrt{2})*r$. Therefore the total number of layers is $5/(\sqrt{2})*r = 5/(\sqrt{2}*0.03) = 118$. Then, the average prorosity is:

$$Poro = 1 - \frac{\frac{N}{2}(n_{more} + n_{less})*\frac{4}{3}*\pi*r^3}{l^2*H} = 1 - \frac{\frac{118}{2}(25+16)*\frac{4}{3}*3.14*0.03^3}{0.3^2*5} = 0.392$$

Eq. 3-26

N: the total layers of the pebbles,

n_{more}: the total numbers of pebbles of a layer with more pebbles,

n_{less}: the total numbers of pebbles of a layer with less pebbles,

r: the radium of the pebbles,

l: the side length of cross section of the square channel,

H: The height of the pebble bed region

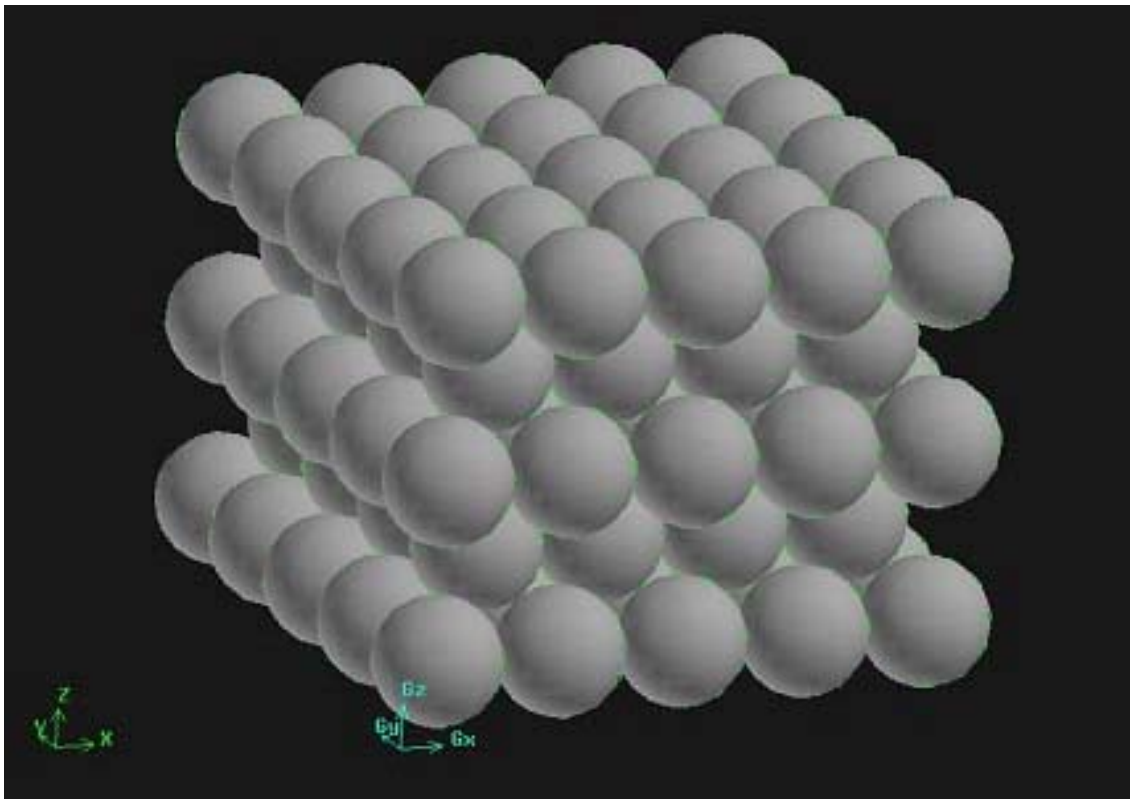

Figure 3-45: The Configuration of Pebble Bed

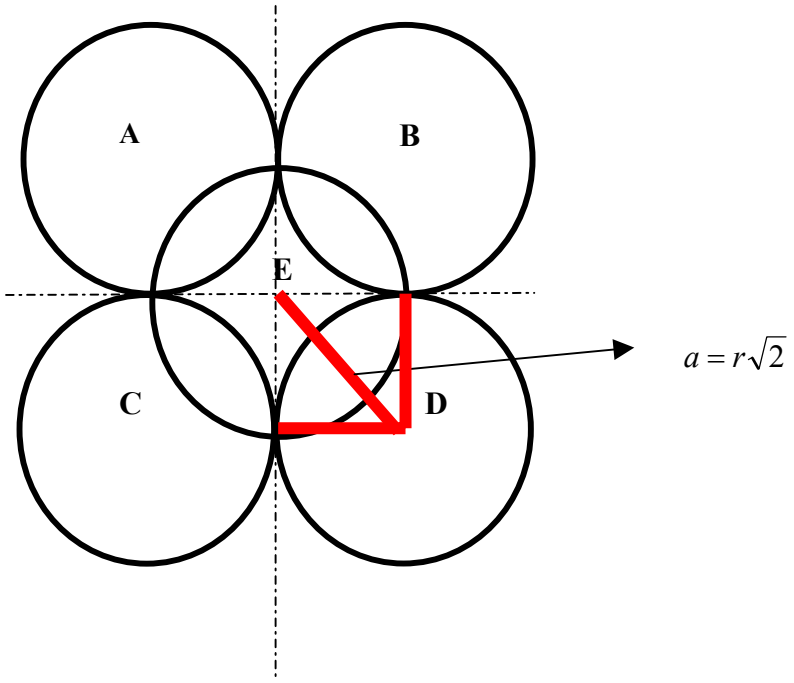

Figure 3-46: Cell Configuration of the Pebble Bed

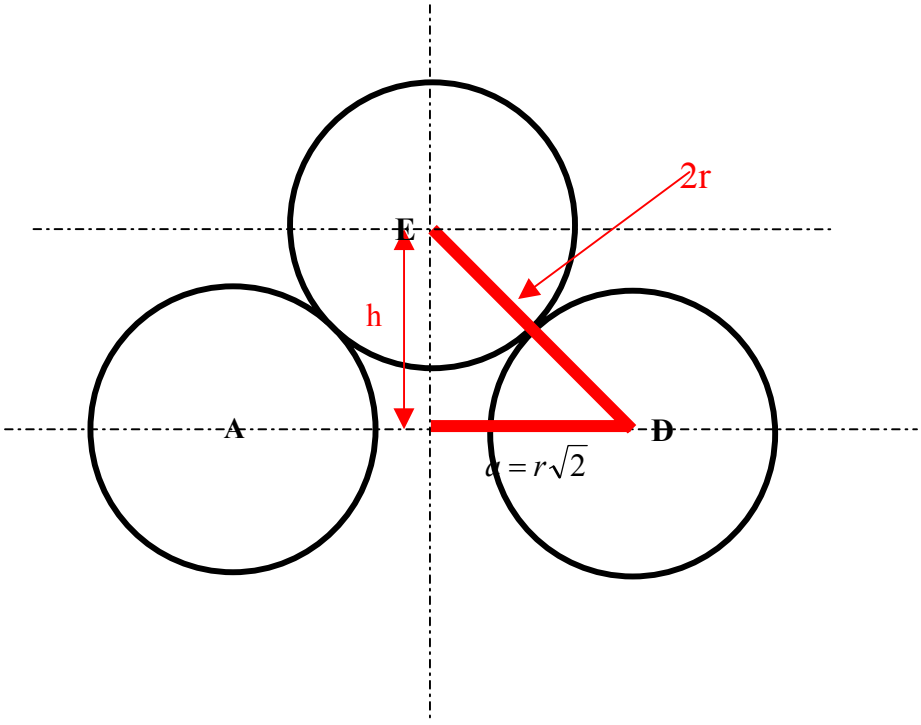

Figure 3-47: The Side View of the Pebble Geometry

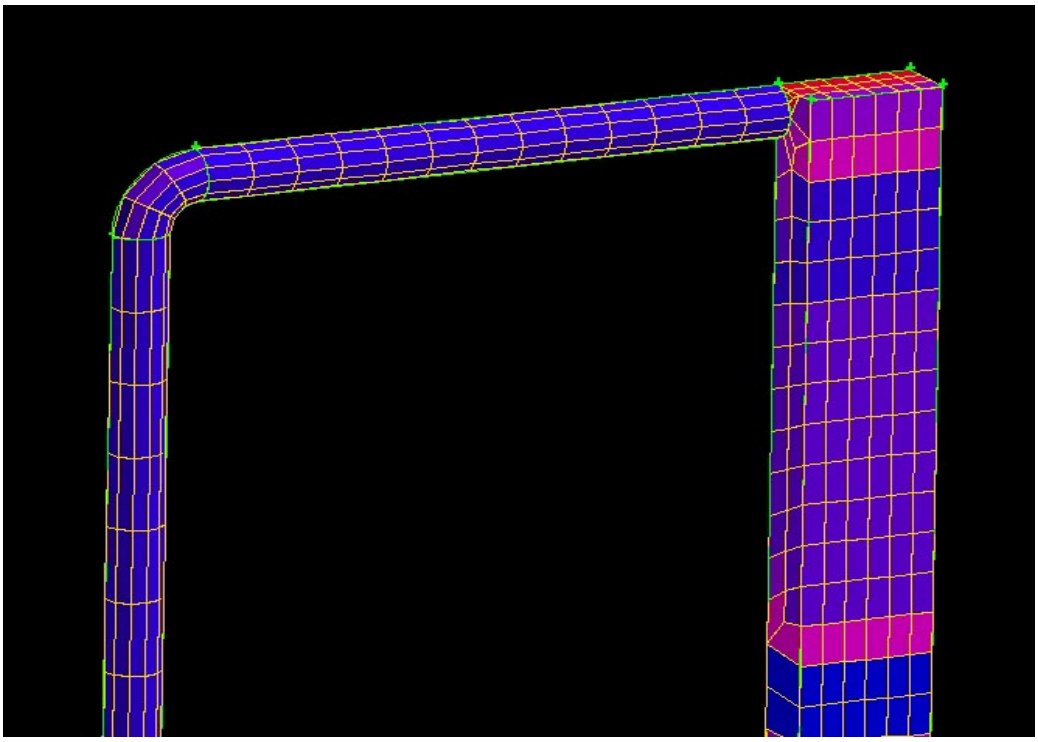

Figure 3-48: The Meshes Generated for the Top Structure

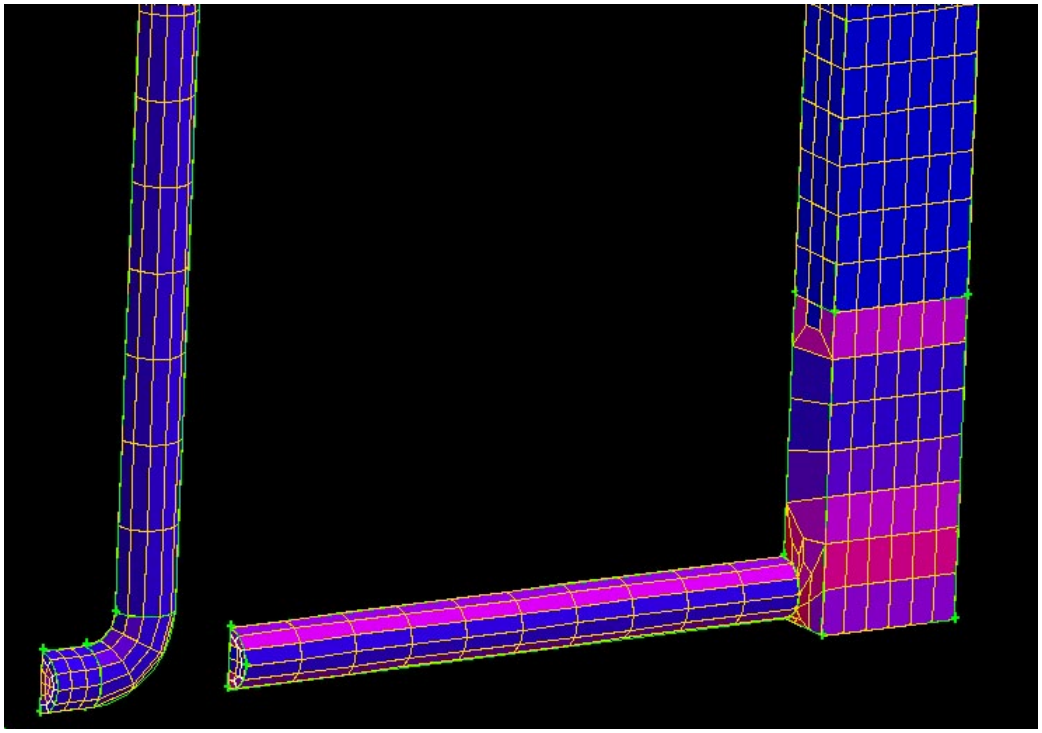

Figure 3-49: The Meshes Generated for the Bottom Structures

Compared with the lower laminar pressure loss in the return pipe and horizontal pipe, the pressure loss in the pebble bed region is much higher: Besides the much higher surface areas of the pebbles, the gas complicated flow path among the pebble lead to a higher form pressure loss. The pressure drop used in the pebble region is the pressure drop formula recommended by Julich Research Institue for this NACOK configuration [14]:

$$\Delta P = -\frac{a}{\mathrm{Re}/(1-\varepsilon)} - \frac{b}{(\mathrm{Re}/(1-\varepsilon))^{0.1}}$$

Eq. 3-27

a: the coefficient for laminar pressure loss,

b: the coefficient for form pressure loss

d: the diameter of the pebbles

ρ: the fluid density

η: fluid dynamic viscosity

u: the gas velocity

ε: the porosity of the pebble bed

This pressure drop could not defined directly in FLUENT, however, it could be converted into the following format from Eq. 3-27:

$$\Delta P = -C_1 * \eta * u_z - C_2 \rho^{0.9} * \eta^{0.1} * u_z^{1.9}$$

Eq. 3-28

C_1, C_2: constants

η: fluid dynamic viscosity

ρ: the fluid density

u_z: the fluid velocity in z-coordinate direction

User Defined Function was developed to define the pressure drop (see Appendix 15). In every iteration, the FLUENT server will access to the UDF to calculate the pressure drop using current and local thermal properties and velocity in z direction.

The structures and mesh generated using GAMBIT2.0 are shown in Figure 3-48 and , and the total mesh number is 11,682.

The conductivity and specific heat of the pebbles are shown in
Figure **3-50** and Figure 3-51 [6]. The conductivity, specific heat, density and viscosity of the air are defined accurately using 12 samples as a function of temperature (Shown in Figure 3-52, Figure 3-53, Figure 3-54 and Figure 3-55, respectively). See Appendix 14 For detailed model description on the NACOK experiment.

3.4.2.3.Results and Conclusions

Shown on Figure 3-56 re the mass flow rates predicted versus the experimental results for the four series of experiments. The FLUENT code as applied yields excellent agreement with experiment. In order to achieve such good results, the pressure drop equation (see Eq. 3-7) described above was benchmarked at a point (the experiment with 400 °C cold leg and 700°C hot leg) to calculate the friction loss constants (a and b in Eq. 3-28) which was used for all subsequent experiments. Instead of the 505 used by the Germans in their analysis [14], 202 was found to be the appropriate constant. This adjustment was necessary since FLUENT calculates the laminar pressure loss on the channel wall automatically, the value of a should be lower than 505 in the UDF.

In the experimental results, the mass flow rate decreases with the temperature increase in the returning pipe since the buoyancy would be reduced by the lower temperature difference between the cold leg and the hot leg. More importantly, the interesting result is that the mass flow rate not always increase with temperature increase in the experiment channel. Actually, in the former theoretical analysis, these results were predicted.

In conclusion, the FLUENT code with appropriate understanding of the experimental configuration and how FLUENT actually performs its analysis, has been shown to represent the natural steady state circulation in a pebble bed in a large range of hot and

cold leg temperature differences. This capability will be applied to future modeling of the NACOK experiments in which air, a reflector and graphite pebbles will be introduced.

3.4.3. Future Work

In order to develop a benchmarked computational fluid dynamics capability to analyze the complexity of air ingress accidents, the next NACOK test in which actual corrosion in graphite pebbles was tested will be analyzed. This test is documented in [14]. While this test was an open chimney test, it will allow the CFD modeling to be benchmarked for future tests planned at NACOK.

The Julich Research Center is planning another series of tests in the fall of 2004. This series of tests is intended to be representative of hot and cold legs in an actual pebble bed reactor air ingress condition. Once this methodology is benchmarked using the open chimney NACOK test, it will be used to provide pre-test predictions of this new series of tests. It is hoped that MIT will be participating in the actual test program in the data collection phase. Once completed, the post test analysis will be performed and the code methodology will be benchmarked for use in reactor calculations.

Once benchmarked, this methodology will be applied to the actual pebble bed reactor to predict the progress of air ingress events. Shown in Figure 3-57 and Figure 3-58 are early models of the actual pebble bed reactor that will form the structure of the model. Since FLUENT is a code that takes a long time to run, it is likely that only a 30 degree segment would be modeled (shown in Figure 3-59). The future work also includes linking the FLUENT code with a systems analysis code that better represents the balance of plant of an actual reactor.

In order to simplify future calculations, single and multiple pebbles will be modeled to understand the details of the surface chemical reactions in a pebble bed reactor. Shown in Figure 3-60 are the five pebbles in which surface chemical reactions were modeled with

air flowing around the pebbles. These smaller models will be used to provide a better understanding of the pebble dynamics that would be used to confirm the more simplistic porosity assumption used in FLUENT. Should this be successful, tens or hundreds of pebbles would be modeled in detail to generate the desired database, such as regional chemical reaction rates in the pebble bed. This database obtained will be used in the real PBMR calculation, in which the pebble bed would be modeled as porous media and a bottom reflector would be analyzed in detail since it is expected that most of the chemical reactions occur in this area.

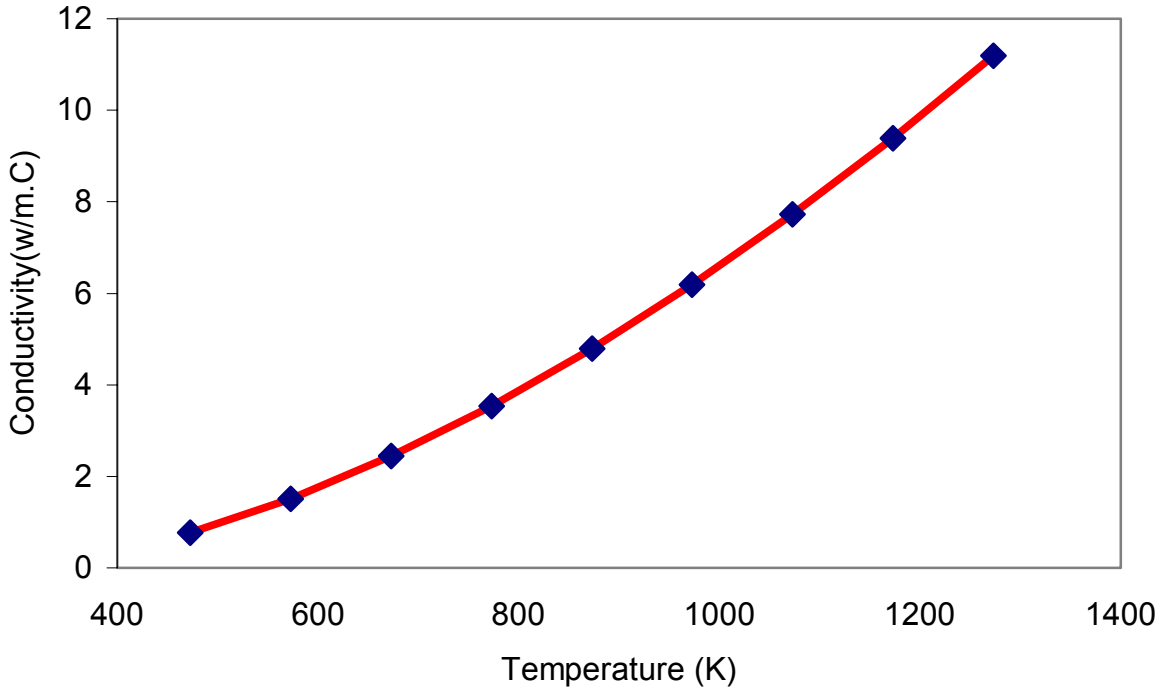

Figure 3-50: Conductivity of the Pebbles

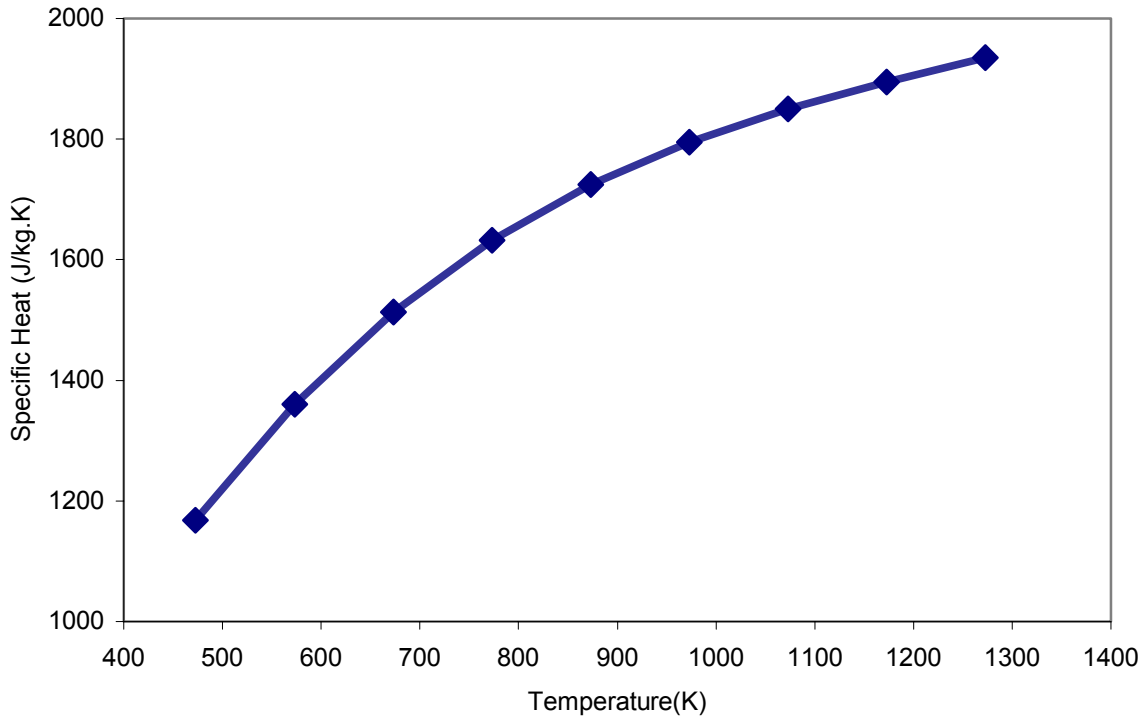

Figure 3-51: The Specific Heat of the Pebbles

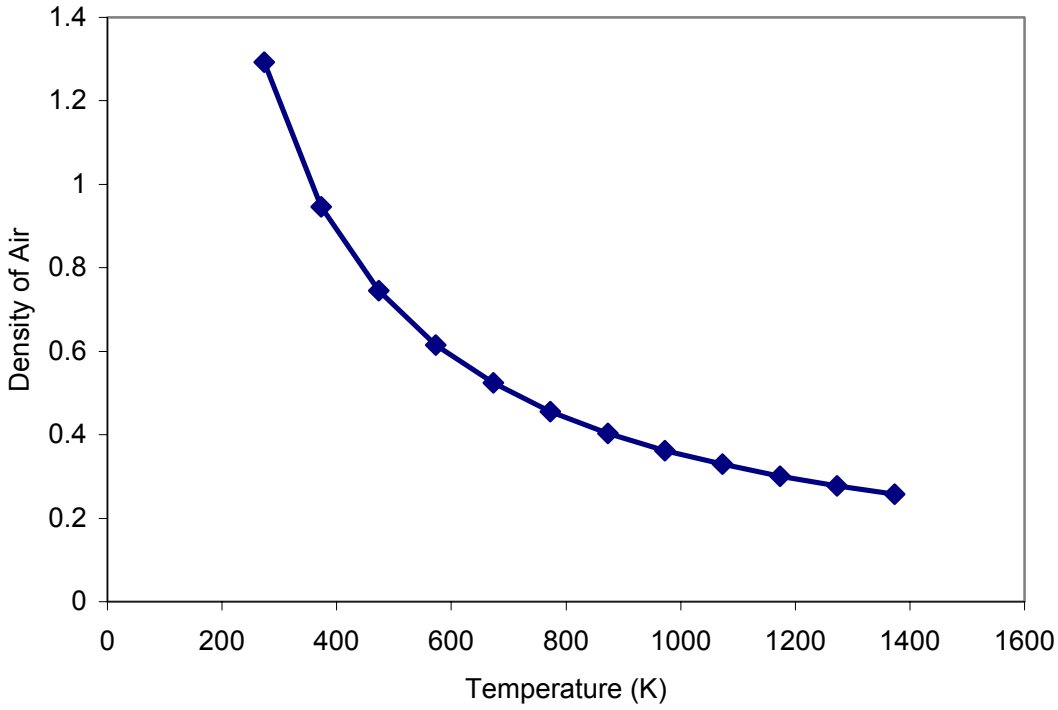

Figure 3-52: The density of Air

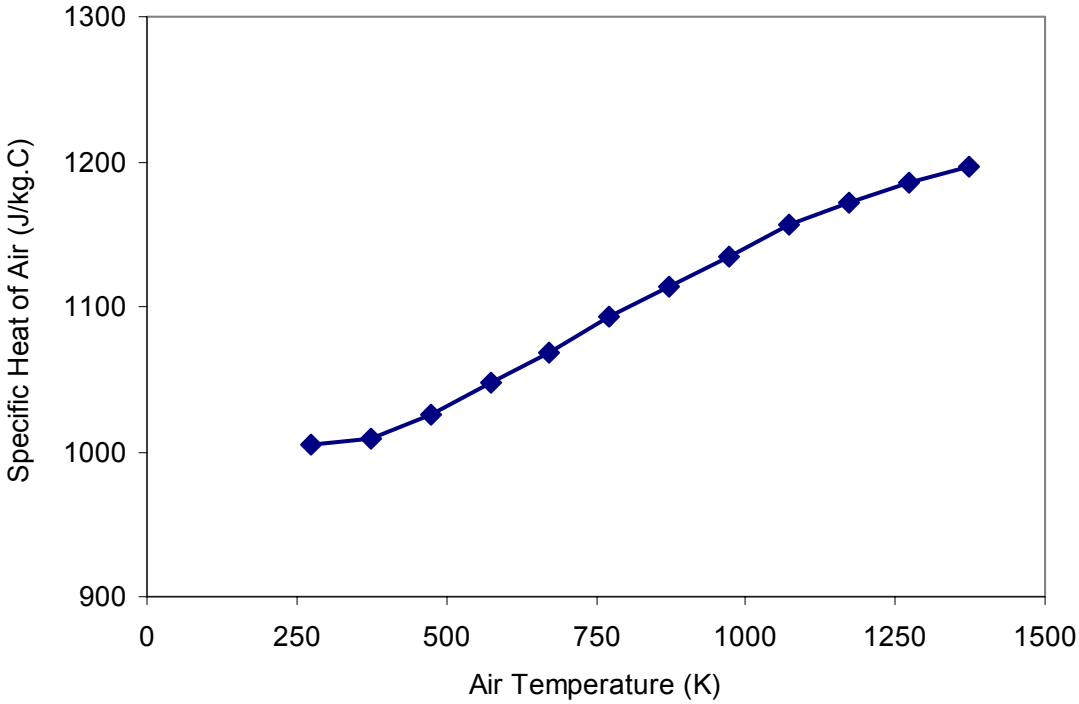

Figure 3-53: The Specific Heat of Air

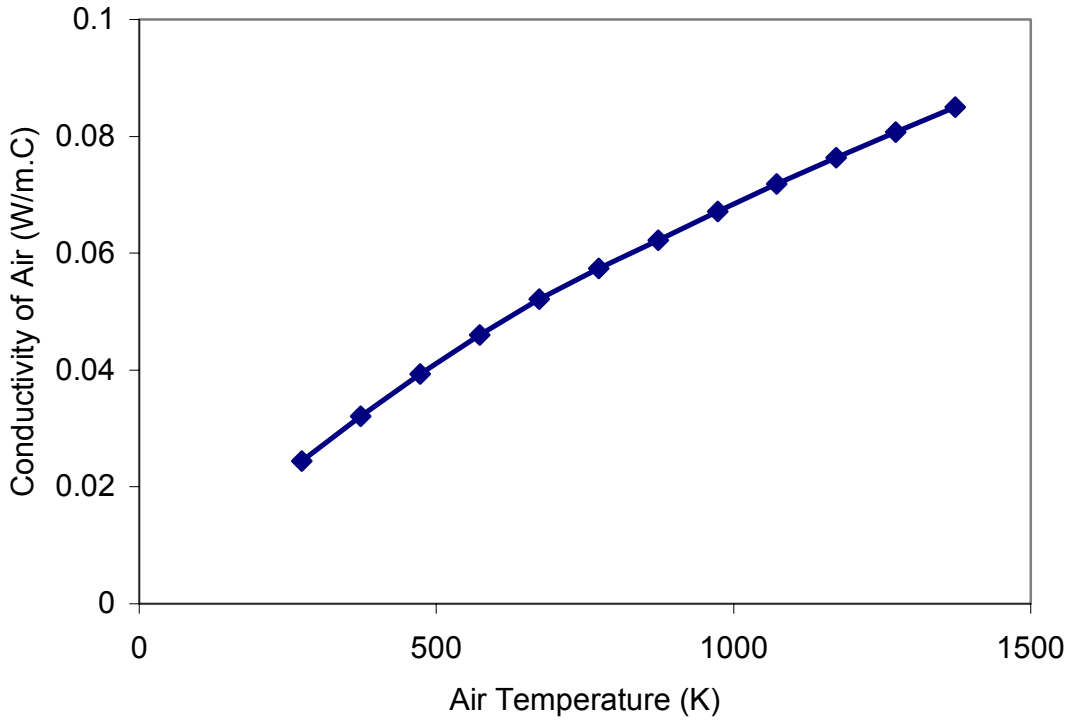

Figure 3-54: The Conductivity of Air

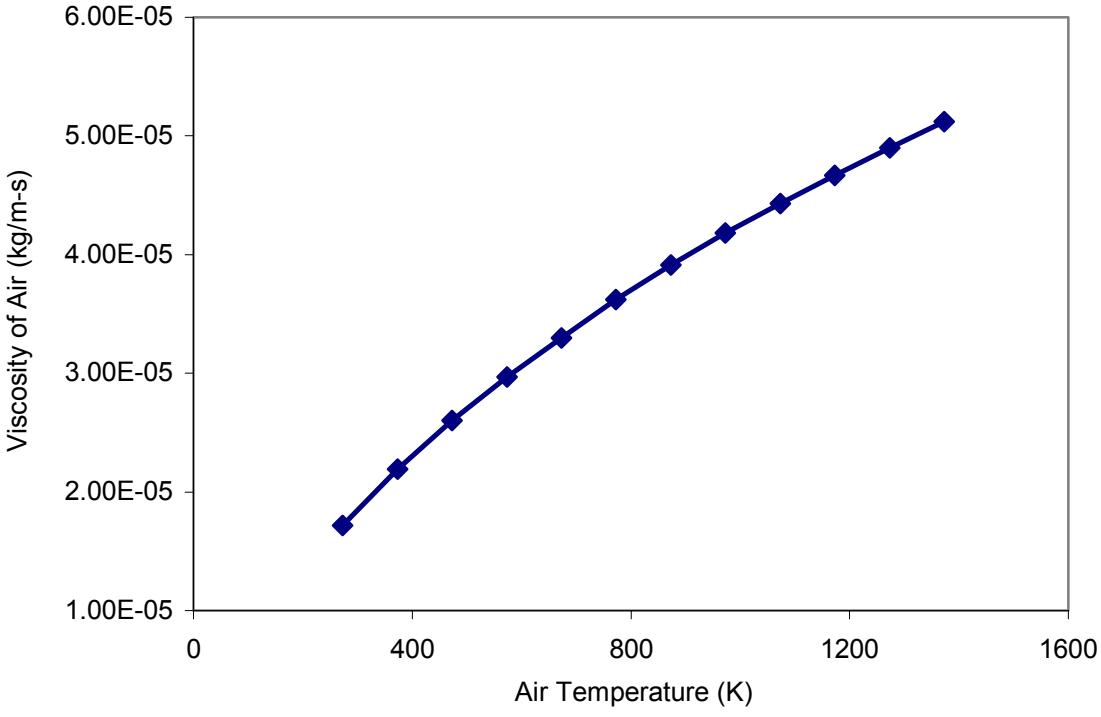

Figure 3-55: The Viscosity of Air

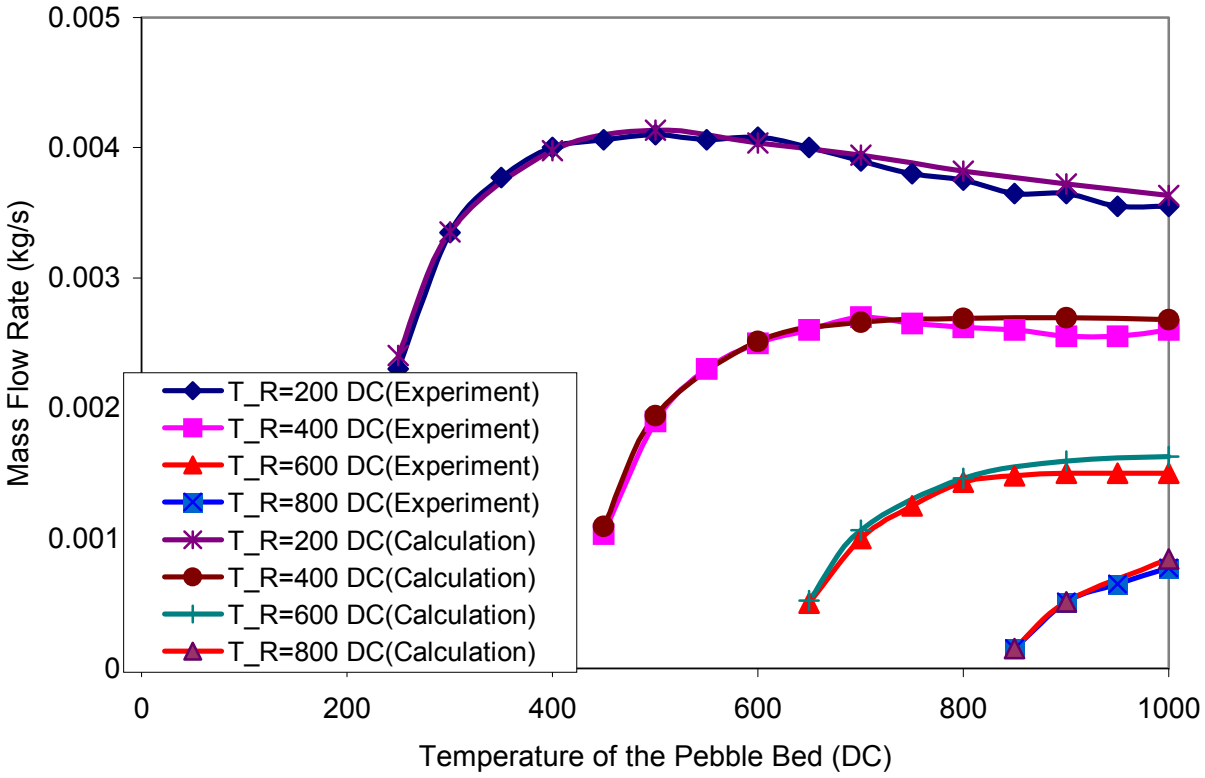

Figure 3-56: The Comparison between Experiments and Calculations

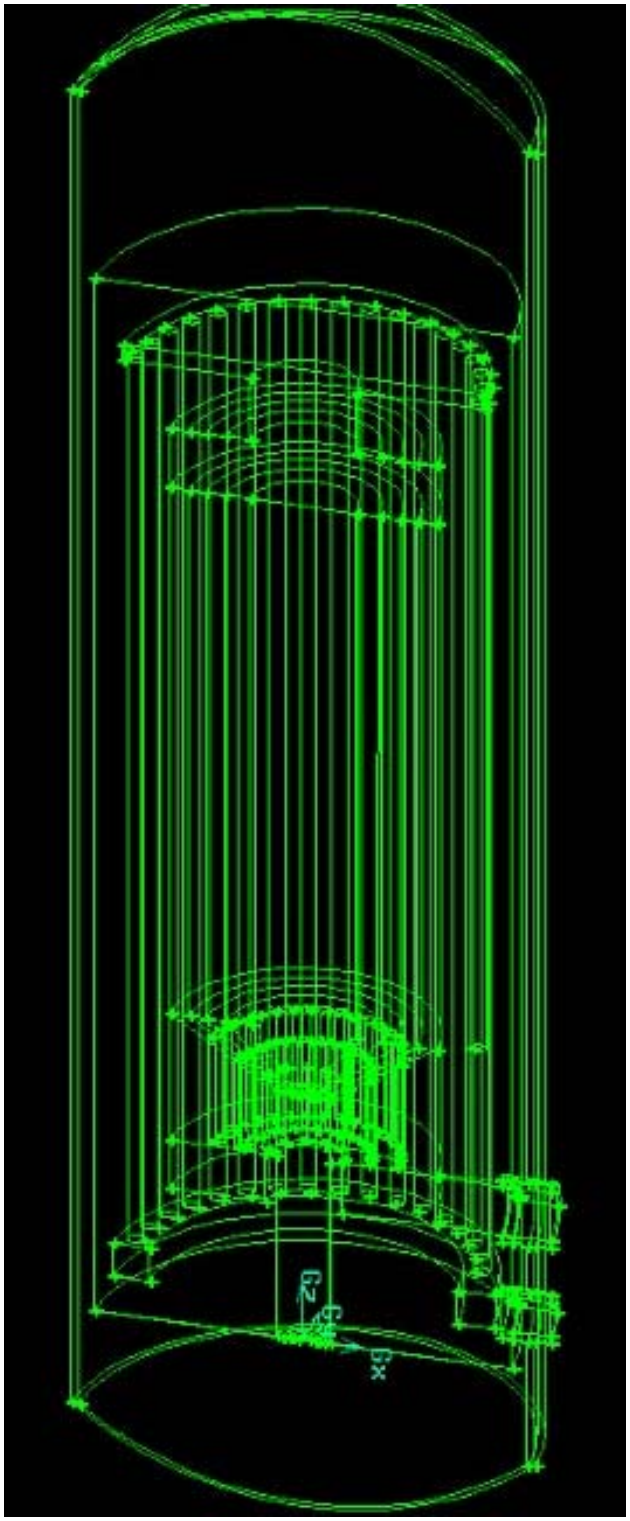

Figure 3-57: The Overall Geometry of a PBMR

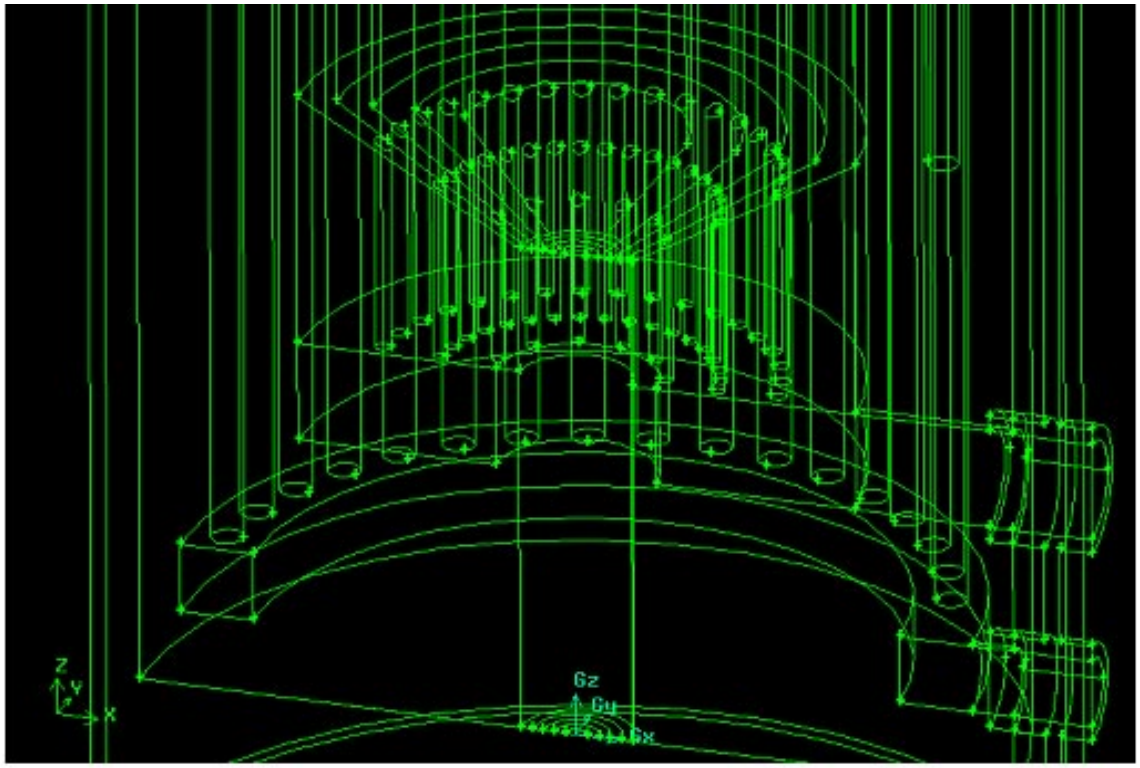

Figure 3-58: The Bottom Reflector of a PBMR

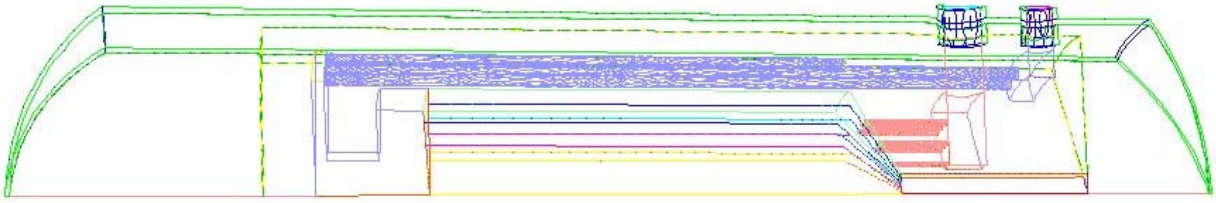

Figure 3-59: The 30-degree Model for a PBMR

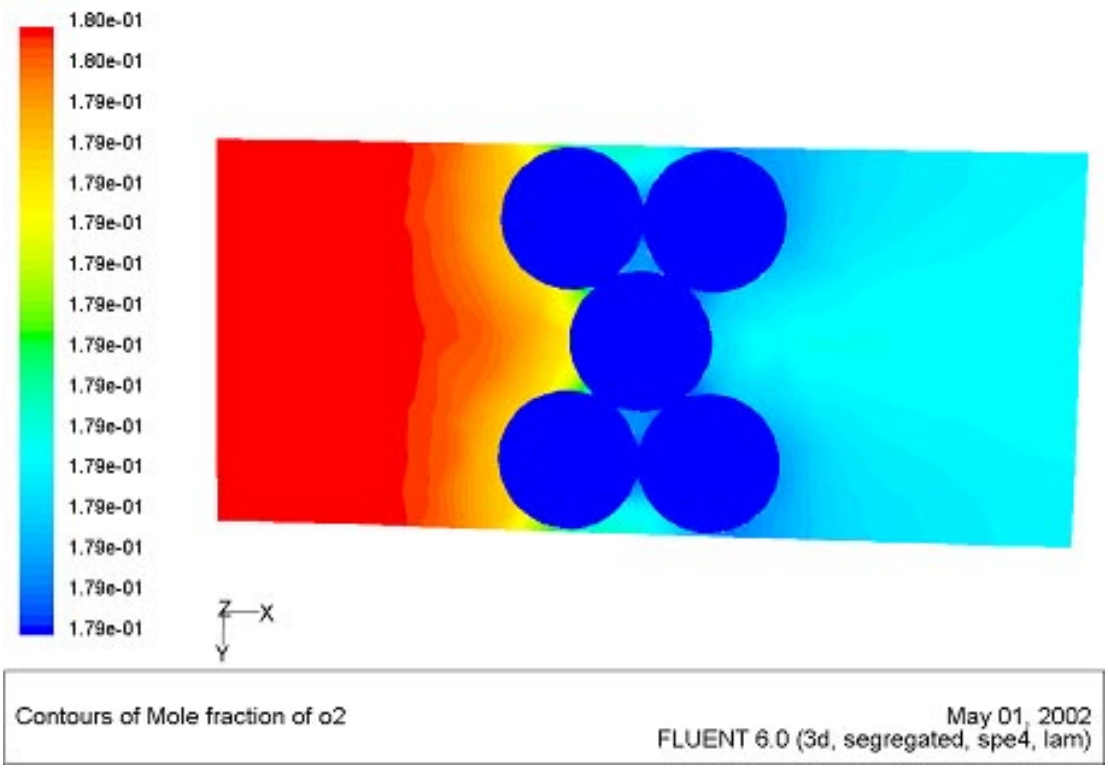

Figure 3-60: The Test Model to the Future Detailed Study

4. Conclusions and Future Work

The objective of this thesis was to investigate the key safety features of the pebble bed reactor under challenging conditions. The first part of the thesis explored the "no meltdown" claim of the proponents of the technology without the use of any active emergency core cooling systems after a loss of coolant accident. Using a conservative HEATING-7 analysis which modeled the PBMR core, reactor vessel, reactor cavity, concrete and soil ultimate heat sink in which no convective heat transfer as assumed, it was shown that the peak fuel temperature was approximately 1642 C approximately 92 hours after the initial loss of coolant which is about 1000 °C below the UO2 fuel melting temperature, ~2700 °C [27]. Sensitivity studies also showed that the peak fuel temperature was insensitive to many parameters, the most important of which was believed to be the emissivity of the reactor vessel.

It was established that although the fuel would not melt, the temperature of the reactor vessel and the reactor cavity concrete exceeded design limits. A separate study by Professor Hee Cheon No using new code developed for this application (PEB-SIM) confirmed the HEATING-7 peak temperature results without convection cooling in the reactor cavity. His analysis was extended to perform a sensitivity study to determine how much air would have to be circulated in the reactor cavity to bring the temperatures of the reactor vessel and reactor cavity within design limits. This study showed that approximately 6 m/s of air flow would be required. The study also showed that the peak fuel temperature was unaffected by the reactor cavity cooling system. The conclusion was that although the core will not melt even under these very conservative conditions by a large margin, some form of reactor cavity cooling system will be required to keep the reactor vessel and reactor cavity concrete within design limits. Future work in this area will be the design of a passive reactor cavity core cooling system based on the design inferences identified in this study.

The second part of this thesis was to develop a better understanding of the details of air ingress accidents in pebble bed and prismatic reactors. A theoretical study of an open cylinder of pebbles to better understand the key processes involved in air ingress was performed using the previous results from the LOCA analysis as initial conditions. The HEATING-7 model with side calculations to model the buoyancy and resistance to flow in a pebble was used to predict the peak fuel temperatures and air ingress velocity. The results of this simple analysis showed that that heat source contribution from the chemical reaction was relatively low and confined to the lower reflector region. The peak temperature increase from the non-chemical LOCA analysis was about 21 °C (a maximum of 1663 °C at 92 hours). Dr. No's analysis using PEB-SIM with chemical reactions showed similar results (peak temperature of 1617°C at 80 hours). The other interesting result was that the air ingress velocity decreased after about 350 °C. This negative feedback could be a significant factor in air ingress accidents in real reactors since the average post LOCA temperature in the reactor is on the order of 1300 °C.

Using these fundamental insights, attention was then focused on developing a benchmarked computational fluid dynamics modeling capability for air ingress events. Two series of tests were used to benchmark the CFD code selected for this analysis – FLUENT 6.0. The first series of tests were performed at the Japan Atomic Energy Research Institute (JAERI). These tests were aimed at understanding the fundamental processes of air ingress accidents in separate effects tests. There are initial diffusion, natural circulation and the chemical reactions with heated graphite in a prismatic reactor configuration. The FLUENT model and methodology developed was able to predict each of these tests quite well.

The second experimental benchmark was the Julich Research Center test performed at the NACOK facility. This series of tests was to model natural circulation in a pebble bed reactor under varying hot and cold leg temperatures to assess air mass flow rate. The FLUENT methodology developed was able to predict the mass flow rates for the 40 experiments with very good results. This work will be used to benchmark the NACOK chemical corrosion tests in the future. A outline for the work plan for continuation of this

work has been prepared for development of a benchmarked CFD capability to analyze the details of air ingress accidents for real reactors.

Reference:

[1] Moormann, R., November 1983. "Graphite oxidation phenomena during massive air ingress accidents in nuclear high temperature gas cooled reactors with pebble bed core," Berichte der Bunsengesellschaft fuer Physikalische Chemie. Ber. Bunsenges. Phys. Chem. V. 87(11) p. 1086-1090. CODEN: BBPCA.

[2] Kadak, A.C., Ballinger, R.G., "Modular Pebble Bed Reactor Project, Fourth Annual Report" MIT-ANP-PR-094, December 2002.

[3] Lyman, Edwin S. "The Pebble-Bed Modular Reactor (PBMR): Safety Issues", Forumon, Physics Y society of the of The American Physical Society, October 2001.

[4] Childs, K. W., February 1993, "HEATING 7.2 USER'S MANUAL", Oak Ridge National Laboratory ORNL/TM-12262.

[5] Lebenhaft, J., "PBMR Temperature Map in the normal operation calculated by VSOP", August, 2000.

[6] Yan, Xinglong, June, 1990, "Dynamic Analysis and Control System Design for an Advanced Nuclear Gas Turbine Power Plant". MIT Ph.D thesis.

[7] Yang, S., "Heat Transfer", second edition, Beijing, 1989.

[8] Rohsenow, M. W. and P. J. Hartnett, 1973. Handbook of Heat Transfer.

[9] Wichner, R.P., April 1999, "Potential Damage to Gas-Cooled Graphite Reactors Due to Severe Accidents", Oak Ridge National Laboratory.

[10] No, H. C., 2001. "PBR System Simulation Code for Depressurization Accident Analysis in a Modular Pebble Bed Reactor," Massachusetts Institute of Technology.

[11] Hishida, M., and T. Takeda, 1991. "Study on air ingress during an early stage of a primary-pipe rupture accident of a high-temperature gas-cooled reactor," Nuclear Engineering and Design, 126, 175-187.

[12] Takeda, T., and M. Hishida, 1992. "Studies on diffusion and natural convection of two-component gases," Nuclear Engineering and Design, 135, 341-354.

[13] Takeda T. and Hishida, M., "Studies on molecular diffusion and natural convection in a multicomponent gas system," Int. J. Heat Mass Transfer", Vol. 39, No. 3, pp. 527-536, 1996.

[14] Kuhlmann, M. B., "Experiments to investigate flow transfer and graphite corrosion in case of air ingress accidents in a high-temperature reactor". 1999.

[15] Hohn. H., "NACOK, Natural Convection in Core". Forchungszentrum Julich, Auslegung, Ergebnisse.

[16] Katscher, W.More, Man, R. Moorland, Roes, J., "Experimental Results of corrosion investigations."

[17] FLUENT Inc. 2002, "FLUENT 6.0 User's Guide"

[18] FLUENT Inc. 2002, "GAMBIT 2.0 User's Guide"

[19] Rehm, W., W. John, and K. Verfondern, 1988. "Present Results and Further Developments on Safety Analysis of Small and Medium-Sized HTRs for Core Heat-Up Accidents," Nuclear Engineering and Design 109, pp. 281-287.

[20] Tang, Chunhe, Guan, Jie, "Improvement in oxidation resistance of the nuclear graphite by reaction-coated SiC coating", Institute of Nuclear Energy Technology, Tsinghua University.

[21] Oh, C., Merrill, B., Moore, R., and D. Petti, January, 2001, "Oxidation Model for a MPBR Graphite Pebble," Idaho National Engineering & Environmental Laboratory.

[22] Liu, G. N-K., August 1973. "High temperature oxidation of graphite by a dissociated oxygen beam," Master thesis of MIT.

[23] Fenech, Henri, "Heat Transfer and Fluid Flow in Nuclear Systems", Pergamon Press, 1980, P382-401.

[24] O'Brien, M. H., B. J. Merrill, and S. N. Ugaki, September 1988. "Combustion Testing and Thermal Modeling of Proposed CIT Graphite Tile Material," EGG-FSP-8255, Idaho National Engineering Laboratory.

[25] Gao, Z., Li, B., Wang, C., Jiang, Z., Institute of Nuclear Energy Technology, Tsinghua University, "Transient Analysis of Air Ingress From Broken Pipe into the HTR-10 Reactor Pressure Vessel", Beijing, China.

[26] Bird, R. B., W. E. Stewart, and E. N. Lightfoot, 1960, Transport Phenomena, John Wiley and Sons, New York, p. 269.

[27] Solomon, A., "Enhanced Thermal Conductivity of Oxide Fuels", Purdue University, Nuclear Energy Research Initiative", 2002.

[28] Bazant, Z.P, 1996. "Material Properties and Mathematical Models", Harlow Longman.

[29] Carlson, K. E., P. A. Roth, and V. H. Ransom, ATHENA Code Manual Vol. I: Code Structure, System Models, and Solution Methods, EGG-RTH-7397, September 1986.

[30] Gauntt, R. O., R. K. Cole, S. A. Hodge, S. B. Rodriguez, R. L. Sanders, R. C. Smith, D. S. Stuart, R. M. Summers, and M. F. Young, 1997. "MELCOR Computer Code Manuals," NUREG/CR-6119, Vol. 1, Rev. 1, SAND97-2397-2398.

[31] Kadak, A.C, Zhai, T., "(The Annual Report on PBMR) The Loss of Coolant Accident with Depressurization", July, 2001, Massachusetts Institute of Technology.

[32] Merrill, B. J., R. L. Moore, S. T. Polkinghorne, and D. A. Petti, 2000. Fusion Engineering and Design, 51-52, 555-563.

[33] Moorman, R., and W. Katscher, 5-10 June 1988. "Examination of graphite burning in high temperature gas cooled reactors," Nuclear reactor severe accident chemistry symposium, Toronto (Canada).

[34] Mosevitskij, I.S., and A. V. Djakov, 5-8 November 1990. "Problems of investigation of HTGR fuel elements under loss-of-pressure accidents," Specialists meeting on behavior of gas cooled reactor fuel under accident conditions. Oak Ridge, TN (United States).

[35] Neale, G. H., and W. K. Nader, May 1974. "Prediction of Transport Processes Within Porous Media: Creeping Flow Relative to a Fixed Swarm of Spherical Particles," AIChE Journal (Vol. 20, No. 3.).

[36] Nieben, H.F., B. Stocker, O. Amoignon, Z. Gao, and J. Liu, September 30-October 4, 1997. "Sana Experiments for Self-Acting Removal of the After-Heat in

Reactors with Pebble Bed Fuel and Their Interpretation," Eighth International Topical Meeting on Nuclear Thermal-Hydraulic. Kyoto, Japan.

[37] Nightingale, R.E., "Nuclear Graphite", Handford Laboratories, General Electric Company, Academic Press-1962.

[38] Ogawa, M., B. Stauch, R. Moormann, and W. Katscher, November 1985. "An experimental investigation on mass transfer in presence of chemical reactions on a graphite cylinder in crossflow," Juel-Spez—336 {JuelSpez336}, p. 42.

[39] Ozisik, M. N., 1993. Heat Conduction (Second Edition).

[40] Petersen, K., H. Barthels, and G. Breitbach, 30 March 1976. "Natural convection in the core of a pebble-bed reactor," Reactor Meeting, Duesseldorf, F.R. Germany.

[41] Petersen, K., H. Barthels, and R. Schulten, 14 November 1976. "Natural-convection afterheat removal from the pebble-bed HTGR," Transactions of the American Nuclear Society 1976 international meeting, Washington, DC.

[42] Peterson, K., K. Verfondern, H. Barthels, and J. Banaschek, 9-12 October 1980. "Thermal hydraulics of the pebble bed high temperature reactor under accident conditions," ANS/ASME topical meeting on reactor thermal-hydraulics, Saratoga, NY.

[43] Rehm, W., J. Altes, and H. Barthels, 1990. "Thermodynamic Investigations of Passive Decay Heat Removal From HTR Cores and Component Behaviour," Nuclear Engineering and Design 121, pp. 211-218.

[44] Rehm, W., W. John, and H. Barthels. "Comparison of Theoretical and Experimental Studies of Afterheat Removal by Natural Convection/Circulation From an HTR."

[45] Shih, W. C. L., 1975. "Molecular Beam Studies of Graphite Oxidation."

Appendix

Appendix 1: Input Files for LOCA Analysis Using HEATING-7

Version : HEATING 7.3beta

```
1  Benchmark TRANSIENT RUN,                                    title
2  36000 1 0 1                                                 p
3  REGIONS
4  1 1  0  0.69  0 6.283 -3.77 3.77                            r1
5  1 1                                                         r2
6  2 1  0.69  1.01 0 6.283 -3.77 3.77                          r1
7  2 2                                                         r2
8  3 1  1.01  1.27 0 6.283 -3.77 3.77                          r1
9  3 3                                                         r2
10  4 1  1.27 1.50 0 6.283 -3.77 3.77                          r1
11  4 4                                                        r2
12  5 1  1.50  1.75 0 6.283 -3.77 3.77                         r1
13  5 5                                                        r2
14  101 101  0  1.75 0 6.283 3.77 5.33                         r1
15  101 0                                                      r2
16  102 101 1.75 3.31 0 6.283 -5.33 5.33                       r1
17  102 0                                                      r2
18  103 101 0  1.75 0 6.283 -5.33 -3.77                        r1
19  103 0                                                      r2
20  104 104 0 3.31 0 6.283 5.33 5.83                           r1
21  104 0 0 0 0 0 104 104                                      r2
22  105 104 3.31  3.41  0 6.283 -5.33 5.83                     r1
23  105 0 104 104                                              r2
24  107 107 0 3.41 0 6.283 5.83 5.93                           r1
25  107 0                                                      r2
```

```
26  108 107 3.41  3.51  0 6.283 -5.43 5.93                    r1
27  108 0                                                    r2
28  109 107 0 3.41 0 6.283 -5.43 -5.33                       r1
29  109 0                                                    r2
30  110 110 0 3.51 0 6.283 5.93 6.93                         r1
31  110 0 0 0 0 0 110 110                                    r2
32  111 110 3.51 4.82 0 6.283 -6.43 6.93                     r1
33  110 0 110 110                                            r2
34  112 110 0 3.51 0 6.283 -6.43 -5.43                       r1
35  110 0 0 0 0 0 110 110                                    r2
36  113 113 0 4.82 0 6.283 6.93 7.13                         r1
37  113 0 0 0 0 0 0 113                                      r2
38  114 113 4.82 5.02 0 6.283 -6.63 7.13                     r1
39  113 0 0 0 0 0 0 113                                      r2
40  115 113 0 4.82 0 6.283 -6.63 -6.43                       r1
41  113 0                                                    r2
42  116 116 5.02 20.02 0 6.283 -6.63 7.13                    r1
43  116 0 0 0 0 0 0 113                                      r2
44  117 116 0 20.02 0 6.283 -26.63 -6.63                     r1
45  116 0                                                    r2
46  MATERIALS
47  1 pebble 1.0 871.47 1.0 -1 0 -2                          m1
48  101 refle 1.0 1394.8 1.0 -3 0 -4                         ml
49  104 heliumgap 1.0 1.0 5193.0 -10 -5                      m1
50  107 vessel 1.0 7833.35 1.0 -11 0 -12                     m1
51  110 air 1.0 1.0 1.0 -6 -7 -8                             ml
52  113 wall  0.79 1930.0 1.0 0 0 -13                        m1
53  116 soil 0.52 2050.0 1840.0                              m1
54  INITIAL TEMPERATURES
55  1 1.0 0 0 -31                                            i
```

```
56  2 1.0 0 0 -32                                   i
57  3 1.0 0 0 -33                                   i
58  4 1.0 0 0 -34                                   i
59  5 1.0 0 0 -35                                   i
60  101 1.0 0 0 -41                                  i
61  102 1.0 0 0 -42                                  i
62  103 1.0 0 0 -43                                  i
63  104 279.0                                       i
64  105 279.0                                       i
65  107 279.0                                       i
66  108 279.0                                       i
67  109 279.0                                       i
68  110 279.0                                       i
69  111 279.0                                       i
70  112 279.0                                       i
71  113 50.0                                        i
72  114 50.0                                        i
73  115 50.0                                        i
74  116 35.0                                        i
75  117 35.0                                        i
76  HEAT GENERATION
77  1 3652700 -9 0 0 0 -51                                g
78  2 3652700 -9 0 0 0 -52                                g
79  3 3652700 -9 0 0 0 -53                                g
80  4 3652700 -9 0 0 0 -54                                g
81  5 3652700 -9 0 0 0 -55                                g
82  BOUNDARY CONDITIONS
83  104 3                                           b1
84  0 2.349E-8                                       b2
85  110 3                                           b1
```

```
86  0 3.112E-8                                                    b2
87  113 1 35                                                     b1
88  0 3.899E-8 1.904 0.333                                            b2
89  XGRID
90  0.0 0.69 1.01 1.27 1.50 1.75 3.31 3.41 3.51 4.82 5.02 20.02
91     7    3    3    3    3   16   1     1   13    2   50
92  YGRID
93  0 6.283
94  2
95  ZGRID
96  -26.63 -6.63 -6.43 -5.43 -5.33 -3.77 3.77 5.33 5.83 5.93  6.93 7.13
97        50    2    10    1     16    75   16   5     1    10    2
98  TABULAR FUNCTIONS
99  1                                                          t1
100  200.0 1.51, 400.0 3.53, 600.0 6.18, 800.0 9.39,
    @ 1000.0 13.10, 1200.0 17.30, 1400.0 21.95, 1600.0 27.02,
    @ 1800.0 32.51, 2000.0 38.39, 2200.0 44.66                        t2
101  2                                                           t1
102  200 1.47E+03, 400 1.90E+03, 600 2.17E+03, 800 2.32E+03,
    @ 1000 2.43E+03, 1200 2.54E+03, 1400 2.72E+03,
    @ 1600 3.02E+03, 1800 3.50E+03, 2000 4.22E+03, 2200 5.23E+03          t2
103  3                                                           t1
104  20.0 8.3, 400.0 14.0, 600.0 17.0, 800.0 22.0,
    @ 1000.0 24.0, 1200.0 31.0, 1400.0 37.0,
    @ 1600.0 41.0, 1800.0 41.5, 2000.0 40.0,
    @ 2200.0 37.0                                                t2
105  4                                                           t1
106  20.0 984.7, 300.0 1330.0, 600.0 1700.0, 900.0 1870.0,
    @ 1200.0 1980.0, 1500.0 2060.0, 1800.0 2110.0,
    @ 2100.0 2170.0, 2400.0 2210.0                                   t2
```

```
107  5                                                    t1
108  20.0 12.77, 100 10.031, 200 7.967, 300 6.606, 400 5.641,
     @ 500 4.922, 600 4.365, 700 3.922, 800 3.560, 900 3.259,
     @ 1000 3.005, 1100 2.788, 1200 2.600, 1300 2.436, 1400 2.291,
     @ 1500 2.162, 1600 2.048, 1700 1.944, 1800 1.851,
     @ 1900 1.766, 2000 1.689, 2100 1.618, 2200 1.553,
     @ 2300 1.492, 2400 1.437, 2500 1.385, 2600 1.337,
     @ 2700 1.292, 2800 1.250, 2900 1.211                    t2
109  6                                                    t1
110  0.0 0.02415, 100.0 0.03066, 200.0 0.03709,
     @ 300.0 0.04326, 400.0 0.04901, 500.0 0.05481,
     @ 600.0 0.06048, 700.0 0.06510, 800.0 0.07014,
     @ 900.0 0.07447, 1000.0 0.07896, 1100.0 0.08295,
     @ 1800.0 0.11088                                    t2
111  7                                                    t1
112  20.0 1.205, 50.0 1.093, 100.0 0.946, 200.0 0.746
     @ 300.0 0.615, 400.0 0.524, 500.0 0.456,
     @ 600.0 0.404, 700.0 0.362, 800.0 0.329,
     @ 900.0 0.301, 1000.0 0.277, 1100.0 0.257
     @ 1200.0 0.239,  1800.0 0.131                       t2
113  8                                                    t1
114  20.0 1005.0, 50.0 1005.0, 100.0 1009.0,
     @ 200.0 1026.0, 300.0 1047.0, 400.0 1068,
     @ 500.0 1093.0, 600.0 1114.0, 700.0 1135.0
     @ 800.0 1156.0, 900.0 1172.0, 1000.0 1185.0
     @ 1100.0 1197.0, 1200.0 1210.0, 1800.0 1288.0          t2
115  9                                                    t1
116  0 1.0, 1 0.042, 2 0.039, 5 0.036, 10 0.033, 80 0.032, 150 0.028,
     @ 1000 0.018, 10000 8.87E-03, 100000 4.28E-03,
     @ 1000000 1.89E-03, 10000000 6.55E-04, 100000000 1.11E-04    t2
```

```
117  10                                                    t1
118  27 0.1564, 77 0.1692, 127 0.1872, 227 0.2206,
     @ 327 0.2516, 427 0.2792, 527 0.3052, 627 0.3312,
     @ 727 0.3352, 827 0.3802, 927 0.406, 1027 0.4302,
     @ 1127 0.4552, 1227 0.4792, 1827 0.4792                  t2
119  11                                                    t1
120  20 44.32, 300.0 39.53, 600.0 34.39, 900.0 29.26,
     @ 1200.0 24.12, 1500.0 18.99, 1800.0 13.85               t2
121  12                                                    t1
122  20.0 492.99, 100.0 511.36, 200.0 529.54
     @ 300.0 544.1, 600.0 584.2, 900.0 657.0,
     @ 1200.0 811.6, 1500.0 1097.0, 1800.0 1562.0,
     @ 2100.0 2256.0  2400.0 3227.0                           t2
123  13                                                    t1
124  20 970, 200 1300, 300 1200, 400 1400, 500 1520,
     @ 600 1700, 700 1780, 800 1770,
     @ 900 1760, 1000 1750, 1100 1740 1500 1740               t2
125  31                                                    t1
126  -3.77 859.1, -3.6145 862.9, -3.5509 862.3, -3.412 860.8,
     @ -2.7591 814.4, -2.1062 753.1, -1.4533 721.3,
     @ -0.8004 694.8, -0.1475 668.8, 0.5055 640.2, 1.1584 613.1,
     @ 1.8113 588.4, 2.4642 567.5, 3.1171 551.7, 3.77 542.5   t2
127  32                                                    t1
128  -3.77 973., -3.6145 978.2, -3.5509 976.2, -3.412 977.4,
     @ -2.7591 957.6, -2.1062 919.1, -1.4533 881.8,
     @ -0.8004 839.7, -0.1475 793.7, 0.5055 743.7,
     @ 1.1584 692.6, 1.8113 643, 2.4642 600.1,
     @ 3.1171 567.7, 3.77 548.1                               t2
129  33                                                    t1
130  -3.77 968.9, -3.6145 971.8, -3.5509 977.4,
```

@ -3.412 980.5, -2.7591 966.5, -2.1062 936.8,

@ -1.4533 903.5, -0.8004 862, -0.1475 813.2, 0.5055 760,

@ 1.1584 704.7, 1.8113 650.6, 2.4642 604.1,

@ 3.1171 570.2, 3.77 549.4 t2

131 34 t1

132 -3.77 973.1, -3.412 978.5, -2.7591 957.7, -2.1062 924.5,

@ -1.4533 890.5, -0.8004 847.8, -0.1475 799.7, 0.5055 747.2,

@ 1.1584 693.1, 1.8113 640.5, 2.4642 596.5,

@ 3.1171 566.2, 3.77 548.5 t2

133 35 t1

134 -3.77 926.6, -3.412 963.3, -2.7591 942.8, -2.1062 912.5,

@ -1.4533 879.7, -0.8004 838.6, -0.1475 792.2, 0.5055 741.2,

@ 1.1584 688.3, 1.8113 636.8, 2.4642 593.8,

@ 3.1171 564.8, 3.77 548.2 t2

135 41 t1

136 3.77 549.4, 4.61 540.5, 4.74 540.1, 4.86 539.8,

@ 4.96 539.3, 5.06 537.1, 5.33 479.8 t2

137 42 t1

138 -5.33 25.1, -4.56 725.5, -4.28 726.8, -4.1469 728.2,

@ -4.0196 730.3, -3.8749 734.7, -3.7337 744.1, -3.6145 771.2,

@ -3.5509 834.3, -3.412 889.8, -2.7591 882, -2.1062 856.8,

@ -1.4533 828.8, -0.8004 793.9, -0.1475 754.5, 0.5055 711.2,

@ 1.1584 666.3, 1.8113 622.7, 2.4642 586.2, 3.1171 561.4,

@ 3.77 547.3, 4.61 539.5, 4.735 536.4, 4.86 532,

@ 4.96 529.5, 5.06 525.1, 5.33 476.4 t2

139 43 t1

140 -5.33 873.3, -3.77 973.1 t2

141 51 t1

142 -3.77 0.011126, -3.35113 0.011126, -2.51335 0.014114,

@ -1.67557 0.016232, -0.83779 0.017734, -0.00001 0.018081,

@ 0.83777 0.017129, 1.67555 0.014212, 2.51333 0.010295,

@ 3.35111 0.005818, 3.77 0.005818 t2

143 52 t1

144 -3.77 0.762057, -3.393 0.762057, -2.639 0.926468, -1.885 1.138509,

@ -1.131 1.308254, -0.377 1.409298, 0.377 1.402658,

@ 1.131 1.289141, 1.885 1.038878,

@ 2.639 0.728655, 3.393 0.421222, 3.77 0.421222 t2

145 53 t1

146 -3.77 1.028516, -3.42723 1.028516, -2.74178 1.252647,

@ -2.05633 1.443015, -1.37088 1.651595, -0.68543 1.800878,

@ 0.00002 1.878047, 0.68547 1.854554, 1.37092 1.704583,

@ 2.05637 1.327315, 2.74182 0.915033, 3.42727 0.541849

@ 3.77 0.541849 t2

147 54 t1

148 -3.77, 0.844293, -3.4558 0.844293, -2.82747 0.945036,

@ -2.19914 1.112876, -1.57081 1.262258, -0.94248 1.454724,

@ -0.31415 1.598541, 0.31418 1.69581, 0.94251 1.676789,

@ 1.57084 1.524377, 2.19917 1.143208, 2.8275 0.753729,

@ 3.45583 0.459489, 3.77 0.459489 t2

149 55 t1

150 -3.77 0.785065, -3.51872 0.785065, -3.01605 0.767299,

@ -2.51338 0.770856, -2.01071 0.841702, -1.50804 0.922295,

@ -1.00537 1.070319, -0.5027 1.241168, 0 1.432057,

@ 0.50264 1.598229, 1.00531 1.70759, 1.50798 1.712877,

@ 2.01065 1.563896, 2.51332 1.156261, 3.01599 0.711366,

@ 3.51867 0.426499, 3.77 0.426499 t2

151 PRINTOUT TIMES

152 1800 3600 7200 10800 18000 36000 43200 50400 57600 64800

@ 72000 79200 158400 201600 244800 288000 331200 360000

@ 374400 604800 1296000 2592000 432000 5184000 5616000

@ 6048000 6480000 6912000 7344000 7776000 O

153 TRANSIENT

154 2 7776000 tr

155 0.7 10E-3 1 10E-3 tr2

156 0 1.1 tr3

157 %

********** CASE DESCRIPTION

****

Benchmark TRANSIENT RUN, t

********** SUMMARY OF PARAMETER CARD DATA

****

Maximum cpu time - 36000.00 seconds

Geometry type number - 1 (rtz)

Initial time - 0.0000000E+00

This is a restart of previous case - No

Read node-to-node connector data file - No

Redirect or suppress convergence information - Yes (Suppress)

Output selected information during calculations - No

Write surface heat fluxes to plot file - No

Units used in problem solution and in material properties library

	Problem	Library
Time	s	s
Length	m	cm
Mass	kg	g
Energy	J	cal

Temperature - C C

********** SUMMARY OF REGION DATA **********

Region Number	Material Number	Initial Temp. No.	Heat Gen. Number
1	1	1	1
2	1	2	2
3	1	3	3
4	1	4	4
5	1	5	5
101	101	101	0
102	101	102	0
103	101	103	0
104	104	104	0
105	104	105	0
107	107	107	0
108	107	108	0
109	107	109	0
110	110	110	0
111	110	110	0
112	110	110	0
113	113	113	0
114	113	113	0
115	113	113	0
116	116	116	0
117	116	116	0

---------- Dimensions / Boundary Numbers ----------

Region	First Axis		Second Axis		Third Axis	
Number	Smaller	Larger	Smaller	Larger	Smaller	Larger
1	0.0000E+00	6.9000E-01	0.0000E+00	6.2830E+00	-3.7700E+00	3.7700E+00
	0	0	0	0	0	0
2	6.9000E-01	1.0100E+00	0.0000E+00	6.2830E+00	-3.7700E+00	3.7700E+00
	0	0	0	0	0	0
3	1.0100E+00	1.2700E+00	0.0000E+00	6.2830E+00	-3.7700E+00	3.7700E+00
	0	0	0	0	0	0
4	1.2700E+00	1.5000E+00	0.0000E+00	6.2830E+00	-3.7700E+00	3.7700E+00
	0	0	0	0	0	0
5	1.5000E+00	1.7500E+00	0.0000E+00	6.2830E+00	-3.7700E+00	3.7700E+00
	0	0	0	0	0	0
101	0.0000E+00	1.7500E+00	0.0000E+00	6.2830E+00	3.7700E+00	5.3300E+00
	0	0	0	0	0	0
102	1.7500E+00	3.3100E+00	0.0000E+00	6.2830E+00	-5.3300E+00	5.3300E+00
	0	0	0	0	0	0
103	0.0000E+00	1.7500E+00	0.0000E+00	6.2830E+00	-5.3300E+00	-3.7700E+00
	0	0	0	0	0	0
104	0.0000E+00	3.3100E+00	0.0000E+00	6.2830E+00	5.3300E+00	5.8300E+00
	0	0	0	0	104	104
105	3.3100E+00	3.4100E+00	0.0000E+00	6.2830E+00	-5.3300E+00	5.8300E+00
	104	104	0	0	0	0
107	0.0000E+00	3.4100E+00	0.0000E+00	6.2830E+00	5.8300E+00	5.9300E+00
	0	0	0	0	0	0
108	3.4100E+00	3.5100E+00	0.0000E+00	6.2830E+00	-5.4300E+00	5.9300E+00
	0	0	0	0	0	0
109	0.0000E+00	3.4100E+00	0.0000E+00	6.2830E+00	-5.4300E+00	-5.3300E+00
	0	0	0	0	0	0
110	0.0000E+00	3.5100E+00	0.0000E+00	6.2830E+00	5.9300E+00	6.9300E+00

```
      0         0         0         0       110       110
  111  3.5100E+00  4.8200E+00  0.0000E+00  6.2830E+00 -6.4300E+00  6.9300E+00
     110       110         0         0         0         0
  112  0.0000E+00  3.5100E+00  0.0000E+00  6.2830E+00 -6.4300E+00 -5.4300E+00
      0         0         0         0       110       110
  113  0.0000E+00  4.8200E+00  0.0000E+00  6.2830E+00  6.9300E+00  7.1300E+00
      0         0         0         0         0       113
  114  4.8200E+00  5.0200E+00  0.0000E+00  6.2830E+00 -6.6300E+00  7.1300E+00
      0         0         0         0         0       113
  115  0.0000E+00  4.8200E+00  0.0000E+00  6.2830E+00 -6.6300E+00 -6.4300E+00
      0         0         0         0         0         0
  116  5.0200E+00  2.0020E+01  0.0000E+00  6.2830E+00 -6.6300E+00  7.1300E+00
      0         0         0         0         0       113
  117  0.0000E+00  2.0020E+01  0.0000E+00  6.2830E+00 -2.6630E+01 -6.6300E+00
      0         0         0         0         0         0


 ************************* SUMMARY OF MATERIAL DATA
*************************

 Material   Material     ------------ Thermal Parameters ------------   Phase
  Number      Name       -- Temperature-Dependent Function Numbers --  Change
                      Conductivity      Density     Specific Heat
    1      pebble       1.000000E+00    8.714700E+02    1.000000E+00     No
                        -1              0              -2
  101      refle        1.000000E+00    1.394800E+03    1.000000E+00     No
                        -3              0              -4
  104      heliumga     1.000000E+00    1.000000E+00    5.193000E+03     No
                       -10             -5              0
  107      vessel       1.000000E+00    7.833350E+03    1.000000E+00     No
```

		-11	0	-12	
110	air	1.000000E+00	1.000000E+00	1.000000E+00	No
		-6	-7	-8	
113	wall	7.900000E-01	1.930000E+03	1.000000E+00	No
		0	0	-13	
116	soil	5.200000E-01	2.050000E+03	1.840000E+03	No
		0	0	0	

********** SUMMARY OF INITIAL TEMPERATURE DATA **********

Number	Initial Temperature	Position-Dependent Function Numbers x or r	y or th	z or p
1	1.00000E+00	0	0	-31
2	1.00000E+00	0	0	-32
3	1.00000E+00	0	0	-33
4	1.00000E+00	0	0	-34
5	1.00000E+00	0	0	-35
101	1.00000E+00	0	0	-41
102	1.00000E+00	0	0	-42
103	1.00000E+00	0	0	-43
104	2.79000E+02	0	0	0
105	2.79000E+02	0	0	0
107	2.79000E+02	0	0	0
108	2.79000E+02	0	0	0
109	2.79000E+02	0	0	0
110	2.79000E+02	0	0	0
111	2.79000E+02	0	0	0
112	2.79000E+02	0	0	0
113	5.00000E+01	0	0	0

114	5.00000E+01	0	0	0
115	5.00000E+01	0	0	0
116	3.50000E+01	0	0	0
117	3.50000E+01	0	0	0

********** SUMMARY OF HEAT GENERATION RATE DATA **********

Number	Power	Time-, Temperature-, and Position-Dependent Function Numbers				
	Density	Time	Temperature	X or R	Y or Theta	Z or Phi
1	3.65270E+06	-9	0	0	0	-51
2	3.65270E+06	-9	0	0	0	-52
3	3.65270E+06	-9	0	0	0	-53
4	3.65270E+06	-9	0	0	0	-54
5	3.65270E+06	-9	0	0	0	-55

********** SUMMARY OF BOUNDARY CONDITION DATA **********

Number: 104 Type: Surface-to-Surface

Heat Transfer Coefficients and Any Functions Used to Define Dependence:

Radiation : 2.349000E-08

Number: 110 Type: Surface-to-Surface

Heat Transfer Coefficients and Any Functions Used to Define Dependence:

Radiation : 3.112000E-08

Number: 113 Type: Surface-to-Environment

Temperature and Any Functions Used to Define Dependence:

Temperature : 3.500000E+01

Heat Transfer Coefficients and Any Functions Used to Define Dependence:

Radiation : 3.899000E-08

Natural Convection : 1.904000E+00 (Multiplier)

Natural Convection : 3.330000E-01 (Exponent)

********** SUMMARY OF GRID STRUCTURE **********

X (or R) Gross Grid Lines and Number of Divisions

0.000000E+00 6.900000E-01 1.010000E+00 1.270000E+00 1.500000E+00

1.750000E+00 3.310000E+00 3.410000E+00 3.510000E+00 4.820000E+00

5.020000E+00 2.002000E+01

7 3 3 3 3

16 1 1 13 2

50

X (or R) Fine Grid Lines Generated by HEATING

1 0.00000E+00 2 9.85714E-02 3 1.97143E-01 4 2.95714E-01

5 3.94286E-01 6 4.92857E-01 7 5.91429E-01 8 6.90000E-01

9 7.96667E-01 10 9.03333E-01 11 1.01000E+00 12 1.09667E+00

13 1.18333E+00 14 1.27000E+00 15 1.34667E+00 16 1.42333E+00

17 1.50000E+00 18 1.58333E+00 19 1.66667E+00 20 1.75000E+00

21 1.84750E+00 22 1.94500E+00 23 2.04250E+00 24 2.14000E+00

25 2.23750E+00 26 2.33500E+00 27 2.43250E+00 28 2.53000E+00

29 2.62750E+00 30 2.72500E+00 31 2.82250E+00 32 2.92000E+00

33 3.01750E+00 34 3.11500E+00 35 3.21250E+00 36 3.31000E+00

37 3.41000E+00 38 3.51000E+00 39 3.61077E+00 40 3.71154E+00

41 3.81231E+00 42 3.91308E+00 43 4.01385E+00 44 4.11462E+00
45 4.21538E+00 46 4.31615E+00 47 4.41692E+00 48 4.51769E+00
49 4.61846E+00 50 4.71923E+00 51 4.82000E+00 52 4.92000E+00
53 5.02000E+00 54 5.32000E+00 55 5.62000E+00 56 5.92000E+00
57 6.22000E+00 58 6.52000E+00 59 6.82000E+00 60 7.12000E+00
61 7.42000E+00 62 7.72000E+00 63 8.02000E+00 64 8.32000E+00
65 8.62000E+00 66 8.92000E+00 67 9.22000E+00 68 9.52000E+00
69 9.82000E+00 70 1.01200E+01 71 1.04200E+01 72 1.07200E+01
73 1.10200E+01 74 1.13200E+01 75 1.16200E+01 76 1.19200E+01
77 1.22200E+01 78 1.25200E+01 79 1.28200E+01 80 1.31200E+01
81 1.34200E+01 82 1.37200E+01 83 1.40200E+01 84 1.43200E+01
85 1.46200E+01 86 1.49200E+01 87 1.52200E+01 88 1.55200E+01
89 1.58200E+01 90 1.61200E+01 91 1.64200E+01 92 1.67200E+01
93 1.70200E+01 94 1.73200E+01 95 1.76200E+01 96 1.79200E+01
97 1.82200E+01 98 1.85200E+01 99 1.88200E+01 100 1.91200E+01
101 1.94200E+01 102 1.97200E+01 103 2.00200E+01

Y (or Theta) Gross Grid Lines and Number of Divisions
0.000000E+00 6.283000E+00
2

Y (or Theta) Fine Grid Lines Generated by HEATING
1 0.00000E+00 2 3.14150E+00 3 6.28300E+00

Z (or Phi) Gross Grid Lines and Number of Divisions
-2.663000E+01 -6.630000E+00 -6.430000E+00 -5.430000E+00 -5.330000E+00
-3.770000E+00 3.770000E+00 5.330000E+00 5.830000E+00 5.930000E+00
6.930000E+00 7.130000E+00
50 2 10 1 16
75 16 5 1 10

2

Z (or Phi) Fine Grid Lines Generated by HEATING

1 -2.66300E+01	2 -2.62300E+01	3 -2.58300E+01	4 -2.54300E+01
5 -2.50300E+01	6 -2.46300E+01	7 -2.42300E+01	8 -2.38300E+01
9 -2.34300E+01	10 -2.30300E+01	11 -2.26300E+01	12 -2.22300E+01
13 -2.18300E+01	14 -2.14300E+01	15 -2.10300E+01	16 -2.06300E+01
17 -2.02300E+01	18 -1.98300E+01	19 -1.94300E+01	20 -1.90300E+01
21 -1.86300E+01	22 -1.82300E+01	23 -1.78300E+01	24 -1.74300E+01
25 -1.70300E+01	26 -1.66300E+01	27 -1.62300E+01	28 -1.58300E+01
29 -1.54300E+01	30 -1.50300E+01	31 -1.46300E+01	32 -1.42300E+01
33 -1.38300E+01	34 -1.34300E+01	35 -1.30300E+01	36 -1.26300E+01
37 -1.22300E+01	38 -1.18300E+01	39 -1.14300E+01	40 -1.10300E+01
41 -1.06300E+01	42 -1.02300E+01	43 -9.83000E+00	44 -9.43000E+00
45 -9.03000E+00	46 -8.63000E+00	47 -8.23000E+00	48 -7.83000E+00
49 -7.43000E+00	50 -7.03000E+00	51 -6.63000E+00	52 -6.53000E+00
53 -6.43000E+00	54 -6.33000E+00	55 -6.23000E+00	56 -6.13000E+00
57 -6.03000E+00	58 -5.93000E+00	59 -5.83000E+00	60 -5.73000E+00
61 -5.63000E+00	62 -5.53000E+00	63 -5.43000E+00	64 -5.33000E+00
65 -5.23250E+00	66 -5.13500E+00	67 -5.03750E+00	68 -4.94000E+00
69 -4.84250E+00	70 -4.74500E+00	71 -4.64750E+00	72 -4.55000E+00
73 -4.45250E+00	74 -4.35500E+00	75 -4.25750E+00	76 -4.16000E+00
77 -4.06250E+00	78 -3.96500E+00	79 -3.86750E+00	80 -3.77000E+00
81 -3.66947E+00	82 -3.56893E+00	83 -3.46840E+00	84 -3.36787E+00
85 -3.26733E+00	86 -3.16680E+00	87 -3.06627E+00	88 -2.96573E+00
89 -2.86520E+00	90 -2.76467E+00	91 -2.66413E+00	92 -2.56360E+00
93 -2.46307E+00	94 -2.36253E+00	95 -2.26200E+00	96 -2.16147E+00
97 -2.06093E+00	98 -1.96040E+00	99 -1.85987E+00	100 -1.75933E+00
101 -1.65880E+00	102 -1.55827E+00	103 -1.45773E+00	104 -1.35720E+00
105 -1.25667E+00	106 -1.15613E+00	107 -1.05560E+00	108 -9.55067E-01

109 -8.54533E-01 110 -7.54000E-01 111 -6.53467E-01 112 -5.52933E-01
113 -4.52400E-01 114 -3.51867E-01 115 -2.51333E-01 116 -1.50800E-01
117 -5.02667E-02 118 5.02667E-02 119 1.50800E-01 120 2.51333E-01
121 3.51867E-01 122 4.52400E-01 123 5.52933E-01 124 6.53467E-01
125 7.54000E-01 126 8.54533E-01 127 9.55067E-01 128 1.05560E+00
129 1.15613E+00 130 1.25667E+00 131 1.35720E+00 132 1.45773E+00
133 1.55827E+00 134 1.65880E+00 135 1.75933E+00 136 1.85987E+00
137 1.96040E+00 138 2.06093E+00 139 2.16147E+00 140 2.26200E+00
141 2.36253E+00 142 2.46307E+00 143 2.56360E+00 144 2.66413E+00
145 2.76467E+00 146 2.86520E+00 147 2.96573E+00 148 3.06627E+00
149 3.16680E+00 150 3.26733E+00 151 3.36787E+00 152 3.46840E+00
153 3.56893E+00 154 3.66947E+00 155 3.77000E+00 156 3.86750E+00
157 3.96500E+00 158 4.06250E+00 159 4.16000E+00 160 4.25750E+00
161 4.35500E+00 162 4.45250E+00 163 4.55000E+00 164 4.64750E+00
165 4.74500E+00 166 4.84250E+00 167 4.94000E+00 168 5.03750E+00
169 5.13500E+00 170 5.23250E+00 171 5.33000E+00 172 5.43000E+00
173 5.53000E+00 174 5.63000E+00 175 5.73000E+00 176 5.83000E+00
177 5.93000E+00 178 6.03000E+00 179 6.13000E+00 180 6.23000E+00
181 6.33000E+00 182 6.43000E+00 183 6.53000E+00 184 6.63000E+00
185 6.73000E+00 186 6.83000E+00 187 6.93000E+00 188 7.03000E+00
189 7.13000E+00

********** LISTING OF TABULAR FUNCTIONS **********

Table number - 1 Number of pairs - 11

Argument Value (Min) <- Relative Value -> (Max)
2.00000000E+02 1.51000000E+00 *

4.00000000E+02	3.53000000E+00	**
6.00000000E+02	6.18000000E+00	***
8.00000000E+02	9.39000000E+00	*****
1.00000000E+03	1.31000000E+01	*******
1.20000000E+03	1.73000000E+01	**********
1.40000000E+03	2.19500000E+01	************
1.60000000E+03	2.70200000E+01	**************
1.80000000E+03	3.25100000E+01	******************
2.00000000E+03	3.83900000E+01	**********************
2.20000000E+03	4.46600000E+01	**************************

Table number - 2 Number of pairs - 11

Argument	Value	(Min) <- Relative Value -> (Max)
2.00000000E+02	1.47000000E+03	*
4.00000000E+02	1.90000000E+03	***
6.00000000E+02	2.17000000E+03	*****
8.00000000E+02	2.32000000E+03	******
1.00000000E+03	2.43000000E+03	*******
1.20000000E+03	2.54000000E+03	********
1.40000000E+03	2.72000000E+03	*********
1.60000000E+03	3.02000000E+03	**********
1.80000000E+03	3.50000000E+03	************
2.00000000E+03	4.22000000E+03	******************
2.20000000E+03	5.23000000E+03	**************************

Table number - 3 Number of pairs - 11

Argument	Value	(Min) <- Relative Value -> (Max)
2.00000000E+01	8.30000000E+00	*

4.00000000E+02	1.40000000E+01	*****
6.00000000E+02	1.70000000E+01	*******
8.00000000E+02	2.20000000E+01	**********
1.00000000E+03	2.40000000E+01	**********
1.20000000E+03	3.10000000E+01	**********
1.40000000E+03	3.70000000E+01	**********
1.60000000E+03	4.10000000E+01	**********
1.80000000E+03	4.15000000E+01	**********
2.00000000E+03	4.00000000E+01	**********
2.20000000E+03	3.70000000E+01	**********

Table number - 4 Number of pairs - 9

Argument	Value	(Min) <- Relative Value -> (Max)
2.00000000E+01	9.84700000E+02	*
3.00000000E+02	1.33000000E+03	********
6.00000000E+02	1.70000000E+03	**********
9.00000000E+02	1.87000000E+03	**********
1.20000000E+03	1.98000000E+03	**********
1.50000000E+03	2.06000000E+03	**********
1.80000000E+03	2.11000000E+03	**********
2.10000000E+03	2.17000000E+03	**********
2.40000000E+03	2.21000000E+03	**********

Table number - 5 Number of pairs - 30

Argument	Value	(Min) <- Relative Value -> (Max)
2.00000000E+01	1.27700000E+01	**********
1.00000000E+02	1.00310000E+01	**********
2.00000000E+02	7.96700000E+00	**********

3.00000000E+02	6.60600000E+00	**********
4.00000000E+02	5.64100000E+00	*********
5.00000000E+02	4.92200000E+00	********
6.00000000E+02	4.36500000E+00	*******
7.00000000E+02	3.92200000E+00	******
8.00000000E+02	3.56000000E+00	******
9.00000000E+02	3.25900000E+00	*****
1.00000000E+03	3.00500000E+00	****
1.10000000E+03	2.78800000E+00	****
1.20000000E+03	2.60000000E+00	****
1.30000000E+03	2.43600000E+00	***
1.40000000E+03	2.29100000E+00	***
1.50000000E+03	2.16200000E+00	***
1.60000000E+03	2.04800000E+00	**
1.70000000E+03	1.94400000E+00	**
1.80000000E+03	1.85100000E+00	**
1.90000000E+03	1.76600000E+00	**
2.00000000E+03	1.68900000E+00	**
2.10000000E+03	1.61800000E+00	*
2.20000000E+03	1.55300000E+00	*
2.30000000E+03	1.49200000E+00	*
2.40000000E+03	1.43700000E+00	*
2.50000000E+03	1.38500000E+00	*
2.60000000E+03	1.33700000E+00	*
2.70000000E+03	1.29200000E+00	*
2.80000000E+03	1.25000000E+00	*
2.90000000E+03	1.21100000E+00	*

Table number - 6 Number of pairs - 13

Argument	Value	(Min) <- Relative Value -> (Max)
0.00000000E+00	2.41500000E-02	*
1.00000000E+02	3.06600000E-02	**
2.00000000E+02	3.70900000E-02	****
3.00000000E+02	4.32600000E-02	******
4.00000000E+02	4.90100000E-02	********
5.00000000E+02	5.48100000E-02	*********
6.00000000E+02	6.04800000E-02	**********
7.00000000E+02	6.51000000E-02	**********
8.00000000E+02	7.01400000E-02	**********
9.00000000E+02	7.44700000E-02	**********
1.00000000E+03	7.89600000E-02	**********
1.10000000E+03	8.29500000E-02	**********
1.80000000E+03	1.10880000E-01	**********

Table number - 7 Number of pairs - 15

Argument	Value	(Min) <- Relative Value -> (Max)
2.00000000E+01	1.20500000E+00	**********
5.00000000E+01	1.09300000E+00	**********
1.00000000E+02	9.46000000E-01	**********
2.00000000E+02	7.46000000E-01	**********
3.00000000E+02	6.15000000E-01	**********
4.00000000E+02	5.24000000E-01	**********
5.00000000E+02	4.56000000E-01	********
6.00000000E+02	4.04000000E-01	*******
7.00000000E+02	3.62000000E-01	******
8.00000000E+02	3.29000000E-01	*****
9.00000000E+02	3.01000000E-01	****
1.00000000E+03	2.77000000E-01	****

1.10000000E+03	2.57000000E-01	***
1.20000000E+03	2.39000000E-01	***
1.80000000E+03	1.31000000E-01	*

Table number - 8 Number of pairs - 15

Argument	Value	(Min) <- Relative Value -> (Max)
2.00000000E+01	1.00500000E+03	*
5.00000000E+01	1.00500000E+03	*
1.00000000E+02	1.00900000E+03	*
2.00000000E+02	1.02600000E+03	**
3.00000000E+02	1.04700000E+03	****
4.00000000E+02	1.06800000E+03	******
5.00000000E+02	1.09300000E+03	********
6.00000000E+02	1.11400000E+03	**********
7.00000000E+02	1.13500000E+03	**********
8.00000000E+02	1.15600000E+03	**********
9.00000000E+02	1.17200000E+03	**********
1.00000000E+03	1.18500000E+03	**********
1.10000000E+03	1.19700000E+03	**********
1.20000000E+03	1.21000000E+03	**********
1.80000000E+03	1.28800000E+03	**********

Table number - 9 Number of pairs - 13

Argument	Value	(Min) <- Relative Value -> (Max)
0.00000000E+00	1.00000000E+00	**********
1.00000000E+00	4.20000000E-02	**
2.00000000E+00	3.90000000E-02	*
5.00000000E+00	3.60000000E-02	*

1.00000000E+01	3.30000000E-02	*
8.00000000E+01	3.20000000E-02	*
1.50000000E+02	2.80000000E-02	*
1.00000000E+03	1.80000000E-02	*
1.00000000E+04	8.87000000E-03	*
1.00000000E+05	4.28000000E-03	*
1.00000000E+06	1.89000000E-03	*
1.00000000E+07	6.55000000E-04	*
1.00000000E+08	1.11000000E-04	*

Table number - 10 Number of pairs - 15

Argument	Value	(Min) <- Relative Value -> (Max)
2.70000000E+01	1.56400000E-01	*
7.70000000E+01	1.69200000E-01	*
1.27000000E+02	1.87200000E-01	***
2.27000000E+02	2.20600000E-01	*****
3.27000000E+02	2.51600000E-01	********
4.27000000E+02	2.79200000E-01	**********
5.27000000E+02	3.05200000E-01	************
6.27000000E+02	3.31200000E-01	**************
7.27000000E+02	3.35200000E-01	**************
8.27000000E+02	3.80200000E-01	******************
9.27000000E+02	4.06000000E-01	********************
1.02700000E+03	4.30200000E-01	**********************
1.12700000E+03	4.55200000E-01	************************
1.22700000E+03	4.79200000E-01	**************************
1.82700000E+03	4.79200000E-01	**************************

Table number - 11 Number of pairs - 7

Argument	Value	(Min) <- Relative Value -> (Max)
2.00000000E+01	4.43200000E+01	*************************
3.00000000E+02	3.95300000E+01	**********************
6.00000000E+02	3.43900000E+01	*****************
9.00000000E+02	2.92600000E+01	************
1.20000000E+03	2.41200000E+01	*********
1.50000000E+03	1.89900000E+01	*****
1.80000000E+03	1.38500000E+01	*

Table number - 12 Number of pairs - 11

Argument	Value	(Min) <- Relative Value -> (Max)
2.00000000E+01	4.92990000E+02	*
1.00000000E+02	5.11360000E+02	*
2.00000000E+02	5.29540000E+02	*
3.00000000E+02	5.44100000E+02	*
6.00000000E+02	5.84200000E+02	*
9.00000000E+02	6.57000000E+02	**
1.20000000E+03	8.11600000E+02	***
1.50000000E+03	1.09700000E+03	******
1.80000000E+03	1.56200000E+03	**********
2.10000000E+03	2.25600000E+03	*****************
2.40000000E+03	3.22700000E+03	*************************

Table number - 13 Number of pairs - 12

Argument	Value	(Min) <- Relative Value -> (Max)
2.00000000E+01	9.70000000E+02	*
2.00000000E+02	1.30000000E+03	***********

3.00000000E+02	1.20000000E+03	********
4.00000000E+02	1.40000000E+03	**********
5.00000000E+02	1.52000000E+03	**********
6.00000000E+02	1.70000000E+03	**********
7.00000000E+02	1.78000000E+03	**********
8.00000000E+02	1.77000000E+03	**********
9.00000000E+02	1.76000000E+03	**********
1.00000000E+03	1.75000000E+03	**********
1.10000000E+03	1.74000000E+03	**********
1.50000000E+03	1.74000000E+03	**********

Table number - 31 Number of pairs - 15

Argument	Value	(Min) <- Relative Value -> (Max)
-3.77000000E+00	8.59100000E+02	**********
-3.61450000E+00	8.62900000E+02	**********
-3.55090000E+00	8.62300000E+02	**********
-3.41200000E+00	8.60800000E+02	**********
-2.75910000E+00	8.14400000E+02	**********
-2.10620000E+00	7.53100000E+02	**********
-1.45330000E+00	7.21300000E+02	**********
-8.00400000E-01	6.94800000E+02	**********
-1.47500000E-01	6.68800000E+02	**********
5.05500000E-01	6.40200000E+02	********
1.15840000E+00	6.13100000E+02	******
1.81130000E+00	5.88400000E+02	****
2.46420000E+00	5.67500000E+02	**
3.11710000E+00	5.51700000E+02	*
3.77000000E+00	5.42500000E+02	*

Table number - 32 Number of pairs - 15

Argument	Value	(Min) <- Relative Value -> (Max)
-3.77000000E+00	9.73000000E+02	**********
-3.61450000E+00	9.78200000E+02	**********
-3.55090000E+00	9.76200000E+02	**********
-3.41200000E+00	9.77400000E+02	**********
-2.75910000E+00	9.57600000E+02	**********
-2.10620000E+00	9.19100000E+02	**********
-1.45330000E+00	8.81800000E+02	**********
-8.00400000E-01	8.39700000E+02	**********
-1.47500000E-01	7.93700000E+02	**********
5.05500000E-01	7.43700000E+02	**********
1.15840000E+00	6.92600000E+02	*********
1.81130000E+00	6.43000000E+02	******
2.46420000E+00	6.00100000E+02	****
3.11710000E+00	5.67700000E+02	**
3.77000000E+00	5.48100000E+02	*

Table number - 33 Number of pairs - 15

Argument	Value	(Min) <- Relative Value -> (Max)
-3.77000000E+00	9.68900000E+02	**********
-3.61450000E+00	9.71800000E+02	**********
-3.55090000E+00	9.77400000E+02	**********
-3.41200000E+00	9.80500000E+02	**********
-2.75910000E+00	9.66500000E+02	**********
-2.10620000E+00	9.36800000E+02	**********
-1.45330000E+00	9.03500000E+02	**********
-8.00400000E-01	8.62000000E+02	**********

-1.47500000E-01 8.13200000E+02 **********

5.05500000E-01 7.60000000E+02 **********

1.15840000E+00 7.04700000E+02 **********

1.81130000E+00 6.50600000E+02 ******

2.46420000E+00 6.04100000E+02 ****

3.11710000E+00 5.70200000E+02 **

3.77000000E+00 5.49400000E+02 *

Table number - 34 Number of pairs - 13

Argument Value (Min) <- Relative Value -> (Max)

-3.77000000E+00 9.73100000E+02 **********

-3.41200000E+00 9.78500000E+02 **********

-2.75910000E+00 9.57700000E+02 **********

-2.10620000E+00 9.24500000E+02 **********

-1.45330000E+00 8.90500000E+02 **********

-8.00400000E-01 8.47800000E+02 **********

-1.47500000E-01 7.99700000E+02 **********

5.05500000E-01 7.47200000E+02 **********

1.15840000E+00 6.93100000E+02 *********

1.81130000E+00 6.40500000E+02 ******

2.46420000E+00 5.96500000E+02 ***

3.11710000E+00 5.66200000E+02 **

3.77000000E+00 5.48500000E+02 *

Table number - 35 Number of pairs - 13

Argument Value (Min) <- Relative Value -> (Max)

-3.77000000E+00 9.26600000E+02 **********

-3.41200000E+00 9.63300000E+02 **********

-2.75910000E+00	9.42800000E+02	**********
-2.10620000E+00	9.12500000E+02	**********
-1.45330000E+00	8.79700000E+02	**********
-8.00400000E-01	8.38600000E+02	**********
-1.47500000E-01	7.92200000E+02	**********
5.05500000E-01	7.41200000E+02	**********
1.15840000E+00	6.88300000E+02	*********
1.81130000E+00	6.36800000E+02	******
2.46420000E+00	5.93800000E+02	***
3.11710000E+00	5.64800000E+02	*
3.77000000E+00	5.48200000E+02	*

Table number - 41 Number of pairs - 7

Argument	Value	(Min) <- Relative Value -> (Max)
3.77000000E+00	5.49400000E+02	**********
4.61000000E+00	5.40500000E+02	**********
4.74000000E+00	5.40100000E+02	**********
4.86000000E+00	5.39800000E+02	**********
4.96000000E+00	5.39300000E+02	**********
5.06000000E+00	5.37100000E+02	**********
5.33000000E+00	4.79800000E+02	*

Table number - 42 Number of pairs - 27

Argument	Value	(Min) <- Relative Value -> (Max)
-5.33000000E+00	2.51000000E+01	*
-4.56000000E+00	7.25500000E+02	**********
-4.28000000E+00	7.26800000E+02	**********
-4.14690000E+00	7.28200000E+02	**********

-4.01960000E+00	7.30300000E+02	**********
-3.87490000E+00	7.34700000E+02	**********
-3.73370000E+00	7.44100000E+02	**********
-3.61450000E+00	7.71200000E+02	**********
-3.55090000E+00	8.34300000E+02	**********
-3.41200000E+00	8.89800000E+02	**********
-2.75910000E+00	8.82000000E+02	**********
-2.10620000E+00	8.56800000E+02	**********
-1.45330000E+00	8.28800000E+02	**********
-8.00400000E-01	7.93900000E+02	**********
-1.47500000E-01	7.54500000E+02	**********
5.05500000E-01	7.11200000E+02	**********
1.15840000E+00	6.66300000E+02	**********
1.81130000E+00	6.22700000E+02	**********
2.46420000E+00	5.86200000E+02	**********
3.11710000E+00	5.61400000E+02	**********
3.77000000E+00	5.47300000E+02	**********
4.61000000E+00	5.39500000E+02	**********
4.73500000E+00	5.36400000E+02	**********
4.86000000E+00	5.32000000E+02	**********
4.96000000E+00	5.29500000E+02	**********
5.06000000E+00	5.25100000E+02	**********
5.33000000E+00	4.76400000E+02	**********

Table number - 43 Number of pairs - 2

Argument	Value	(Min) <- Relative Value -> (Max)
-5.33000000E+00	8.73300000E+02	*
-3.77000000E+00	9.73100000E+02	**********

Table number - 51 Number of pairs - 11

Argument	Value	(Min) <- Relative Value -> (Max)
-3.77000000E+00	1.11260000E-02	**********
-3.35113000E+00	1.11260000E-02	**********
-2.51335000E+00	1.41140000E-02	**********
-1.67557000E+00	1.62320000E-02	**********
-8.37790000E-01	1.77340000E-02	**********
-1.00000000E-05	1.80810000E-02	**********
8.37770000E-01	1.71290000E-02	**********
1.67555000E+00	1.42120000E-02	**********
2.51333000E+00	1.02950000E-02	**********
3.35111000E+00	5.81800000E-03	*
3.77000000E+00	5.81800000E-03	*

Table number - 52 Number of pairs - 12

Argument	Value	(Min) <- Relative Value -> (Max)
-3.77000000E+00	7.62057000E-01	**********
-3.39300000E+00	7.62057000E-01	**********
-2.63900000E+00	9.26468000E-01	**********
-1.88500000E+00	1.13850900E+00	**********
-1.13100000E+00	1.30825400E+00	**********
-3.77000000E-01	1.40929800E+00	**********
3.77000000E-01	1.40265800E+00	**********
1.13100000E+00	1.28914100E+00	**********
1.88500000E+00	1.03887800E+00	**********
2.63900000E+00	7.28655000E-01	**********
3.39300000E+00	4.21222000E-01	*
3.77000000E+00	4.21222000E-01	*

Table number - 53 Number of pairs - 13

Argument	Value	(Min) <- Relative Value -> (Max)
-3.77000000E+00	1.02851600E+00	**********
-3.42723000E+00	1.02851600E+00	**********
-2.74178000E+00	1.25264700E+00	**********
-2.05633000E+00	1.44301500E+00	**********
-1.37088000E+00	1.65159500E+00	**********
-6.85430000E-01	1.80087800E+00	**********
2.00000000E-05	1.87804700E+00	**********
6.85470000E-01	1.85455400E+00	**********
1.37092000E+00	1.70458300E+00	**********
2.05637000E+00	1.32731500E+00	**********
2.74182000E+00	9.15033000E-01	*******
3.42727000E+00	5.41849000E-01	*
3.77000000E+00	5.41849000E-01	*

Table number - 54 Number of pairs - 14

Argument	Value	(Min) <- Relative Value -> (Max)
-3.77000000E+00	8.44293000E-01	********
-3.45580000E+00	8.44293000E-01	********
-2.82747000E+00	9.45036000E-01	**********
-2.19914000E+00	1.11287600E+00	**********
-1.57081000E+00	1.26225800E+00	**********
-9.42480000E-01	1.45472400E+00	**********
-3.14150000E-01	1.59854100E+00	**********
3.14180000E-01	1.69581000E+00	**********
9.42510000E-01	1.67678900E+00	**********

1.57084000E+00	1.52437700E+00	**********
2.19917000E+00	1.14320800E+00	**********
2.82750000E+00	7.53729000E-01	******
3.45583000E+00	4.59489000E-01	*
3.77000000E+00	4.59489000E-01	*

Table number - 55 Number of pairs - 17

Argument	Value	(Min) <- Relative Value -> (Max)
-3.77000000E+00	7.85065000E-01	*******
-3.51872000E+00	7.85065000E-01	*******
-3.01605000E+00	7.67299000E-01	*******
-2.51338000E+00	7.70856000E-01	*******
-2.01071000E+00	8.41702000E-01	*********
-1.50804000E+00	9.22295000E-01	**********
-1.00537000E+00	1.07031900E+00	**********
-5.02700000E-01	1.24116800E+00	**********
0.00000000E+00	1.43205700E+00	**********
5.02640000E-01	1.59822900E+00	**********
1.00531000E+00	1.70759000E+00	**********
1.50798000E+00	1.71287700E+00	**********
2.01065000E+00	1.56389600E+00	**********
2.51332000E+00	1.15626100E+00	**********
3.01599000E+00	7.11366000E-01	******
3.51867000E+00	4.26499000E-01	*
3.77000000E+00	4.26499000E-01	*

********** TABLE OF SPECIFIED OUTPUT TIMES

****

1 1.80000E+03 2 3.60000E+03 3 7.20000E+03 4 1.08000E+04
5 1.80000E+04 6 3.60000E+04 7 4.32000E+04 8 5.04000E+04
9 5.76000E+04 10 6.48000E+04 11 7.20000E+04 12 7.92000E+04
13 1.58400E+05 14 2.01600E+05 15 2.44800E+05 16 2.88000E+05
17 3.31200E+05 18 3.60000E+05 19 3.74400E+05 20 4.32000E+05
21 6.04800E+05 22 1.29600E+06 23 2.59200E+06 24 5.18400E+06
25 5.61600E+06 26 6.04800E+06 27 6.48000E+06 28 6.91200E+06
29 7.34400E+06 30 7.77600E+06

********** SUMMARY OF SHARED NODAL LOCATIONS **********

Shared nodes occur at the following location(s) in the model:
Radius of zero in cylindrical geometry
Surface where 360 degree cylinder joins together

********** SOURCES OF NON-LINEARITY IN THE MODEL **********

Radiation (in calculations 273.15 will be added to temperatures to
convert them to absolute)
Natural convection
Temperature dependent conductivity
Temperature dependent density or specific heat (transient calculations)

********** SUMMARY OF AREAS AND VOLUMES
****

These values are for model checking only and are not used in
any calculations. Some roundoff errors may occur in cases
with a large number of small nodes. User-defined node-to-node
connectors may cause incorrect surface areas to be displayed.
To check areas, run the case without node-to-node connectors.

Boundary Condition	Surface Area
104	2.665101E+02
110	3.720397E+02
113	1.259114E+03

Material	Volume
1	7.254116E+01
101	0.000000E+00
104	0.000000E+00
107	0.000000E+00
110	0.000000E+00
113	0.000000E+00
116	0.000000E+00

Heat Gen.	Volume
1	1.127734E+01
2	1.288568E+01
3	1.404160E+01
4	1.509093E+01
5	1.924561E+01

********** NUMBER OF PARAMETERS SPECIFIED BY THE INPUT DATA **********

Regions	21
Materials	7
Phase changes	0
Initial temperatures	21
Heat generations	5
Boundary conditions	3
Gross grid lines along x or r axis	12
Fine grid lines along x or r axis	103
Gross grid lines along y or theta axis	2
Fine grid lines along y or theta axis	3
Gross grid lines along z or phi axis	12
Fine grid lines along z or phi axis	189
Analytic functions	0
Tabular functions	26
Node-to-node connectors	0
Transient printout times	30
Nodes for monitoring of temperatures	0
Number of nodes	58401
Number of specified-temperature nodes	0
Position-dependent boundary temperature nodes	0

********** INITIAL CONDITIONS **********

Number of time steps completed = 0

Current time step = 0.00000000E+00

Current problem time = 0.00000000E+00

Elapsed wallclock time (h:m:s) = 00:00:28.00

Minimum Temperature = 3.50000E+01 at node 8416

Maximum Temperature = 9.79554E+02 at node 25659

HEAT GENERATION

Number	Current Rate (energy/time)		Net for Transient (energy)	
	(Modeled)	(Neglected)	(Modeled)	(Neglected)
1	5.70926E+05	0.00000E+00	0.00000E+00	0.00000E+00
2	4.90685E+07	0.00000E+00	0.00000E+00	0.00000E+00
3	7.17985E+07	0.00000E+00	0.00000E+00	0.00000E+00
4	6.64736E+07	0.00000E+00	0.00000E+00	0.00000E+00
5	7.83008E+07	0.00000E+00	0.00000E+00	0.00000E+00
---	---	---	---	---
Sum	2.66212E+08	0.00000E+00	0.00000E+00	0.00000E+00

BOUNDARY HEAT FLOW

Number	Environment Temperature	Current Rate (energy/time) (Modeled)	(Neglected)	Net for Transient (energy) (Modeled)	(Neglected)
104	------	0.00000E+00	0.00000E+00	0.00000E+00	0.00000E+00
110	------	0.00000E+00	0.00000E+00	0.00000E+00	0.00000E+00
113	3.50000E+01	-1.12721E+04	0.00000E+00	0.00000E+00	0.00000E+00
---		---	---	---	---
Sum		-1.12721E+04	0.00000E+00	0.00000E+00	0.00000E+00

Appendix 2: The Geometries and Positions of the Layers

	Number of Layer	Height of Layer	R (m)	H (m)	V (m^3)
Channel 1	9	0.838	0.69	7.54	11.43
Channel 2	10	0.754	1.01	7.54	12.70
Channel 3	11	0.685	1.27	7.54	13.97
Channel 4	12	0.628	1.50	7.54	15.24
Channel 5	15	0.503	1.75	7.54	19.05

Appendix 3: The Volume and Power Density of the Patches

Patch Reference #	Volume	Power Density	Power
1	636.417	1.64737	1048.414
2	637.963	1.54798	987.554
3	638.863	1.40508	897.6536
4	639.764	1.26455	809.0136
5	640.666	1.13857	729.4431
6	641.569	1.02835	659.7575
7	642.474	0.932485	599.0974
8	643.380	0.849251	546.3911
9	644.287	0.777106	500.6793
10	645.195	0.714685	461.1112
11	0.126641E+07	0.118295E-03	149.81
12	636.417	2.92252	1859.941
13	637.963	2.74197	1749.275
14	638.863	2.48557	1587.939
15	639.764	2.23539	1430.122
16	640.666	2.01158	1288.751
17	641.569	1.81593	1165.044
18	642.474	1.64583	1057.403
19	643.380	1.49822	963.9248
20	644.287	1.37033	882.8858
21	645.195	1.25975	812.7844
22	0.126641E+07	0.218639E-03	276.8866
23	636.417	4.06230	2585.317
24	637.963	3.79121	2418.652
25	638.863	3.42874	2190.495
26	639.764	3.07942	1970.102
27	640.666	2.76803	1773.383

28	641.569	2.49615	1601.452
29	642.474	2.25997	1451.972
30	643.380	2.05519	1322.268
31	644.287	1.87790	1209.907
32	645.195	1.72477	1112.813
33	0.126641E+07	0.325974E-03	412.8167
34	636.417	4.94107	3144.581
35	637.963	4.57802	2920.607
36	638.863	4.12768	2637.022
37	639.764	3.70047	2367.427
38	640.666	3.32140	2127.908
39	641.569	2.99102	1918.946
40	642.474	2.70436	1737.481
41	643.380	2.45608	1580.193
42	644.287	2.24137	1444.086
43	645.195	2.05617	1326.631
44	0.126641E+07	0.433621E-03	549.142
45	636.417	5.26559	3351.111
46	637.963	4.84012	3087.817
47	638.863	4.34953	2778.754
48	639.764	3.89185	2489.866
49	640.666	3.48779	2234.508
50	641.569	3.13633	2012.172
51	642.474	2.83178	1819.345
52	643.380	2.56836	1652.431
53	644.287	2.34081	1508.153
54	645.195	2.14485	1383.846
55	0.126641E+07	0.509295E-03	644.9763
56	636.417	5.20956	3315.453

57	637.963	4.75235	3031.823
58	638.863	4.25717	2719.748
59	639.764	3.80232	2432.587
60	640.666	3.40270	2179.994
61	641.569	3.05578	1960.494
62	642.474	2.75558	1770.389
63	643.380	2.49624	1606.031
64	644.287	2.27249	1464.136
65	645.195	2.08009	1342.064
66	0.126641E+07	0.552767E-03	700.0297
67	636.417	4.80058	3055.171
68	637.963	4.35092	2775.726
69	638.863	3.88728	2483.439
70	639.764	3.46689	2217.991
71	640.666	3.09906	1985.462
72	641.569	2.78028	1783.741
73	642.474	2.50475	1609.237
74	643.380	2.26701	1458.549
75	644.287	2.06211	1328.591
76	645.195	1.88616	1216.941
77	0.126641E+07	0.553058E-03	700.3982
78	636.417	4.19310	2668.56
79	637.963	3.78096	2412.113
80	638.863	3.37131	2153.805
81	639.764	3.00363	1921.614
82	640.666	2.68294	1718.868
83	641.569	2.40538	1543.217
84	642.474	2.16572	1391.419
85	643.380	1.95913	1260.465

86	644.287	1.78124	1147.63
87	645.195	1.62865	1050.797
88	0.126641E+07	0.518122E-03	656.1549
89	636.417	3.35976	2138.208
90	637.963	3.00380	1916.313
91	638.863	2.66510	1702.634
92	639.764	2.36541	1513.304
93	640.666	2.10555	1348.954
94	641.569	1.88135	1207.016
95	642.474	1.68822	1084.637
96	643.380	1.52209	979.2823
97	644.287	1.37930	888.6651
98	645.195	1.25704	811.0359
99	0.126641E+07	0.426139E-03	539.6667
100	63641.7	1.21962	77618.69
101	63729.4	1.14527	72987.37
102	63819.3	1.03920	66321.02
103	63909.3	0.935082	59760.44
104	63999.4	0.841824	53876.23
105	64089.6	0.760268	48725.27
106	64180.0	0.689345	44242.16
107	64270.5	0.627777	40347.54
108	64361.1	0.574417	36970.11
109	64451.9	0.528252	34046.85
110	632370.	0.885165E-04	55.97518
111	63641.7	2.11031	134303.7
112	63729.4	1.98145	126276.6
113	63819.3	1.79706	114687.1
114	63909.3	1.61694	103337.5

115	63999.4	1.45579	93169.69
116	64089.6	1.31491	84272.06
117	64180.0	1.19243	76530.16
118	64270.5	1.08612	69805.48
119	64361.1	0.994009	63975.51
120	64451.9	0.914352	58931.72
121	632370.	0.161054E-03	101.8457
122	63641.7	3.01806	192074.5
123	63729.4	2.82567	180078.3
124	63819.3	2.56048	163408
125	63909.3	2.30337	147206.8
126	63999.4	2.07378	132720.7
127	64089.6	1.87319	120052
128	64180.0	1.69885	109032.2
129	64270.5	1.54760	99465.03
130	64361.1	1.41659	91173.29
131	64451.9	1.30338	84005.32
132	632370.	0.251238E-03	158.8754
133	63641.7	3.76357	239520
134	63729.4	3.50792	223557.6
135	63819.3	3.17444	202590.5
136	63909.3	2.85461	182436.1
137	63999.4	2.56986	164469.5
138	64089.6	2.32133	148773.1
139	64180.0	2.10547	135129.1
140	64270.5	1.91833	123292
141	64361.1	1.75631	113038
142	64451.9	1.61643	104182
143	632370.	0.350372E-03	221.5647

144	63641.7	4.11832	262096.9
145	63729.4	3.81831	243338.6
146	63819.3	3.44989	220169.6
147	63909.3	3.10102	198184
148	63999.4	2.79154	178656.9
149	64089.6	2.52179	161620.5
150	64180.0	2.28769	146823.9
151	64270.5	2.08491	133998.2
152	64361.1	1.90948	122896.2
153	64451.9	1.75817	113317.4
154	632370.	0.432698E-03	273.6252
155	63641.7	4.16190	264870.4
156	63729.4	3.83769	244573.7
157	63819.3	3.46173	220925.2
158	63909.3	3.11034	198779.7
159	63999.4	2.79985	179188.7
160	64089.6	2.52961	162121.7
161	64180.0	2.29532	147313.6
162	64270.5	2.09255	134489.2
163	64361.1	1.91727	123397.6
164	64451.9	1.76626	113838.8
165	632370.	0.490028E-03	309.879
166	63641.7	3.88282	247109.3
167	63729.4	3.56264	227044.9
168	63819.3	3.20902	204797.4
169	63909.3	2.88242	184213.4
170	63999.4	2.59486	166069.5
171	64089.6	2.34495	150286.9
172	64180.0	2.12847	136605.2

173	64270.5	1.94129	124767.7
174	64361.1	1.77961	114537.7
175	64451.9	1.64046	105730.8
176	632370.	0.504995E-03	319.3437
177	63641.7	3.39165	215850.4
178	63729.4	3.09928	197515.3
179	63819.3	2.78858	177965.2
180	63909.3	2.50444	160057
181	63999.4	2.25505	144321.8
182	64089.6	2.03856	130650.5
183	64180.0	1.85120	118810
184	64270.5	1.68931	108572.8
185	64361.1	1.54957	99732.03
186	64451.9	1.42941	92128.19
187	632370.	0.479257E-03	303.0677
188	63641.7	2.73429	174014.9
189	63729.4	2.50194	159447.1
190	63819.3	2.25678	144026.1
191	63909.3	2.03258	129900.8
192	63999.4	1.83553	117472.8
193	64089.6	1.66427	106662.4
194	64180.0	1.51592	97291.75
195	64270.5	1.38767	89186.24
196	64361.1	1.27691	82183.33
197	64451.9	1.18165	76159.59
198	632370.	0.425527E-03	269.0905
199	63641.7	2.31375	147251
200	63729.4	2.09068	133237.8
201	63819.3	1.87113	119414.2

202	63909.3	1.67486	107039.1
203	63999.4	1.50402	96256.38
204	64089.6	1.35630	86924.72
205	64180.0	1.22879	78863.74
206	64270.5	1.11888	71910.98
207	64361.1	1.02419	65918
208	64451.9	0.942926	60773.37
209	632370.	0.352777E-03	223.0856
210	127283.	0.772045	98268.2
211	127463.	0.731902	93290.42
212	127643.	0.667869	85248.8
213	127823.	0.603477	77138.24
214	128003.	0.545264	69795.43
215	128184.	0.494125	63338.92
216	128365.	0.449533	57704.3
217	128545.	0.410750	52799.86
218	128727.	0.377086	48541.15
219	120779.	0.347927	42022.28
220	1.00000	0.567821E-04	5.68E-05
221	127283.	1.29699	165084.8
222	127463.	1.23225	157066.3
223	127643.	1.12556	143669.9
224	127823.	1.01826	130157
225	128003.	0.921163	117911.6
226	128184.	0.835786	107134.4
227	128365.	0.761277	97721.32
228	128545.	0.696436	89523.37
229	128727.	0.640125	82401.37
230	120779.	0.591340	71421.45

231	1.00000	0.100438E-03	0.0001
232	127283.	1.87058	238093
233	127463.	1.77864	226710.8
234	127643.	1.62718	207698.1
235	127823.	1.47474	188505.7
236	128003.	1.33658	171086.2
237	128184.	1.21489	155729.5
238	128365.	1.10856	142300.3
239	128545.	1.01594	130594
240	128727.	0.935441	120416.5
241	120779.	0.865676	104555.5
242	1.00000	0.158710E-03	0.000159
243	127283.	2.39048	304267.5
244	127463.	2.27159	289543.7
245	127643.	2.08106	265632.7
246	127823.	1.88979	241558.6
247	128003.	1.71629	219690.3
248	128184.	1.56325	200383.6
249	128365.	1.42936	183479.8
250	128545.	1.31261	168729.5
251	128727.	1.21106	155896.1
252	120779.	1.12303	135638.4
253	1.00000	0.229082E-03	0.000229
254	127283.	2.59236	329963.4
255	127463.	2.45830	313342.3
256	127643.	2.25420	287732.9
257	127823.	2.05072	262129.2
258	128003.	1.86622	238881.8
259	128184.	1.70332	218338.4

260	128365.	1.56066	200334.1
261	128545.	1.43617	184612.5
262	128727.	1.32781	170925
263	120779.	1.23386	149024.4
264	1.00000	0.284304E-03	0.000284
265	127283.	2.62063	333561.6
266	127463.	2.47776	315822.7
267	127643.	2.27314	290150.4
268	127823.	2.07112	264736.8
269	128003.	1.88821	241696.5
270	128184.	1.72665	221328.9
271	128365.	1.58505	203464.9
272	128545.	1.46142	187858.2
273	128727.	1.35377	174266.8
274	120779.	1.26043	152233.5
275	1.00000	0.326439E-03	0.000326
276	127283.	2.51078	319579.6
277	127463.	2.36631	301617
278	127643.	2.17138	277161.5
279	127823.	1.98093	253208.4
280	128003.	1.80885	231538.2
281	128184.	1.65685	212381.7
282	128365.	1.52356	195571.8
283	128545.	1.40715	180882.1
284	128727.	1.30575	168085.3
285	120779.	1.21784	147089.5
286	1.00000	0.349316E-03	0.000349
287	127283.	2.30211	293019.5
288	127463.	2.16290	275689.7

289	127643.	1.98481	253347.1
290	127823.	1.81258	231689.4
291	128003.	1.65730	212139.4
292	128184.	1.52016	194860.2
293	128365.	1.39989	179696.9
294	128545.	1.29482	166442.6
295	128727.	1.20328	154894.6
296	120779.	1.12392	135745.9
297	1.00000	0.350881E-03	0.000351
298	127283.	2.01223	256122.7
299	127463.	1.88502	240270.3
300	127643.	1.72953	220762.4
301	127823.	1.58061	202038.3
302	128003.	1.44666	185176.8
303	128184.	1.32840	170279.6
304	128365.	1.22468	157206
305	128545.	1.13407	145779
306	128727.	1.05512	135822.4
307	120779.	0.986694	119171.9
308	1.00000	0.329903E-03	0.00033
309	127283.	1.75233	223041.8
310	127463.	1.63562	208481
311	127643.	1.49932	191377.7
312	127823.	1.37018	175140.5
313	128003.	1.25441	160568.2
314	128184.	1.15230	147706.4
315	128365.	1.06279	136425
316	128545.	0.984622	126568.2
317	128727.	0.916527	117981.8

318	120779.	0.857525	103571
319	1.00000	0.302584E-03	0.000303
320	127283.	1.43986	183269.7
321	127463.	1.34110	170940.6
322	127643.	1.22904	156878.4
323	127823.	1.12359	143620.6
324	128003.	1.02924	131745.8
325	128184.	0.946072	121271.3
326	128365.	0.873174	112085
327	128545.	0.809520	104059.7
328	128727.	0.754076	97069.94
329	120779.	0.706032	85273.84
330	1.00000	0.260114E-03	0.00026
331	127283.	0.654751	83338.67
332	127463.	0.620700	79116.28
333	127643.	0.566380	72294.44
334	127823.	0.511756	65414.19
335	128003.	0.462379	59185.9
336	128184.	0.419004	53709.61
337	128365.	0.381183	48930.56
338	128545.	0.348290	44770.94
339	128727.	0.319741	41159.3
340	120781.	0.295011	35631.72
341	1.00000	0.481541E-04	4.82E-05
342	127283.	1.06810	135951
343	127463.	1.01511	129389
344	127643.	0.927266	118359
345	127823.	0.838845	107223.7
346	128003.	0.758828	97132.26

347	128184.	0.688469	88250.71
348	128365.	0.627073	80494.23
349	128545.	0.573645	73739.2
350	128727.	0.527247	67870.92
351	120781.	0.487050	58826.39
352	1.00000	0.822150E-04	8.22E-05
353	127283.	1.60928	204834
354	127463.	1.53182	195250.4
355	127643.	1.40180	178930
356	127823.	1.27054	162404.2
357	128003.	1.15150	147395.5
358	128184.	1.04664	134162.5
359	128365.	0.955018	122590.9
360	128545.	0.875208	112503.6
361	128727.	0.805843	103733.8
362	120781.	0.745725	90069.41
363	1.00000	0.134187E-03	0.000134
364	127283.	2.13367	271579.9
365	127463.	2.03120	258902.8
366	127643.	1.86177	237641.9
367	127823.	1.69084	216128.2
368	128003.	1.53558	196558.8
369	128184.	1.39860	179278.1
370	128365.	1.27874	164145.5
371	128545.	1.17424	150942.7
372	128727.	1.08333	139453.8
373	120781.	1.00452	121326.9
374	1.00000	0.198727E-03	0.000199
375	127283.	2.33843	297642.4

376	127463.	2.22265	283305.6
377	127643.	2.03938	260312.6
378	127823.	1.85546	237170.5
379	128003.	1.68841	216121.5
380	128184.	1.54086	197513.6
381	128365.	1.41162	181202.6
382	128545.	1.29884	166959.4
383	128727.	1.20066	154557.4
384	120781.	1.11554	134736
385	1.00000	0.247238E-03	0.000247
386	127283.	2.36029	300424.8
387	127463.	2.23764	285216.3
388	127643.	2.05428	262214.5
389	127823.	1.87182	239261.6
390	128003.	1.70627	218407.7
391	128184.	1.55998	199964.5
392	128365.	1.43175	183786.6
393	128545.	1.31978	169651.1
394	128727.	1.22226	157337.9
395	120781.	1.13771	137413.8
396	1.00000	0.282083E-03	0.000282
397	127283.	2.22271	282913.2
398	127463.	2.10106	267807.4
399	127643.	1.92940	246274.4
400	127823.	1.76021	224995.3
401	128003.	1.60698	205698.3
402	128184.	1.47154	188627.9
403	128365.	1.35277	173648.3
404	128545.	1.24903	160556.6

405	128727.	1.15864	149148.3
406	120781.	1.08028	130477.3
407	1.00000	0.295971E-03	0.000296
408	127283.	2.02179	257339.5
409	127463.	1.90575	242912.6
410	127643.	1.75023	223404.6
411	127823.	1.59837	204308.4
412	128003.	1.46112	187027.7
413	128184.	1.33981	171742.2
414	128365.	1.23339	158324.1
415	128545.	1.14042	146595.3
416	128727.	1.05940	136373.4
417	120781.	0.989158	119471.5
418	1.00000	0.294586E-03	0.000295
419	127283.	1.75504	223386.8
420	127463.	1.64969	210274.4
421	127643.	1.51483	193357.4
422	127823.	1.38436	176953
423	128003.	1.26669	162140.1
424	128184.	1.16272	149042.1
425	128365.	1.07152	137545.7
426	128545.	0.991838	127495.8
427	128727.	0.922391	118736.6
428	120781.	0.862188	104135.9
429	1.00000	0.274875E-03	0.000275
430	127283.	1.55264	197624.7
431	127463.	1.45408	185341.4
432	127643.	1.33389	170261.7
433	127823.	1.21889	155802.2

434	128003.	1.11552	142789.9
435	128184.	1.02429	131297.6
436	128365.	0.944301	121215.2
437	128545.	0.874433	112404
438	128727.	0.813554	104726.4
439	120781.	0.760792	91889.22
440	1.00000	0.256112E-03	0.000256
441	127283.	1.32065	168096.3
442	127463.	1.23368	157248.6
443	127643.	1.13114	144382.1
444	127823.	1.03380	132143.4
445	128003.	0.946510	121156.1
446	128184.	0.869527	111459.4
447	128365.	0.802047	102954.8
448	128545.	0.743117	95523.97
449	128727.	0.691780	89050.76
450	120781.	0.647287	78179.97
451	1.00000	0.228017E-03	0.000228
452	127283.	1.17948	150127.8
453	127463.	1.10029	140246.3
454	127643.	1.00889	128777.7
455	127823.	0.922547	117922.7
456	128003.	0.845208	108189.2
457	128184.	0.777019	99601.4
458	128365.	0.717248	92069.54
459	128545.	0.665050	85488.85
460	128727.	0.619579	79756.55
461	120781.	0.580159	70072.18
462	1.00000	0.212031E-03	0.000212

463	127283.	0.607095	77272.87
464	127463.	0.575864	73401.35
465	127643.	0.525627	67092.61
466	127823.	0.475027	60719.38
467	128003.	0.429260	54946.57
468	128184.	0.389046	49869.47
469	128365.	0.353976	45438.13
470	128545.	0.323471	41580.58
471	128727.	0.296992	38230.89
472	120784.	0.274054	33101.34
473	1.00000	0.444227E-04	4.44E-05
474	127283.	1.00670	128135.8
475	127463.	0.957593	122057.7
476	127643.	0.875062	111695.5
477	127823.	0.791792	101209.2
478	128003.	0.716373	91697.89
479	128184.	0.650034	83323.96
480	128365.	0.592132	76009.02
481	128545.	0.541738	69637.71
482	128727.	0.497969	64102.06
483	120784.	0.460045	55566.08
484	1.00000	0.765580E-04	7.66E-05
485	127283.	1.62555	206904.9
486	127463.	1.54892	197430
487	127643.	1.41798	180995.2
488	127823.	1.28541	164305
489	128003.	1.16505	149129.9
490	128184.	1.05898	135744.3
491	128365.	0.966280	124036.5

492	128545.	0.885512	113828.1
493	128727.	0.815304	104951.6
494	120784.	0.754449	91125.37
495	1.00000	0.132430E-03	0.000132
496	127283.	2.18792	278485
497	127463.	2.08458	265706.8
498	127643.	1.91107	243934.7
499	127823.	1.73553	221840.7
500	128003.	1.57593	201723.8
501	128184.	1.43505	183950.4
502	128365.	1.31175	168382.8
503	128545.	1.20422	154796.5
504	128727.	1.11067	142973.2
505	120784.	1.02956	124354.4
506	1.00000	0.196836E-03	0.000197
507	127283.	2.39048	304267.5
508	127463.	2.27319	289747.6
509	127643.	2.08554	266204.6
510	127823.	1.89682	242457.2
511	128003.	1.72527	220839.7
512	128184.	1.57368	201720.6
513	128365.	1.44087	184957.3
514	128545.	1.32496	170317
515	128727.	1.22404	157567
516	120784.	1.13654	137275.8
517	1.00000	0.241441E-03	0.000241
518	127283.	2.38145	303118.1
519	127463.	2.25793	287802.5
520	127643.	2.07204	264481.4

521	127823.	1.88677	241172.6
522	128003.	1.71858	219983.4
523	128184.	1.56990	201236.1
524	128365.	1.43953	184785.3
525	128545.	1.32569	170410.8
526	128727.	1.22653	157887.5
527	120784.	1.14056	137761.4
528	1.00000	0.269234E-03	0.000269
529	127283.	2.22953	283781.3
530	127463.	2.10704	268569.6
531	127643.	1.93347	246793.9
532	127823.	1.76222	225252.2
533	128003.	1.60705	205707.2
534	128184.	1.46985	188411.3
535	128365.	1.34951	173229.9
536	128545.	1.24439	159960.1
537	128727.	1.15280	148396.5
538	120784.	1.07339	129648.3
539	1.00000	0.278410E-03	0.000278
540	127283.	1.99915	254457.8
541	127463.	1.88343	240067.6
542	127643.	1.72796	220562
543	127823.	1.57604	201454.2
544	128003.	1.43867	184154.1
545	128184.	1.31722	168846.5
546	128365.	1.21066	155406.4
547	128545.	1.11756	143656.8
548	128727.	1.03643	133416.5
549	120784.	0.966104	116689.9

550	1.00000	0.271202E-03	0.000271
551	127283.	1.73473	220801.6
552	127463.	1.62956	207708.6
553	127643.	1.49456	190770.1
554	127823.	1.36381	174326.3
555	128003.	1.24583	159470
556	128184.	1.14156	146329.7
557	128365.	1.05007	134792.2
558	128545.	0.970125	124704.7
559	128727.	0.900457	115913.1
560	120784.	0.840068	101466.8
561	1.00000	0.251462E-03	0.000251
562	127283.	1.50277	191277.1
563	127463.	1.40607	179221.9
564	127643.	1.28793	164395.2
565	127823.	1.17481	150167.7
566	128003.	1.07308	137357.5
567	128184.	0.983284	126041.3
568	128365.	0.904533	116110.4
569	128545.	0.835748	107431.2
570	128727.	0.775818	99868.72
571	120784.	0.723885	87433.73
572	1.00000	0.228136E-03	0.000228
573	127283.	1.29819	165237.5
574	127463.	1.21135	154402.3
575	127643.	1.10878	141528
576	127823.	1.01133	129271.2
577	128003.	0.923914	118263.8
578	128184.	0.846797	108545.8

579	128365.	0.779191	100020.9
580	128545.	0.720154	92572.2
581	128727.	0.668728	86083.35
582	120784.	0.624169	75389.63
583	1.00000	0.205352E-03	0.000205
584	127283.	1.18684	151064.6
585	127463.	1.10508	140856.8
586	127643.	1.01099	129045.8
587	127823.	0.922165	117873.9
588	128003.	0.842620	107857.9
589	128184.	0.772494	99021.37
590	128365.	0.711032	91271.62
591	128545.	0.657369	84501.5
592	128727.	0.610634	78605.08
593	120784.	0.570134	68863.07
594	1.00000	0.194467E-03	0.000194
595	127283.	1.08819	138508.1
596	127463.	1.01152	128931.4
597	127643.	0.925078	118079.7
598	127823.	0.843889	107868.4
599	128003.	0.771287	98727.05
600	128184.	0.707308	90665.57
601	128365.	0.651246	83597.19
602	128545.	0.602303	77423.04
603	128727.	0.559687	72046.83
604	120784.	0.522747	63139.47
605	1.00000	0.183931E-03	0.000184
606	127283.	1.08393	137965.9
607	127463.	1.00620	128253.3

608	127643.	0.920028	117435.1
609	127823.	0.839416	107296.7
610	128003.	0.767410	98230.78
611	128184.	0.703973	90238.08
612	128365.	0.648390	83230.58
613	128545.	0.599867	77109.9
614	128727.	0.557625	71781.39
615	120784.	0.520994	62927.74
616	1.00000	0.188185E-03	0.000188
617	127283.	1.10942	141210.3
618	127463.	1.02876	131128.8
619	127643.	0.940554	120055.1
620	127823.	0.858321	109713.2
621	128003.	0.784925	100472.8
622	128184.	0.720273	92327.47
623	128365.	0.663624	85186.09
624	128545.	0.614168	78948.23
625	128727.	0.571123	73518.95
626	120784.	0.533773	64471.24
627	1.00000	0.197166E-03	0.000197

Appendix 4: The MathCad file in Theoretical Study

1Constants

$H := 7.54$

$D := 3.5$

$d := 0.06$

$g := 9.8$

$poro := 0.39$

$T\_air\_in := 20$

$P\_atm := 1.01 \cdot 10^5$ *

$\rho\_air\_in := 1.205$

$Cp\_air := 1185$

$Cp\_CO := 1267$

$Ratio\_CO\_out := 0.31$

2. The outlet temperature of the gas

Important_Value

$T\_air\_out := 800$

3. The velocity of the gas(through resistance balance)

Important_Value

$u\_air\_in := 0.0415$

$$Mole\_air\_in := \frac{\left[u\_air\_in \cdot poro \cdot 3.14 \left(\frac{D}{2}\right)^2 \cdot \rho\_air\_in\right]}{0.029}$$

$Mole\_air\_in = 6.467$

$M\_air\_rate := Mole\_air\_in \cdot 0.029$ *

$M\_air\_rate = 0.188$

$T\_CO\_out := T\_air\_out$

$T\_air\_ave := T\_air\_out$

$T\_air\_ave = 800$

$T\_CO\_ave := T\_air\_ave$

$T\_CO\_ave = 800$

$Cp\_air\_in := 1005$

$Cp\_out := [1043 + 0.1435(T\_air\_out - 27)] \cdot (1 - Ratio\_CO\_out) + [1041 + 0.1494(T\_air\_out - 27)] \cdot Ratio\_CO\_out$

$Cp\_out = 1.155 \times 10^{3}$

$$Cp\_ave := \frac{(Cp\_air\_in + Cp\_out)}{2}$$

$Cp\_ave = 1.08 \times 10^{3}$

$k\_N\_ave := 0.0267 + 5.135 10^{-5} \cdot (T\_air\_ave - 27)$ *

$k\_N\_ave = 0.066$

$k\_O\_ave := 0.0274 + 5.8 \cdot 10^{-5} \cdot (T\_air\_ave - 27)$ *

$k\_N\_ave = 0.066$

$k\_CO\_ave := 0.026 + 5.8 \cdot 10^{-5} \cdot (T\_CO\_ave - 27)$ *

$k\_CO\_ave = 0.071$

$$k\_ave := k\_N\_ave \cdot (1 - Ratio\_CO\_out) + k\_O\_ave \cdot \frac{Ratio\_CO\_out}{2} + k\_CO\_ave \cdot \frac{Ratio\_CO\_out}{2}$$ *

$k\_ave = 0.068$

$$\rho\_CO\_ave := \frac{336.82}{(T\_CO\_ave + 273)}$$ *

$\rho\_CO\_ave = 0.314$

$$\rho\_CO\_out := \frac{336.82}{T\_CO\_out + 273}$$

$\rho\_CO\_out = 0.314$

$$\rho\_N\_ave := \frac{341.4}{(T\_CO\_ave + 273)}$$ *

$\rho\_N\_ave = 0.318$

$$\rho\_N\_out := \frac{341.4}{T\_CO\_out + 273}$$

$\rho\_N\_out = 0.318$

$$\rho\_O\_ave := \frac{389.7}{(T\_CO\_ave + 273)}$$ *

$$\rho\_O\_ave = 0.363$$

$$\rho\_O\_out := \frac{389.7}{T\_CO\_out + 273}$$

$$\rho\_O\_out = 0.363$$

$$\rho\_out := \rho\_N\_out \cdot (1 - Ratio\_CO\_out) + \rho\_CO\_out \cdot Ratio\_CO\_out \quad *$$

$$\rho\_out = 0.317$$

$$\rho\_ave := \rho\_N\_ave \cdot (1 - Ratio\_CO\_out) + \rho\_O\_ave \cdot \frac{Ratio\_CO\_out}{2} + \rho\_CO\_ave \cdot \frac{Ratio\_CO\_out}{2} \quad *$$

$$\rho\_ave = 0.324$$

$$\eta\_CO\_ave := 10^{-6} \cdot [\, 27.1 + 0.0249 (T\_CO\_ave - 327) \,] \quad *$$

$$\eta\_CO\_ave = 3.888 \times 10^{-5}$$

$$\eta\_N\_ave := 10^{-6} \cdot [\, 28.3 + 0.024 (T\_CO\_ave - 327) \,] \quad *$$

$$\eta\_N\_ave = 3.965 \times 10^{-5}$$

$$\eta\_O\_ave := 10^{-6} \cdot [\, 33.9 + 0.0293 (T\_CO\_ave - 327) \,] \quad *$$

$$\eta\_O\_ave = 4.776 \times 10^{-5}$$

$$\eta\_ave := \eta\_N\_ave \cdot (1 - Ratio\_CO\_out) + \eta\_O\_ave \cdot \frac{Ratio\_CO\_out}{2} + \eta\_CO\_ave \cdot \frac{Ratio\_CO\_out}{2} \quad *$$

$$\eta\_ave = 4.079 \times 10^{-5}$$

$$\eta\_N\_out := 10^{-6} \cdot [\, 28.3 + 0.024 (T\_CO\_out - 327) \,] \quad *$$

$$\eta\_N\_out = 3.965 \times 10^{-5}$$

$$\eta\_CO2\_out := 10^{-6} \cdot [\, 28.3 + 0.024 (T\_CO\_out - 327) \,] \quad *$$

$$\eta\_N\_out = 3.965 \times 10^{-5}$$

$$\eta\_out := \eta\_N\_out \cdot (1 - Ratio\_CO\_out) + \eta\_CO2\_out \cdot Ratio\_CO\_out \quad *$$

$$\eta\_out = 3.965 \times 10^{-5}$$

$$Pr\_ave := 0.7$$

$$u\_out := \left(\frac{\rho\_air\_in}{\rho\_out} \right) \cdot u\_air\_in \quad *$$

$$u\_out = 0.158$$

$$u\_ave := \left(\frac{\rho\_air\_in}{\rho\_ave}\right)\cdot u\_air\_in \quad *$$

$$u\_ave = 0.154$$

3. Resistance Balance

3.1. friction loss

$$\Delta P\_buoy := (\rho\_air\_in - \rho\_out)\cdot g\cdot\frac{H}{2} \quad *$$

$$\Delta P\_buoy = 32.814$$

$$Re := \frac{d\cdot u\_out\cdot\rho\_out}{\eta\_out}$$

$$Re = 75.67$$

$$\psi := 320\left(\frac{Re}{1-poro}\right)^{-1} + 6\cdot\left(\frac{Re}{1-poro}\right)^{-0.1} \quad *$$

$$\psi = 6.285$$

$$\Delta p\_fric := \left[\psi\cdot\left(\frac{H}{d}\right)\cdot\left(\frac{1-poro}{poro^3}\right)\cdot\frac{\rho\_ave\cdot u\_out^2}{2}\right] \quad *$$

$$\Delta p\_fric = 32.822$$

3.2. Total pressure loss

$$\Delta p\_resis := \Delta p\_fric$$

$$\Delta p\_resis = 32.822$$

$$u\_out := u\_air\_in\cdot\frac{\rho\_air\_in}{\rho\_out} \quad *$$

$$u\_out = 0.158$$

4.The temperature of the graphite (through heat balance)

$$Q\_generated := 0.2\cdot 2Mole\_air\_in\cdot 1.11\cdot 10^5 \quad *$$

$$Q\_generated = 2.871\times 10^5$$

$$Q\_removed = 1.671\times 10^5$$

$$Q\_removed\_by\_heating\_7 := Q\_generated - Q\_removed \quad *$$

$$Q\_removed\_by\_heating\_7 = 1.201\times 10^5$$

$$Q\_density\_removed\_by\_heating\_7 := \frac{(Q\_generated - Q\_removed)}{15} *$$

$$Q\_density\_removed\_by\_heating\_7 = 8.003 \times 10^{3}$$

$$hc := 0.664\left(\frac{k\_ave}{d}\right)\cdot\left(\frac{Re}{poro}\right)^{\frac{1}{2}}\cdot Pr\_ave^{\frac{1}{3}} *$$

$$hc = 9.305$$

$$T\_graphite\_ave := T\_air\_ave + \frac{Q\_removed}{hc\cdot 3600003.14\left(\frac{d}{2}\right)^{2}} *$$

$$T\_graphite\_ave = 817.649$$

5. Graphite consumed

$$W\_graphite := 0.2\cdot 2\cdot Mole\_air\_in\cdot 0.012 *$$

$$W\_graphite = 0.031$$

$$TotalW\_graphite\_daily := W\_graphite\cdot 24\cdot 3600 *$$

$$TotalW\_graphite\_daily = 2.682 \times 10^{3}$$

Appendix 5: The Input for Non-Isothermal Experiment

FLUENT

Version: 3d, dp, segregated, spe2, lam, unsteady (3d, double precision, segregated, 2 species, laminar, unsteady)

Release: 6.0.20

Title:

Models

Model	Settings
Space	3D
Time	Unsteady, 2nd-Order Implicit
Viscous	Laminar
Heat Transfer	Enabled
Solidification and Melting	Disabled
Radiation	None
Species Transport	Non-Reacting (2 species)
Coupled Dispersed Phase	Disabled
Pollutants	Disabled
Soot	Disabled

Boundary Conditions

Zones

name	id	type

---

he-region	2	fluid
n_region	3	fluid
region01_outside	4	wall
region09_outside	5	wall
tank_region_wall	6	wall
region02_outside	7	wall
region08_outside	8	wall
region03_outside	9	wall
region07_outside	10	wall
region04_outside	11	wall
region06_outside	12	wall
region05_outside	13	wall
all_symmetry_faces	14	symmetry
default-interior	16	interior
all_symmetry_faces:001	1	symmetry
default-interior:015	15	interior
default-interior:017	17	interior

Boundary Conditions

he-region

Condition	Value
Material Name	mixture-template

Specify source terms? no

Source Terms ((mass (inactive . #f) (constant . 0) (profile)) (x-momentum (inactive . #f) (constant . 0) (profile)) (y-momentum (inactive . #f) (constant . 0) (profile)) (z-momentum (inactive . #f) (const
nt . 0) (profile)) (species-0 (inactive . #f) (constant . 0) (profile)) (energy (inactive . #f) (constant . 0) (profile)))

Specify fixed values? no

Local Coordinate System for Fixed Velocities no

Fixed Values ((x-velocity (constant . 0) (profile)) (y-velocity (constant . 0) (profile)) (z-velocity (constant . 0) (profile)) (species-0 (profile udf he_profile) (constant . 0)) (temperature (constant .
291.14999) (profile)))

Motion Type 0

X-Velocity Of Zone 0

Y-Velocity Of Zone 0

Z-Velocity Of Zone 0

Rotation speed 0

X-Origin of Rotation-Axis 0

Y-Origin of Rotation-Axis 0

Z-Origin of Rotation-Axis 0

X-Component of Rotation-Axis 0

Y-Component of Rotation-Axis 0

Z-Component of Rotation-Axis 1

Porous zone? no

Conical porous zone? no

X-Component of Direction-1 Vector 1

Y-Component of Direction-1 Vector 1

Z-Component of Direction-1 Vector 1

X-Component of Direction-2 Vector 0

Y-Component of Direction-2 Vector 1

Z-Component of Direction-2 Vector 0

X-Coordinate of Point on Cone Axis 1

Y-Coordinate of Point on Cone Axis 0

Z-Coordinate of Point on Cone Axis 0

Half Angle of Cone Relative to its Axis 0

Direction-1 Viscous Resistance 0

Direction-2 Viscous Resistance 0

Direction-3 Viscous Resistance 0

Direction-1 Inertial Resistance 0

Direction-2 Inertial Resistance 0

Direction-3 Inertial Resistance 0

C0 Coefficient for Power-Law 0

C1 Coefficient for Power-Law 0

Porosity 1

Solid Material Name aluminum

n_region

Condition Value

Material Name mixture-template

Specify source terms? no

Source Terms ((mass (inactive . #f) (constant . 0) (profile)) (x-momentum (inactive . #f) (constant . 0) (profile)) (y-momentum (inactive . #f) (constant . 0) (profile)) (z-momentum (inactive . #f) (const
nt . 0) (profile)) (species-0 (inactive . #f) (constant . 0) (profile)) (energy (inactive . #f) (constant . 0) (profile)))

Specify fixed values? no

Local Coordinate System for Fixed Velocities no

Fixed Values ((x-velocity (constant . 0) (profile)) (y-velocity (constant . 0) (profile)) (z-velocity (constant . 0) (profile)) (species-0 (profile udf he_profile) (constant . 0)) (temperature (constant .
291.14999) (profile)))

Motion Type 0

X-Velocity Of Zone 0

Y-Velocity Of Zone 0

Z-Velocity Of Zone 0

Rotation speed	0
X-Origin of Rotation-Axis	0
Y-Origin of Rotation-Axis	0
Z-Origin of Rotation-Axis	0
X-Component of Rotation-Axis	0
Y-Component of Rotation-Axis	0
Z-Component of Rotation-Axis	1
Porous zone?	no
Conical porous zone?	no
X-Component of Direction-1 Vector	1
Y-Component of Direction-1 Vector	1
Z-Component of Direction-1 Vector	1
X-Component of Direction-2 Vector	0
Y-Component of Direction-2 Vector	1
Z-Component of Direction-2 Vector	0

X-Coordinate of Point on Cone Axis 1

Y-Coordinate of Point on Cone Axis 0

Z-Coordinate of Point on Cone Axis 0

Half Angle of Cone Relative to its Axis 0

Direction-1 Viscous Resistance 0

Direction-2 Viscous Resistance 0

Direction-3 Viscous Resistance 0

Direction-1 Inertial Resistance 0

Direction-2 Inertial Resistance 0

Direction-3 Inertial Resistance 0

C0 Coefficient for Power-Law 0

C1 Coefficient for Power-Law 0

Porosity 1

Solid Material Name aluminum

region01_outside

Condition	Value

Wall Thickness	0
Heat Generation Rate	0
Material Name	aluminum
Thermal BC Type	0
Temperature	291.14999
Heat Flux	0
Convective Heat Transfer Coefficient	0
Free Stream Temperature	300
Enable shell conduction?	no
Wall Motion	0
Shear Boundary Condition	0
Define wall motion relative to adjacent cell zone?	yes
Apply a rotational velocity to this wall?	no
Velocity Magnitude	0
X-Component of Wall Translation	1
Y-Component of Wall Translation	0
Z-Component of Wall Translation	0
Define wall velocity components?	no
X-Component of Wall Translation	0
Y-Component of Wall Translation	0
Z-Component of Wall Translation	0
External Emissivity	1
External Radiation Temperature	300
	(0)
	(((constant . 0) (profile)))
Rotation Speed	0
X-Position of Rotation-Axis Origin	0
Y-Position of Rotation-Axis Origin	0
Z-Position of Rotation-Axis Origin	0

X-Component of Rotation-Axis Direction	0
Y-Component of Rotation-Axis Direction	0
Z-Component of Rotation-Axis Direction	1
X-component of shear stress	0
Y-component of shear stress	0
Z-component of shear stress	0
Surface tension gradient	0

region09_outside

Condition	Value
Wall Thickness	0
Heat Generation Rate	0
Material Name	aluminum
Thermal BC Type	0
Temperature	291.14999
Heat Flux	0
Convective Heat Transfer Coefficient	0
Free Stream Temperature	300
Enable shell conduction?	no
Wall Motion	0
Shear Boundary Condition	0
Define wall motion relative to adjacent cell zone?	yes
Apply a rotational velocity to this wall?	no
Velocity Magnitude	0
X-Component of Wall Translation	1
Y-Component of Wall Translation	0
Z-Component of Wall Translation	0
Define wall velocity components?	no

X-Component of Wall Translation	0
Y-Component of Wall Translation	0
Z-Component of Wall Translation	0
External Emissivity	1
External Radiation Temperature	300
	(0)
	(((constant . 0) (profile)))
Rotation Speed	0
X-Position of Rotation-Axis Origin	0
Y-Position of Rotation-Axis Origin	0
Z-Position of Rotation-Axis Origin	0
X-Component of Rotation-Axis Direction	0
Y-Component of Rotation-Axis Direction	0
Z-Component of Rotation-Axis Direction	1
X-component of shear stress	0
Y-component of shear stress	0
Z-component of shear stress	0
Surface tension gradient	0

tank_region_wall

Condition	Value
Wall Thickness	0
Heat Generation Rate	0
Material Name	aluminum
Thermal BC Type	0
Temperature	291.14999
Heat Flux	0
Convective Heat Transfer Coefficient	0

Free Stream Temperature 300

Enable shell conduction? no

Wall Motion 0

Shear Boundary Condition 0

Define wall motion relative to adjacent cell zone? yes

Apply a rotational velocity to this wall? no

Velocity Magnitude 0

X-Component of Wall Translation 1

Y-Component of Wall Translation 0

Z-Component of Wall Translation 0

Define wall velocity components? no

X-Component of Wall Translation 0

Y-Component of Wall Translation 0

Z-Component of Wall Translation 0

External Emissivity 1

External Radiation Temperature 300

(0)

(((constant . 0) (profile)))

Rotation Speed 0

X-Position of Rotation-Axis Origin 0

Y-Position of Rotation-Axis Origin 0

Z-Position of Rotation-Axis Origin 0

X-Component of Rotation-Axis Direction 0

Y-Component of Rotation-Axis Direction 0

Z-Component of Rotation-Axis Direction 1

X-component of shear stress 0

Y-component of shear stress 0

Z-component of shear stress 0

Surface tension gradient 0

region02_outside

Condition	Value
Wall Thickness	0
Heat Generation Rate	0
Material Name	aluminum
Thermal BC Type	0
Temperature	291.14999
Heat Flux	0
Convective Heat Transfer Coefficient	0
Free Stream Temperature	300
Enable shell conduction?	no
Wall Motion	0
Shear Boundary Condition	0
Define wall motion relative to adjacent cell zone?	yes
Apply a rotational velocity to this wall?	no
Velocity Magnitude	0
X-Component of Wall Translation	1
Y-Component of Wall Translation	0
Z-Component of Wall Translation	0
Define wall velocity components?	no
X-Component of Wall Translation	0
Y-Component of Wall Translation	0
Z-Component of Wall Translation	0
External Emissivity	1
External Radiation Temperature	300
	(0)
	(((constant . 0) (profile)))
Rotation Speed	0

X-Position of Rotation-Axis Origin	0
Y-Position of Rotation-Axis Origin	0
Z-Position of Rotation-Axis Origin	0
X-Component of Rotation-Axis Direction	0
Y-Component of Rotation-Axis Direction	0
Z-Component of Rotation-Axis Direction	1
X-component of shear stress	0
Y-component of shear stress	0
Z-component of shear stress	0
Surface tension gradient	0

region08_outside

Condition	Value
Wall Thickness	0
Heat Generation Rate	0
Material Name	aluminum
Thermal BC Type	0
Temperature	291.14999
Heat Flux	0
Convective Heat Transfer Coefficient	0
Free Stream Temperature	300
Enable shell conduction?	no
Wall Motion	0
Shear Boundary Condition	0
Define wall motion relative to adjacent cell zone?	yes
Apply a rotational velocity to this wall?	no
Velocity Magnitude	0
X-Component of Wall Translation	1

Y-Component of Wall Translation	0
Z-Component of Wall Translation	0
Define wall velocity components?	no
X-Component of Wall Translation	0
Y-Component of Wall Translation	0
Z-Component of Wall Translation	0
External Emissivity	1
External Radiation Temperature	300
	(0)
	(((constant . 0) (profile)))
Rotation Speed	0
X-Position of Rotation-Axis Origin	0
Y-Position of Rotation-Axis Origin	0
Z-Position of Rotation-Axis Origin	0
X-Component of Rotation-Axis Direction	0
Y-Component of Rotation-Axis Direction	0
Z-Component of Rotation-Axis Direction	1
X-component of shear stress	0
Y-component of shear stress	0
Z-component of shear stress	0
Surface tension gradient	0

region03_outside

Condition	Value
Wall Thickness	0
Heat Generation Rate	0
Material Name	aluminum
Thermal BC Type	0

Temperature 291.14999

Heat Flux 0

Convective Heat Transfer Coefficient 0

Free Stream Temperature 300

Enable shell conduction? no

Wall Motion 0

Shear Boundary Condition 0

Define wall motion relative to adjacent cell zone? yes

Apply a rotational velocity to this wall? no

Velocity Magnitude 0

X-Component of Wall Translation 1

Y-Component of Wall Translation 0

Z-Component of Wall Translation 0

Define wall velocity components? no

X-Component of Wall Translation 0

Y-Component of Wall Translation 0

Z-Component of Wall Translation 0

External Emissivity 1

External Radiation Temperature 300

(0)

(((constant . 0) (profile)))

Rotation Speed 0

X-Position of Rotation-Axis Origin 0

Y-Position of Rotation-Axis Origin 0

Z-Position of Rotation-Axis Origin 0

X-Component of Rotation-Axis Direction 0

Y-Component of Rotation-Axis Direction 0

Z-Component of Rotation-Axis Direction 1

X-component of shear stress 0

Y-component of shear stress 0

Z-component of shear stress	0
Surface tension gradient	0

region07_outside

Condition	Value
Wall Thickness	0
Heat Generation Rate	0
Material Name	aluminum
Thermal BC Type	0
Temperature	291.14999
Heat Flux	0
Convective Heat Transfer Coefficient	0
Free Stream Temperature	300
Enable shell conduction?	no
Wall Motion	0
Shear Boundary Condition	0
Define wall motion relative to adjacent cell zone?	yes
Apply a rotational velocity to this wall?	no
Velocity Magnitude	0
X-Component of Wall Translation	1
Y-Component of Wall Translation	0
Z-Component of Wall Translation	0
Define wall velocity components?	no
X-Component of Wall Translation	0
Y-Component of Wall Translation	0
Z-Component of Wall Translation	0
External Emissivity	1
External Radiation Temperature	300

	(0)
	(((constant . 0) (profile)))
Rotation Speed	0
X-Position of Rotation-Axis Origin	0
Y-Position of Rotation-Axis Origin	0
Z-Position of Rotation-Axis Origin	0
X-Component of Rotation-Axis Direction	0
Y-Component of Rotation-Axis Direction	0
Z-Component of Rotation-Axis Direction	1
X-component of shear stress	0
Y-component of shear stress	0
Z-component of shear stress	0
Surface tension gradient	0

region04_outside

Condition	Value
Wall Thickness	0
Heat Generation Rate	0
Material Name	aluminum
Thermal BC Type	0
Temperature	291.14999
Heat Flux	0
Convective Heat Transfer Coefficient	0
Free Stream Temperature	300
Enable shell conduction?	no
Wall Motion	0
Shear Boundary Condition	0
Define wall motion relative to adjacent cell zone?	yes

Apply a rotational velocity to this wall?	no
Velocity Magnitude	0
X-Component of Wall Translation	1
Y-Component of Wall Translation	0
Z-Component of Wall Translation	0
Define wall velocity components?	no
X-Component of Wall Translation	0
Y-Component of Wall Translation	0
Z-Component of Wall Translation	0
External Emissivity	1
External Radiation Temperature	300
	(0)
	(((constant . 0) (profile)))
Rotation Speed	0
X-Position of Rotation-Axis Origin	0
Y-Position of Rotation-Axis Origin	0
Z-Position of Rotation-Axis Origin	0
X-Component of Rotation-Axis Direction	0
Y-Component of Rotation-Axis Direction	0
Z-Component of Rotation-Axis Direction	1
X-component of shear stress	0
Y-component of shear stress	0
Z-component of shear stress	0
Surface tension gradient	0

region06_outside

Condition	Value
Wall Thickness	0

Heat Generation Rate	0
Material Name	aluminum
Thermal BC Type	0
Temperature	291.14999
Heat Flux	0
Convective Heat Transfer Coefficient	0
Free Stream Temperature	300
Enable shell conduction?	no
Wall Motion	0
Shear Boundary Condition	0
Define wall motion relative to adjacent cell zone?	yes
Apply a rotational velocity to this wall?	no
Velocity Magnitude	0
X-Component of Wall Translation	1
Y-Component of Wall Translation	0
Z-Component of Wall Translation	0
Define wall velocity components?	no
X-Component of Wall Translation	0
Y-Component of Wall Translation	0
Z-Component of Wall Translation	0
External Emissivity	1
External Radiation Temperature	300
	(0)
	(((constant . 0) (profile)))
Rotation Speed	0
X-Position of Rotation-Axis Origin	0
Y-Position of Rotation-Axis Origin	0
Z-Position of Rotation-Axis Origin	0
X-Component of Rotation-Axis Direction	0
Y-Component of Rotation-Axis Direction	0

Z-Component of Rotation-Axis Direction	1
X-component of shear stress	0
Y-component of shear stress	0
Z-component of shear stress	0
Surface tension gradient	0

region05_outside

Condition	Value
Wall Thickness	0
Heat Generation Rate	0
Material Name	aluminum
Thermal BC Type	0
Temperature	291.14999
Heat Flux	0
Convective Heat Transfer Coefficient	0
Free Stream Temperature	300
Enable shell conduction?	no
Wall Motion	0
Shear Boundary Condition	0
Define wall motion relative to adjacent cell zone?	yes
Apply a rotational velocity to this wall?	no
Velocity Magnitude	0
X-Component of Wall Translation	1
Y-Component of Wall Translation	0
Z-Component of Wall Translation	0
Define wall velocity components?	no
X-Component of Wall Translation	0
Y-Component of Wall Translation	0

Z-Component of Wall Translation 0

External Emissivity 1

External Radiation Temperature 300

(0)

(((constant . 0) (profile)))

Rotation Speed 0

X-Position of Rotation-Axis Origin 0

Y-Position of Rotation-Axis Origin 0

Z-Position of Rotation-Axis Origin 0

X-Component of Rotation-Axis Direction 0

Y-Component of Rotation-Axis Direction 0

Z-Component of Rotation-Axis Direction 1

X-component of shear stress 0

Y-component of shear stress 0

Z-component of shear stress 0

Surface tension gradient 0

all_symmetry_faces

Condition Value

---

default-interior

Condition Value

---

all_symmetry_faces:001

Condition Value

---

default-interior:015

Condition Value

---

default-interior:017

Condition Value

```
        -----------------
Solver Controls
---------------
  Equations
    Equation   Solved
    -----------------
    Flow       yes
    he         yes
    Energy     yes
  Numerics
    Numeric                        Enabled
    ---------------------------------------
    Absolute Velocity Formulation   yes

  Unsteady Calculation Parameters
    -----------------------------------
    Time Step (s)                  2
    Max. Iterations Per Time Step   10000

  Relaxation
    Variable      Relaxation Factor
    -------------------------------
    Pressure      0.30000001
    Density       1
    Body Forces   1
    Momentum      0.15000001
    he            1
    Energy        0.60000002
  Linear Solver
                Solver     Termination   Residual Reduction
```

Variable Type Criterion Tolerance

Pressure V-Cycle 0.1

X-Momentum Flexible 0.1 0.7

Y-Momentum Flexible 0.1 0.7

Z-Momentum Flexible 0.1 0.7

he Flexible 0.1 0.7

Energy Flexible 0.1 0.7

Discretization Scheme

Variable Scheme

Pressure PRESTO!

Pressure-Velocity Coupling PISO

Density Second Order Upwind

Momentum Second Order Upwind

he Second Order Upwind

Energy Second Order Upwind

Solution Limits

Quantity Limit

Minimum Absolute Pressure 1

Maximum Absolute Pressure 5000000

Minimum Temperature 1

Maximum Temperature 5000

Material Properties

Material: aluminum (solid)

Property	Units	Method	Value(s)
Density	kg/m3	constant	2719
Cp (Specific Heat)	j/kg-k	constant	871
Thermal Conductivity	w/m-k	constant	202.4

Material: air (fluid)

Property	Units	Method	Value(s)
Cp (Specific Heat)	j/kg-k	constant	1006.43
Thermal Conductivity	w/m-k	constant	0.0242
Viscosity	kg/m-s	constant	1.7894e-05
Molecular Weight	kg/kgmol	constant	28.966
L-J Characteristic Length	angstrom	constant	3.711
L-J Energy Parameter	k	constant	78.6
Degrees of Freedom		constant	0

Material: water-vapor (fluid)

Property	Units	Method	Value(s)
Cp (Specific Heat)	j/kg-k	constant	2014
Thermal Conductivity	w/m-k	constant	0.0261
Viscosity	kg/m-s	constant	1.34e-05
Molecular Weight	kg/kgmol	constant	18.01534
L-J Characteristic Length	angstrom	constant	2.605
L-J Energy Parameter	k	constant	572.4
Degrees of Freedom		constant	0

Material: oxygen (fluid)

Property	Units	Method	Value(s)
Cp (Specific Heat)	j/kg-k	constant	919.31
Thermal Conductivity	w/m-k	constant	0.0246
Viscosity	kg/m-s	constant	1.919e-05
Molecular Weight	kg/kgmol	constant	31.9988
L-J Characteristic Length	angstrom	constant	3.458
L-J Energy Parameter	k	constant	107.4
Degrees of Freedom		constant	0

Material: nitrogen (fluid)

Property	Units	Method	Value(s)
Cp (Specific Heat)	j/kg-k	constant	1040.67
Thermal Conductivity	w/m-k	constant	0.0242
Viscosity	kg/m-s	constant	1.663e-05
Molecular Weight	kg/kgmol	constant	28.0134
L-J Characteristic Length	angstrom	constant	3.621
L-J Energy Parameter	k	constant	97.53
Degrees of Freedom		constant	0

Material: mixture-template (mixture)

Property	Units	Method	Value(s)

Mixture Species names ((he n2)())

Density kg/m3 ideal-gas #f

Cp(Specific Heat) j/kg-k mixing-law #f

Thermal Conductivity w/m-k ideal-gas-mixing-law #f

Viscosity kg/m-s ideal-gas-mixing-law #f

Mass Diffusivity m2/s multicomponent ((n2 o2 (polynomial -4.3e-06 4.0389999e-08 1.52e-10 -1.689e-14 1.955e-18) (constant . 0)) (he o2 (polynomial -1.5e-05 1.4e-07 5.2659999e-10 -5.8520002e-14 6.774e-18) (constant . 0)) (
e n2 (constant . 6.7300003e-05) (polynomial -1.48e-05 1.3659999e-07 5.1389998e-10 -5.7100002e-14 6.6089998e-18)))

Thermal Expansion Coefficient 1/k constant 0

Material: helium (fluid)

Property	Units	Method	Value(s)
Cp (Specific Heat)	j/kg-k	constant	5193
Thermal Conductivity	w/m-k	constant	0.152
Viscosity	kg/m-s	constant	1.99e-05
Molecular Weight	kg/kgmol	constant	4.0026
L-J Characteristic Length	angstrom	constant	0
L-J Energy Parameter	k	constant	0
Degrees of Freedom		constant	0

Appendix 6: UDF to Define the Gas Initial Conditions

```
#include "udf.h"

DEFINE_PROFILE (he_profile, t, i)
{
  real x[ND_ND]; /*this will hold the position vector*/
  real z;
  face_t f;

  begin_f_loop(f, t)
    {
     F_CENTROID(x, f, t);
     z = x[2];

/* lower pipe begin*/
            if (z < 0.65)
                    F_PROFILE(f, t, i) = 0;
            else if (z > 0.65)
                    F_PROFILE(f, t, i) = 1;
    }
   end_f_loop(f, t)
}
```

Appendix 7: The Model Summary for Non-Isothermal Experiment

FLUENT

Version: 3d, dp, segregated, spe2, lam, unsteady (3d, double precision, segregated, 2 species, laminar, unsteady)

Release: 6.0.20

Title:

Models

Model	Settings
Space	3D
Time	Unsteady, 2nd-Order Implicit
Viscous	Laminar
Heat Transfer	Enabled
Solidification and Melting	Disabled
Radiation	None
Species Transport	Non-Reacting (2 species)
Coupled Dispersed Phase	Disabled
Pollutants	Disabled
Soot	Disabled

Boundary Conditions

Zones

name	id	type

```
-------------------------------------
he-region              2    fluid
n_region               3    fluid
region01_outside       4    wall
region09_outside       5    wall
tank_region_wall       6    wall
region02_outside       7    wall
region08_outside       8    wall
region03_outside       9    wall
region07_outside       10   wall
region04_outside       11   wall
region06_outside       12   wall
region05_outside       13   wall
all_symmetry_faces     14   symmetry
default-interior       16   interior
all_symmetry_faces:001 1    symmetry
default-interior:015   15   interior
default-interior:017   17   interior
```

Boundary Conditions

he-region

Condition	Value
Material Name	mixture-template

Specify source terms? no

Source Terms ((mass (inactive . #f) (constant . 0) (profile)) (x-momentum (inactive . #f) (constant . 0) (profile)) (y-momentum (inactive . #f) (constant . 0) (profile)) (z-momentum (inactive . #f) (const nt . 0) (profile)) (species-0 (inactive . #f) (constant . 0) (profile)) (energy (inactive . #f) (constant . 0) (profile)))

Specify fixed values? no

Local Coordinate System for Fixed Velocities no

Fixed Values ((x-velocity (constant . 0) (profile)) (y-velocity (constant . 0) (profile)) (z-velocity (constant . 0) (profile)) (species-0 (profile udf he_profile) (constant . 0)) (temperature (inactive . #f) (constant . 0) (profile)))

Motion Type 0

X-Velocity Of Zone 0

Y-Velocity Of Zone 0

Z-Velocity Of Zone 0

Rotation speed 0

X-Origin of Rotation-Axis	0
Y-Origin of Rotation-Axis	0
Z-Origin of Rotation-Axis	0
X-Component of Rotation-Axis	0
Y-Component of Rotation-Axis	0
Z-Component of Rotation-Axis	1
Porous zone?	no
Conical porous zone?	no
X-Component of Direction-1 Vector	1
Y-Component of Direction-1 Vector	1
Z-Component of Direction-1 Vector	1
X-Component of Direction-2 Vector	0
Y-Component of Direction-2 Vector	1
Z-Component of Direction-2 Vector	0
X-Coordinate of Point on Cone Axis	1

Y-Coordinate of Point on Cone Axis 0

Z-Coordinate of Point on Cone Axis 0

Half Angle of Cone Relative to its Axis 0

Direction-1 Viscous Resistance 0

Direction-2 Viscous Resistance 0

Direction-3 Viscous Resistance 0

Direction-1 Inertial Resistance 0

Direction-2 Inertial Resistance 0

Direction-3 Inertial Resistance 0

C0 Coefficient for Power-Law 0

C1 Coefficient for Power-Law 0

Porosity 1

Solid Material Name aluminum

n_region

Condition Value

Material Name mixture-template

Specify source terms? no

Source Terms ((mass (inactive . #f) (constant . 0) (profile)) (x-momentum (inactive . #f) (constant . 0) (profile)) (y-momentum (inactive . #f) (constant . 0) (profile)) (z-momentum (inactive . #f) (const
nt . 0) (profile)) (species-0 (inactive . #f) (constant . 0) (profile)) (energy (inactive . #f) (constant . 0) (profile)))

Specify fixed values? yes

Local Coordinate System for Fixed Velocities no

Fixed Values ((x-velocity (inactive . #f) (constant . 0) (profile)) (y-velocity (inactive . #f) (constant . 0) (profile)) (z-velocity (inactive . #f) (constant . 0) (profile)) (species-0 (inactive . #f) (
onstant . 0) (profile)) (temperature (constant . 291.64999) (profile)))

Motion Type 0

X-Velocity Of Zone 0

Y-Velocity Of Zone 0

Z-Velocity Of Zone 0

Rotation speed	0
X-Origin of Rotation-Axis	0
Y-Origin of Rotation-Axis	0
Z-Origin of Rotation-Axis	0
X-Component of Rotation-Axis	0
Y-Component of Rotation-Axis	0
Z-Component of Rotation-Axis	1
Porous zone?	no
Conical porous zone?	no
X-Component of Direction-1 Vector	1
Y-Component of Direction-1 Vector	1
Z-Component of Direction-1 Vector	1
X-Component of Direction-2 Vector	0
Y-Component of Direction-2 Vector	1
Z-Component of Direction-2 Vector	0

X-Coordinate of Point on Cone Axis	1
Y-Coordinate of Point on Cone Axis	0
Z-Coordinate of Point on Cone Axis	0
Half Angle of Cone Relative to its Axis	0
Direction-1 Viscous Resistance	0
Direction-2 Viscous Resistance	0
Direction-3 Viscous Resistance	0
Direction-1 Inertial Resistance	0
Direction-2 Inertial Resistance	0
Direction-3 Inertial Resistance	0
C0 Coefficient for Power-Law	0
C1 Coefficient for Power-Law	0
Porosity	1
Solid Material Name	aluminum

region01_outside

Condition	Value
Wall Thickness	0
Heat Generation Rate	0
Material Name	aluminum
Thermal BC Type	0
Temperature	292.45001
Heat Flux	0
Convective Heat Transfer Coefficient	0
Free Stream Temperature	300
Enable shell conduction?	no
Wall Motion	0
Shear Boundary Condition	0
Define wall motion relative to adjacent cell zone?	yes
Apply a rotational velocity to this wall?	no
Velocity Magnitude	0
X-Component of Wall Translation	1
Y-Component of Wall Translation	0
Z-Component of Wall Translation	0
Define wall velocity components?	no
X-Component of Wall Translation	0
Y-Component of Wall Translation	0
Z-Component of Wall Translation	0
External Emissivity	1
External Radiation Temperature	300
	(0)
	(((constant . 0) (profile)))
Rotation Speed	0
X-Position of Rotation-Axis Origin	0

Y-Position of Rotation-Axis Origin	0
Z-Position of Rotation-Axis Origin	0
X-Component of Rotation-Axis Direction	0
Y-Component of Rotation-Axis Direction	0
Z-Component of Rotation-Axis Direction	1
X-component of shear stress	0
Y-component of shear stress	0
Z-component of shear stress	0
Surface tension gradient	0

region09_outside

Condition	Value
Wall Thickness	0
Heat Generation Rate	0
Material Name	aluminum
Thermal BC Type	0
Temperature	290.85001
Heat Flux	0
Convective Heat Transfer Coefficient	0
Free Stream Temperature	300
Enable shell conduction?	no
Wall Motion	0
Shear Boundary Condition	0
Define wall motion relative to adjacent cell zone?	yes
Apply a rotational velocity to this wall?	no
Velocity Magnitude	0
X-Component of Wall Translation	1
Y-Component of Wall Translation	0

Z-Component of Wall Translation	0
Define wall velocity components?	no
X-Component of Wall Translation	0
Y-Component of Wall Translation	0
Z-Component of Wall Translation	0
External Emissivity	1
External Radiation Temperature	300
	(0)
	(((constant . 0) (profile)))
Rotation Speed	0
X-Position of Rotation-Axis Origin	0
Y-Position of Rotation-Axis Origin	0
Z-Position of Rotation-Axis Origin	0
X-Component of Rotation-Axis Direction	0
Y-Component of Rotation-Axis Direction	0
Z-Component of Rotation-Axis Direction	1
X-component of shear stress	0
Y-component of shear stress	0
Z-component of shear stress	0
Surface tension gradient	0

tank_region_wall

Condition	Value
Wall Thickness	0
Heat Generation Rate	0
Material Name	aluminum
Thermal BC Type	0
Temperature	291.64999

Heat Flux 0

Convective Heat Transfer Coefficient 0

Free Stream Temperature 300

Enable shell conduction? no

Wall Motion 0

Shear Boundary Condition 0

Define wall motion relative to adjacent cell zone? yes

Apply a rotational velocity to this wall? no

Velocity Magnitude 0

X-Component of Wall Translation 1

Y-Component of Wall Translation 0

Z-Component of Wall Translation 0

Define wall velocity components? no

X-Component of Wall Translation 0

Y-Component of Wall Translation 0

Z-Component of Wall Translation 0

External Emissivity 1

External Radiation Temperature 300

(0)

(((constant . 0) (profile)))

Rotation Speed 0

X-Position of Rotation-Axis Origin 0

Y-Position of Rotation-Axis Origin 0

Z-Position of Rotation-Axis Origin 0

X-Component of Rotation-Axis Direction 0

Y-Component of Rotation-Axis Direction 0

Z-Component of Rotation-Axis Direction 1

X-component of shear stress 0

Y-component of shear stress 0

Z-component of shear stress 0

Surface tension gradient	0

region02_outside

Condition	Value
Wall Thickness	0
Heat Generation Rate	0
Material Name	aluminum
Thermal BC Type	0
Temperature	292.45001
Heat Flux	0
Convective Heat Transfer Coefficient	0
Free Stream Temperature	300
Enable shell conduction?	no
Wall Motion	0
Shear Boundary Condition	0
Define wall motion relative to adjacent cell zone?	yes
Apply a rotational velocity to this wall?	no
Velocity Magnitude	0
X-Component of Wall Translation	1
Y-Component of Wall Translation	0
Z-Component of Wall Translation	0
Define wall velocity components?	no
X-Component of Wall Translation	0
Y-Component of Wall Translation	0
Z-Component of Wall Translation	0
External Emissivity	1
External Radiation Temperature	300

(0)

	(((constant . 0) (profile)))
Rotation Speed	0
X-Position of Rotation-Axis Origin	0
Y-Position of Rotation-Axis Origin	0
Z-Position of Rotation-Axis Origin	0
X-Component of Rotation-Axis Direction	0
Y-Component of Rotation-Axis Direction	0
Z-Component of Rotation-Axis Direction	1
X-component of shear stress	0
Y-component of shear stress	0
Z-component of shear stress	0
Surface tension gradient	0

region08_outside

Condition	Value
Wall Thickness	0
Heat Generation Rate	0
Material Name	aluminum
Thermal BC Type	0
Temperature	290.85001
Heat Flux	0
Convective Heat Transfer Coefficient	0
Free Stream Temperature	300
Enable shell conduction?	no
Wall Motion	0
Shear Boundary Condition	0
Define wall motion relative to adjacent cell zone?	yes
Apply a rotational velocity to this wall?	no

Velocity Magnitude	0
X-Component of Wall Translation	1
Y-Component of Wall Translation	0
Z-Component of Wall Translation	0
Define wall velocity components?	no
X-Component of Wall Translation	0
Y-Component of Wall Translation	0
Z-Component of Wall Translation	0
External Emissivity	1
External Radiation Temperature	300
	(0)
	(((constant . 0) (profile)))
Rotation Speed	0
X-Position of Rotation-Axis Origin	0
Y-Position of Rotation-Axis Origin	0
Z-Position of Rotation-Axis Origin	0
X-Component of Rotation-Axis Direction	0
Y-Component of Rotation-Axis Direction	0
Z-Component of Rotation-Axis Direction	1
X-component of shear stress	0
Y-component of shear stress	0
Z-component of shear stress	0
Surface tension gradient	0

region03_outside

Condition	Value
Wall Thickness	0
Heat Generation Rate	0

Material Name aluminum

Thermal BC Type 0

Temperature (profile udf wall_Temp)

Heat Flux 0

Convective Heat Transfer Coefficient 0

Free Stream Temperature 300

Enable shell conduction? no

Wall Motion 0

Shear Boundary Condition 0

Define wall motion relative to adjacent cell zone? yes

Apply a rotational velocity to this wall? no

Velocity Magnitude 0

X-Component of Wall Translation 1

Y-Component of Wall Translation 0

Z-Component of Wall Translation 0

Define wall velocity components? no

X-Component of Wall Translation 0

Y-Component of Wall Translation 0

Z-Component of Wall Translation 0

External Emissivity 1

External Radiation Temperature 300

(0)

(((constant . 0) (profile)))

Rotation Speed 0

X-Position of Rotation-Axis Origin 0

Y-Position of Rotation-Axis Origin 0

Z-Position of Rotation-Axis Origin 0

X-Component of Rotation-Axis Direction 0

Y-Component of Rotation-Axis Direction 0

Z-Component of Rotation-Axis Direction 1

X-component of shear stress	0
Y-component of shear stress	0
Z-component of shear stress	0
Surface tension gradient	0

region07_outside

Condition	Value
Wall Thickness	0
Heat Generation Rate	0
Material Name	aluminum
Thermal BC Type	0
Temperature	(profile udf wall_Temp)
Heat Flux	0
Convective Heat Transfer Coefficient	0
Free Stream Temperature	300
Enable shell conduction?	no
Wall Motion	0
Shear Boundary Condition	0
Define wall motion relative to adjacent cell zone?	yes
Apply a rotational velocity to this wall?	no
Velocity Magnitude	0
X-Component of Wall Translation	1
Y-Component of Wall Translation	0
Z-Component of Wall Translation	0
Define wall velocity components?	no
X-Component of Wall Translation	0
Y-Component of Wall Translation	0
Z-Component of Wall Translation	0

External Emissivity	1
External Radiation Temperature	300
	(0)
	(((constant . 0) (profile)))
Rotation Speed	0
X-Position of Rotation-Axis Origin	0
Y-Position of Rotation-Axis Origin	0
Z-Position of Rotation-Axis Origin	0
X-Component of Rotation-Axis Direction	0
Y-Component of Rotation-Axis Direction	0
Z-Component of Rotation-Axis Direction	1
X-component of shear stress	0
Y-component of shear stress	0
Z-component of shear stress	0
Surface tension gradient	0

region04_outside

Condition	Value
Wall Thickness	0
Heat Generation Rate	0
Material Name	aluminum
Thermal BC Type	0
Temperature	(profile udf wall_Temp)
Heat Flux	0
Convective Heat Transfer Coefficient	0
Free Stream Temperature	300
Enable shell conduction?	no
Wall Motion	0

Shear Boundary Condition	0
Define wall motion relative to adjacent cell zone?	yes
Apply a rotational velocity to this wall?	no
Velocity Magnitude	0
X-Component of Wall Translation	1
Y-Component of Wall Translation	0
Z-Component of Wall Translation	0
Define wall velocity components?	no
X-Component of Wall Translation	0
Y-Component of Wall Translation	0
Z-Component of Wall Translation	0
External Emissivity	1
External Radiation Temperature	300
	(0)
	(((constant . 0) (profile)))
Rotation Speed	0
X-Position of Rotation-Axis Origin	0
Y-Position of Rotation-Axis Origin	0
Z-Position of Rotation-Axis Origin	0
X-Component of Rotation-Axis Direction	0
Y-Component of Rotation-Axis Direction	0
Z-Component of Rotation-Axis Direction	1
X-component of shear stress	0
Y-component of shear stress	0
Z-component of shear stress	0
Surface tension gradient	0

region06_outside

Condition	Value

Wall Thickness 0

Heat Generation Rate 0

Material Name aluminum

Thermal BC Type 0

Temperature (profile udf wall_Temp)

Heat Flux 0

Convective Heat Transfer Coefficient 0

Free Stream Temperature 300

Enable shell conduction? no

Wall Motion 0

Shear Boundary Condition 0

Define wall motion relative to adjacent cell zone? yes

Apply a rotational velocity to this wall? no

Velocity Magnitude 0

X-Component of Wall Translation 1

Y-Component of Wall Translation 0

Z-Component of Wall Translation 0

Define wall velocity components? no

X-Component of Wall Translation 0

Y-Component of Wall Translation 0

Z-Component of Wall Translation 0

External Emissivity 1

External Radiation Temperature 300

(0)

(((constant . 0) (profile)))

Rotation Speed 0

X-Position of Rotation-Axis Origin 0

Y-Position of Rotation-Axis Origin 0

Z-Position of Rotation-Axis Origin 0

X-Component of Rotation-Axis Direction	0
Y-Component of Rotation-Axis Direction	0
Z-Component of Rotation-Axis Direction	1
X-component of shear stress	0
Y-component of shear stress	0
Z-component of shear stress	0
Surface tension gradient	0

region05_outside

Condition	Value
Wall Thickness	0
Heat Generation Rate	0
Material Name	aluminum
Thermal BC Type	0
Temperature	(profile udf wall_Temp)
Heat Flux	0
Convective Heat Transfer Coefficient	0
Free Stream Temperature	300
Enable shell conduction?	no
Wall Motion	0
Shear Boundary Condition	0
Define wall motion relative to adjacent cell zone?	yes
Apply a rotational velocity to this wall?	no
Velocity Magnitude	0
X-Component of Wall Translation	1
Y-Component of Wall Translation	0
Z-Component of Wall Translation	0
Define wall velocity components?	no

X-Component of Wall Translation 0

Y-Component of Wall Translation 0

Z-Component of Wall Translation 0

External Emissivity 1

External Radiation Temperature 300

(0)

(((constant . 0) (profile)))

Rotation Speed 0

X-Position of Rotation-Axis Origin 0

Y-Position of Rotation-Axis Origin 0

Z-Position of Rotation-Axis Origin 0

X-Component of Rotation-Axis Direction 0

Y-Component of Rotation-Axis Direction 0

Z-Component of Rotation-Axis Direction 1

X-component of shear stress 0

Y-component of shear stress 0

Z-component of shear stress 0

Surface tension gradient 0

all_symmetry_faces

Condition Value

---

default-interior

Condition Value

---

all_symmetry_faces:001

Condition Value

---

default-interior:015

Condition Value

---

default-interior:017

Condition Value

Solver Controls

Equations

Equation Solved

Flow yes

he yes

Energy yes

Numerics

Numeric Enabled

Absolute Velocity Formulation yes

Unsteady Calculation Parameters

Time Step (s) 0.5

Max. Iterations Per Time Step 1000

Relaxation

Variable Relaxation Factor

Pressure 0.30000001

Density 0.69999999

Body Forces 0.69999999

Momentum 0.80000001

he 0.69999999

Energy 0.69999999

Linear Solver

Variable	Solver Type	Termination Criterion	Residual Reduction Tolerance
Pressure	V-Cycle	0.1	
X-Momentum	Flexible	0.1	0.7
Y-Momentum	Flexible	0.1	0.7
Z-Momentum	Flexible	0.1	0.7
he	Flexible	0.1	0.7
Energy	Flexible	0.1	0.7

Discretization Scheme

Variable	Scheme
Pressure	PRESTO!
Pressure-Velocity Coupling	PISO
Density	QUICK
Momentum	QUICK
he	QUICK
Energy	QUICK

Solution Limits

Quantity	Limit

Minimum Absolute Pressure 1

Maximum Absolute Pressure 5000000

Minimum Temperature 1

Maximum Temperature 5000

Material Properties

Material: helium (fluid)

Property	Units	Method	Value(s)
Cp (Specific Heat)	j/kg-k	constant	5193
Thermal Conductivity	w/m-k	constant	0.152
Viscosity	kg/m-s	constant	1.9900001e-05
Molecular Weight	kg/kgmol	constant	4.0026002
L-J Characteristic Length	angstrom	constant	2.576
L-J Energy Parameter	k	constant	10.2
Degrees of Freedom		constant	0

Material: mixture-template (mixture)

Property	Units	Method	Value(s)
Mixture Species		names	((he n2) ())
Density	kg/m3	ideal-gas	#f
Cp (Specific Heat)	j/kg-k	mixing-law	#f
Thermal Conductivity	w/m-k	ideal-gas-mixing-law	#f
Viscosity	kg/m-s	ideal-gas-mixing-law	#f

Mass Diffusivity	m2/s	kinetic-theory	#f
Thermal Diffusion Coefficient	kg/m-s	kinetic-theory	#f
Thermal Expansion Coefficient	1/k	constant	0

Material: nitrogen (fluid)

Property	Units	Method	Value(s)
Cp (Specific Heat)	j/kg-k	constant	1040.67
Thermal Conductivity	w/m-k	constant	0.0242
Viscosity	kg/m-s	constant	1.663e-05
Molecular Weight	kg/kgmol	constant	28.013399
L-J Characteristic Length	angstrom	constant	3.6210001
L-J Energy Parameter	k	constant	97.529999
Degrees of Freedom		constant	0

Material: oxygen (fluid)

Property	Units	Method	Value(s)
Cp (Specific Heat)	j/kg-k	constant	919.31
Thermal Conductivity	w/m-k	constant	0.0246
Viscosity	kg/m-s	constant	1.919e-05
Molecular Weight	kg/kgmol	constant	31.9988
L-J Characteristic Length	angstrom	constant	3.458
L-J Energy Parameter	k	constant	107.4
Degrees of Freedom		constant	0

Material: water-vapor (fluid)

Property	Units	Method	Value(s)
Cp (Specific Heat)	j/kg-k	constant	2014
Thermal Conductivity	w/m-k	constant	0.0261
Viscosity	kg/m-s	constant	1.34e-05
Molecular Weight	kg/kgmol	constant	18.01534
L-J Characteristic Length	angstrom	constant	2.605
L-J Energy Parameter	k	constant	572.4
Degrees of Freedom		constant	0

Material: air (fluid)

Property	Units	Method	Value(s)
Cp (Specific Heat)	j/kg-k	constant	1006.43
Thermal Conductivity	w/m-k	constant	0.0242
Viscosity	kg/m-s	constant	1.7894e-05
Molecular Weight	kg/kgmol	constant	28.966
L-J Characteristic Length	angstrom	constant	3.711
L-J Energy Parameter	k	constant	78.6
Degrees of Freedom		constant	0

Material: aluminum (solid)

Property	Units	Method	Value(s)
Density	kg/m3	constant	2719
Cp (Specific Heat)	j/kg-k	constant	871
Thermal Conductivity	w/m-k	constant	202.4

Appendix 8: UDF for Gas Initial Profile (Non-Isothermal Experiment)

```
#include "udf.h"

DEFINE_PROFILE (he_profile, t, i)
{
  real x[ND_ND]; /*this will hold the position vector*/
  real z;
  face_t f;

  begin_f_loop(f, t)
    {
     F_CENTROID(x, f, t);
     z = x[2];

/* lower pipe begin*/
          if (z < 0.65)
                F_PROFILE(f, t, i) = 0.00000001;
          else if (z > 0.65)
                F_PROFILE(f, t, i) = 0.99999999;
    }
   end_f_loop(f, t)
}
```

Appendix 9: UDF for Wall Temperature (Non-Isothermal Experiment)

```
DEFINE_PROFILE (wall_Temp, t, i)
{
  real x[ND_ND]; /*this will hold the position vector*/
  real y; /*here y refer to x coordinate)*/
  real z;
  face_t f;

  begin_f_loop(f, t)
    {
     F_CENTROID(x, f, t);
          y = x[0];
     z = x[2];

/* lower pipe begin*/
          if (y > 0.2 && z >= 1.0 && z < 1.2)
               F_PROFILE(f, t, i) = 292.45+(z-1)*(574.1-292.45)/0.2;
          else if (y > 0.2 && z >= 1.2 && z < 1.7)
               F_PROFILE(f, t, i) = 574.1;
          else if (y > 0.2 && z >= 1.7 && z < 1.8)
               F_PROFILE(f, t, i) = 574.1+(z-1.7)*(416.3-574.6)/0.1;
          else if (y > 0.2 && z >= 1.8 && z < 1.97635)
               F_PROFILE(f, t, i) = 416.3+(z-1.8)*(438 - 416.25)/0.17635;
          else if (y >= -0.22365 && y <= 0.22365 &&  z > 1.923)
               F_PROFILE(f, t, i) = 356 + (y + 0.22365)*(438 - 356)/0.4473;
          else if (y < -0.2 && z >= 1.8 && z < 1.97635)
               F_PROFILE(f, t, i) = 308.05+(z-1.8)*(356.25-308.05)/0.17635;
          else if (y < -0.2 && z >= 1.0 && z < 1.8)
               F_PROFILE(f, t, i) = 290.85+(z-1)*(308.05-290.85)/0.8;
```

```
        else
                F_PROFILE(f, t, i) = 290.85;
}
end_f_loop(f, t)
                                                }
```

Appendix 10: The Model Summary for Multi-Component Experiment

FLUENT

Version: 3d, dp, segregated, spe6, lam, unsteady (3d, double precision, segregated, 6 species, laminar, unsteady)

Release: 6.0.20

Title:

Models

Model	Settings
Space	3D
Time	Unsteady, 2nd-Order Implicit
Viscous	Laminar
Heat Transfer	Enabled
Solidification and Melting	Disabled
Radiation	None
Species Transport	Reacting (6 species)
Coupled Dispersed Phase	Disabled
Pollutants	Disabled
Soot	Disabled

Boundary Conditions

Zones

name	id	type

---

region_pipe 2 fluid

region_tank 3 fluid

wall03_up_and_cool 4 wall

wall02_graphite 5 wall

wall01_lower 6 wall

wall04_tank 7 wall

all_symm_faces 8 symmetry

default-interior 10 interior

all_symm_faces:001 1 symmetry

default-interior:009 9 interior

default-interior:011 11 interior

Boundary Conditions

region_pipe

Condition Value

MaterialName mixture-template

Specify source terms? no

Source Terms ((mass (inactive . #f) (constant . 0) (profile)) (x-momentum (inactive . #f) (constant . 0) (profile)) (y-momentum (inactive . #f) (constant . 0) (profile)) (z-momentum (inactive . #f) (constant . 0) (profile)) (species-0 (inactive . #f) (constant . 0) (profile)) (species-1 (inactive . #f) (constant . 0) (profile)) (species-2 (inactive . #f) (constant . 0) (profile)) (species-3 (inactive . #f) (constant . 0)

(profile)) (species-4 (inactive . #f) (constant . 0) (profile)) (energy (inactive . #f) (constant . 0) (profile)))

Specify fixed values? no

Local Coordinate System for Fixed Velocities no

Fixed Values ((x-velocity (constant . 0) (profile)) (y-velocity (constant . 0) (profile)) (z-velocity (constant . 0) (profile)) (species-0 (constant . 0) (profile)) (species-1 (constant . 0) (profile)) (species-2 (constant . 0) (profile)) (species-3 (constant . 0.99633998) (profile)) (species-4 (constant . 0.0036599999) (profile))(temperature (inactive . #f) (constant . 0) (profile)))

Motion Type 0

X-Velocity Of Zone 0

Y-Velocity Of Zone 0

Z-Velocity Of Zone 0

Rotation speed 0

X-Origin of Rotation-Axis 0

Y-Origin of Rotation-Axis 0

Z-Origin of Rotation-Axis 0

X-Component of Rotation-Axis 0

Y-ComponentofRotation-Axis 0

Z-ComponentofRotation-Axis 1

Porous-zone? no

Conical-porous-zone? no

X-ComponentofDirection-1-Vector 1

Y-ComponentofDirection-1-Vector 1

Z-ComponentofDirection-1-Vector 1

X-ComponentofDirection-2-Vector 0

Y-ComponentofDirection-2-Vector 1

Z-ComponentofDirection-2-Vector 0

X-CoordinateofPointonConeAxis 1

Y-CoordinateofPointonConeAxis 0

Z-CoordinateofPointonConeAxis 0

Half-AngleofConeRelativetoAxis 0

Direction-1-Viscous-Resistance 0

Direction-2ViscousResistance 0

Direction-3ViscousResistance 0

Direction-1InertialResistance 0

Direction-2InertialResistance 0

Direction-3InertialResistance 0

C0CoefficientforPowerLaw 0

C1CoefficientforPowerLaw 0

Porosity 1

SolidMaterialName aluminum

region_tank

Condition Value

MaterialName mixturetemplate

Specifysourceterms? no

Source Terms ((mass (inactive . #f) (constant . 0) (profile)) (x-momentum (inactive . #f) (constant . 0) (profile)) (y-momentum (inactive . #f) (constant . 0) (profile)) (z-momentum (inactive . #f) (constant . 0) (profile)) (species-0 (inactive . #f) (constant . 0) (profile)) (species-1 (inactive . #f) (constant . 0) (profile)) (species-2 (inactive . #f) (constant . 0) (profile)) (species-3 (inactive . #f) (constant . 0) (profile)) (species-4 (inactive . #f) (constant . 0) (profile)) (energy (inactive . #f) (constant . 0) (profile)))

Specify fixed values? yes

Local Coordinate System for Fixed Velocities no

Fixed Values ((x-velocity (inactive . #f) (constant . 0) (profile)) (y-velocity (inactive . #f) (constant . 0) (profile)) (z-velocity (inactive . #f) (constant . 0) (profile)) (species-0 (inactive . #f) (constant . 0) (profile)) (species-1 (inactive . #f) (constant . 0) (profile)) (species-2 (inactive . #f) (constant . 0) (profile)) (species-3 (inactive . #f) (constant . 0) (profile)) (species-4 (inactive . #f) (constant . 0) (profile)) (temperature (constant . 289.45001) (profile)))

Motion Type 0

X-Velocity Of Zone 0

Y-Velocity Of Zone 0

Z-Velocity Of Zone 0

Rotation speed 0

X-Origin of Rotation-Axis 0

Y-Origin of Rotation-Axis 0

Z-OriginofRotation-Axis 0

X-ComponentofRotation-Axis 0

Y-ComponentofRotation-Axis 0

Z-ComponentofRotation-Axis 1

Porus-zone? no

Conicalporus-zone? no

X-ComponentofDirection-1Vector 1

Y-ComponentofDirection-1Vector 1

Z-ComponentofDirection-1Vector 1

X-ComponentofDirection-2Vector 0

Y-ComponentofDirection-2Vector 1

Z-ComponentofDirection-2Vector 0

X-CoordinateofPointonCone-Axis 1

Y-CoordinateofPointonCone-Axis 0

Z-CoordinateofPointonCone-Axis 0

HalfAngleofConeRelativetoAxis 0

Direction-1ViscousResistance 0

Direction-2ViscousResistance 0

Direction-3ViscousResistance 0

Direction-1InertialResistance 0

Direction-2InertialResistance 0

Direction-3InertialResistance 0

C0CoefficientforPowerLaw 0

C1CoefficientforPowerLaw 0

Porosity 1

SolidMaterialName aluminum

wall03_up_and_cool

Condition Value

Wall Thickness 0

Heat Generation Rate 0

Material Name aluminum

Thermal BC Type 0

Temperature (profile udf wall_Temp)

Heat Flux 0

Convective Heat Transfer Coefficient 0

Free Stream Temperature 300

Enable shell conduction? no

Wall Motion 0

Shear Boundary Condition 0

Define wall motion relative to adjacent cell zone? yes

Apply a rotational velocity to this wall? no

Velocity Magnitude 0

X-Component of Wall Translation 1

Y-Component of Wall Translation 0

Z-Component of Wall Translation 0

Define wall velocity components? no

X-Component of Wall Translation 0

Y-Component of Wall Translation 0

Z-Component of Wall Translation 0

External Emissivity 1

External Radiation Temperature 300

Activate surface reactions? no

(0 0 0 0 0)

(((constant . 0) (profile)) ((constant . 0) (profile)) ((constant . 0) (profile)) ((constant . 0) (profile)) ((constant . 0) (profile)))

Rotation Speed 0

X-Position of Rotation-Axis Origin 0

Y-Position of Rotation-Axis Origin 0

Z-Position of Rotation-Axis Origin 0

X-Component of Rotation-Axis Direction 0

Y-Component of Rotation-Axis Direction 0

Z-Component of Rotation-Axis Direction 1

X-component of shear stress 0

Y-component of shear stress 0

Z-component of shear stress 0

Surface tension gradient 0

wall02_graphite

Condition Value

Wall Thickness 0

Heat Generation Rate 0

Material Name aluminum

Thermal BC Type 0

Temperature (profile udf wall_Temp)

Heat Flux 0

Convective Heat Transfer Coefficient 0

Free Stream Temperature 300

Enable shell conduction? no

Wall Motion 0

Shear Boundary Condition 0

Define wall motion relative to adjacent cell zone? yes

Apply a rotational velocity to this wall? no

Velocity Magnitude 0

X-Component of Wall Translation 1

Y-Component of Wall Translation 0

Z-Component of Wall Translation 0

Define wall velocity components? no

X-Component of Wall Translation 0

Y-Component of Wall Translation 0

Z-Component of Wall Translation 0

External Emissivity 1

External Radiation Temperature 300

Activate surface reactions? yes

(0 0 0 0 0)

(((constant . 0) (profile)) ((constant . 0) (profile)) ((constant . 0) (profile)) ((constant . 0) (profile)) ((constant . 0) (profile)))

Rotation Speed 0

X-Position of Rotation-Axis Origin 0

Y-Position of Rotation-Axis Origin 0

Z-Position of Rotation-Axis Origin 0

X-Component of Rotation-Axis Direction 0

Y-Component of Rotation-Axis Direction 0

Z-Component of Rotation-Axis Direction 1

X-component of shear stress 0

Y-component of shear stress 0

Z-component of shear stress 0

Surface tension gradient 0

wall01_lower

Condition Value

Wall Thickness 0

Heat Generation Rate 0

Material Name aluminum

Thermal BC Type 0

Temperature (profile udf wall_Temp)

Heat Flux 0

Convective Heat Transfer Coefficient 0

Free Stream Temperature 300

Enable shell conduction? no

Wall Motion 0

Shear Boundary Condition 0

Define wall motion relative to adjacent cell zone? yes

Apply a rotational velocity to this wall? no

Velocity Magnitude 0

X-Component of Wall Translation 1

Y-Component of Wall Translation 0

Z-Component of Wall Translation 0

Define wall velocity components? no

X-Component of Wall Translation 0

Y-Component of Wall Translation 0

Z-Component of Wall Translation 0

External Emissivity 1

External Radiation Temperature 300

Activate surface reactions? no

(0 0 0 0 0)

(((constant . 0) (profile)) ((constant . 0) (profile)) ((constant . 0) (profile)) ((constant . 0) (profile)) ((constant . 0) (profile)))

Rotation Speed 0

X-Position of Rotation-Axis Origin 0

Y-Position of Rotation-Axis Origin 0

Z-Position of Rotation-Axis Origin 0

X-Component of Rotation-Axis Direction 0

Y-Component of Rotation-Axis Direction 0

Z-Component of Rotation-Axis Direction 1

X-component of shear stress 0

Y-component of shear stress 0

Z-component of shear stress 0

Surface tension gradient 0

wall04_tank

Condition	Value
Wall Thickness	0
Heat Generation Rate	0
Material Name	aluminum
Thermal BC Type	0
Temperature	289.45001
Heat Flux	0
Convective Heat Transfer Coefficient	0
Free Stream Temperature	300
Enable shell conduction?	no
Wall Motion	0
Shear Boundary Condition	0
Define wall motion relative to adjacent cell zone?	yes

Apply a rotational velocity to this wall? no

Velocity Magnitude 0

X-Component of Wall Translation 1

Y-Component of Wall Translation 0

Z-Component of Wall Translation 0

Define wall velocity components? no

X-Component of Wall Translation 0

Y-Component of Wall Translation 0

Z-Component of Wall Translation 0

External Emissivity 1

External Radiation Temperature 300

Activate surface reactions? no

(0 0 0 0 0)

(((constant . 0) (profile)) ((constant . 0) (profile)) ((constant . 0) (profile)) ((constant . 0) (profile)) ((constant . 0) (profile)))

Rotation Speed 0

X-Position of Rotation-Axis Origin 0

Y-Position of Rotation-Axis Origin 0

Z-Position of Rotation-Axis Origin 0

X-Component of Rotation-Axis Direction 0

Y-Component of Rotation-Axis Direction 0

Z-Component of Rotation-Axis Direction 1

X-component of shear stress 0

Y-component of shear stress 0

Z-component of shear stress 0

Surface tension gradient 0

all_symm_faces

Condition Value

---

default-interior

Condition Value

---

all_symm_faces:001

Condition Value

---

default-interior:009

Condition Value

---

default-interior:011

Condition Value

Solver Controls

Equations

Equation Solved

Flow yes

co yes

co2 yes

o2 yes

he yes

h2o yes

Energy yes

Numerics

Numeric Enabled

Absolute Velocity Formulation yes

Unsteady Calculation Parameters

Time Step (s) 1

Max. Iterations Per Time Step 2000

Relaxation

Variable	Relaxation Factor
Pressure	0.30000001
Density	0.69999999
Body Forces	0.69999999
Momentum	0.1
co	0.69999999
co2	0.69999999
o2	0.69999999
he	0.69999999
h2o	0.69999999
Energy	0.69999999

Linear Solver

Variable	Solver Type	Termination Criterion	Residual Reduction Tolerance
Pressure	V-Cycle	0.1	
X-Momentum	Flexible	0.1	0.7
Y-Momentum	Flexible	0.1	0.7
Z-Momentum	Flexible	0.1	0.7
co	Flexible	0.1	0.7
co2	Flexible	0.1	0.7
o2	Flexible	0.1	0.7
he	Flexible	0.1	0.7
h2o	Flexible	0.1	0.7

Energy Flexible 0.1 0.7

Discretization Scheme

Variable	Scheme
Pressure	PRESTO!
Pressure-Velocity Coupling	PISO
Density	QUICK
Momentum	QUICK
co	First Order Upwind
co2	First Order Upwind
o2	First Order Upwind
he	First Order Upwind
h2o	First Order Upwind
Energy	QUICK

Solution Limits

Quantity	Limit
Minimum Absolute Pressure	1
Maximum Absolute Pressure	5000000
Minimum Temperature	1
Maximum Temperature	5000

Material Properties

Material: aluminum (solid)

Property	Units	Method	Value(s)
Density	kg/m3	constant	2719
Cp (Specific Heat)	j/kg-k	constant	871
Thermal Conductivity	w/m-k	constant	202.4

Material: air (fluid)

Property	Units	Method	Value(s)
Cp (Specific Heat)	j/kg-k	constant	1006.43
Thermal Conductivity	w/m-k	constant	0.0242
Viscosity	kg/m-s	constant	1.7894001e-05
Molecular Weight	kg/kgmol	constant	28.966
Standard State Enthalpy	j/kgmol	constant	0
Standard State Entropy	j/kgmol-k	constant	0
Reference Temperature	k	constant	298.14999
L-J Characteristic Length	angstrom	constant	3.711
L-J Energy Parameter	k	constant	78.599998
Degrees of Freedom		constant	0

Material: water-vapor (fluid)

Property	Units	Method	Value(s)
Cp (Specific Heat)	j/kg-k	constant	2014
Thermal Conductivity	w/m-k	kinetic-theory	#f
Viscosity	kg/m-s	kinetic-theory	#f
Molecular Weight	kg/kgmol	constant	18.015341

Standard State Enthalpy	j/kgmol	constant	-2.418379e+08
Standard State Entropy	j/kgmol-k	constant	188696.41
Reference Temperature	k	constant	298.14999
L-J Characteristic Length	angstrom	constant	2.605
L-J Energy Parameter	k	constant	572.40002
Degrees of Freedom		constant	0

Material: oxygen (fluid)

Property	Units	Method	Value(s)
Cp (Specific Heat)	j/kg-k	constant	919.31
Thermal Conductivity	w/m-k	kinetic-theory	#f
Viscosity	kg/m-s	kinetic-theory	#f
Molecular Weight	kg/kgmol	constant	31.9988
Standard State Enthalpy	j/kgmol	constant	0
Standard State Entropy	j/kgmol-k	constant	205026.86
Reference Temperature	k	constant	298.14999
L-J Characteristic Length	angstrom	constant	3.4330001
L-J Energy Parameter	k	constant	113
Degrees of Freedom		constant	0

Material: nitrogen (fluid)

Property	Units	Method	Value(s)
Cp (Specific Heat)	j/kg-k	constant	1040.67
Thermal Conductivity	w/m-k	kinetic-theory	#f
Viscosity	kg/m-s	kinetic-theory	#f
Molecular Weight	kg/kgmol	constant	28.013399

Standard State Enthalpy	j/kgmol	constant	0
Standard State Entropy	j/kgmol-k	constant	191494.78
Reference Temperature	k	constant	298.14999
L-J Characteristic Length	angstrom	constant	3.681
L-J Energy Parameter	k	constant	91.5
Degrees of Freedom		constant	0

Material: mixture-template (mixture)

Property Units Method Value(s)

Mixture Species names ((co2 o2 he h2o n2 (c<s>))

Reaction finite-rate ((reaction-1 ((c<s> 1 0 1) (o2 0.55500001 1 1)) ((co 0.88999999 0 1) (co2 0.11 0 1)) ((he 0 1) (h2o 0 1) (n2 0 1)) (stoichiometry 1c<s> + 0.55500001o2 --> 0.88999999co + 0.11co2) (arrhenius 3938000 2.09e+08 0) (mixing-rate 4 0.5) (use-third-body-efficiencies? . #f) (surface-reaction? . #t)) (reaction-2 ((co 1 1 1) (o2 0.5 0.25 1)) ((co2 1 0 1) (h2o 0 0.5 1)) ((he 0 1) (n2 0 1)) (stoichiometry 1co + 0.5o2 --> 1co2 + 0h2o) (arrhenius 2.239e+12 1.7e+08 0) (mixing-rate 4 0.5) (use-third-body-efficiencies? . #f)) (reaction-3 ((co2 1 1 1)) ((co 1 0 1) (o2 0.5 0 1)) ((he 0 1) (h2o 0 1) (n2 0 1)) (stoichiometry 1co2 --> 1co + 0.5o2) (arrhenius 1.75e+08 1.7e+08 0) (mixing-rate 4 0.5) (use-third
body-efficiencies? . #f)))

Density kg/m3 ideal-gas #f

Cp(Specific Heat) j/kg-k mixing-law #f

Thermal Conductivity w/m-k ideal-gas-mixing-law #f

Viscosity kg/m-s ideal-gas-mixing-law #f

Mass Diffusivity m2/s kinetic-theory #f

Thermal Diffusion Coefficient kg/m-s kinetic-theory #f

Thermal Expansion Coefficient 1/k constant 0

Material: carbon-solid (fluid)

Property Units Method Value(s)

Cp (Specific Heat) j/kg-k polynomial (300-1000: -464.17822 4.9711663 -0.0038992118 1.4829381e-06 -2.8855555e-10) (1000-5000: 1031.5207 1.150554 -0.00046290062 8.9357071e-08 -6.372102e-12)

Thermal Conductivity w/m-k constant 0.0454

Viscosity kg/m-s constant 1.72e-05

Molecular Weight kg/kgmol constant 12.01115

Standard State Enthalpy j/kgmol constant -101.268

Standard State Entropy j/kgmol-k constant 5731.747

Reference Temperature k constant 298

L-J Characteristic Length angstrom constant 0

L-J Energy Parameter k constant 0

Degrees of Freedom constant 0

Material: carbon-monoxide (fluid)

Property	Units	Method	Value(s)
Cp (Specific Heat)	j/kg-k	constant	1043
Thermal Conductivity	w/m-k	kinetic-theory	#f
Viscosity	kg/m-s	kinetic-theory	#f
Molecular Weight	kg/kgmol	constant	28.01055
Standard State Enthalpy	j/kgmol	constant	-1.1053956e+08
Standard State Entropy	j/kgmol-k	constant	197531.64
Reference Temperature	k	constant	298.14999
L-J Characteristic Length	angstrom	constant	3.5899999
L-J Energy Parameter	k	constant	110
Degrees of Freedom		constant	0

Material: carbon-dioxide (fluid)

Property	Units	Method	Value(s)

Cp (Specific Heat)	j/kg-k	constant	840.37
Thermal Conductivity	w/m-k	kinetic-theory	#f
Viscosity	kg/m-s	kinetic-theory	#f
Molecular Weight	kg/kgmol	constant	44.009949
Standard State Enthalpy	j/kgmol	constant	-3.9353235e+08
Standard State Entropy	j/kgmol-k	constant	213715.88
Reference Temperature	k	constant	298.14999
L-J Characteristic Length	angstrom	constant	3.9960001
L-J Energy Parameter	k	constant	190
Degrees of Freedom		constant	0

Material: helium (fluid)

Property	Units	Method	Value(s)
Cp (Specific Heat)	j/kg-k	constant	5193
Thermal Conductivity	w/m-k	kinetic-theory	#f
Viscosity	kg/m-s	kinetic-theory	#f
Molecular Weight	kg/kgmol	constant	4.0026002
Standard State Enthalpy	j/kgmol	constant	-3117.7102
Standard State Entropy	j/kgmol-k	constant	126029.45
Reference Temperature	k	constant	298.14999
L-J Characteristic Length	angstrom	constant	2.576
L-J Energy Parameter	k	constant	10.2
Degrees of Freedom		**constant**	**0**

Appendix 11: UDF for the Initial Condition of the Gas Concentration

(Multi-Component Experiment)

```
#include "udf.h"

DEFINE_PROFILE (he_profile, t, i)
{
  real x[ND_ND]; /*this will hold the position vector*/
  real z;
  face_t f;

  begin_f_loop(f, t)
    {
     F_CENTROID(x, f, t);
     z = x[2];

/* lower pipe begin*/
            if (z < 0.2)
                    F_PROFILE(f, t, i) = 0;
            else if (z >= 0.2)
                    F_PROFILE(f, t, i) = 1;
    }
   end_f_loop(f, t)
}
```

Appendix 12: UDF to Define the Initial Concentration of the Oxygen (Multi-Component Experiment)

```
DEFINE_PROFILE (oxygen_profile, t, i)
{
  real x[ND_ND]; /*this will hold the position vector*/
  real z;
  face_t f;

  begin_f_loop(f, t)
    {
     F_CENTROID(x, f, t);
     z = x[2];

/* lower pipe begin*/
            if (z < 0.2)
                    F_PROFILE(f, t, i) = 0.232;
            else if (z >= 0.2)
                    F_PROFILE(f, t, i) = 0;
    }
    end_f_loop(f, t)
}
```

Appendix 13: UDF for Wall Temperature Distribution (Multi-Component Experiment)

```
DEFINE_PROFILE (wall_Temp, t, i)
{
 real x[ND_ND]; /*this will hold the position vector*/
 real y; /*here y refer to x coordinate)*/
 real z;
 face_t f;

 begin_f_loop(f, t)
  {
   F_CENTROID(x, f, t);
        y = x[0];
   z = x[2];

/* lower pipe begin*/
        if (y > 0.2 && z > 0.4 && z < 0.56)
                F_PROFILE(f, t, i) = 289.3 + (793 - 289.3)*(z - 0.4)/(0.56 - 0.4);
        else if (y > 0.2 && z > 0.56 && z < 0.72)
                F_PROFILE(f, t, i) = 793 + (938 - 793)*(z - 0.56)/(0.72 - 0.56);
        else if (y > 0.2 && z > 0.72 && z < 0.78)
                F_PROFILE(f, t, i) = 938 + (1018 - 938)*(z - 0.72)/(0.78 - 0.72);
        else if (y > 0.2 && z > 0.78 && z < 0.87)
                F_PROFILE(f, t, i) = 1018 + (1063 - 1018)*(z - 0.78)/(0.87 - 0.78);

/*graphite wall begion*/
        else if (y > 0.2 && z > 0.87 && z < 0.95)
                F_PROFILE(f, t, i) = 1063 + (1073 - 1063)*(z - 0.87)/(0.95 - 0.87);
```

```
        else if (y > 0.2 && z > 0.95 && z < 1.08)
                F_PROFILE(f, t, i) = 1073;
        else if (y > 0.2 && z > 1.08 && z < 1.32)
                F_PROFILE(f, t, i) = 1073 + (1123 - 1073)*(z - 1.08)/(1.32 - 1.08);


/*up and cool pipe begion*/
        else if (y > 0.2 && z > 1.32 && z < 1.4)
                F_PROFILE(f, t, i) = 1123 + (1118 - 1123)*(z - 1.32)/(1.4 - 1.32);
        else if (y > 0.2 && z > 1.4 && z < 1.6)
                F_PROFILE(f, t, i) = 1118 + (1003 - 1118)*(z - 1.4)/(1.6 - 1.4);
        else if (y > 0.2 && z > 1.6 && z < 1.68)
                F_PROFILE(f, t, i) = 1003 + (858 - 1003)*(z - 1.6)/(1.68 - 1.6);
        else if (y > 0.2 && z > 1.68 && z < 1.77)
                F_PROFILE(f, t, i) = 858 + (880 - 858)*(z - 1.68)/(1.77 - 1.68);
        else if (y > 0.2 && z > 1.77 && z < 1.89975)
                F_PROFILE(f, t, i) = 880 + (1003 - 880)*(z - 1.77)/(1.89975 - 1.77);

        else if (y > 0.17 && y < 0.27025 && z > 1.89975)
                F_PROFILE(f, t, i) = 1003 + (1073 - 1003)*(y - 0.27025)/(0.17 -
0.27025);
        else if (y > -0.17 && y < 0.17 && z > 1.89975)
                F_PROFILE(f, t, i) = 1073;
        else if (y > -0.27025 && y < -0.17 && z > 1.89975)
                F_PROFILE(f, t, i) = 1073 + (808 - 1073)*(y - (-0.17))/(-0.27025 - (-
0.17));

        else if (y < -0.2 && z > 1.62 && z < 1.89975)
                F_PROFILE(f, t, i) = 808 + (393 - 808)*(z - 1.89975)/(1.62 - 1.89975);
        else if (y < -0.2 && z > 1.22 && z < 1.62)
```

```
            F_PROFILE(f, t, i) = 393 + (289.45 - 393)*(z - 1.62)/(1.22 - 1.62);
        else
            F_PROFILE(f, t, i) = 289.449;
}
end_f_loop(f, t)
                                                    }
```

Appendix 14: The Fluent Model Summary for NACOK Experiment

FLUENT

Version: 3d, dp, segregated, lam (3d, double precision, segregated, laminar)

Release: 6.0.20

Title:

Models

Model	Settings
Space	3D
Time	Steady
Viscous	Laminar
Heat Transfer	Enabled
Solidification and Melting	Disabled
Radiation	None
Species Transport	Disabled
Coupled Dispersed Phase	Disabled
Pollutants	Disabled
Soot	Disabled

oundary Conditions

Zones

name	id	type
fluid	2	fluid
region_bottomsquare	3	fluid
region_topsquare	4	fluid
return_horizonpipe	5	fluid

region_returnpipe 6 fluid

region_pebbles 7 fluid

region_inletpipe 8 fluid

outlet 9 pressure-outlet

inlet 10 pressure-inlet

wall_returnpipe 11 wall

wall_horizonpipe 12 wall

wall_topsquare 13 wall

wall_pebblebed 14 wall

wall_bottomsquare 15 wall

wall_inletpipe 16 wall

symmetry.25 17 symmetry

default-interior 19 interior

wall_topsquare:001 1 wall

symmetry.25:018 18 symmetry

symmetry.25:020 20 symmetry

symmetry.25:021 21 symmetry

symmetry.25:022 22 symmetry

symmetry.25:023 23 symmetry

symmetry.25:024 24 symmetry

default-interior:025 25 interior

default-interior:026 26 interior

default-interior:027 27 interior

default-interior:028 28 interior

default-interior:029 29 interior

default-interior:030 30 interior

default-interior:031 31 interior

default-interior:032 32 interior

default-interior:033 33 interior

default-interior:034 34 interior

default-interior:035 35 interior

default-interior:036 36 interior

Boundary Conditions

fluid

Condition Value

Material Name air

Specify source terms? no

Source Terms ((mass (inactive . #f) (constant . 0) (profile)) (x-momentum (inactive . #f) (constant . 0) (profile)) (y-momentum (inactive . #f) (constant . 0) (profile)) (z-momentum (inactive . #f) (const
nt . 0) (profile)) (energy (inactive . #f) (constant . 0) (profile)))

Specify fixed values? no

Local Coordinate System for Fixed Velocities no

Fixed Values ()

Motion Type 0

X-Velocity Of Zone 0

Y-Velocity Of Zone 0

Z-Velocity Of Zone 0

Rotation speed 0

X-Origin of Rotation-Axis 0

Y-Origin of Rotation-Axis 0

Z-Origin of Rotation-Axis 0

X-Component of Rotation-Axis 0

Y-Component of Rotation-Axis 0

Z-Component of Rotation-Axis 1

Porous zone? no

Conical porous zone? no

X-Component of Direction-1 Vector 1

Y-Component of Direction-1 Vector 0

Z-Component of Direction-1 Vector 0

X-Component of Direction-2 Vector 0

Y-Component of Direction-2 Vector 1

Z-Component of Direction-2 Vector	0
X-Coordinate of Point on Cone Axis	1
Y-Coordinate of Point on Cone Axis	0
Z-Coordinate of Point on Cone Axis	0
Half Angle of Cone Relative to its Axis	0
Direction-1 Viscous Resistance	0
Direction-2 Viscous Resistance	0
Direction-3 Viscous Resistance	0
Direction-1 Inertial Resistance	0
Direction-2 Inertial Resistance	0
Direction-3 Inertial Resistance	0
C0 Coefficient for Power-Law	0
C1 Coefficient for Power-Law	0
Porosity	1
Solid Material Name	aluminum

region_bottomsquare

Condition Value

Material Name air

Specify source terms? no

Source Terms ((mass (inactive . #f) (constant . 0) (profile)) (x-momentum (inactive . #f) (constant . 0) (profile)) (y-momentum (inactive . #f) (constant . 0) (profile)) (z-momentum (inactive . #f) (const
nt . 0) (profile)) (energy (inactive . #f) (constant . 0) (profile)))

Specify fixed values? no

Local Coordinate System for Fixed Velocities no

Fixed Values ((x-velocity (inactive . #f) (constant . 0) (profile)) (y-velocity (inactive . #f) (constant . 0) (profile)) (z-velocity (inactive . #f) (constant . 0) (profile)) (temperature (constant . 873
(profile)))

Motion Type 0

X-Velocity Of Zone 0

Y-Velocity Of Zone 0

Z-Velocity Of Zone 0

Rotation speed 0

X-Origin of Rotation-Axis 0

Y-Origin of Rotation-Axis 0

Z-Origin of Rotation-Axis 0

X-Component of Rotation-Axis 0

Y-Component of Rotation-Axis 0

Z-Component of Rotation-Axis 1

Porous zone? no

Conical porous zone? no

X-Component of Direction-1 Vector 1

Y-Component of Direction-1 Vector 0

Z-Component of Direction-1 Vector 0

X-Component of Direction-2 Vector 0

Y-Component of Direction-2 Vector 1

Z-Component of Direction-2 Vector 0

X-Coordinate of Point on Cone Axis 1

Y-Coordinate of Point on Cone Axis 0

Z-Coordinate of Point on Cone Axis 0

Half Angle of Cone Relative to its Axis 0

Direction-1 Viscous Resistance 0

Direction-2 Viscous Resistance 0

Direction-3 Viscous Resistance 0

Direction-1 Inertial Resistance 0

Direction-2 Inertial Resistance 0

Direction-3 Inertial Resistance 0

C0 Coefficient for Power-Law 0

C1 Coefficient for Power-Law 0

Porosity 1

Solid Material Name aluminum

region_topsquare

Condition Value

Material Name air

Specify source terms? no

Source Terms ((mass (inactive . #f) (constant . 0) (profile)) (x-momentum (inactive . #f) (constant . 0) (profile)) (y-momentum (inactive . #f) (constant . 0) (profile)) (z-momentum (inactive . #f) (const
nt . 0) (profile)) (energy (inactive . #f) (constant . 0) (profile)))

Specify fixed values? no

Local Coordinate System for Fixed Velocities no

Fixed Values ((x-velocity (inactive . #f) (constant . 0) (profile)) (y-velocity (inactive . #f) (constant . 0) (profile)) (z-velocity (inactive . #f) (constant . 0) (profile)) (temperature (constant . 873
(profile)))

Motion Type 0

X-Velocity Of Zone 0

Y-Velocity Of Zone 0

Z-Velocity Of Zone 0

Rotation speed 0

X-Origin of Rotation-Axis 0

Y-Origin of Rotation-Axis 0

Z-Origin of Rotation-Axis 0

X-Component of Rotation-Axis 0

Y-Component of Rotation-Axis 0

Z-Component of Rotation-Axis 1

Porous zone? no

Conical porous zone? no

X-Component of Direction-1 Vector 1

Y-Component of Direction-1 Vector 0

Z-Component of Direction-1 Vector 0

X-Component of Direction-2 Vector 0

Y-Component of Direction-2 Vector 1

Z-Component of Direction-2 Vector 0

X-Coordinate of Point on Cone Axis 1

Y-Coordinate of Point on Cone Axis 0

Z-Coordinate of Point on Cone Axis 0

Half Angle of Cone Relative to its Axis 0

Direction-1 Viscous Resistance 0

Direction-2 Viscous Resistance 0

Direction-3 Viscous Resistance 0

Direction-1 Inertial Resistance 0

Direction-2 Inertial Resistance 0

Direction-3 Inertial Resistance 0

C0 Coefficient for Power-Law 0

C1 Coefficient for Power-Law 0

Porosity 1

Solid Material Name aluminum

return_horizonpipe

Condition Value

Material Name air

Specify source terms? no

Source Terms ((mass (inactive . #f) (constant . 0) (profile)) (x-momentum (inactive . #f) (constant . 0) (profile)) (y-momentum (inactive . #f) (constant . 0) (profile)) (z-momentum (inactive . #f) (const
nt . 0) (profile)) (energy (inactive . #f) (constant . 0) (profile)))

Specify fixed values? no

Local Coordinate System for Fixed Velocities no

Fixed Values ((x-velocity (inactive . #f) (constant . 0) (profile)) (y-velocity (inactive . #f) (constant . 0) (profile)) (z-velocity (inactive . #f) (constant . 0) (profile)) (temperature (constant . 473
(profile)))

Motion Type 0

X-Velocity Of Zone 0

Y-Velocity Of Zone 0

Z-Velocity Of Zone 0

Rotation speed 0

X-Origin of Rotation-Axis 0

Y-Origin of Rotation-Axis 0

Z-Origin of Rotation-Axis 0

X-Component of Rotation-Axis	0
Y-Component of Rotation-Axis	0
Z-Component of Rotation-Axis	1
Porous zone?	no
Conical porous zone?	no
X-Component of Direction-1 Vector	1
Y-Component of Direction-1 Vector	0
Z-Component of Direction-1 Vector	0
X-Component of Direction-2 Vector	0
Y-Component of Direction-2 Vector	1
Z-Component of Direction-2 Vector	0
X-Coordinate of Point on Cone Axis	1
Y-Coordinate of Point on Cone Axis	0
Z-Coordinate of Point on Cone Axis	0

Half Angle of Cone Relative to its Axis 0

Direction-1 Viscous Resistance 0

Direction-2 Viscous Resistance 0

Direction-3 Viscous Resistance 0

Direction-1 Inertial Resistance 0

Direction-2 Inertial Resistance 0

Direction-3 Inertial Resistance 0

C0 Coefficient for Power-Law 0

C1 Coefficient for Power-Law 0

Porosity 1

Solid Material Name aluminum

region_returnpipe

Condition Value

Material Name air

Specify source terms? no

Source Terms ((mass (inactive . #f) (constant . 0) (profile)) (x-momentum (inactive . #f) (constant . 0) (profile)) (y-momentum (inactive . #f) (constant . 0) (profile)) (z-momentum (inactive . #f) (const
nt . 0) (profile)) (energy (inactive . #f) (constant . 0) (profile)))

Specify fixed values? no

Local Coordinate System for Fixed Velocities no

Fixed Values ((x-velocity (inactive . #f) (constant . 0) (profile)) (y-velocity (inactive . #f) (constant . 0) (profile)) (z-velocity (inactive . #f) (constant . 0) (profile)) (temperature (constant . 473
(profile)))

Motion Type 0

X-Velocity Of Zone 0

Y-Velocity Of Zone 0

Z-Velocity Of Zone 0

Rotation speed 0

X-Origin of Rotation-Axis 0

Y-Origin of Rotation-Axis 0

Z-Origin of Rotation-Axis 0

X-Component of Rotation-Axis 0

Y-Component of Rotation-Axis 0

Z-Component of Rotation-Axis 1

Porous zone? no

Conical porous zone? no

X-Component of Direction-1 Vector 1

Y-Component of Direction-1 Vector 0

Z-Component of Direction-1 Vector 0

X-Component of Direction-2 Vector 0

Y-Component of Direction-2 Vector 1

Z-Component of Direction-2 Vector 0

X-Coordinate of Point on Cone Axis 1

Y-Coordinate of Point on Cone Axis 0

Z-Coordinate of Point on Cone Axis 0

Half Angle of Cone Relative to its Axis 0

Direction-1 Viscous Resistance 0

Direction-2 Viscous Resistance 0

Direction-3 Viscous Resistance 0

Direction-1 Inertial Resistance 0

Direction-2 Inertial Resistance 0

Direction-3 Inertial Resistance 0

C0 Coefficient for Power-Law 0

C1 Coefficient for Power-Law 0

Porosity 1

Solid Material Name aluminum

region_pebbles

Condition Value

Material Name air

Specify source terms? yes

Source Terms ((mass (inactive . #f) (constant . 0) (profile)) (x-momentum (inactive . #f) (constant . 0) (profile)) (y-momentum (inactive . #f) (constant . 0) (profile)) (z-momentum (profile udf zmom_sour

e) (constant . 0)) (energy (inactive . #f) (constant . 0) (profile)))

Specify fixed values? no

Local Coordinate System for Fixed Velocities no

Fixed Values ((x-velocity (inactive . #f) (constant . 0) (profile)) (y-velocity (inactive . #f) (constant . 0) (profile)) (z-velocity (inactive . #f) (constant . 0) (profile)) (temperature (constant . 873 (profile)))

Motion Type 0

X-Velocity Of Zone 0

Y-Velocity Of Zone 0

Z-Velocity Of Zone 0

Rotation speed 0

X-Origin of Rotation-Axis 0

Y-Origin of Rotation-Axis 0

Z-Origin of Rotation-Axis 0

X-Component of Rotation-Axis 0

Y-Component of Rotation-Axis 0

Z-Component of Rotation-Axis 1

Porous zone? yes

Conical porous zone? no

X-Component of Direction-1 Vector 1

Y-Component of Direction-1 Vector 0

Z-Component of Direction-1 Vector 0

X-Component of Direction-2 Vector 0

Y-Component of Direction-2 Vector 1

Z-Component of Direction-2 Vector 0

X-Coordinate of Point on Cone Axis 1

Y-Coordinate of Point on Cone Axis 0

Z-Coordinate of Point on Cone Axis 0

Half Angle of Cone Relative to its Axis 0

Direction-1 Viscous Resistance 0

Direction-2 Viscous Resistance 0

Direction-3 Viscous Resistance 0

Direction-1 Inertial Resistance 0

Direction-2 Inertial Resistance 0

Direction-3 Inertial Resistance 0

C0 Coefficient for Power-Law 0

C1 Coefficient for Power-Law 0

Porosity 0.39500001

Solid Material Name aluminum

region_inletpipe

Condition Value

Material Name air

Specify source terms? no

Source Terms ((mass (inactive . #f) (constant . 0) (profile)) (x-momentum (inactive . #f) (constant . 0) (profile)) (y-momentum (inactive . #f) (constant . 0) (profile)) (z-momentum (inactive . #f) (const
nt . 0) (profile)) (energy (inactive . #f) (constant . 0) (profile)))

Specify fixed values? no

Local Coordinate System for Fixed Velocities no

Fixed Values ((x-velocity (inactive . #f) (constant . 0) (profile)) (y-velocity (inactive . #f) (constant . 0) (profile)) (z-velocity (inactive . #f) (constant . 0) (profile)) (temperature (constant . 473 (profile)))

Motion Type 0

X-Velocity Of Zone 0

Y-Velocity Of Zone 0

Z-Velocity Of Zone 0

Rotation speed 0

X-Origin of Rotation-Axis 0

Y-Origin of Rotation-Axis 0

Z-Origin of Rotation-Axis 0

X-Component of Rotation-Axis 0

Y-Component of Rotation-Axis 0

Z-Component of Rotation-Axis 1

Porous zone? no

Conical porous zone?	no
X-Component of Direction-1 Vector	1
Y-Component of Direction-1 Vector	0
Z-Component of Direction-1 Vector	0
X-Component of Direction-2 Vector	0
Y-Component of Direction-2 Vector	1
Z-Component of Direction-2 Vector	0
X-Coordinate of Point on Cone Axis	1
Y-Coordinate of Point on Cone Axis	0
Z-Coordinate of Point on Cone Axis	0
Half Angle of Cone Relative to its Axis	0
Direction-1 Viscous Resistance	0
Direction-2 Viscous Resistance	0
Direction-3 Viscous Resistance	0
Direction-1 Inertial Resistance	0

Direction-2 Inertial Resistance 0

Direction-3 Inertial Resistance 0

C0 Coefficient for Power-Law 0

C1 Coefficient for Power-Law 0

Porosity 1

Solid Material Name aluminum

outlet

Condition	Value
Gauge Pressure	0
Radial Equilibrium Pressure Distribution	no
Backflow Total Temperature	473
is zone used in mixing-plane model?	no

inlet

Condition	Value
Gauge Total Pressure	0
Supersonic/Initial Gauge Pressure	0
Total Temperature	473
Direction Specification Method	1
Coordinate System	0
X-Component of Flow Direction	1

Y-Component of Flow Direction	0
Z-Component of Flow Direction	0
X-Component of Axis Direction	1
Y-Component of Axis Direction	0
Z-Component of Axis Direction	0
X-Coordinate of Axis Origin	0
Y-Coordinate of Axis Origin	0
Z-Coordinate of Axis Origin	0
is zone used in mixing-plane model?	no

wall_returnpipe

Condition	Value
Wall Thickness	0
Heat Generation Rate	0
Material Name	aluminum
Thermal BC Type	0
Temperature	473
Heat Flux	0
Convective Heat Transfer Coefficient	0
Free Stream Temperature	300
Enable shell conduction?	no
Wall Motion	0
Shear Boundary Condition	0
Define wall motion relative to adjacent cell zone?	yes
Apply a rotational velocity to this wall?	no
Velocity Magnitude	0
X-Component of Wall Translation	1
Y-Component of Wall Translation	0

Z-Component of Wall Translation	0
Define wall velocity components?	no
X-Component of Wall Translation	0
Y-Component of Wall Translation	0
Z-Component of Wall Translation	0
External Emissivity	1
External Radiation Temperature	300
Rotation Speed	0
X-Position of Rotation-Axis Origin	0
Y-Position of Rotation-Axis Origin	0
Z-Position of Rotation-Axis Origin	0
X-Component of Rotation-Axis Direction	0
Y-Component of Rotation-Axis Direction	0
Z-Component of Rotation-Axis Direction	1
X-component of shear stress	0
Y-component of shear stress	0
Z-component of shear stress	0
Surface tension gradient	0

wall_horizonpipe

Condition	Value
Wall Thickness	0
Heat Generation Rate	0
Material Name	aluminum
Thermal BC Type	0
Temperature	473
Heat Flux	0
Convective Heat Transfer Coefficient	0

Free Stream Temperature	300
Enable shell conduction?	no
Wall Motion	0
Shear Boundary Condition	0
Define wall motion relative to adjacent cell zone?	yes
Apply a rotational velocity to this wall?	no
Velocity Magnitude	0
X-Component of Wall Translation	1
Y-Component of Wall Translation	0
Z-Component of Wall Translation	0
Define wall velocity components?	no
X-Component of Wall Translation	0
Y-Component of Wall Translation	0
Z-Component of Wall Translation	0
External Emissivity	1
External Radiation Temperature	300
Rotation Speed	0
X-Position of Rotation-Axis Origin	0
Y-Position of Rotation-Axis Origin	0
Z-Position of Rotation-Axis Origin	0
X-Component of Rotation-Axis Direction	0
Y-Component of Rotation-Axis Direction	0
Z-Component of Rotation-Axis Direction	1
X-component of shear stress	0
Y-component of shear stress	0
Z-component of shear stress	0
Surface tension gradient	0

wall_topsquare

Condition	Value
Wall Thickness	0
Heat Generation Rate	0
Material Name	aluminum
Thermal BC Type	0
Temperature	1273
Heat Flux	0
Convective Heat Transfer Coefficient	0
Free Stream Temperature	300
Enable shell conduction?	no
Wall Motion	0
Shear Boundary Condition	0
Define wall motion relative to adjacent cell zone?	yes
Apply a rotational velocity to this wall?	no
Velocity Magnitude	0
X-Component of Wall Translation	1
Y-Component of Wall Translation	0
Z-Component of Wall Translation	0
Define wall velocity components?	no
X-Component of Wall Translation	0
Y-Component of Wall Translation	0
Z-Component of Wall Translation	0
External Emissivity	1
External Radiation Temperature	300
Rotation Speed	0
X-Position of Rotation-Axis Origin	0
Y-Position of Rotation-Axis Origin	0
Z-Position of Rotation-Axis Origin	0
X-Component of Rotation-Axis Direction	0

Y-Component of Rotation-Axis Direction	0
Z-Component of Rotation-Axis Direction	1
X-component of shear stress	0
Y-component of shear stress	0
Z-component of shear stress	0
Surface tension gradient	0

wall_pebblebed

Condition	Value
Wall Thickness	0
Heat Generation Rate	0
Material Name	aluminum
Thermal BC Type	0
Temperature	1273
Heat Flux	0
Convective Heat Transfer Coefficient	0
Free Stream Temperature	300
Enable shell conduction?	no
Wall Motion	0
Shear Boundary Condition	0
Define wall motion relative to adjacent cell zone?	yes
Apply a rotational velocity to this wall?	no
Velocity Magnitude	0
X-Component of Wall Translation	1
Y-Component of Wall Translation	0
Z-Component of Wall Translation	0
Define wall velocity components?	no
X-Component of Wall Translation	0

Y-Component of Wall Translation	0
Z-Component of Wall Translation	0
External Emissivity	1
External Radiation Temperature	300
Rotation Speed	0
X-Position of Rotation-Axis Origin	0
Y-Position of Rotation-Axis Origin	0
Z-Position of Rotation-Axis Origin	0
X-Component of Rotation-Axis Direction	0
Y-Component of Rotation-Axis Direction	0
Z-Component of Rotation-Axis Direction	1
X-component of shear stress	0
Y-component of shear stress	0
Z-component of shear stress	0
Surface tension gradient	0

wall_bottomsquare

Condition	Value
Wall Thickness	0
Heat Generation Rate	0
Material Name	aluminum
Thermal BC Type	0
Temperature	1273
Heat Flux	0
Convective Heat Transfer Coefficient	0
Free Stream Temperature	300
Enable shell conduction?	no
Wall Motion	0

Shear Boundary Condition	0
Define wall motion relative to adjacent cell zone?	yes
Apply a rotational velocity to this wall?	no
Velocity Magnitude	0
X-Component of Wall Translation	1
Y-Component of Wall Translation	0
Z-Component of Wall Translation	0
Define wall velocity components?	no
X-Component of Wall Translation	0
Y-Component of Wall Translation	0
Z-Component of Wall Translation	0
External Emissivity	1
External Radiation Temperature	300
Rotation Speed	0
X-Position of Rotation-Axis Origin	0
Y-Position of Rotation-Axis Origin	0
Z-Position of Rotation-Axis Origin	0
X-Component of Rotation-Axis Direction	0
Y-Component of Rotation-Axis Direction	0
Z-Component of Rotation-Axis Direction	1
X-component of shear stress	0
Y-component of shear stress	0
Z-component of shear stress	0
Surface tension gradient	0

wall_inletpipe

Condition	Value
Wall Thickness	0

Heat Generation Rate	0
Material Name	aluminum
Thermal BC Type	0
Temperature	473
Heat Flux	0
Convective Heat Transfer Coefficient	0
Free Stream Temperature	300
Enable shell conduction?	no
Wall Motion	0
Shear Boundary Condition	0
Define wall motion relative to adjacent cell zone?	yes
Apply a rotational velocity to this wall?	no
Velocity Magnitude	0
X-Component of Wall Translation	1
Y-Component of Wall Translation	0
Z-Component of Wall Translation	0
Define wall velocity components?	no
X-Component of Wall Translation	0
Y-Component of Wall Translation	0
Z-Component of Wall Translation	0
External Emissivity	1
External Radiation Temperature	300
Rotation Speed	0
X-Position of Rotation-Axis Origin	0
Y-Position of Rotation-Axis Origin	0
Z-Position of Rotation-Axis Origin	0
X-Component of Rotation-Axis Direction	0
Y-Component of Rotation-Axis Direction	0
Z-Component of Rotation-Axis Direction	1
X-component of shear stress	0

Y-component of shear stress	0
Z-component of shear stress	0
Surface tension gradient	0

symmetry.25

Condition	Value

default-interior

Condition	Value

wall_topsquare:001

Condition	Value
Wall Thickness	0
Heat Generation Rate	0
Material Name	aluminum
Thermal BC Type	0
Temperature	1273
Heat Flux	0
Convective Heat Transfer Coefficient	0
Free Stream Temperature	300
Enable shell conduction?	no
Wall Motion	0
Shear Boundary Condition	0
Define wall motion relative to adjacent cell zone?	yes

Apply a rotational velocity to this wall?	no
Velocity Magnitude	0
X-Component of Wall Translation	1
Y-Component of Wall Translation	0
Z-Component of Wall Translation	0
Define wall velocity components?	no
X-Component of Wall Translation	0
Y-Component of Wall Translation	0
Z-Component of Wall Translation	0
External Emissivity	1
External Radiation Temperature	300
Rotation Speed	0
X-Position of Rotation-Axis Origin	0
Y-Position of Rotation-Axis Origin	0
Z-Position of Rotation-Axis Origin	0
X-Component of Rotation-Axis Direction	0
Y-Component of Rotation-Axis Direction	0
Z-Component of Rotation-Axis Direction	1
X-component of shear stress	0
Y-component of shear stress	0
Z-component of shear stress	0
Surface tension gradient	0

symmetry.25:018

Condition	Value

symmetry.25:020

Condition	Value

symmetry.25:021

Condition Value

---

symmetry.25:022

Condition Value

---

symmetry.25:023

Condition Value

---

symmetry.25:024

Condition Value

---

default-interior:025

Condition Value

---

default-interior:026

Condition Value

---

default-interior:027

Condition Value

---

default-interior:028

Condition Value

---

default-interior:029

Condition Value

---

default-interior:030

Condition Value

---

default-interior:031

Condition Value

---

default-interior:032

Condition Value

---

default-interior:033

Condition Value

---

default-interior:034

Condition Value

---

default-interior:035

Condition Value

---

default-interior:036

Condition Value

---

olver Controls

Equations

Equation Solved

Flow yes

Energy yes

Numerics

Numeric Enabled

Absolute Velocity Formulation yes

Relaxation

Variable Relaxation Factor

Pressure 0.2

Density 0.30000001

Body Forces 0.30000001

Momentum 0.050000001

Energy 0.2

Linear Solver

Variable	Solver Type	Termination Criterion	Residual Reduction Tolerance
Pressure	V-Cycle	0.1	
X-Momentum	Flexible	0.1	0.7
Y-Momentum	Flexible	0.1	0.7
Z-Momentum	Flexible	0.1	0.7
Energy	Flexible	0.1	0.7

Discretization Scheme

Variable	Scheme
Pressure	PRESTO!
Pressure-Velocity Coupling	PISO
Momentum	Second Order Upwind
Energy	Second Order Upwind

Solution Limits

Quantity	Limit
Minimum Absolute Pressure	1
Maximum Absolute Pressure	5000000
Minimum Temperature	1
Maximum Temperature	5000

FLUENT

Version: 3d, dp, segregated, lam (3d, double precision, segregated, laminar)

Release: 6.0.20

Title:

Material Properties

Material: aluminum (solid)

Property	Units	Method	Value(s)
Density	kg/m3	constant	2719
Cp (Specific Heat)	j/kg-k	constant	871
Thermal Conductivity	w/m-k	constant	202.4

Material: air (fluid)

Property	Units	Method	Value(s)
Density	kg/m3	polynomial	(273 1.293) (373 0.94599998) (473 0.74599999) (573 0.61500001) (673 0.52399999) (773 0.456) (873 0.40400001) (973 0.36199999) (1073 0.329) (1173 0.301) (1273 0.27700001) (1373 0.257)
Cp (Specific Heat)	j/kg-k	polynomial	(273 1005) (373 1009) (473 1026) (573 1047) (673 1068) (773 1093) (873 1114) (973 1135) (1073 1156) (1173 1172) (1273 1185) (1373 1197)
Thermal Conductivity	w/m-k	polynomial	(273 0.0244) (373 0.032099999) (473 0.039299998) (573 0.046) (673 0.052099999) (773 0.057399999) (873

0.062199999) (973 0.067100003) (1073 0.071800001) (1173 0.076300003) (1273 0.080700003) (
373 0.085000001)

Viscosity kg/m-s polynomial (273 1.72e-05) (373 2.1899999e-05) (473 2.6e-05) (573 2.9700001e-05) (673 3.3e-05) (773 3.6199999e-05) (873 3.9099999e-05) (973 4.1800002e-05) (1073 4.4299999e-05) (1173 4.6699999e-05) (1273 .8999998e-05) (1373 5.1200001e-05)

Molecular Weight kg/kgmol constant 28.966

L-J Characteristic Length angstrom constant 3.711

L-J Energy Parameter k constant 78.599998

Thermal Expansion Coefficient 1/k constant 0.0035000001

Appendix 15: UDF to Define the Pressure Drop in Pebble Bed Region

```
#include "udf.h"
#define C1 170000
#define C2 10.3
DEFINE_SOURCE (zmom_source, c, t, dS, eqn)
{
   real source;
  source = -C1*C_MU_L(c,t)*C_W(c,t)-C2*pow(C_R(c,t), 0.9)*pow(C_MU_L(c,t),
0.1)*pow(C_W(c,t), 1.9);
  dS[eqn] = -C1*C_MU_L(c,t)-1.9*C2*pow(C_R(c,t), 0.9)*pow(C_MU_L(c,t),
0.1)*pow(C_W(c,t), 0.9);

  return source;
}
```